The Dissertation Committee for Prinda Wanakule Certifies that this is the approved version of the following dissertation:

Development and Evaluation of Enzymatically-Degradable Hydrogel Microparticles for Pulmonary Delivery of Nanoparticles and Biologics

Committee:

Krishnendu Roy, Supervisor

Laura J. Suggs

Konstantin V. Sokolov

Robert O. Williams, III

Jason T. McConville

Development and Evaluation of Enzymatically-Degradable Hydrogel Microparticles for Pulmonary Delivery of Nanoparticles and Biologics

by

Prinda Wanakule, B.S.; M.S.E.

Dissertation

Presented to the Faculty of the Graduate School of

The University of Texas at Austin

in Partial Fulfillment

of the Requirements

for the Degree of

Doctor of Philosophy

The University of Texas at Austin

December 2012

Dedication

This work is dedicated to my loving family for all of their support and encouragement throughout my education:

My father, Dr. Nisai Wanakule, who received his Ph.D. in engineering from the University of Texas at Austin in the same year and month that I was born, and laid the early foundations that resulted in my pursuit of engineering and science.

My mother, Paulla Wanakule, whom I take after in creativity and imagination, and who gave me the inspiration to understand and improve pulmonary disorders and treatment.

My sister, Dr. Nisita Wanakule, also a Ph.D. engineer, who helped me with my homework when we were kids, got me started in research early on, and whom I have always looked up to as a mentor and role model.

Acknowledgements

I would first like to thank my advisor, Dr. Krishnendu Roy, for taking a chance on me and letting me join his lab, despite my vastly different research background and complete lack of experience in biomaterials. I am especially grateful that he believed in me and gave me the opportunity and challenge of creating my own project, and was there to motivate and guide me when I needed it. He has truly been a great mentor from the first day we met, and has always encouraged me to pursue my passions and other opportunities for personal and professional development.

Next, I must give thanks to all of my committee members for their support and advice in all the different areas of my work. Dr. Williams and Dr. McConville were absolutely invaluable with their advice on pulmonary formulations and particle synthesis methods. I could not have achieved my end goal without their support, expertise, and generosity with their time and equipment. Dr. Sokolov also provided valuable guidance in various imaging methods, and was always happy to share equipment. Dr. Suggs provided helpful advice and insight for the chemistry and materials aspects of my project, and always served as a great role model.

I would also like to thank several research staff members, both currently and formerly at the University of Texas at Austin. Dwight Romanowicz, Angela Bardo, and Julie Hayes of the Institute for Cellular and Molecular Biology Core Facility spent countless hours training and helping me to use the SEM, cryoSEM, and confocal microscopes. Klaus Linse, formerly in the Protein Core Facility, helped to demystify protein and peptide biochemistry. Greg Lyness and Jamye O'Neal in TherapUTex also spent countless hours in support of my research. The staff at the Animal Resources

Center were especially invaluable in the last year of my work: Kathryn Starr, Dr. Kathleen Roellich, Dr. Glen Otto, Jennifer Cassaday, Jocelyn Franklin, and Nachi Shukla and his facilities support team.

Special thanks go out to all my friends and colleagues for their support throughout the years. First and most especially, I must recognize other members from the Roy Lab. I could not have made it to the end without the help of my undergrad Gary Liu, and labmate Asha Fleury, who helped me tremendously with many experiments. Mary Caldorera-Moore taught me the basics of peptide acrylation and made my first UV-polymerized hydrogel with me. Bilal Ghosn introduced me into the lab, and taught me the basics of chitosan chemistry and mouse necropsy. Ankur Singh started me on the path to Michael addition chemistries, and helped me create my first Michael addition hydrogels. Nathalie Guimard further worked with me on chitosan chemistry, mentored me, and taught me so many other aspects of proper laboratory safety and practices. Myung Hee Michelle Kim patiently taught me how to do cell culture, and always helped me to troubleshoot various aspects of my project. Eileen Dawson was always willing to discuss issues, and helped bring out our best work with her high standards and scientific scrutiny. Krista Fridley and Rachit Agarwal taught me how to do flow cytometry, and Tracy Ooi helped me further along and demystified Flow Jo. I must also thank my former undergrads Amy Bergeron and James Chang for their hard work and dedication in the lab. Lonnissa Nguyen, Jian Lin, Jardin Leleux, Pallab Pradhan, Kathryn Erickson, and all other members of "Klub Krish," your support and camaraderie helped to get me through these years! I am so grateful to have you all both as friends and labmates.

Many thanks go to my other colleagues from different labs that have impacted my work in various ways. Eric Spivey helped with optical trapping; Thiago, Yoen-Ju, and Ju from Pharmaceutics were always helpful in discussing a field that I was unfamiliar with.

Special thanks go to colleagues from Jeffrey Hubbell's and Melody Swartz's labs at EPFL: Evan, Jennifer, Sachiko, and Armando, all of whom I learned a remarkable amount from in just one summer.

To my other BME-affiliated colleagues and friends, I am so grateful to have you in my lives: Thomas, Justina, Deanna, Navid, Arnold, Eric, Ashwin, Vaish, Mark, and Michelle. Most sincere heartfelt thanks must go out to the SWE@UT Graduate Committee founding and early members for being my graduate school cheerleaders: Anne, Richelle, Katie, and Ellison. Of course, I must also include my nationwide SWEsters for always encouraging me: Ruby, Pree, Cristina, Chelsea, and Tabitha.

I must express my most heartfelt love and appreciation for my family, and my deepest gratitude for their encouragement, inspiration, and support all throughout my life. For their many personal sacrifices in always putting my education and happiness first, I am forever in their debt. My parents were both the motivation for me to pursue graduate study in engineering, and also the inspiration that led me to my field, and I try my best everyday to make them proud. My sister was also there to lend a supportive and understanding ear, and always gave me the best advice in both professional and personal matters. I know that I could not have gotten to where I am without her mentorship and guidance. I must also thank Shasta, who always kept me company, and made sure I stayed healthy and active.

Finally, this research would not have been possible without the financial support from the National Science Foundation Division of Materials Research, as well as generous support from the National Science Foundation Graduate Research Fellowship Program, the University of Texas THRUST, Bruton, Heuer, and WEP Fellowship and Scholarship Programs, and the Society of Women Engineers Scholarship Program.

Development and Evaluation of Enzymatically-Degradable Hydrogel Microparticles for Pulmonary Delivery of Nanoparticles and Biologics

Prinda Wanakule, Ph.D.

The University of Texas at Austin, 2012

Supervisor: Krishnendu Roy

The emerging class of biologic drugs, including proteins, peptides, and gene therapies, are widely administered by injection, despite potential systemic side effects. Rational design of targeted carriers that can be delivered non-invasively, with reduced side effects, is essential for the success of these therapies, as well as for the improvement of patient compliance and quality of life.

One potential approach is to take advantage of specific physiological cues, such as enzymes, which would trigger drug release from a drug carrier. Enzymatic cleavage is highly specific and could be tailored for certain diseased tissues where specific enzymes are up regulated. Enzymatically-degradable hydrogels, which incorporate an enzyme-cleavable peptide into the network structure, have been extensively reported for releasing drugs for tissue engineering applications. These studies showed that a rapid response and corresponding drug release occurs upon enzyme exposure, whereas minimal degradation occurs without enzyme. Recently, Michael addition reactions have been developed for the synthesis of such enzymatically-degradable hydrogels. Michael addition reactions occur under mild physiological conditions, making them ideally suited for polymerizing hydrogels with encapsulated biologic drugs without affecting its bioactivity, as in traditional polymerization and particle synthesis. The focus of my research was to create

enzymatically-degradable hydrogel microparticles, using Michael addition chemistry, to evaluate for use as an inhalable, disease-responsive delivery system for biologic drugs and nanoparticles.

In this dissertation, I utilize bioconjugation and Michael addition chemistries in the design and development of enzymatically-degradable hydrogels, which may be tailored to a multitude of disease applications. I then introduce a new method of hydrogel microparticle, or microgel, synthesis known as the Michael Addition During Emulsion (MADE) method. These microgel carriers were evaluated *in vitro*, and found to exhibit triggered release of encapsulated biologic drugs in response to enzyme, no significant cytotoxic effects, and the ability the avoid rapid clearance by macrophages. Lastly, *in vivo* studies in mice were conducted, and microgels were found to exhibit successful delivery to the deep lung, as well as prolonged pulmonary retention after intratracheal aerosol delivery. In conclusion, a new class of enzymatically-degradable microgels were successfully developed and characterized as a versatile and promising new system for pulmonary, disease-responsive delivery of biologic drugs.

Table of Contents

List of Tables

List of Figures

Chapter 1: Introduction, Specific Aims, and Overview

1.1 INTRODUCTION

In recent years, a series of highly sophisticated drugs, rationally designed to target various cellular pathways (e.g. signal transduction cascades, transcription factors, apoptosis etc.) have emerged [1-3]. They range from proteins and peptides designed to interfere with specific cell functions to DNA, siRNA, oligonucleotides, and aptamers that produce therapeutic proteins or block transcription/translation. Even though these drugs are very specific in their effect, most of them interfere with key cellular processes and therefore are highly cytotoxic. Moreover, the majority of these sophisticated drugs, especially those that target chronic and advanced diseases are primarily given via systemic administration and often through multiple, regular doses. Needless to say this severely interferes with the quality of life of these patients while leading to major systemic side effects. Rational design of targeted therapies that enhance patient compliance, improve quality of life while still being highly effective in treating the disease, is therefore essential [1-8].

It is well appreciated that delivery of therapeutic agents through the pulmonary route could provide significant improvement in patient compliance and reduce systemic toxicity [9-13] for a variety of diseases. This is particularly relevant for chronic pulmonary disorders like airway allergy, asthma, and pulmonary fibrosis, as well as for lung cancers. Traditional drugs for inhalation suffer from low respirable fractions and high emitted (exhaled) fractions, clearance by alveolar macrophages, and target non-specificity. Therefore, the design of effective pulmonary drug carriers must possess the following attributes: (i) optimal aerodynamic properties for respirable efficiency, (ii)

avoidance of alveolar macrophage clearance, (iii) site-specific delivery at diseased tissue to avoid local bystander and systemic side effects, and (iv) enhanced intra-cellular delivery of drugs.

These criteria pose several unique engineering and biomaterial challenges. The established range for optimal aerodynamic particle diameter to achieve efficient deep lung deposition following inhalation ranges between 1-5 μm [9]. However, avoidance of phagocytosis and clearance by alveloar macrophages requires particle sizes that are significantly larger (larger than 10μm). Even then, drugs that are targeted to intracellular pathways and molecules, e.g. siRNA, DNA or intracellularly targeted proteins or peptides, require nanoscale carriers, on the order of 50-300 nm which can undergo efficient endocytosis or macropinocytosis by epithelial cells. This is a complex design space where the carrier should be (a) 1-3 μm during inhalation (b) >10 μm following lung deposition and (c) 50-300 nm to deliver the drug intracellularly. Moreover, it is also beneficial to incorporate disease-triggered release of the drug following lung deposition, in order to minimize non-specific side effects on normal cells.

The body of research described in this treatise proposes an innovative solution to this problem through design and use of a nanoparticle-in-microparticle formulation, comprised of swellable, peptide-crosslinked microgel-carriers encapsulating therapeutic nanoparticles and/or free biologic drugs. Specifically, the focus of this work has been on the development of the platform hydrogel microparticle (microgel) carrier system that could be used for multiple applications. These inhalable microgel carriers were designed with the following criteria in mind:

- patient-friendly method of administration by achieving efficient aerodynamic delivery to airway epithelial cells with uniform lung distribution,

- prolonged residence time in the lungs by avoiding alveolar macrophage uptake, due to *in situ* swelling (large geometric size) and stealth properties,
- reduced side effects and toxicity by incorporating disease-triggered release of nanoparticles/drugs from microgels, specifically, degradation of the microcarriers by up regulated enzymes, only at the site of diseased tissue,
- mild and easily scalable manufacturing process, suitable for use with biologic drugs, a relatively new class of pharmaceuticals, and
- applicability to multiple disease indications, as well as the option to include enhanced intracellular drug delivery mechanisms using nanoparticles.

Through the design and realization of such a system, several engineering and biomaterials topics were studied and incorporated. The overarching themes with more detail on the specific innovations are summarized in the following sub-sections, along with a table provided on page 5 (Table 1.1). The step-by-step specific aims are then laid out in the next section.

1.1.1 Disease-triggered drug release

A potential approach for site-specific or disease-specific therapy is to take advantage of specific physiological and pathological cues, such as enzymes, which could trigger drug release from the carrier. Enzymatic cleavage is highly specific and could be tailored for certain up regulated enzymes in diseased tissues. Enzymatically-degradable hydrogels, which incorporate an enzyme-cleavable peptide into the network structure, have been extensively reported for tissue engineering applications [14-18], along with limited work in drug delivery applications [19-22]. These studies showed that rapid degradation of the hydrogels occur upon enzyme exposure, whereas minimal degradation

occurs without enzyme. Collectively, they demonstrate the possibility that similar peptide-based hydrogels could be used to control drug release from micro- and nanoparticle carriers. Previous students in the research advisor's group have worked on the fabrication of nanoparticles, using top-down nanoimprinting techniques, that are degraded in the presence of enzymes [23]. However, such enzymatically degradable microparticulate carriers for pulmonary delivery drugs are yet to be reported.

1.1.2 Enzyme-responsive microgels for improved pulmonary delivery

Hydrogel microparticles (microgels) in the dry state are collapsed in comparison to their swollen or relaxed state. When hydrated, for example, upon contact with physiological fluids or in high humidity airways, the particles should begin to swell, increasing in diameter and density. The combination of the initial dry powder state and "in-transit" density change could provide optimal aerodynamic properties for pulmonary delivery leading to increased particle deposition within the lungs [9,10,12]. A hydrogel microparticle carrier system has recently been reported for sustained drug release by biodegradation, however, particle morphology was non-uniform and more mild fabrication conditions would be necessary for biological drugs [10]. To our knowledge, specific disease-responsive microgels designed for efficient pulmonary delivery of nanoparticles and biologic drugs are yet to be reported.

1.1.3 Michael addition during emulsion (MADE) microgel synthesis method

In this body of work, a new method of synthesizing fairly uniform, spherical, enzyme-responsive microgels was developed. The method involves using a simple Michael addition-type reaction within a water-in-oil emulsion, using low homogenization

Table 1.1 Summary of engineered material and method innovations to address design criteria and challenges

Design Criteria/Challenge	Material and/or Method Innovation
Optimal aerodynamic properties for efficient, non-invasive, patient-compliant delivery by inhalation	Aerosolized dry microgels of appropriate aerodynamic diameter undergo in-transit swelling to increase both diameter and density, thus increasing particle impaction and minimizing exhaled fraction
Delivery of cellular-pathway-interfering siRNA to the site of diseased tissue only in non-homogeneous pulmonary diseases	Enzyme-triggered drug release mechanism from microgels in response to enzymes secreted extracellularly at site of diseased tissue 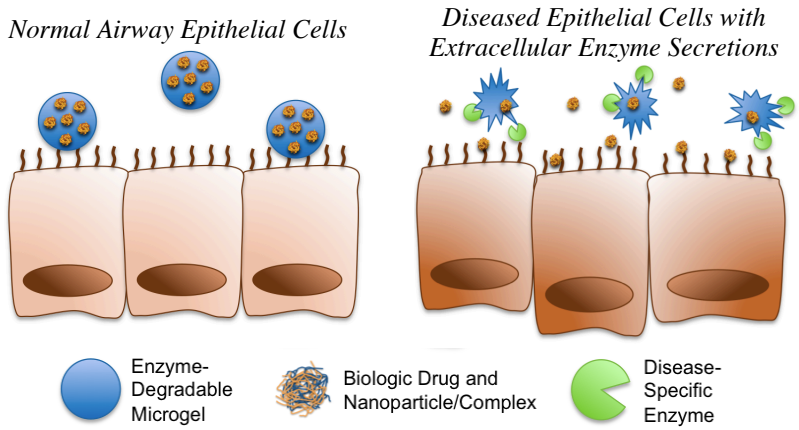
Avoid rapid clearance of drug-containing particles by alveolar macrophages	"Stealth" microgels that avoid uptake and clearance by alveolar macrophages – due to hydrophilicity, stealth, and swelling capacity of poly(ethylene glycol)
Eventual clearance of particles over the long term	Primarily, the mucociliary escalator will clear any un-triggered microgels after more than two days. Additionally, as microgels undergo hydrolysis over a 2-week time period, softening of the gel improves clearance with mucosal turnover. Microgels are designed with hydrolytic linkages as a "fail-safe" to prevent accumulation over the long term.
Encapsulation of biologic drugs, avoiding degradative conditions (such as UV light, high temperatures, and organic solvents)	Newly-developed method of Michael addition during emulsion at low shear homogenization and physiological conditions eliminates need for photo-initiators or UV cross-linking, used in traditional hydrogel cross-linking. Encapsulation is achieved by simply incorporating the therapeutic with the aqueous pre-cursor polymer solution prior to emulsion.
Applicable to multiple disease indications and ability to incorporate enhanced intracellular delivery mechanisms using nanoparticles	Peptide cross-linker may be easily interchanged to tailor the system for multiple disease indications. The ability to encapsulate nanoparticles allows for a second delivery stage to improve intracellular delivery and endosomal escape for intracellularly-targeted drugs, such as siRNA. 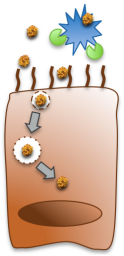

energy input and mild aqueous conditions under physiological pH and temperature. This method is shown to produce particles within the desired particle size distribution for optimal aerodynamic diameter for delivery to the airways by inhalation. Overall, these microgel particles exhibit enzyme-triggered degradation and drug release, a mild manufacturing process, as well as stealth and swelling for avoidance of macrophage clearance.

1.2 SPECIFIC AIMS

The specific aims of this exploratory and development research treatise are as follows.

1.2.1 Aim 1A: To rationally design and optimize Michael addition and bioconjugation chemistries to create enzyme-degradable hydrogels

In this aim, enzyme-degradable hydrogels will be created by cross-linking enzyme-degradable peptides with multi-armed poly(ethylene glycol) acrylates (PEG-acrylates) or multi-acrylated chitosan using a Michael addition-type reaction. This aim will include work in developing a library of optimal enzyme-specific peptide sequences for various disease applications, bioconjugation chemistry to add functional groups to the peptide, polymers, and polysaccharides to enable the Michael addition reaction, and optimizing the Michael addition reaction. I hypothesize that these hydrogels would exhibit triggered degradation and drug release in response to specific enzymes.

1.2.2 Aim 1B: To rationally design, develop, and optimize a method to produce enzyme-degradable hydrogel microparticles, using chemistries developed in Aim 1A, that are suitable for pulmonary delivery via inhalation

In this aim, the chemistries developed in Aim 1A will be incorporated into a method to produce hydrogel microparticles, or microgels, in a suitable size range for pulmonary delivery via inhalation. Work in this aim will include exploration of various particle manufacturing techniques, and determining feasibility for use with the chemistry developed and end goals. I hypothesize that these microgels will exhibit optimal aerodynamic properties for efficient pulmonary delivery, and retain the material properties, designed in Aim 1A, of exhibiting enzyme-triggered degradation. The final method will be easily scalable, use mild fabrication conditions, and be tailorable for multiple disease indications.

1.2.3 Aim 2: To perform *in vitro* characterization and evaluation of the microgels in terms of drug release and cellular interactions

In this aim, microgels developed in Aim 1 will be evaluated and characterized for their performance *in vitro*. This will include the study of drug and nanoparticle release from enzymatic degradation, hydrolytic degradation, and diffusion. The microgels will also be evaluated for cytotoxic effects on multiple cell lines, and the extent of phagocytic uptake by macrophages will be studied. I hypothesize that the microgels will exhibit rapidly triggered release of drug in response to enzyme, in stark contrast to drug release by diffusion and hydrolytic degradation. Furthermore, I hypothesize that the swelling capacity of the microgels, and in one formulation, the PEG composition, will contribute to the reduced uptake and clearance of the microgels by macrophages.

1.2.4 Aim 3: To evaluate the *in vivo* pulmonary distribution and clearance of microgels after delivery to murine lungs by an intratracheal aerosolizer

The objective of this aim is to evaluate the pulmonary distribution and clearance of the microgels in mouse lungs over a two-week time period. Microgels will be simultaneously aerosolized and delivered intratracheally to mice using a Penn-Century microsprayer device. The distribution will be evaluated using fluorescent IVIS imaging and fluorescent quantification from lung homogenates over a two-week time course. I hypothesize that the microgels will exhibit uniform distribution throughout the lungs following delivery, and show improved retention (as compared to non-swellable polymer particles) over the course of the study.

1.3 OVERVIEW

The following chapter, **Chapter 2**, will discuss background material in the field of Drug Delivery and its applications, especially for delivery of proteins and other biologic drugs. **Chapter 3** then focuses on the background and significance of the concept of Disease-Responsive Drug Delivery, providing greater context for this dissertation work within the greater field of Drug Delivery. **Chapter 4** describes the bioconjugation and Michael addition chemistry used to create enzymatically-degradable hydrogel networks from different biopolymers, including the design and incorporation of peptide sequences to create the disease-specific trigger. **Chapter 5** then details the numerous particle synthesis methods that were attempted before developing and optimizing the Michael Addition During Emulsion (MADE) method for synthesizing microgels. **Chapter 6** describes the *in vitro* characterization of the microgels in terms of material properties, drug release, and interactions with cell. **Chapter 7** then discusses the performance, distribution, and clearance patterns of microgels from the lungs after

simultaneous aerosolization and intratracheal delivery to mice, *in vivo*. Lastly, **Chapter 8** will discuss the implications of the research, as well as potential future studies and development.

1.4 REFERENCES

[1] Y. Darcan-Nicolaisen, H. Meinicke, G. Fels, O. Hegend, A. Haberland, A. Kühl, et al., Small interfering RNA against transcription factor STAT6 inhibits allergic airway inflammation and hyperreactivity in mice, J Immunol. 182 (2009) 7501–7508.

[2] S.P. Kasturi, K. Sachaphibulkij, K. Roy, Covalent conjugation of polyethyleneimine on biodegradable microparticles for delivery of plasmid DNA vaccines, Biomaterials. 26 (2005) 6375–6385.

[3] H. Katas, H.O. Alpar, Development and characterisation of chitosan nanoparticles for siRNA delivery, J Control Release. 115 (2006) 216–225.

[4] B. Ghosn, S.P. Kasturi, K. Roy, Enhancing polysaccharide-mediated delivery of nucleic acids through functionalization with secondary and tertiary amines, Current Topics in Medicinal Chemistry. 8 (2008) 331–340.

[5] X. Jiang, H. Dai, K.W. Leong, S.-H. Goh, H.-Q. Mao, Y.-Y. Yang, Chitosan-g-PEG/DNA complexes deliver gene to the rat liver via intrabiliary and intraportal infusions, J Gene Med. 8 (2006) 477–487.

[6] I. Kadiyala, Y. Loo, K. Roy, J. Rice, K.W. Leong, Transport of chitosan-DNA nanoparticles in human intestinal M-cell model versus normal intestinal enterocytes, Eur J Pharm Sci. 39 (2010) 103–109.

[7] M. Kumar, A.K. Behera, R.F. Lockey, J. Zhang, G. Bhullar, C.P. De La Cruz, et al., Intranasal gene transfer by chitosan-DNA nanospheres protects BALB/c mice against acute respiratory syncytial virus infection, Hum Gene Ther. 13 (2002) 1415–1425.

[8] X. Liu, K.A. Howard, M. Dong, M.Ø. Andersen, U.L. Rahbek, M.G. Johnsen, et al., The influence of polymeric properties on chitosan/siRNA nanoparticle formulation and gene silencing, Biomaterials. 28 (2007) 1280–1288.

[9] D.A. Edwards, C. Dunbar, Bioengineering of therapeutic aerosols, Annu Rev Biomed Eng. 4 (2002) 93–107.

[10] I.M. El-Sherbiny, S. McGill, H.D.C. Smyth, Swellable microparticles as carriers for sustained pulmonary drug delivery, J Pharm Sci. 99 (2010) 2343–2356.

[11] L. Garcia-Contreras, J. Fiegel, M.J. Telko, K. Elbert, A. Hawi, M. Thomas, et al., Inhaled large porous particles of capreomycin for treatment of tuberculosis in a guinea pig model, Antimicrob Agents Chemother. 51 (2007) 2830–2836.

[12] J.C. Sung, B.L. Pulliam, D.A. Edwards, Nanoparticles for drug delivery to the lungs, Trends Biotechnol. 25 (2007) 563–570.

[13] N. Tsapis, D. Bennett, B. Jackson, D.A. Weitz, D.A. Edwards, Trojan particles: large porous carriers of nanoparticles for drug delivery, Proc Natl Acad Sci U S A. 99 (2002) 12001–12005.

[14] M. Ehrbar, A. Metters, P. Zammaretti, J.A. Hubbell, A.H. Zisch, Endothelial cell proliferation and progenitor maturation by fibrin-bound VEGF variants with differential susceptibilities to local cellular activity, J Control Release. 101 (2005) 93–109.

[15] A.S. Gobin, J.L. West, Cell migration through defined, synthetic ECM analogs, Faseb J. 16 (2002) 751–753.

[16] M.P. Lutolf, F.E. Weber, H.G. Schmoekel, J.C. Schense, T. Kohler, R. Müller, et al., Repair of bone defects using synthetic mimetics of collagenous extracellular matrices, Nat Biotechnol. 21 (2003) 513–518.

[17] M. Lutolf, J.A. Hubbell, Synthesis and physicochemical characterization of end-linked poly(ethylene glycol)-co-peptide hydrogels formed by Michael-type addition, Biomacromolecules. 4 (2003) 713–722.

[18] B.K. Mann, A.S. Gobin, A.T. Tsai, R.H. Schmedlen, J.L. West, Smooth muscle cell growth in photopolymerized hydrogels with cell adhesive and proteolytically degradable domains: synthetic ECM analogs for tissue engineering, Biomaterials. 22 (2001) 3045–3051.

[19] J.R. Tauro, R.A. Gemeinhart, Extracellular protease activation of chemotherapeutics from hydrogel matrices: a new paradigm for local chemotherapy, Mol Pharm. 2 (2005) 435–438.

[20] J.R. Tauro, R.A. Gemeinhart, Matrix metalloprotease triggered delivery of cancer chemotherapeutics from hydrogel matrixes, Bioconjug Chem. 16 (2005) 1133–1139.

[21] J.R. Tauro, B.-S. Lee, S.S. Lateef, R.A. Gemeinhart, Matrix metalloprotease selective peptide substrates cleavage within hydrogel matrices for cancer chemotherapy activation, Peptides. 29 (2008) 1965–1973.

[22] D.G. Vartak, R.A. Gemeinhart, Matrix metalloproteases: underutilized targets for drug delivery, Journal of Drug Targeting. 15 (2007) 1–20.

[23] L.C. Glangchai, M. Caldorera-Moore, L. Shi, K. Roy, Nanoimprint lithography based fabrication of shape-specific, enzymatically-triggered smart nanoparticles, J Control Release. 125 (2008) 263–272.

Chapter 2: Drug Delivery Strategies for Eliciting Cellular Responses in Tissue Engineering and Drug Therapy

[This chapter has been adapted, with permission, from P. Wanakule & K. Roy† (2012). Chapter 17: Drug Delivery. In J. P. Fisher, et al, (Eds.), Tissue Engineering: Principles and Practices. CRC Press, Taylor & Francis Group.]*

2.1 INTRODUCTION

Drug delivery has proven to be an integral part in manipulating cellular responses in various diseases, and directing the development and differentiation of cells into functional tissues, specifically, the controlled delivery of pharmacologically active or bioactive agents, such as cytokines, growth factors, and morphogens. By controlling the delivery of these drugs at different time points and concentrations, a direct effect is exerted on the cell proliferation, differentiation, or migration, with the potential for controlling the phenotype and functionality of cells and tissues [1-8].

The goals of drug delivery are manifold, and include (1) the targeting of drug to specific cells or sites in the body, (2) overcoming tissue barriers associated with delivery routes, including the epithelial layers of the skin, lungs, and intestine, (3) overcoming cellular barriers which control cellular uptake, and (4) controlled release.

Controlled release concepts encompass the ability to control release of bioactive molecules at target sites, the effective concentration of drug in the body, as well as its

† Statement of co-author contribution: This chapter was written by Prinda Wanakule, with editorial and content assistance by Krishnendu Roy (research supervisor).

duration of activity [9]. The use of controlled drug delivery, more so than the other goals of drug delivery, has come into greater use in recent years [1,3,8]. While it is possible to directly infuse drugs directly into culture flasks and plates (*in vitro*) or by injection (*in vivo*), this may be undesirable for several reasons. For example, many proteins and peptides have short half-lives in serum or media due to inactivation by proteases and enzymes, and thus, need continual replenishment to maintain a certain minimum effective concentration (see Figure 2.1). Additionally, unconstrained repeated doses may result in toxic effects. The controlled temporal and spatial release of these drugs may then reduce the amount of expensive drug and chemical signals required, as well as the potential toxic effects [1-3,6,8-10]. This temporal and spatial control has also given rise to new possibilities and advances in tissue engineering, for example, the use of three-dimensional scaffolds to spatially differentiate cells into various "zones" consisting of different cell types [1-8,11].

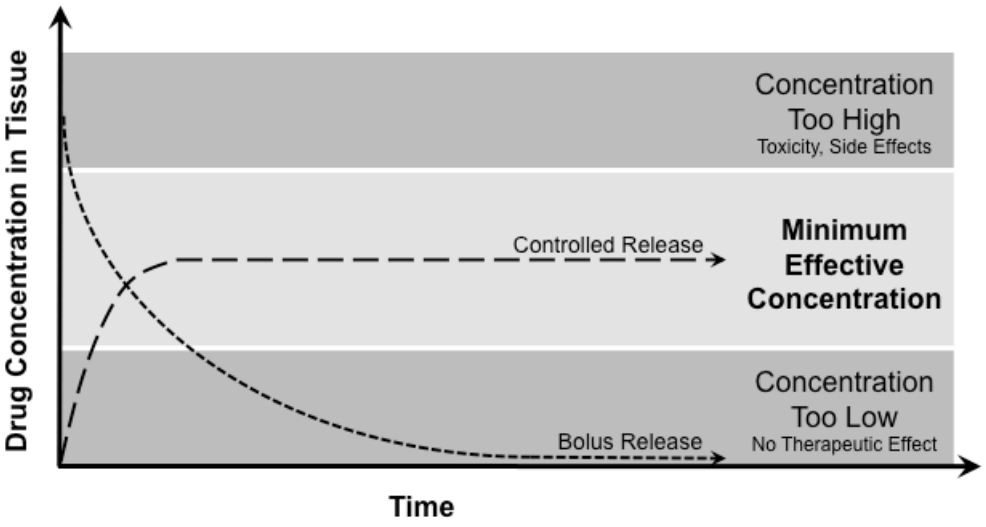

Figure 2.1 In classical drug delivery, controlled release systems aim to achieve a constant minimum effective concentration of bioactive drug.

This section will encompass the basics of drug delivery, an overview of controlled drug delivery technologies, as well as their applicability to and significance in eliciting cellular responses for tissue engineering and drug therapies. We first begin by providing a brief review on the modes of drug delivery, or drug release, from drug delivery systems. Next, we move on to discuss some biological drugs of interest in cell therapy applications, as well as their properties that affect the design of the delivery system. We then explore the methods used to control the release of drugs, with special emphasis on the release of drugs from scaffolds, matrices, and particulates.

2.2 MECHANISMS OF DRUG DELIVERY

There are myriad mechanisms from which we may choose to drive the release of drugs in a controlled manner. We can classify the drug delivery mechanisms of special interest in cellular therapies into three main categories: diffusion from non-degradable systems, bioerodible systems, and stimuli-responsive systems.

2.2.1 Diffusion from Non-Degradable Systems

Diffusion is one of the most kinetically well-defined concepts of transport phenomena, and is especially applicable in the diffusion of drug molecules from some of the early non-degradable drug delivery systems [9,12,13]. Thermodynamically driven, it is the result of the random walk of submicron particles, called Brownian motion. Although movement may seem random at the microscopic level, at the macroscopic level, movement of particles along a concentration gradient is observed. Fick's second law of diffusion describes the temporal and spatial net movement of particles by diffusion:

$$\frac{\partial C(x,y,z,t)}{\partial t} = \frac{\partial^2 C}{\partial x^2} + \frac{\partial^2 C}{\partial y^2} + \frac{\partial^2 C}{\partial z^2}$$

Numerous solutions for this equation have been derived in order to describe the diffusion of drug molecules from several types of drug delivery devices under several conditions; for details, we refer the reader to an excellent text by Truskey, et al. [1,3,8,12]. However, the two main diffusive conditions of special interest in drug delivery for tissue engineering are the diffusion of drug from a polymer matrix and the diffusion of drug from a reservoir through a membrane (see Figure 2.2), both of which are predictably well-defined. The solutions to the problem are highly dependent on the initial drug concentration and the geometry of the device, and as such, the diffusion of drug out of the system may be changed by altering the device geometry, and prolonged by increasing the initial concentration [1-3,6,8-10,12,13].

Along the same lines, however, the disadvantage of this system lies in its dependence on drug concentration to define the flux of drug out of the system. As the drug concentration decreases over time and there is less of a concentration gradient, the release rate also decreases over time. This is especially pronounced in the diffusion of drug from a polymer matrix. However, by using a highly saturated drug reservoir with diffusion of drug driven through a membrane, a constant release of drug may be achieved over an extended period of time – longer than may be typically achieved through use of a matrix alone[9,12,13].

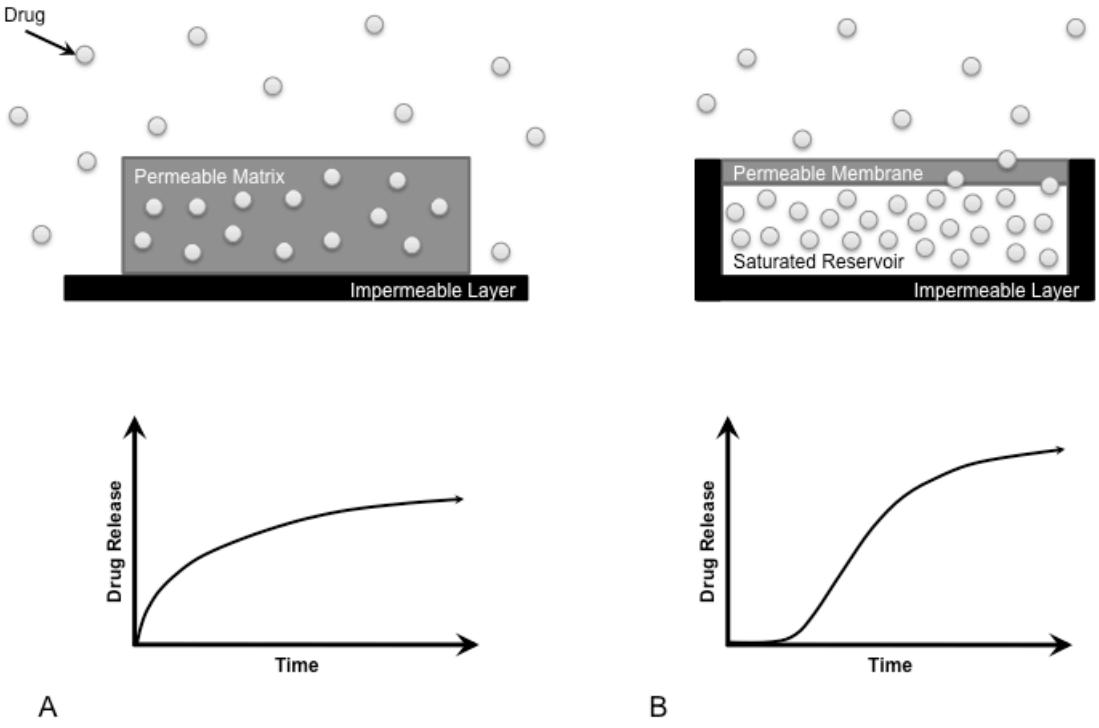

Figure 2.2 (A) Diffusion-driven release of drug from a matrix. (B) Diffusion-driven release of drug from a saturated reservoir through a membrane.

2.2.1.2 Diffusion from Swellable Polymers

Diffusion of drugs may also be controlled by the use of swellable polymers, including swellable cross-linked hydrogels. In this case, there is an increase in polymer chain mobility due to the uptake of a solvent, such as water, that decreases the glass transition of the polymer (T_g). Drugs that are entrapped and immobilized by the non-swollen polymer matrix may then begin to diffuse out due to the increased flexibility, resulting in a heightened release rate. In order to achieve this, the pore size of the polymer matrix must be sufficiently small so as to restrict a drug of known hydrodynamic radius. Upon swelling, the pore size increases, thus allowing movement and diffusion of

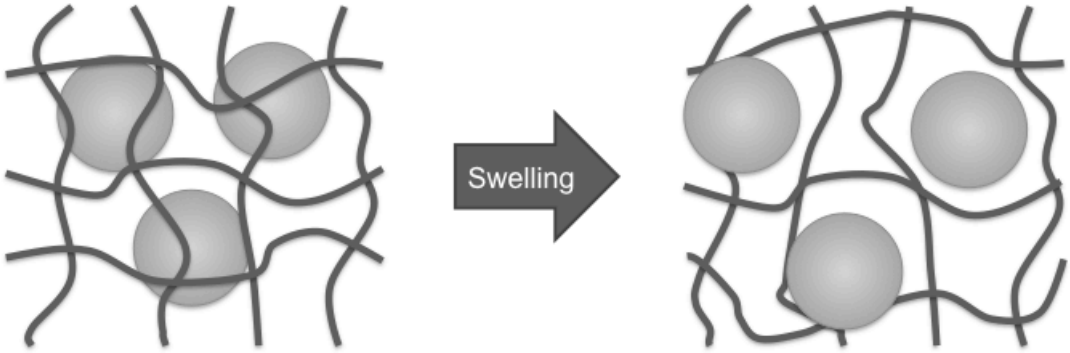

Figure 2.3 Diffusion of drug from a swellable polymer matrix. In the pre-swollen state, drug molecules are entrapped within the network structure. Swelling of the polymer network results in increased polymer chain mobility or pore size, allowing diffusion of the drug out of the network.

the drug out from the matrix (see Figure 2.3) [9,13,14]. The diffusion of drugs from swellable polymer matrices has been well studied for macroporous (pore size between 0.1-1.0μm), microporous (100-1000Å), and nonporous (10-100Å) hydrogels by several groups, and tunable drug release profiles from swellable polymers have been achieved [9,15].

2.2.2 Bioerosion

By definition, bioerosion refers to the erosion of a polymer into water-soluble products under physiological conditions, including both physical and chemical processes (according to the European Society for Biomaterials Consensus Conference in 1986) [16]. As a side note, biodegradation refers to the degradation by biological molecules, such as enzymes, which will be covered in the following section on stimuli-responsive

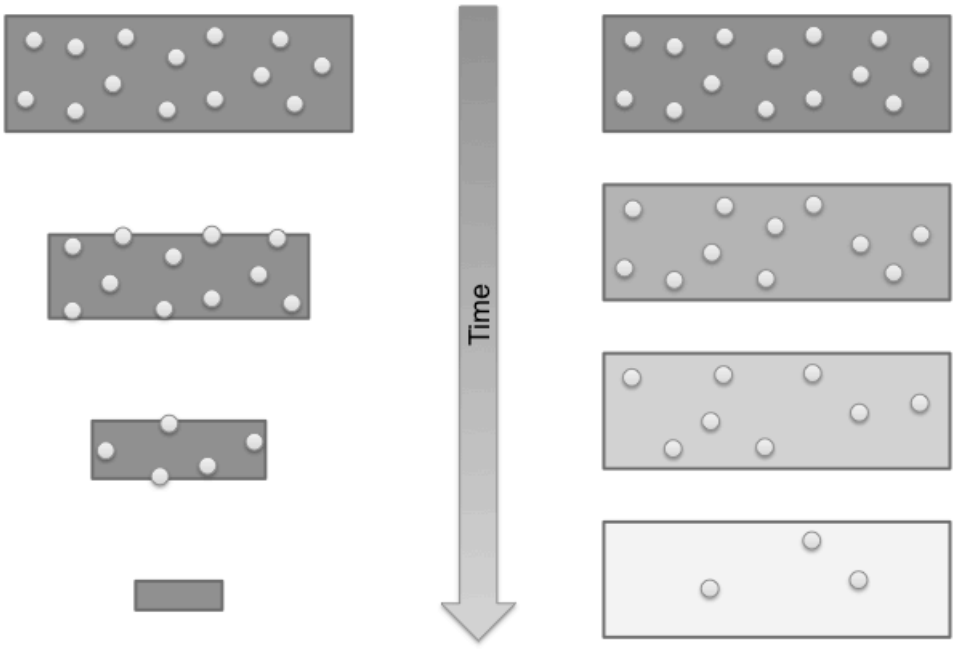

Figure 2.4 Surface erosion (left) and bulk erosion (right) of polymeric devices, resulting in differing release kinetics.

systems. The most common mechanism of bioerosion is by hydrolysis of a polymer backbone by neutral water, however, accelerated hydrolysis may occur in the presence of ion catalysts and acidic pH. Erosion may proceed by either surface erosion or bulk erosion (see Figure 4). In surface erosion, the rate at which water is able to penetrate the device is slower than the erosion rate. On the other hand, bulk erosion occurs when the rate of water penetration into the device is greater than the rate of erosion [17-19].

Bioerodible drug delivery systems have been designed to both provide a mechanism of controlled drug release, as well as to eliminate the need for device extraction after the lifetime of the system. As the device erodes, drug that has been solubilized or suspended within the device are slowly released. In general, surface eroding systems (heterogeneous) have a release rate proportional to the surface erosion

rate, are driven primarily driven by erosion rather than diffusion, and can be varied according to device geometry. Bulk eroding systems (homogeneous) are driven by a combination of erosion and diffusion kinetics, with first order kinetics for the rate of erosion, as well as the permeability of the device. Several parameters affect the rate of hydrolysis, and thus, release rate, including lability of the polymer backbone, hydrophobicity or hydrophilicity of the polymer, morphology, and molecular weight [17-21].

2.2.3 Stimuli-Responsive Systems

In recent decades, a greater interest in the stimuli-responsive subfield in controlled drug delivery has been developing as a means to deliver drug only when or where it is needed. These stimuli-responsive types of systems often rely on physicochemical changes due to disease pathology or the cell microenvironment. Common stimuli include pH, temperature, ions, enzymes, light, and biomolecules, all of which have been designed it elicit a response in drug carriers to trigger drug release [3,10,22-26].

2.2.3.1 pH-Responsive Systems

Several hydrogel-based drug delivery systems with the ability to swell or shrink in response to pH changes have been developed as triggered-release delivery systems. The pH triggered swelling and shrinking mechanisms are primarily due to the properties of the side chain pendant group, which are cationic or anionic [10,27,28]. Anionic hydrogels are ionized at pHs above their pKa, and thus exhibit high swelling at these higher pHs

due to repulsion of the ionized groups [28]. In contrast, cationic hydrogels are ionized at pHs below their pKa, exhibiting high swelling below their pKa [27].

Changes in pH exist throughout the body at the organ, tissue, and cellular level, and even due to various disease states. For example, pH triggered drug delivery systems have been developed that are capable of triggering drug release when moving from the acidic gastric cavity to the more neutral small intestine [29,30], where much drug absorption occurs, as well as from the neutral extracellular environment to the slightly more acidic early endosome (intracellular) [31,32]. Thus, pH-responsive systems offer a versatile way in which to trigger drug release in response to environmental cues.

2.2.3.2 Enzyme-Responsive Systems

A relatively new strategy in drug delivery is to incorporate enzyme sensitive components into the drug carriers, which are primarily hydrogel-based. Enzyme-degradable hydrogels have been shown to exhibit minimal release without the presence of enzyme, and triggered release in the presence of enzyme [10,26,33-36]. This strategy has been used extensively in tissue engineering applications [37,38], however, it also provides an effective means of physiologically controlled release of drugs [36,39]. Enzyme-responsive systems are suitable for site-specific delivery because enzymatic cleavage is highly specific, and many enzymes are upregulated in several diseases, such various cancers and inflammatory diseases [10,22,25,36,39,40]. In most cases, enzyme-cleavable proteins, peptides, or extracellular matrix (ECM) components are incorporated into the hydrogel cross-links [26,33,34,38]. In another set-up, enzyme-degradable components are used as covalent linkers to conjugate drugs as pendant groups off the

polymer backbone [10,41]. Upon encountering the enzyme, the cross-links are broken, releasing any encapsulated drug.

2.2.4 Overall Release Profiles

Oftentimes, the overall drug release mechanism may be due to a combination of the aforementioned modes. For example, diffusion plays a role in each of these mechanisms in that the drug must diffuse out of eroding scaffolds, or swollen matrices. Stimuli-responsive carriers may also release drug by stimuli-induced erosion or swelling. In choosing a release mechanism, the temporal requirements of drug in the system, as well as drug pharmacokinetics, must be considered.

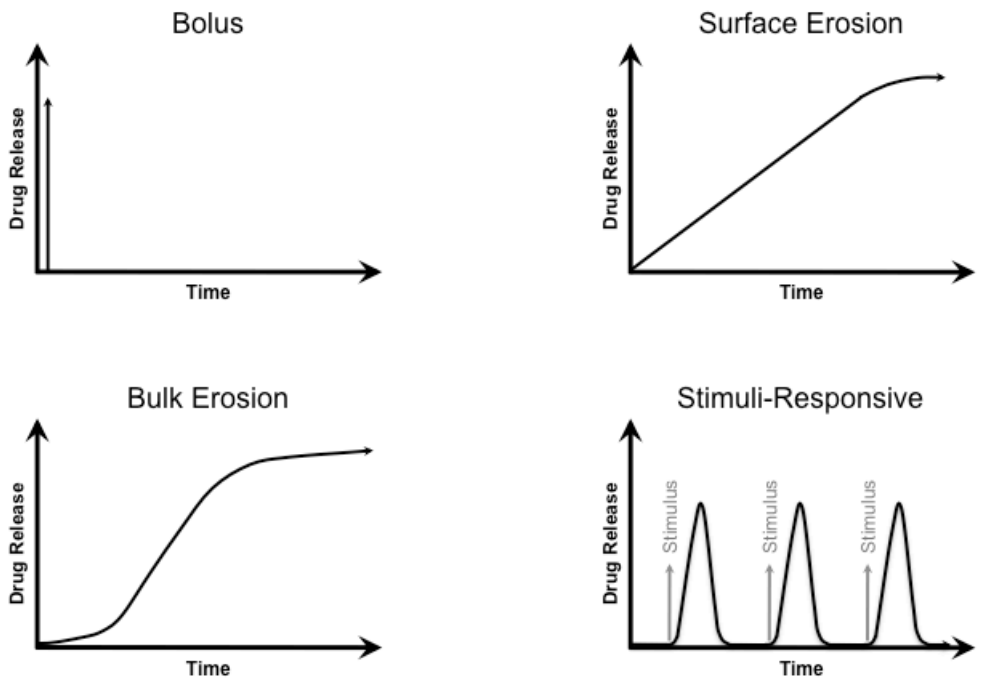

Figure 2.5 Release profiles of various delivery mechanisms. See Figure 2.2 for diffusion-driven release profiles.

There are several release profiles that may be achieved by the delivery systems described here (see Figure 2.5). Several classical drug delivery systems were designed with the aim of achieving a zero order, or linear, release rate, which results in a constant level of drug in the tissues. However, newer drug delivery systems are designed to release drug when and where it is needed, thereby reducing side effects [1,9,12,13]. Since spatial and temporal control over drug release is often required to guide the differentiation of cells into their appropriate niches, highly ordered systems with a combination of mechanisms may be required.

2.3 Biological Drugs of Interest in Cellular and Drug Therapies

The primary drugs of interest for eliciting cellular responses and next generation drug therapies include biologic drugs, or biologics. These include nucleotides, proteins, and peptides, such as siRNA, DNA, cytokines, growth factors, and adhesion factors. Growth factors are cell signaling proteins or hormones that have an effect on cell differentiation, proliferation, and maturation through a process of ligand-receptor binding. Some examples of growth factors include bone morphogenetic proteins, vascular endothelial growth factors, and some cytokines. Adhesion factors are proteins and peptides that are typically bound to the extracellular matrix and relay mechanical stress feedback to the cell. Adhesion factors include vitronectin and fibronectin, as well as the fibronectin-derived peptide sequence, RGD. Some common biologics used in cell-based therapies, as well as the intended function or purpose, are summarized in Table 2.1 [7,9,13,38,42].

2.3.1 Drug Properties and Design Considerations

Given that the majority of growth factors and adhesion factors are composed of bioactive proteins, or derivatives thereof, there are many considerations that must be made in order to design suitable systems for the delivery of these proteins in active forms. The most prominent consideration is the need to deliver the proteins in their native forms, that is, with their tertiary structure intact. Several methods of drug incorporation into delivery systems may cause proteins to denature from processing and encapsulation conditions, such as the application of heat, high shear forces, pH changes, UV, and exposure to organic solvents. Also considering that the majority of these proteins are hydrophilic, the choice of delivery materials is important in that exposure to hydrophobic materials may cause protein denaturation [43-45]. Lastly, the conditions that lead to drug release must also be evaluated to verify that they do not damage the protein. For example, in the case of hydrolytically degradable polyester drug carriers, a slightly acidic microenvironment is often created, which could affect protein activity [46]. The final conformation of the protein must be such that its bioactivity is not affected, and there are no forms present that may elicit ill effects or immunogenicity [9].

Along the same lines, the biological environment that the protein drugs are exposed to, whether *in vitro* or *in vivo*, may affect the protein conformation and activity. Several components in serum, including enzymes and peptidases, cause protein degradation often within minutes, decreasing the half-life dramatically. Glomerular, or renal, filtration also plays a key role in decreasing the half-life of proteins. For example, *in vivo*, the half-lives of PDGF, bFGF, and VEGF are approximately 2, 3 and 50 minutes respectively. A common strategy to improve the circulating half-lives of these proteins is to encapsulate them within polymers, however, care must be taken to ensure that the encapsulating material does not cause protein agglomeration or activate clotting factors

Table 2.1 Common biologic drugs used in cell-based therapies

Abbreviation	Bioactive Agent	Application
BMP	Bone morphogenetic protein	Osteogenesis
PTH	Human parathyroid hormone	Osteogeneisis
TGF-β	Transforming growth factor beta	Differentiation, anti-proliferation
HGF	Hepatocyte growth factor	Proliferation
G-CSF	Granulocyte colony-stimulating factor	Proliferation
GM-CSF	Granulocyte-macrophage colony-stimulating factor	Proliferation
VEGF	Vascular endothelial growth factor	Angiogenesis
FGF	Fibroblast growth factor	Angiogenesis
EPO	Erythropoietin	Angiogenesis
OPG	Osteoprotegerin	Angiogenesis
Ang1	Angiopoietin-1	Angiogenesis, vessel maturation
PDGF	Platelet-derived growth factor	Angiogenesis, vessel maturation
NGF	Nerve growth factor	Nerve regeneration
GDNF	Glial-derived neurotrophic factor	Nerve regeneration
	Fibronectin	Adhesion, cell substrate
	Vitronectin	Adhesion, cell substrate
	Fibrinogen	Adhesion, cell substrate
	Laminin	Adhesion, cell substrate
RGD	Arginine-Glycine-Asparagine	Adhesion
S1P	Sphingosine 1-phosphate	Chemoattractant
MIP3α	Macrophage inflammatory protein 3 alpha	Chemoattractant

[43-45]. Another common strategy is the conjugation of poly(ethylene glycol), or PEG, referred to as PEGylation [47-50]. PEGylation of proteins has been shown to increase circulation time *in vivo* and decrease the rate of protein degradation by enzymes [51,52].

Aside from classical cell culture flasks and dishes, there has recently been an increased usage of ECM-mimicking gel matrices to serve both as a cell scaffold and a controlled drug delivery device [33,53]. These bio-inspired matrices may be either a hybrid of synthetic and biomaterial or biomaterial alone, offer improved compatibility

and stability with proteins, and have been designed to mimic the ways in which growth factors are released in the body [53-56]. In the body, growth factors are either stored within the extracellular matrix or secreted by cells for short-term signaling. The ECM serves as a responsive delivery system for these growth factors, which may be controlled dynamically by cell movement and secretion of enzymes that degrade the matrix [9,33]. Adhesion factors in the ECM also relay mechanical feedback to the cells, and help the cells migrate as controlled by cellular signals [23,57,58]. These ECM-mimicking systems offer several advantages over classical systems, as we will discuss in the following section.

2.4 Drug Delivery at the Cellular Level

Given the complex temporal and spatial control of drug delivery required at the local cellular level, several strategies have been developed to meet the needs of this growing field. The strategies may be roughly classified into four major categories:

- Classical drug delivery systems for use in cell culture or *in vivo* at local sites
- Drug delivery from tissue engineering scaffolds and matrices
- Cells (genetically altered or otherwise) to produce drugs in the system
- Biomimetic systems with conjugated drugs.

The primary focus of this chapter will be to discuss in greater detail the first two strategies, the use of classical drug delivery systems, and especially the delivery of drugs from the cell scaffolds and matrices. The third strategy is beyond the scope of this work, and will not be discussed. The final strategy will be covered in the following chapter on disease-responsive drug delivery.

2.4.1 Classical Drug Delivery Systems

Several classical drug delivery systems for tissue engineering are still in use for a wide variety of applications. The majority of these systems are employed to provide a means of long term, controlled release of drugs into the local environment, whether *in vitro* or *in vivo*. The required release profile may be chosen based on several factors, including the rate of drug clearance from the system, pharmacokinetics, and stability. Thereafter, a system will be designed or chosen based on these requirements, considering parameters such as material properties, degradation rate, and device geometry. Generally, the major types of classical systems used include monolithic or slab-type systems, particulate systems, and gel-like systems.

2.4.1.1 Monolithic Systems

Monolithic polymer systems have a long history in drug delivery in that they were the first types of systems to be used for the controlled release of bioactive proteins and peptides. Among the first systems reported for controlled release was the polymeric membrane system composed of poly(ethylene-co-vinyl acetate) or EVAc, as described by Folkman and Langer in 1976 [59]. Although these systems were not biodegradable, the excellent controlled release profiles set the stage for an entirely new strategy of controlled release. In the following decade, several new biodegradable or bioerodible materials were developed with the aim of achieving sustained release *in vivo* without the need for removal after transplantation. Some of the materials included polyanhydrides [21], poly(ortho esters) [20], and poly(α-hydroxyesters) [60], with several more described in the literature. However, with the advent of these erodible systems came new unforeseen challenges due to the new intricacies of the system, including pH changes and side reactions with encapsulated drug due to the degraded products [46,61,62].

These early delivery systems were made in the form of monolithic devices because of their ease of manufacture by solvent casting, extrusion, and injection molding. These bulk devices were also able to carry a large payload of drug, and could be tailored for different release rates by changing material composition, drug loading, or including dispersants. As discussed in the previous section on the mechanisms of drug release, release from non-degradable systems is controlled primarily by diffusion. Erosion controlled release provided more control over the release rate, which could be changed by the degradation rate, or by choosing between surface or bulk erosion. Monolithic devices based on the poly(lactic-co-glycolic acid) copolymer, PLGA, were and still are commonly used in the erodible systems because erosion may be well-controlled by changing crystallinity, copolymer composition, and molecular weight [46,62-66]. Other monolithic devices have been based on cross-linked hydrogels, and will be discussed in more detail in following sections.

2.4.1.2 Particulate Systems

Following the progress made in monolithic and erodible devices, microparticulate systems began to surface in the field. Whereas monolithic systems required surgical implantation *in vivo* and are associated with a strong drug gradient, particulate systems offered the possibility of an injectable system and more even distribution in the tissue *in vivo*, or in cell culture. Microparticles also provided the flexibility for cell microencapsulation, or combinatorial delivery from microparticle distribution within monolithic systems or gels [12,13,67]. Aside from microparticles, nanoparticles, liposomes, and other similar particulate technologies have also been explored; however,

microparticles have been most widely applied to tissue engineering, and are the focus of this dissertation.

Microparticulate systems have been widely used for the delivery of growth factors for directing cell differentiation and proliferation. One application that has been extensively studied is the use of both EVAc and PLGA microparticles to deliver nerve growth factor (NGF) for supporting cellular therapy in neurodegenerative diseases [68]. PLGA microparticles are also still in use for delivery of several other proteins, including BMP-2 [69] and interferon-α [65]. Poly(phosphoester) microspheres with encapsulated NGF loaded within silicone nerve conduits showed greater peripheral nerve regeneration as compared to conduits with free NGF loaded [70]. Pfister et al [71] has reviewed other similar systems of NGF loaded microspheres for nerve regeneration. Excellent reviews may be found in the contemporary literature on the important considerations with protein encapsulation within polymer systems [62,64].

Hydrogel microparticles have also been used extensively to encapsulate proteins for drug delivery in tissue engineering. Some of the earliest hydrogel microparticle, or microgel, systems were the alginate beads, easily formed by dropping or spraying into cationic solutions, such as calcium [54,72]. Alginate microbeads are still widely used for delivery of FGF and osteogenic proteins [73-75], as well as for microencapsulation of chondrocytes for co-culture with bone marrow stem cells for osteogenic differentiation [76]. Along with alginate, microgels based on collagen [77], gelatin [78], and hyaluronan and its derivatives [79] are all used to deliver a variety of proteins.

Aside from encapsulation of proteins, much work has been done on the surface functionalization of microparticles for cellular interaction and proliferative effects. Surface modification of PLGA microspheres with an amine-terminated dendrimer improved long-term proliferation of chondrocytes without observed changes in the cell

phenotype, as compared to monolayer culture systems [66]. Additionally, surface functionalization of polystyrene magnetic microbeads with the DLL4 notch ligand used in co-culture has been shown to efficiently generate T cells from mouse bone marrow hematopoietic stem cells [80].

2.4.1.3 Gel-Based and Gel-Like Systems

Several gel-based and gel-like systems also offer the advantage of being injectable *in vivo*, taking on the shape of the tissue cavity. Additionally, the hydrophilic matrix structures of gels offer the advantage of high compatibility with the majority of proteins and peptides of interest in tissue engineering. Gelation occurs by several methods including thermally- or pH-induced cross-linking [38,81], sol-gel transitions, and physical gelation. Early injectable gel-like systems include those composed of alginate, gelatin, and collagen [54-56]. Although gel systems for protein delivery are a classical form of drug delivery, they have in recent decades gained much significance as a combinatorial tissue engineering substrate and drug delivery medium. As such, much attention will be directed towards these systems in the following section.

2.4.2 Drug Delivery from Scaffolds and Matrices

As the previous section focused on controlled delivery strategies separate from a cellular substrate, herein referred to as the substrate, much work has been done in using the substrate itself as a controlled release medium. The use of both scaffolds and matrices have been used to achieve desirable release strategies, where scaffolds refer to macro- or microporous substrates to provide structural support, and matrices refer to more or less continuous nanoporous substrates, such as gels. Several strategies may be used to achieve

the desired effect, including the admixing of drugs within matrices, entrapment of drugs within matrices, covalent binding of drugs to the matrix, affinity binding of drugs to the matrix, and microparticles embedded in matrices for delivery of drug.

2.4.2.1 Drugs Admixed with Cell Substrate

A common form of drug delivery from the cell substrate is by simply admixing the drug with the cell substrate. As previously discussed, various mechanisms may be used to control the release, with the desired effect usually being prolongation of the release. In the case of prolongation, even a small degree of affinity between the substrate materials may serve to slow the release rate. Additionally, poorly soluble drugs may dissolve over time and provide a sustained release profile. The cell substrate may also serve as a diffusion-limiting factor, providing drug release in a localized area of the scaffold, also known as zonal release.

Several examples of drugs admixed within a cell substrate have already resulted in commercial products, especially the release of bone morphogenetic proteins from collagen sponges and matrices [82]. Aside from the collagen sponge, other substrates for BMP delivery have included calcium phosphate cement, both of which have shown excellent orthopedic tissue regeneration *in vivo* [82-85]. Gelatin, a form of denatured collagen, has also been used in both its native self-assembled gel form and as a cross-linked gel to deliver growth factors. During fabrication, gelatin may be modified into either negatively or positively charged gels at physiological pH in order to create low-affinity electrostatic interactions with a protein drug [56,86,87]. These low affinity electrostatic interactions of proteins with gelatin have been shown to prolong release rates as compared to non-electrostatic gelatin [86,88-90].

2.4.2.2 Drugs Entrapped within Cell Substrate

It is also possible to engineer hydrogel cell carriers with structures capable of physically trapping drug molecules within the cell carrier's molecular structure, most commonly, with hydrogels. Hydrogels form somewhat of a 3-dimensional network structure, where the molecular weight and structure of the cross-linking molecule determines the pore size. If the pore size of the hydrogel is sufficiently close to the size of the drug of interest, then the release of the drug from the matrix could then be inhibited by the network structure [14]. In this case, drug release would be driven either by polymer swelling or degradation of cross-links. Commonly, the drug is loaded with the polymer precursor solutions, and the hydrogel network is then reacted to form around the drug [23,91,92].

Common materials used for these systems include PEG, fibrin, collagen, and hyaluronic acid [23,53,91,93,94]. A study by van de Wettering et al. illustrated the ability to tune the release of human growth hormone (hGH) from various PEG-based hydrogels using different cross-linked network architectures. Tighter cross-linked networks were able to significantly prolong the release of hGH over loosely-formed networks [95]. In addition to single-component hydrogel networks, hybrid hydrogels of interpenetrated networks or semi-interpenetrated networks are similarly able to form diverse network structures of varying pore sizes and cross-linking densities [93].

Due to the tight nanoporous properties of these hydrogels, which may prevent cell inter-growth, these systems are often employed as particulate systems within a scaffold. Scott et al. created PEG-based scaffolds using a modular assembly system of hydrogel microspheres with encapsulated sphingosine 1-phosphate (S1P), microspheres for

structural support, and porogen particles. The resulting macro-porous scaffolds with incorporated S1P-loaded microspheres showed an approximate two-fold increase in rate of cell migration into the scaffold as compared to scaffolds without S1P-loaded microspheres [96]. Alternatively, cell ingrowth into such nanoporous hydrogels may be achieved by incorporating enzyme-cleavable moieties into the network structure, thus allowing a cell to easily infiltrate the hydrogel by secreting ECM-degrading enzymes. Examples of these ingrowth matrices with entrapped drug include fibrin-based matrices for controlled release of NGF [94] and PEG-based matrices with matrix metalloproteinase substrates as cross-linkers with entrapped rhBMP [53].

2.4.2.3 Covalent Binding of Drugs to Cell Substrate

It is oftentimes advantageous, if not required, to covalently bind drugs to the cell substrate itself. For example, adhesion peptides must be bound to the substrate in order to elicit the correct response in the cell for migration. Although adhesion sites are already present in naturally derived materials, such as collagen and fibrin, cell substrates composed of synthetic components (such as PEG) must include adhesion peptides to effectively promote cell adhesion and signaling. Scaffolds of naturally derived materials may also benefit from adhesion peptide or growth factor incorporation to provide a higher degree of control over cell migration and differentiation.

In a study by Hern and Hubbell, the cell adhesion peptide RGD (Arg-Gly-Asp) was covalently bound to PEG-based hydrogels either directly, or using a PEG spacer arm, and compared to a non-adhesive control peptide [97]. Due to the greater steric availability of the adhesion peptide bound to the PEG spacer arm, specific mediation of cell spreading was observed in contrast to non-specific cell spreading observed in direct

conjugation of the peptide to the scaffold. Wacker, et al. compared S1P-induced endothelial cell migration in PEG hydrogels with either linear or cyclic RGD peptide sequences for implications in implant endothelialization speed following implantation [57]. Although linear RGD produced greater adhesion strength and long-term adhesion on exposure to shear stress from fluid flow, cyclic RGD produced a faster rate of endothelial cell migration. These studies illustrate the complexity in the incorporation of adhesion peptides into scaffolds, from determining the optimal conformation for steric availability, and finding the balance between high adhesion strength and higher migration rates for tissue regeneration.

In addition to covalent binding of adhesion peptides into cell substrates, drugs may also be covalently bound to the substrates in order to achieve directed differentiation, interaction, or promote migration of a specific cell phenotype. For example, vascularization of regenerated tissues is necessary for nutrient delivery *in vivo*, and requires high order cell and tissue arrangement controlled by growth factors. Leslie-Barbick et al. were able to achieve endothelial cell tubulogenesis in 2D and 3D PEG-based scaffolds by covalently attaching VEGF and an RGD adhesion peptide, in comparison to RGD-immobilized scaffolds alone [98]. Similarly, a study by Chiu and Radisic showed enhanced vascularization of endothelial cells in collagen scaffolds with immobilized VEGF and Angiopoietin-1 over collagen scaffolds alone and soluble factor in collagen scaffolds alone [99].

Furthermore, some drugs require binding to the substrate such that they are released only in response to cell-ingrowth, for example by enzymatic cleavage, providing on-demand delivery of the drug. In the case of bone regeneration, high concentrations of drug may result in overactivation of cells locally, and thus, abnormal tissue regeneration. By incorporating an enzyme-cleavable prodrug of a parathyroid hormone fragment into a

cell-ingrowth matrix, Arrighi et al. were able to circumvent osteoclast overactivation and show dose-dependent bone healing *in vivo* [100].

2.4.2.4 Affinity Binding of Drugs to Cell Substrate

Another strategy for binding drugs to a cell substrate involves the use of affinity binding molecules that have strong interactions with several growth factors and other proteins. A comprehensive review of the myriad molecules is outside the scope of this chapter, and we refer the reader to excellent reviews in the literature [8,101]. Instead, we will focus on two groups of common affinity binding molecules: heparin/heparan sulfate and fibrin/fibrinogen. Other molecules of interest include laminins, collagens, glycosaminoglycans, DNA, poly(amino acids), avidin-biotin [102-104], and other polysaccharides.

Heparan sulfate and heparin are glycosaminoglycans (GAGs) that are present in a variety of tissues throughout the body, regulate many processes, and bind a variety of proteins or growth factors. There are several growth factors that bind to both heparan sulfate and heparin, and are known as heparin binding growth factors (HBGFs). Commonly noted HBGFs include members of the families of FGF, HGF, and VEGFs. Heparan sulfate has been used in micropatterned PEG-based scaffolds for spatiotemporal release of growth factors and multilineage differentiation [105], and widely in other applications [106-108]. However, due to lower costs, heparin is more widely used in cell substrates for HBGFs, and has been incorporated into gels for osteogenic differentiation [109,110], endothelialization [111,112], nerve regeneration [113,114], and a variety of other applications [8,115-117].

Fibrin and fibrinogen are proteins found in the blood that are critical in the clotting and wound sealing process; cleavage of fibrinogen by thrombin yields fibrin [8,118,119]. Fibrinogen is used primarily in fibrin glue systems, where a mixture of fibrinogen solution and calcium-rich thrombin solution are co-delivered for surgical use as a sealant or hemostatic agent [118,119], but has recently gained more interest as a cell substrate with protein immobilization capabilities [118]. Fibrin is widely used for its affinity binding characteristics with other proteins to slowly release growth factors, particularly VEGF and FGF, to loaded cells within the gel [120,121]. Work by the Swartz group used VEGF bound to fibrin-based matrices along with interstitial fluid flow in order to direct blood and lymphatic capillary morphogenesis, resulting in organized tubular structures [122,123]. Hybrid PEG and fibrin matrices have also been used to create cell substrates with the ability to entrap, covalently conjugate, and affinity bind growth factors, and have tunable mechanical properties for directed differentiation [124,125]. PEG-based materials that mimic the fibrin clotting cascade, known as fibrin analogs, have also been created for tissue engineering applications [126].

2.4.2.5 Particulate Systems within Cell Substrate

Microparticles, and to a lesser extent, nanoparticles, may often be incorporated into cell substrates to provide another mechanism of controlled drug release to the cells. The complexities in these systems are vast when considering the combinations of material properties, release profiles, release mechanisms, or substrate construct. In some cases, the particles may be hydrophobic and rely on hydrolysis to control the release of growth factors, as in the release of BMPs from PLGA microspheres in scaffolds and matrices [127-130]. In other cases, the particles provide a facile means in which to

provide controlled delivery of growth factors *in vivo*, for example, by injection [129,131,132] or intratracheally [133]. Particles may also serve as cell carriers themselves, or assemble into a cell substrate at a later stage [96].

2.5 PERSPECTIVE

Drug delivery, and especially controlled drug delivery with engineered biomaterials, has proven to be an essential means for eliciting desired cellular responses in tissue engineering and drug therapy. The complexity of these biological systems, and the response to the concentration and pattern of drug introduced into the system, warrants further study to improve future therapies. The following chapter will further discuss the concept of disease-responsive drug delivery, previously introduced here as a part of the stimuli-responsive release modality.

2.6 REFERENCES

[1] M. Biondi, F. Ungaro, F. Quaglia, P.A. Netti, Controlled drug delivery in tissue engineering, Adv Drug Deliv Rev. 60 (2008) 229–242.

[2] T. Boontheekul, D.J. Mooney, Protein-based signaling systems in tissue engineering, Curr Opin Biotechnol. 14 (2003) 559–565.

[3] O.Z. Fisher, A. Khademhosseini, R. Langer, N.A. Peppas, Bioinspired materials for controlling stem cell fate, Acc Chem Res. 43 (2010) 419–428.

[4] R. Langer, J.P. Vacanti, Tissue engineering, Science. 260 (1993) 920–926.

[5] M. Nomi, A. Atala, P.D. Coppi, S. Soker, Principals of neovascularization for tissue engineering, Mol Aspects Med. 23 (2002) 463–483.

[6] W.M. Saltzman, W.L. Olbricht, Building drug delivery into tissue engineering, Nat Rev Drug Discov. 1 (2002) 177–186.

[7] Y. Tabata, Tissue regeneration based on growth factor release, Tissue Eng. 9 Suppl 1 (2003) S5–15.

[8] L. Uebersax, H.P. Merkle, L. Meinel, Biopolymer-based growth factor delivery for tissue repair: from natural concepts to engineered systems, Tissue Engineering Part B, Reviews. 15 (2009) 263–289.

[9] C. A van Blitterswijk, P. Thomsen, Tissue engineering', Book. (2008) 740.

[10] M. Caldorera-Moore, N.A. Peppas, Micro- and nanotechnologies for intelligent and responsive biomaterial-based medical systems, Adv Drug Deliv Rev. 61 (2009) 1391–1401.

[11] T.J. Klein, J. Malda, R.L. Sah, D.W. Hutmacher, Tissue engineering of articular cartilage with biomimetic zones, Tissue Engineering Part B, Reviews. 15 (2009) 143–157.

[12] G. A Truskey, F. Yuan PhD, F. Yuan, D. F Katz, Transport phenomena in biological systems', 2004.

[13] J.P. Fisher, A.G. Mikos, J. D Bronzino, Tissue Engineering', 2007.

[14] S. Lustig, N. Peppas, Solute diffusion in swollen membranes. IX. Scaling laws for solute diffusion in gels, Journal of Applied Polymer Science. 36 (1988) 735–747.

[15] N. Annabi, J.W. Nichol, X. Zhong, C. Ji, S. Koshy, A. Khademhosseini, et al., Controlling the porosity and microarchitecture of hydrogels for tissue engineering, Tissue Engineering Part B, Reviews. 16 (2010) 371–383.

[16] E.S.F.B.C. Conference, D. Franklyn Williams, E. Society for Biomaterials, Definitions in biomaterials: proceedings of a consensus conference of the

European Society for Biomaterials, Chester, England, March 3-5, 1986, (1987) 72.

[17] W.R. Gombotz, D.K. Pettit, Biodegradable polymers for protein and peptide drug delivery, Bioconjug Chem. 6 (1995) 332–351.

[18] A. Göpferich, Mechanisms of polymer degradation and erosion, Biomaterials. 17 (1996) 103–114.

[19] A. Steinbüchel, S. Matsumura, Biopolymers: Miscellaneous biopolymers and biodegradation of synthetic polymers‖, 2003.

[20] J. Heller, Controlled drug release from poly(ortho esters), Ann N Y Acad Sci. 446 (1985) 51–66.

[21] J.P. Jain, S. Modi, A.J. Domb, N. Kumar, Role of polyanhydrides as localized drug carriers, J Control Release. 103 (2005) 541–563.

[22] M. Caldorera-Moore, N. Guimard, L. Shi, K. Roy, Designer nanoparticles: incorporating size, shape and triggered release into nanoscale drug carriers, Expert Opin Drug Deliv. 7 (2010) 479–495.

[23] X. Jia, K.L. Kiick, Hybrid multicomponent hydrogels for tissue engineering, Macromolecular Bioscience. 9 (2009) 140–156.

[24] D.W.P.M. Löwik, E.H.P. Leunissen, M. van den Heuvel, M.B. Hansen, J.C.M. van Hest, Stimulus responsive peptide based materials, Chem Soc Rev. 39 (2010) 3394–3412.

[25] P. Wanakule, K. Roy, Disease-responsive drug delivery: the next generation of smart delivery devices, Curr Drug Metab. 13 (2012) 42–49.

[26] P. Wanakule, G.W. Liu, A.T. Fleury, K. Roy, Nano-inside-micro: Disease-responsive microgels with encapsulated nanoparticles for intracellular drug delivery to the deep lung, J Control Release. 162 (2012) 429–437.

[27] A.R. Khare, N.A. Peppas, Release behavior of bioactive agents from pH-sensitive hydrogels, J Biomater Sci Polym Ed. 4 (1993) 275–289.

[28] A.R. Khare, N.A. Peppas, Swelling/deswelling of anionic copolymer gels, Biomaterials. 16 (1995) 559–567.

[29] D. Gallardo, B. Skalsky, P. Kleinebudde, Controlled release solid dosage forms using combinations of (meth)acrylate copolymers, Pharm Dev Technol. 13 (2008) 413–423.

[30] F. Liu, A.W. Basit, A paradigm shift in enteric coating: achieving rapid release in the proximal small intestine of man, J Control Release. 147 (2010) 242–245.

[31] O. Boussif, F. Lezoualc'h, M.A. Zanta, M.D. Mergny, D. Scherman, B. Demeneix, et al., A versatile vector for gene and oligonucleotide transfer into cells in culture and in vivo: polyethylenimine, Proc Natl Acad Sci U S A. 92 (1995) 7297–7301.

[32] D. Putnam, C.A. Gentry, D.W. Pack, R. Langer, Polymer-based gene delivery with low cytotoxicity by a unique balance of side-chain termini, Proc Natl Acad Sci U S A. 98 (2001) 1200–1205.

[33] A.S. Gobin, J.L. West, Cell migration through defined, synthetic ECM analogs, Faseb J. 16 (2002) 751–753.

[34] T. Miyata, T. Uragami, K. Nakamae, Biomolecule-sensitive hydrogels, Adv Drug Deliv Rev. 54 (2002) 79–98.

[35] N.A. Peppas, P. Bures, W. Leobandung, H. Ichikawa, Hydrogels in pharmaceutical formulations, Eur J Pharm Biopharm. 50 (2000) 27–46.

[36] D.G. Vartak, R.A. Gemeinhart, Matrix metalloproteases: underutilized targets for drug delivery, Journal of Drug Targeting. 15 (2007) 1–20.

[37] L. Tong, Q. Wei, A. Wei, J.-X. Cheng, Gold nanorods as contrast agents for biological imaging: optical properties, surface conjugation and photothermal effects, Photochemistry and Photobiology. 85 (2009) 21–32.

[38] A.H. Zisch, M.P. Lutolf, J.A. Hubbell, Biopolymeric delivery matrices for angiogenic growth factors, Cardiovasc Pathol. 12 (2003) 295–310.

[39] A.A. Aimetti, A.J. Machen, K.S. Anseth, Poly(ethylene glycol) hydrogels formed by thiol-ene photopolymerization for enzyme-responsive protein delivery, Biomaterials. 30 (2009) 6048–6054.

[40] L.C. Glangchai, M. Caldorera-Moore, L. Shi, K. Roy, Nanoimprint lithography based fabrication of shape-specific, enzymatically-triggered smart nanoparticles, J Control Release. 125 (2008) 263–272.

[41] J. Tauro, B. Lee, S. Lateef, R. Gemeinhart, Matrix metalloprotease selective peptide substrates cleavage within hydrogel matrices for cancer …, Peptides. (2008).

[42] S.N. Robinson, J.E. Talmadge, Sustained release of growth factors, In Vivo. 16 (2002) 535–540.

[43] M.C. Manning, K. Patel, R.T. Borchardt, Stability of protein pharmaceuticals, Pharm Res. 6 (1989) 903–918.

[44] M.C. Manning, D.K. Chou, B.M. Murphy, R.W. Payne, D.S. Katayama, Stability of protein pharmaceuticals: an update, Pharm Res. 27 (2010) 544–575.

[45] W. Wang, Instability, stabilization, and formulation of liquid protein pharmaceuticals, Int J Pharm. 185 (1999) 129–188.

[46] K. Fu, D.W. Pack, A.M. Klibanov, R. Langer, Visual evidence of acidic environment within degrading poly(lactic-co-glycolic acid) (PLGA) microspheres, Pharm Res. 17 (2000) 100–106.

[47] J.F. Eliason, Pegylated cytokines: potential application in immunotherapy of cancer, BioDrugs. 15 (2001) 705–711.

[48] G. Molineux, Pegylation: engineering improved pharmaceuticals for enhanced therapy, Cancer Treat Rev. 28 Suppl A (2002) 13–16.

[49] M.J. Roberts, M.D. Bentley, J.M. Harris, Chemistry for peptide and protein PEGylation, Adv Drug Deliv Rev. 54 (2002) 459–476.

[50] H. Sato, Enzymatic procedure for site-specific pegylation of proteins, Adv Drug Deliv Rev. 54 (2002) 487–504.

[51] G. Molineux, Pegylation: engineering improved biopharmaceuticals for oncology, Pharmacotherapy. 23 (2003) 3S–8S.

[52] B.-B. Yang, P.K. Lum, M.M. Hayashi, L.K. Roskos, Polyethylene glycol modification of filgrastim results in decreased renal clearance of the protein in rats, J Pharm Sci. 93 (2004) 1367–1373.

[53] M.P. Lutolf, F.E. Weber, H.G. Schmoekel, J.C. Schense, T. Kohler, R. Müller, et al., Repair of bone defects using synthetic mimetics of collagenous extracellular matrices, Nat Biotechnol. 21 (2003) 513–518.

[54] S. Wee, W. Gombotz, Protein release from alginate matrices, Adv Drug Deliv Rev. 31 (1998) 267–285.

[55] A. Sano, T. Hojo, M. Maeda, K. Fujioka, Protein release from collagen matrices, Adv Drug Deliv Rev. 31 (1998) 247–266.

[56] Y. Ikada, Y. Tabata, Protein release from gelatin matrices, Adv Drug Deliv Rev. 31 (1998) 287–301.

[57] B.K. Wacker, S.K. Alford, E.A. Scott, M. Das Thakur, G.D. Longmore, D.L. Elbert, Endothelial cell migration on RGD-peptide-containing PEG hydrogels in the presence of sphingosine 1-phosphate, Biophys J. 94 (2008) 273–285.

[58] W.M. Saltzman, S. Baldwin, Materials for protein delivery in tissue engineering, Adv Drug Deliv Rev. 33 (1998) 71–86.

[59] Y. Cao, R. Langer, A review of Judah Folkman's remarkable achievements in biomedicine, Proc Natl Acad Sci U S A. 105 (2008) 13203.

[60] A. Lucke, J. Kiermaier, A. Göpferich, Peptide acylation by poly(alpha-hydroxy esters), Pharm Res. 19 (2002) 175–181.

[61] A. Brunner, K. Mäder, A. Göpferich, pH and osmotic pressure inside biodegradable microspheres during erosion, Pharm Res. 16 (1999) 847–853.

[62] M. van de Weert, W.E. Hennink, W. Jiskoot, Protein instability in poly(lactic-co-glycolic acid) microparticles, Pharm Res. 17 (2000) 1159–1167.

[63] K.A. Athanasiou, C.M. Agrawal, F.A. Barber, S.S. Burkhart, Orthopaedic applications for PLA-PGA biodegradable polymers, Arthroscopy. 14 (1998) 726–737.

[64] F. Mohamed, C.F. van der Walle, Engineering biodegradable polyester particles with specific drug targeting and drug release properties, J Pharm Sci. 97 (2008) 71–87.

[65] A. Sánchez, M. Tobío, L. González, A. Fabra, M.J. Alonso, Biodegradable micro- and nanoparticles as long-term delivery vehicles for interferon-alpha, Eur J Pharm Sci. 18 (2003) 221–229.

[66] H. Thissen, K.-Y. Chang, T.A. Tebb, W.-B. Tsai, V. Glattauer, J.A.M. Ramshaw, et al., Synthetic biodegradable microparticles for articular cartilage tissue engineering, J Biomed Mater Res A. 77 (2006) 590–598.

[67] A. Singh, S. Suri, K. Roy, In-situ crosslinking hydrogels for combinatorial delivery of chemokines and siRNA-DNA carrying microparticles to dendritic cells, Biomaterials. 30 (2009) 5187–5200.

[68] M.F. Haller, W.M. Saltzman, Nerve growth factor delivery systems, J Control Release. 53 (1998) 1–6.

[69] D.H.R. Kempen, L. Lu, T.E. Hefferan, L.B. Creemers, A. Maran, K.L. Classic, et al., Retention of in vitro and in vivo BMP-2 bioactivities in sustained delivery vehicles for bone tissue engineering, Biomaterials. 29 (2008) 3245–3252.

[70] X. Xu, W.-C. Yee, P.Y.K. Hwang, H. Yu, A.C.A. Wan, S. Gao, et al., Peripheral nerve regeneration with sustained release of poly(phosphoester) microencapsulated nerve growth factor within nerve guide conduits, Biomaterials. 24 (2003) 2405–2412.

[71] L.A. Pfister, M. Papaloïzos, H.P. Merkle, B. Gander, Nerve conduits and growth factor delivery in peripheral nerve repair, J Peripher Nerv Syst. 12 (2007) 65–82.

[72] H.H. Tønnesen, J. Karlsen, Alginate in drug delivery systems, Drug Dev Ind Pharm. 28 (2002) 621–630.

[73] M. Lee, W. Li, R.K. Siu, J. Whang, X. Zhang, C. Soo, et al., Biomimetic apatite-coated alginate/chitosan microparticles as osteogenic protein carriers, Biomaterials. 30 (2009) 6094–6101.

[74] M.L. Moya, M.R. Garfinkel, X. Liu, S. Lucas, E.C. Opara, H.P. Greisler, et al., Fibroblast growth factor-1 (FGF-1) loaded microbeads enhance local capillary neovascularization, J Surg Res. 160 (2010) 208–212.

[75] M.L. Moya, M.-H. Cheng, J.-J. Huang, M.E. Francis-Sedlak, S.-W. Kao, E.C. Opara, et al., The effect of FGF-1 loaded alginate microbeads on neovascularization and adipogenesis in a vascular pedicle model of adipose tissue engineering, Biomaterials. 31 (2010) 2816–2826.

[76] A.D. Thompson, M.W. Betz, D.M. Yoon, J.P. Fisher, Osteogenic differentiation of bone marrow stromal cells induced by coculture with chondrocytes

encapsulated in three-dimensional matrices, Tissue Engineering Part A. 15 (2009) 1181–1190.

[77] N. Nagai, N. Kumasaka, T. Kawashima, H. Kaji, M. Nishizawa, T. Abe, Preparation and characterization of collagen microspheres for sustained release of VEGF, J Mater Sci Mater Med. 21 (2010) 1891–1898.

[78] L. Li, H. Okada, G. Takemura, M. Esaki, H. Kobayashi, H. Kanamori, et al., Sustained release of erythropoietin using biodegradable gelatin hydrogel microspheres persistently improves lower leg ischemia, J Am Coll Cardiol. 53 (2009) 2378–2388.

[79] J. Gaffney, S. Matou-Nasri, M. Grau-Olivares, M. Slevin, Therapeutic applications of hyaluronan, Mol Biosyst. 6 (2010) 437–443.

[80] S. Taqvi, L. Dixit, K. Roy, Biomaterial-based notch signaling for the differentiation of hematopoietic stem cells into T cells, J Biomed Mater Res A. 79 (2006) 689–697.

[81] A.H. Zisch, M.P. Lutolf, M. Ehrbar, G.P. Raeber, S.C. Rizzi, N. Davies, et al., Cell-demanded release of VEGF from synthetic, biointeractive cell ingrowth matrices for vascularized tissue growth, Faseb J. 17 (2003) 2260–2262.

[82] H. Seeherman, J.M. Wozney, Delivery of bone morphogenetic proteins for orthopedic tissue regeneration, Cytokine Growth Factor Rev. 16 (2005) 329–345.

[83] H.J. Seeherman, J.M. Archambault, S.A. Rodeo, A.S. Turner, L. Zekas, D. D'Augusta, et al., rhBMP-12 accelerates healing of rotator cuff repairs in a sheep model, J Bone Joint Surg Am. 90 (2008) 2206–2219.

[84] H.J. Seeherman, X.J. Li, M.L. Bouxsein, J.M. Wozney, rhBMP-2 induces transient bone resorption followed by bone formation in a nonhuman primate core-defect model, J Bone Joint Surg Am. 92 (2010) 411–426.

[85] H. Seeherman, R. Li, M. Bouxsein, H. Kim, X.J. Li, E.A. Smith-Adaline, et al., rhBMP-2/calcium phosphate matrix accelerates osteotomy-site healing in a nonhuman primate model at multiple treatment times and concentrations, J Bone Joint Surg Am. 88 (2006) 144–160.

[86] N. Thyagarajapuram, D. Olsen, C.R. Middaugh, The structure, stability, and complex behavior of recombinant human gelatins, J Pharm Sci. 96 (2007) 3363–3378.

[87] S. Young, M. Wong, Y. Tabata, A.G. Mikos, Gelatin as a delivery vehicle for the controlled release of bioactive molecules, J Control Release. 109 (2005) 256–274.

[88] M. Yamamoto, Y. Takahashi, Y. Tabata, Enhanced bone regeneration at a segmental bone defect by controlled release of bone morphogenetic protein-2 from a biodegradable hydrogel, Tissue Eng. 12 (2006) 1305–1311.

[89] M. Ozeki, Y. Tabata, Interaction of hepatocyte growth factor with gelatin as the carrier material, J Biomater Sci Polym Ed. 17 (2006) 163–175.

[90] X. Guo, H. Park, S. Young, J.D. Kretlow, J.J. van den Beucken, L.S. Baggett, et al., Repair of osteochondral defects with biodegradable hydrogel composites encapsulating marrow mesenchymal stem cells in a rabbit model, Acta Biomaterialia. 6 (2010) 39–47.

[91] C.-C. Lin, K.S. Anseth, PEG hydrogels for the controlled release of biomolecules in regenerative medicine, Pharm Res. 26 (2009) 631–643.

[92] A. Metters, J.A. Hubbell, Network formation and degradation behavior of hydrogels formed by Michael-type addition reactions, Biomacromolecules. 6 (2005) 290–301.

[93] S. Suri, C.E. Schmidt, Photopatterned collagen-hyaluronic acid interpenetrating polymer network hydrogels, Acta Biomaterialia. 5 (2009) 2385–2397.

[94] S.E. Sakiyama-Elbert, J.A. Hubbell, Controlled release of nerve growth factor from a heparin-containing fibrin-based cell ingrowth matrix, J Control Release. 69 (2000) 149–158.

[95] P. van de Wetering, A.T. Metters, R.G. Schoenmakers, J.A. Hubbell, Poly(ethylene glycol) hydrogels formed by conjugate addition with controllable swelling, degradation, and release of pharmaceutically active proteins, J Control Release. 102 (2005) 619–627.

[96] E.A. Scott, M.D. Nichols, R. Kuntz-Willits, D.L. Elbert, Modular scaffolds assembled around living cells using poly(ethylene glycol) microspheres with macroporation via a non-cytotoxic porogen, Acta Biomaterialia. 6 (2010) 29–38.

[97] D. Hern, J.A. Hubbell, Incorporation of adhesion peptides into nonadhesive hydrogels useful for tissue resurfacing, J Biomed Mater Res. (1998).

[98] J.E. Leslie-Barbick, J.J. Moon, J.L. West, Covalently-immobilized vascular endothelial growth factor promotes endothelial cell tubulogenesis in poly(ethylene glycol) diacrylate hydrogels, J Biomater Sci Polym Ed. 20 (2009) 1763–1779.

[99] L.L.Y. Chiu, M. Radisic, Scaffolds with covalently immobilized VEGF and Angiopoietin-1 for vascularization of engineered tissues, Biomaterials. 31 (2010) 226–241.

[100] I. Arrighi, S. Mark, M. Alvisi, B. von Rechenberg, J.A. Hubbell, J.C. Schense, Bone healing induced by local delivery of an engineered parathyroid hormone prodrug, Biomaterials. 30 (2009) 1763–1771.

[101] D.J. Maxwell, B.C. Hicks, S. Parsons, S.E. Sakiyama-Elbert, Development of rationally designed affinity-based drug delivery systems, Acta Biomaterialia. 1 (2005) 101–113.

[102] A. Baeza, I. Izquierdo-Barba, M. Vallet-Regí, Biotinylation of silicon-doped hydroxyapatite: a new approach to protein fixation for bone tissue regeneration, Acta Biomaterialia. 6 (2010) 743–749.

[103] J.D. Clapper, M.E. Pearce, C.A. Guymon, A.K. Salem, Biotinylated biodegradable nanotemplated hydrogel networks for cell interactive applications, Biomacromolecules. 9 (2008) 1188–1194.

[104] T. Segura, B.C. Anderson, P.H. Chung, R.E. Webber, K.R. Shull, L.D. Shea, Crosslinked hyaluronic acid hydrogels: a strategy to functionalize and pattern, Biomaterials. 26 (2005) 359–371.

[105] G. Mapili, Y. Lu, S. Chen, K. Roy, Laser-layered microfabrication of spatially patterned functionalized tissue-engineering scaffolds, J Biomed Mater Res B. 75 (2005) 414–424.

[106] M.A. Woodruff, S.N. Rath, E. Susanto, L.M. Haupt, D.W. Hutmacher, V. Nurcombe, et al., Sustained release and osteogenic potential of heparan sulfate-doped fibrin glue scaffolds within a rat cranial model, J Mol Histol. 38 (2007) 425–433.

[107] J.S. Pieper, T. Hafmans, P.B. van Wachem, M.J.A. van Luyn, L.A. Brouwer, J.H. Veerkamp, et al., Loading of collagen-heparan sulfate matrices with bFGF promotes angiogenesis and tissue generation in rats, J Biomed Mater Res. 62 (2002) 185–194.

[108] S.K. Chintala, R.R. Miller, C.A. McDevitt, Role of heparan sulfate in the terminal differentiation of growth plate chondrocytes, Arch Biochem Biophys. 316 (1995) 227–234.

[109] D.S.W. Benoit, K.S. Anseth, Heparin functionalized PEG gels that modulate protein adsorption for hMSC adhesion and differentiation, Acta Biomaterialia. 1 (2005) 461–470.

[110] D.S.W. Benoit, A.R. Durney, K.S. Anseth, The effect of heparin-functionalized PEG hydrogels on three-dimensional human mesenchymal stem cell osteogenic differentiation, Biomaterials. 28 (2007) 66–77.

[111] J.S. McGonigle, G. Tae, P.S. Stayton, A.S. Hoffman, M. Scatena, Heparin-regulated delivery of osteoprotegerin promotes vascularization of implanted hydrogels, J Biomater Sci Polym Ed. 19 (2008) 1021–1034.

[112] G. Tae, M. Scatena, P.S. Stayton, A.S. Hoffman, PEG-cross-linked heparin is an affinity hydrogel for sustained release of vascular endothelial growth factor, J Biomater Sci Polym Ed. 17 (2006) 187–197.

[113] M.D. Wood, A.M. Moore, D.A. Hunter, S. Tuffaha, G.H. Borschel, S.E. Mackinnon, et al., Affinity-based release of glial-derived neurotrophic factor from fibrin matrices enhances sciatic nerve regeneration, Acta Biomaterialia. 5 (2009) 959–968.

[114] M.D. Wood, M.R. MacEwan, A.R. French, A.M. Moore, D.A. Hunter, S.E. Mackinnon, et al., Fibrin matrices with affinity-based delivery systems and neurotrophic factors promote functional nerve regeneration, Biotechnol Bioeng. 106 (2010) 970–979.

[115] K.L. Kiick, Peptide- and protein-mediated assembly of heparinized hydrogels, Soft Matter. 4 (2008) 29–37.

[116] T. Nie, A. Baldwin, N. Yamaguchi, K.L. Kiick, Production of heparin-functionalized hydrogels for the development of responsive and controlled growth factor delivery systems, J Control Release. 122 (2007) 287–296.

[117] L. Zhang, E.M. Furst, K.L. Kiick, Manipulation of hydrogel assembly and growth factor delivery via the use of peptide-polysaccharide interactions, J Control Release. 114 (2006) 130–142.

[118] P.P. Spicer, A.G. Mikos, Fibrin glue as a drug delivery system, J Control Release. 148 (2010) 49–55.

[119] D.H. Sierra, Fibrin sealant adhesive systems: a review of their chemistry, material properties and clinical applications, J Biomater Appl. 7 (1993) 309–352.

[120] M. Ehrbar, S.M. Zeisberger, G.P. Raeber, J.A. Hubbell, C. Schnell, A.H. Zisch, The role of actively released fibrin-conjugated VEGF for VEGF receptor 2 gene activation and the enhancement of angiogenesis, Biomaterials. 29 (2008) 1720–1729.

[121] P. Losi, E. Briganti, A. Magera, D. Spiller, C. Ristori, B. Battolla, et al., Tissue response to poly(ether)urethane-polydimethylsiloxane-fibrin composite scaffolds for controlled delivery of pro-angiogenic growth factors, Biomaterials. 31 (2010) 5336–5344.

[122] C.-L.E. Helm, M.E. Fleury, A.H. Zisch, F. Boschetti, M.A. Swartz, Synergy between interstitial flow and VEGF directs capillary morphogenesis in vitro through a gradient amplification mechanism, Proc Natl Acad Sci U S A. 102 (2005) 15779–15784.

[123] C.-L.E. Helm, A. Zisch, M.A. Swartz, Engineered blood and lymphatic capillaries in 3-D VEGF-fibrin-collagen matrices with interstitial flow, Biotechnol Bioeng. 96 (2007) 167–176.

[124] C.T. Drinnan, G. Zhang, M.A. Alexander, A.S. Pulido, L.J. Suggs, Multimodal release of transforming growth factor-β1 and the BB isoform of platelet derived growth factor from PEGylated fibrin gels, J Control Release. 147 (2010) 180–186.

[125] G. Zhang, C.T. Drinnan, L.R. Geuss, L.J. Suggs, Vascular differentiation of bone marrow stem cells is directed by a tunable three-dimensional matrix, Acta Biomaterialia. 6 (2010) 3395–3403.

[126] M. Ehrbar, S.C. Rizzi, R.G. Schoenmakers, B.S. Miguel, J.A. Hubbell, F.E. Weber, et al., Biomolecular hydrogels formed and degraded via site-specific enzymatic reactions, Biomacromolecules. 8 (2007) 3000–3007.

[127] Y. Ji, G.P. Xu, Z.P. Zhang, J.J. Xia, J.L. Yan, S.H. Pan, BMP-2/PLGA delayed-release microspheres composite graft, selection of bone particulate diameters, and prevention of aseptic inflammation for bone tissue engineering, Ann Biomed Eng. 38 (2010) 632–639.

[128] K. Gavenis, U. Schneider, J. Groll, B. Schmidt-Rohlfing, BMP-7-loaded PGLA microspheres as a new delivery system for the cultivation of human chondrocytes in a collagen type I gel: the common nude mouse model, Int J Artif Organs. 33 (2010) 45–53.

[129] B. Li, T. Yoshii, A.E. Hafeman, J.S. Nyman, J.C. Wenke, S.A. Guelcher, The effects of rhBMP-2 released from biodegradable polyurethane/microsphere composite scaffolds on new bone formation in rat femora, Biomaterials. 30 (2009) 6768–6779.

[130] C.-K. Wang, M.-L. Ho, G.-J. Wang, J.-K. Chang, C.-H. Chen, Y.-C. Fu, et al., Controlled-release of rhBMP-2 carriers in the regeneration of osteonecrotic bone, Biomaterials. 30 (2009) 4178–4186.

[131] N. Sasaki, T. Minami, K. Yamada, H. Yamada, Y. Inoue, M. Kobayashi, et al., In vivo effects of intra-articular injection of gelatin hydrogen microspheres containing basic fibroblast growth factor on experimentally induced defects in third metacarpal bones of horses, Am J Vet Res. 69 (2008) 1555–1559.

[132] A. Inoue, K.A. Takahashi, Y. Arai, H. Tonomura, K. Sakao, M. Saito, et al., The therapeutic effects of basic fibroblast growth factor contained in gelatin hydrogel microspheres on experimental osteoarthritis in the rabbit knee, Arthritis Rheum. 54 (2006) 264–270.

[133] K. Hirose, A. Marui, Y. Arai, T. Kushibiki, Y. Kimura, H. Sakaguchi, et al., Novel approach with intratracheal administration of microgelatin hydrogel microspheres incorporating basic fibroblast growth factor for rescue of rats with monocrotaline-induced pulmonary hypertension, J Thorac Cardiovasc Surg. 136 (2008) 1250–1256.

Chapter 3: Disease-Responsive Drug Delivery

[This chapter was adapted, with permission[‡], from P. Wanakule, K. Roy[§], Disease-responsive drug delivery: the next generation of smart delivery devices, Curr Drug Metab. 13 (2012) 42–49.]

3.1 INTRODUCTION

As more effective and sophisticated drugs begin to emerge, greater emphasis must be placed on the specificity and accuracy by which they are delivered to diseased cells in the body. These new classes of drugs include biological molecules, such as proteins, peptides, DNA, and siRNA, which are designed to target specific cellular pathways (such as signal transduction cascades, transcription factors, and apoptosis). Although these drugs are very specific in their action, many of them interfere with key cellular processes, and are therefore highly cytotoxic. When delivered to physiologically normal cells or tissue, the side effects are potentially damaging and debilitating. Moreover, the majority of these sophisticated drugs, especially those for chronic and advanced diseases, are primarily given via systemic administration, often through multiple, regular doses. The continued endurance of these side effects interferes with the quality of life of these patients, and may further lead to the development of other acute and chronic diseases. Therefore, rational design of targeted therapies that enhance patient compliance and improve quality of life while maintaining efficacy of treatment is essential [1-3].

[§] Statement of co-author contribution: This chapter was written by Prinda Wanakule, with editorial and content assistance by Krishnendu Roy (research supervisor).

Research to improve the mechanisms of controlled drug delivery has seen much success in recent decades, achieving long-lasting zero-order drug release, and reducing issues such as toxic plasma concentrations, short half-lives, and the need for multiple administrations. However, as their underlying mechanisms are uncovered, many diseases are found to follow biological rhythms or aberrant regulatory feedback cycles. Hence, ideal drug delivery systems should be designed to respond and modulate their release profiles to synchronize with the changing physiologic and pathophysiologic condition, both temporally and spatially [1,3].

In response to this, a growing interest in controlled drug delivery has been developing as a means to deliver bioactive agents (drugs) only when or where it is needed, primarily in response to specific stimuli. These stimuli-responsive types of systems often rely on local physicochemical changes arising from disease pathology or the cell microenvironment as well as on external stimuli that could be provided by a device. Common stimuli include pH, temperature, ions, enzymes and other biomolecules as well as light and mechanical forces, all of which have been designed to illicit a response in drug carriers to trigger drug release [1,2,4-11]. Stimuli-responsive systems are also referred to as "smart," "environment-sensitive," and "intelligent" systems, among others.

In this chapter, we focus on systems that respond to local, disease-specific stimuli – pH, ions, and biomolecules. The overwhelming majority of these delivery strategies are based on both natural and synthetic polymers, including biopolymers such as proteins, peptides, nucleic acids, and carbohydrates. We first begin with a detailed description of the disease-triggered drug release mechanisms, as well as advantages and disadvantages. We then move on to provide enabling applications and examples of these disease-specific delivery systems for various pathologies. Finally, we conclude the chapter with future

outlooks. External stimuli like light, magnetic field, ultrasound, electrical, and thermal triggers are not discussed extensively. Instead, we refer the reader to excellent reviews in the literature [2,5,8] that covers these aspects. It is also beyond the scope of this review to thoroughly discuss systems that respond to intracellular pH changes and reductive environments, although a few examples are provided. We again refer the reader to excellent articles in the literature [7,9,12-15] describing such systems.

3.2 Disease-Responsive Drug Release Mechanisms

First, we will begin with a discussion of the various disease cues that may be used to create disease-responsive drug delivery systems. These include pH responsiveness and biomolecule sensitivity, such as enzymes, antibodies, and metabolic products. An illustration of the many types of disease-responsive systems discussed here is shown in Figure 3.1 (page 55). A table is also provided at the end of the chapter, which gives an overview of the mechanisms discussed, a brief description of the mechanism, and a cross-listing of general references and disease-specific references (Table 3.1, page 67).

3.2.1 pH-Responsive

Variations in pH exist throughout the body at the organ, tissue, and cellular level, as well as in the local microenvironment of disease-affected tissues. pH-triggered drug delivery systems have been especially used in oral drug delivery to protect drugs from the acidic gastric cavity, triggering release in the more neutral small intestine [16,17], where much drug absorption occurs. More recently, as gene delivery systems have been gaining increasing significance, pH-responsive carriers have been developed to take advantage of the pH gradient from the extracellular environment through the early and late endosomes

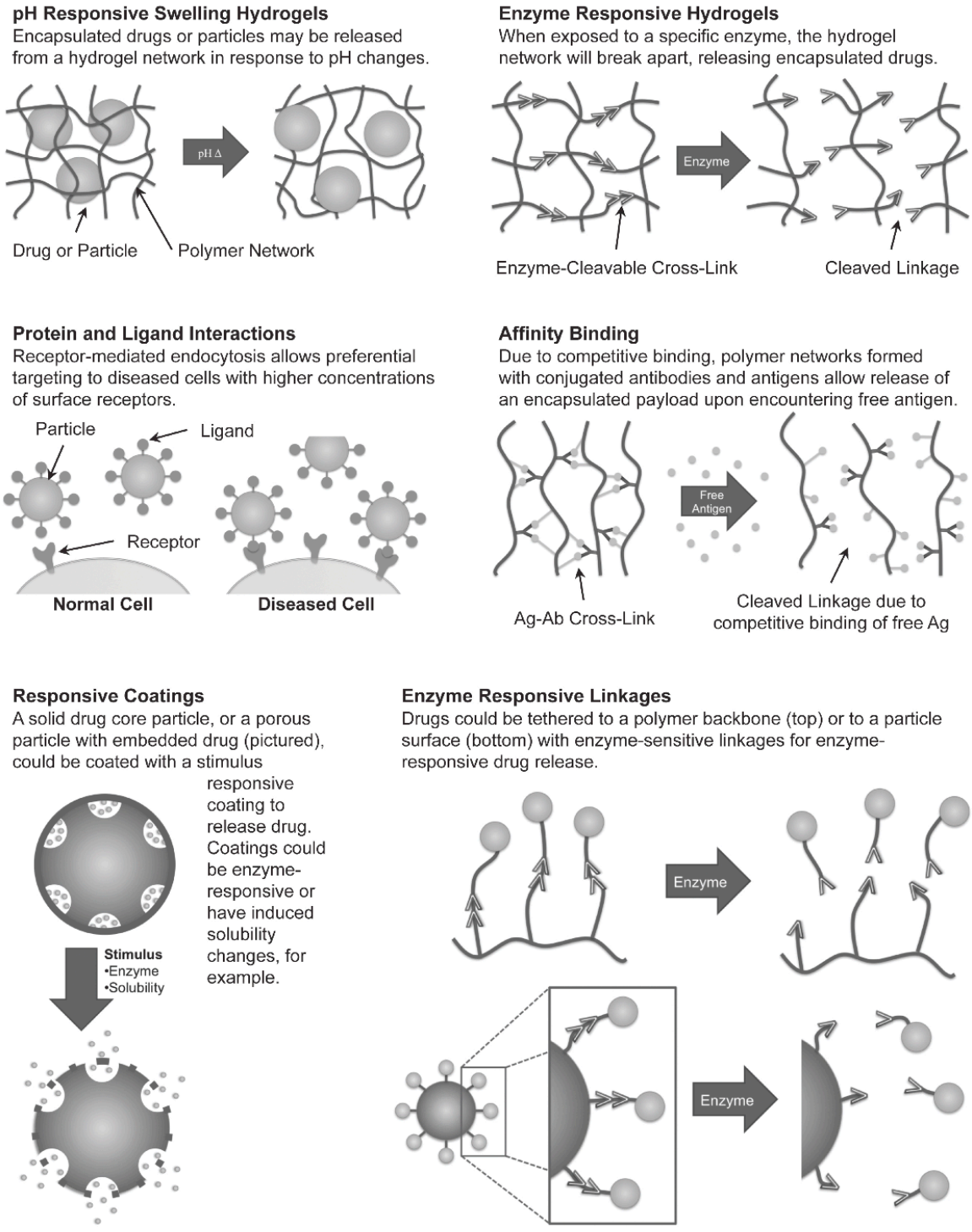

Figure 3.1 Illustrations of select disease-responsive release mechanisms.

[18]. pH variations within the microenvironment of disease-affected tissues have also been observed, including tumors, infarctions [19], and several other conditions connected with acidosis and alkalosis. Thus, pH-responsive systems offer a versatile way in which to trigger drug release in response to physiological or pathological cues.

Several hydrogel-based drug delivery systems with the ability to swell or shrink in response to pH changes have been developed as triggered-release delivery systems. The pH triggered swelling and shrinking mechanisms are primarily due to the properties of the side chain pendant group, which are cationic or anionic [2,6,20,21]. Anionic hydrogels are ionized at pHs above their pKa, and thus exhibit high swelling at these higher pHs due to repulsion of the ionized groups [20]. In contrast, cationic hydrogels are ionized at pHs below their pKa, exhibiting high swelling below their pKa [6]. pH-triggered swelling systems have been developed to be sensitive to minor pH changes, as low as 0.2-0.6 pH [22].

Other pH-responsive delivery systems have been designed to undergo hydrophilic to hydrophobic transitions, based on incorporated acid-degradable linkers, such as acetal [23,24], hydrazone [19], and pH-hydrolysable protecting groups [25]. Some materials with pH-dependent solubility also exhibit pH-dependant drug release, and have also been used [26]. Related to pH-responsive delivery, ionically driven drug release systems have also been developed [27,28].

3.2.2 Biomolecularly-Responsive

Systems that incorporate biomolecular recognition are some of the most relevant stimuli-responsive systems for disease-triggered drug release. Several different types of biomolecules could be used as drug release triggers, including high affinity binding of

proteins and peptides, enzyme-substrate recognition, and metabolically reactive systems. The incorporation of biomolecular recognition often involves the addition of complementary proteins, peptides, ligands, enzymes, substrates, antibodies, antigens, and metabolic products within a polymer system [1-5,8]. Polymer systems with incorporated biomolecules are often referred to as biopolymers or bio-inspired materials. These biomolecules could also be incorporated with non-polymeric delivery systems, for example, gold nanoparticles [29,30] or other theranostic systems [31-35].

Protein and ligand interactions have been used for years as a way to target drugs to certain cells. In the classical system, the drug is tethered to a protein, which binds to a receptor that is over expressed in the target cell type. Due to the higher accumulation of drug at these target cells and the process of receptor-mediated endocytosis, these systems are able to preferentially deliver drugs to the diseased tissue. These protein-ligand systems have also been incorporated into micro- and nanoparticles by conjugating proteins to the particle surfaces [36-39]. Common receptors targeted in cancer include CD44 [40-43], HER2 [37,44], transferrin [45,46], and folate [47,48].

Aside from usage as targeting molecules, affinity binding has also been used to create reversibly swelling hydrogel systems based on antigen-antibody binding [49]. In this system, both antibody and antigen are grafted onto polymer chains, and in combination, the antibody-antigen binding induces hydrogel formation. When the hydrogel is then exposed to free antigen, competitive binding disrupts the hydrogel network, resulting in swelling. When free antigen is removed, the original binding between the grafted antibody-antigen are re-formed, demonstrating a memory-like property. This early system paved the way for extensive work on molecular imprinting in hydrogel systems, which continue to be explored for disease-responsive release [50,51], targeting, and biosensors [2,3,52,53].

Another class of biomolecularly-responsive systems involves incorporation of enzyme-sensitive components into drug carriers, usually peptides, proteins, or polysaccharides. Several of these biomolecules have been integrated into enzyme-degradable hydrogels, either as a cross-linker (short peptide sequences) or as the matrix material, e.g. polysaccharides (chitosan, hyaluronic acid) and protein-based gels (collagen, gelatin). These hydrogels have shown minimal release in the absence of the stimulating enzyme, and triggered release in the presence of the enzyme [2,3,54,55]. This strategy has been used extensively in tissue engineering applications [56,57], however, it could also provide an effective means of disease-responsive drug delivery [58-60]. Enzyme-responsive systems are suitable for site-specific and disease-specific delivery because of the high specificity of enzymatic cleavage, and the up regulation of enzymes in several diseases, such as various cancers and inflammatory diseases [46,55,58,59,61-63]. Aside from enzyme-sensitive hydrogels, enzyme-degradable components are often used as covalent linkers to conjugate drugs as pendant groups off a polymer backbone. Upon encountering the enzyme, the pendant chains are broken, releasing the tethered drug [2,60,64]. Yet another set-up incorporates an enzyme-sensitive peptide-based coating on a porous particle. Drug molecules are loaded within the pores of a particle and encased with a peptide coating such that the coating prevents drug release until it is removed via enzymatic degradation [65].

Common metabolic products and pathways may also be used as stimuli for polymer systems, an exemplary example of which includes the glucose oxidase-containing cationic hydrogels created by Podual and colleagues [66,67] (described in detail under the Diabetes section). Other examples include a carbon dioxide-responsive cationic hydrogel developed as a feedback-regulated drug delivery vehicle [68], as well as a metabolism-mimicking glutathione-triggered drug release system [69]. In normal

cells, glutathione neutralizes reactive oxygen species, preventing free-radical damage to nucleic acids. However, glutathione is elevated in tumor cells, and contributes to chemotherapy drug resistance [70].

With recent advances in computing and bioinformatics, a number of protein and enzyme databases with detailed binding and specificity information are available for researchers to carefully choose appropriate molecules for incorporation into their systems as the stimulus, or stimulus-responsive component. Just to name a few, these databases include the Protein Data Bank (PDB) [71], Braunschweig Enzyme Database (BRENDA) [72], Expert Protein Analysis System (ExPASy) [73], and Universal PBM Resource for Oligonucleotide Binding Evaluation (UniPROBE) [74].

3.2.3 Other Notable Stimuli

Several other common stimuli within the field of stimuli-responsive drug delivery include temperature, light, magnetic field, and ultrasound [1,5,15,75]. Although these stimuli are not specifically disease-responsive, many of these have been incorporated into drug release systems as a means of externally controlling drug release, with the possibility of dosing according to a regimented schedule. These types of stimuli are especially applicable in the newly emerging area of theranostics, in which diagnostics and therapy are combined into one delivery system, and delivered to the patient in a single, combined dosage form. In this way, theranostics allows for simultaneous monitoring of disease progression or regression in response to a prescribed therapy. Combined with imaging-based diagnostics, the accumulation of the theranostic treatment could be monitored until significant levels are achieved at a known disease site, and then triggered for drug release in response to applied stimuli. Several opportunities exist, all of

which we invite the reader to explore in several exceptional reviews in the literature [34,35,76-81].

3.3 Disease Applications

3.3.1 Cancer

Physiological differences found within the tumor microenvironment, or stroma, may be exploited by drug delivery systems in order to trigger drug release. Aside from the leaky vasculature that results in the enhanced permeation and retention (EPR) effect, the tumor-stroma exhibits a slightly acidic pH, around 6.5-7.2. This acidic environment stems from poor perfusion rates and increased glycolysis in tumor cells, which results in a local accumulation of acidic waste products [46,82,83]. Although this low pH slows the uptake of weakly basic drugs like doxorubicin (DOX), several strategies have been employed to improve the uptake and efficacy of DOX [84]. For example, pH-sensitive micelles composed of poly(L-histidine)-poly(ethylene glycol) block copolymers were developed by Bae and coworkers [85,86] that destabilize at the slightly acidic tumor microenvironment. When loaded with DOX and subjected to decreasing pH, a marked increase in release of DOX and corresponding decrease in A2780 cell viability was observed between pH 7.4 and 6.8. Further *in vivo* studies also demonstrated increased tumor suppression using the pH-sensitive micellar formulation versus free DOX. Similar results were obtained with another acidic pH-destabilizing micelle formulation of methyl ether poly(ethylene glycol)-poly(β-amino ester), developed by Kwon and colleagues [87]. Whereas both of these micellar systems utilized the acidic microenvironment to increase the tumor-localized concentration of DOX for increased uptake and efficacy, another system devised by Stayton et al. improved overall DOX efficacy by using pH

responsive polymers to co-deliver siRNA [88]. In this system, pH-responsive poly(styrene-alt-maleic-anhydride) was complexed with siRNA to improve endosomal escape within the tumor cell, and packaged inside a micelle to be co-delivered with DOX. The siRNA used was shown to sensitize multidrug resistant tumor cells to DOX by silencing the gene polo-like kinase 1, demonstrating a potent combinatorial treatment system. Aside from buffering-induced endosomal disruption, pH triggered expansion of hydrogel nanoparticles within the endosome, and thus a bursting of the endosome, has also been conceived as means of cytosolic anti-cancer drug delivery [25].

Enzyme-triggered release is an especially noteworthy method of achieving disease-responsive delivery for tumors and cancer cells. Several enzymes are up regulated in various cancers, both intracellularly and extracellularly, including secretory phospholipase A2 (sPLA2) [89], cathepsins [4,59], Src family kinases [90], and MMPs [60,63,91]. sPLA2 is an extracellularly up regulated lipid hydrolyzing enzyme, and is primarily used as a trigger for liposome-based delivery systems [89]. Several variations of these sPLA2-sensitive liposomal formulations are possible, such as incorporating the enzyme-sensitivity to activate a phospholipid prodrug, or triggering release of anti-cancer drugs encapsulated within a liposome. Kaasgaard and co-workers demonstrated promising cytotoxicity of a novel methotrexate analogue encapsulated within sPLA2-degradable liposomes in KATO III and HT-29 cancer cell lines. However, the cytotoxicity was independent of the enzyme degradation, indicating leakage of the anti-cancer drug from the system, and illustrating the difficulty in ensuring anchoring stability of such drugs in liposomal formulations [92]. Pederson and colleagues demonstrated the sPLA2-mediated cytotoxicity of several retinoid phospholipid prodrugs toward HT-29 and Colo205 colon cancer cells (no significant cell death observed in the absence of enzyme). Furthermore, the phospholipid prodrugs were able to form ~100nm particles

suitable for intravenous administration, demonstrating a marked improvement over previous liposomal formulation strategies that often result in leakage of the drug from the carrier [93].

Our group has recently demonstrated the incorporation of an enzyme-triggered release mechanism within size- and shape-specific hydrogel nanoparticles for cancer treatment [4,59]. Specifically, disease-responsive release is mediated by cathepsin B activity on a di-acrylated peptide sequence, GFLGK, which is incorporated into a PEG hydrogel via UV cross-linking of acrylate groups. The nanoparticles are fabricated using step and flash imprint lithography (S-FIL), allowing precise control over size (down to 50nm), shape, composition, and ease of harvest and recovery. Specific enzyme triggered release from these nanostructures was demonstrated with plasmid DNA and IgG antibodies, with minimal release of both model drugs in the absence of enzyme.

The family of matrix metalloproteinases has perhaps received the most attention of all the up-regulated enzymes in cancer. This is largely due to early interest in the therapeutic potential of down-regulating MMP activity. However, significant work by Gemeinhart and colleagues established MMPs as an effective target for disease-specific triggered drug release [55,60,63,91]. In these systems [60,63,91], cisplatin is used as a model chemotherapeutic drug, and is incorporated within a PEG hydrogel via MMP-sensitive peptide tether. Collectively, the work demonstrates the enzyme-dependant release of drugs from the system, with a PEG chain length of 4000 kDa being sufficient to allow MMP activity within and throughout the hydrogel, and a PEG chain length of 574 Da being insufficient. Cytotoxicity studies of the cisplatin-loaded system using U-87 malignant glioma cells and the 4000 kDa PEG chain showed 0% cell survival in the presence of MMP versus ~50% cell survival in the absence of MMP. This early work has

paved the way for the development of other MMP-responsive systems for localized treatment of cancer and other diseases [64,94-97].

3.3.2 Diabetes

Feedback-regulated control of insulin release, required to maintain optimal blood-glucose levels is of utmost importance in controlling diabetes, preventing diabetic coma, and reducing the risk of developing more serious pathologies as a result of glucose imbalance [98]. Peppas and colleagues developed one of the most significant insulin delivery systems capable of achieving this feedback-regulated control [66,67]. In this system, glucose oxidase and catalase was incorporated into cationic hydrogel microparticles, employing hybrid disease-responsive triggers: biomolecule-sensitivity and pH-responsive swelling. As glucose interacts with glucose oxidase in the hydrogel, it is enzymatically digested into gluconic acid, thereby shifting towards a slightly acidic pH in the hydrogel microenvironment. The cationic hydrogel then swells in response to the acidic pH, releasing insulin, and reversibly shrinks once glucose is removed and local pH returns to the neutral physiological norm.

3.3.3 Inflammatory Diseases

Prolonged inflammation after acute injury or in chronic diseases, such as asthma and arthritis, can severely debilitate a patient and lead to development of more serious conditions, including fibrosis and cancer [23,58,99,100]. Since inflammation is an essential part of the normal immune response, it is undesirable to non-specifically deliver anti-inflammatory or immune-suppressive drugs over the long term. Disease-responsive

drug delivery is therefore needed to treat only the tissue affected with prolonged inflammation.

One strategy to achieve such inflammation-responsive drug delivery involves an enzyme-degradable PEG hydrogel, sensitive to human neutrophil elastase, an enzyme secreted during inflammation [58]. The authors were able to demonstrate enzyme-dependent release of a model protein from the system, and effective retention of the protein without enzyme, by creating hydrogels with sufficiently restrictive mesh size so as to drive the mechanism towards enzyme-mediated surface erosion.

In another system, an intracellular protein kinase that is constantly activated in inflammatory cells was used as a cell-specific stimulus to cleave a transcription-inhibiting polymer complexed with plasmid DNA [99]. This system was able to effectively demonstrate gene activation only in cells exposed to an inflammatory stimulus (lipopolysaccharide), as compared to normal cells, showing potential in targeting only the inflammatory cell types.

3.3.4 Infection

There are many benefits for applying disease-responsive drug delivery to infections, including bacterial, fungal, or viral. In the case of bacterial infection, the rise of antibiotic resistant bacterial strains has created a tangible need to limit and control the improper and/or prophylactic usage of antibiotics. Although antibiotic-treated bandages have been available for years, *in vitro* studies have shown that most antibiotics exert somewhat cytotoxic effects on human fibroblasts. To address these issues, an antibiotic delivery system based on PVA with peptide tethered-gentamicin was created to release the antibiotic only in the presence of infection by *Pseudomonas aeruginosa*. Gentamicin

release was clearly observed from infected samples as compared to negligible release of gentamicin from non-infected control samples [101]. Another system for enzyme-mediated gentamicin release was designed using poly(trimethylene carbonate) for the treatment of osteomyelitis, via lipase degradation [102].

Enzymatic activity due to viral infection has also been used to target and treat only those cells that are infected with the virus. For example, an anti-HIV transgene was coupled with an intelligent gene delivery carrier using enzyme specificity to achieve HIV-infected cell specificity. The authors fabricated an HIV-1 protease sensitive polymer known as CPCHIVtat (cationic polymer possessing a cleavage site for HIV-1 protease), which formed a polyplex with the transgene, suppressing transcription. The presence of the HIV-1 protease caused the cleavage of the CPCHIVtat polymer, releasing the transgene to be expressed in activated HIV-infected cells, whereas other uninfected cells remained intact [103].

3.4 Conclusions and Future Perspectives

Drug release from nano to macroscale delivery systems in response to physiological or disease-specific signals holds significant promise in reducing side effects and increasing efficacy of a variety of therapeutic agents. New particle and device fabrication methods have enabled incorporation of a variety of stimuli-responsiveness within delivery systems. The field is expanding rapidly with more and more new systems being reported. However, a few areas need to be studied more carefully before such systems can find clinical usage. For example, most of the systems developed so far must rely on a threshold level of stimuli signal to "trigger" the drug release. This is critical for distinguishing disease-specific signals from normal physiological levels of the stimulus.

However, inter patient variability and variability between different phenotypes of the disease could significantly complicate the design of such systems. As in the case of pH or enzyme-responsive devices, the threshold of pH or enzyme concentration would dictate drug release, both in terms of when drug is released and at what rate. Variability in enzyme levels or pH levels from tumor to tumor or patient to patient could provide significant differences in those variables. Another critical issue is that of scale up and cost. Drug carriers involving biological molecules (peptides, proteins, nucleic acids) in addition to the drug itself could drive up cost significantly. Therefore, it is necessary to study cost-benefit issues when developing such systems for clinical use. Nevertheless, the recent developments in this area are exciting, and open up new directions in treating complex diseases with reduced side effects and improved efficacy.

Table 3.1 Summary of disease-responsive release mechanisms, with cited references (in-chapter reference list).

Mechanism	Description	References
pH-Responsive Materials	Includes hydrogels with the ability to swell or shrink in response to minor changes in pH, and micelles that destabilize according to pH, triggering release of encapsulated drug.	[2,6,20-22] Cancer: [85-88] Diabetes: [66,67]
pH-Dependent Hydrophilic to Hydrophobic Conversions	Systems release drug after undergoing conversion, using acid-degradable linkages, hydrolysable protecting groups, or pH-dependent solubility.	[19,23,24,26] Cancer: [25]
Ionically-Driven Drug Release Systems	Changes in ion concentration trigger release of drug.	[27,28]
Protein-Ligand Interactions	Addition of a specific protein that binds with an over expressed receptor increases drug accumulation at diseased tissue.	[36-39] Cancer: [37,40-48]
Hydrogels based on Antigen-Antibody Binding	A hydrogel network is formed by affinity binding between conjugated antigens and antibody. Introduction of free antigen disrupts the network, causing release of drug.	[50]
Enzyme Responsive Hydrogels	Hydrogel networks are formed with a cross-linker that is sensitive to an enzyme. The enzyme is either up-regulated in diseased tissue, or may be location-specific. Exposure to the enzyme causes network degradation and release of drug.	[2,3,46,54,55,59-63,96] Cancer: [4,59] Inflammatory Diseases: [58,99]
Enzyme Responsive Linkages	Enzyme sensitive linkages are used to tether drug to a polymer backbone or to a particle. The enzyme is either up-regulated in diseased tissue, or may be location-specific. Exposure to the enzyme causes release of the tethered drug.	[2,60,64,97] Infection: [99,101-103]
Enzyme Responsive Coatings or Membrane Structures	An enzyme sensitive coating is used to cover the surface of a porous particle with embedded drug, or solid drug particle. Upon enzyme exposure, the coating is degraded, triggering drug release. Also realized in micellar and liposomal formulations.	[65,94] Cancer: [55,60,63,89,91-93,95,104]
Systems Responding to Metabolic Products	Systems are designed to respond to metabolic products, usually via chemical reactions, including glucose, carbon dioxide, and glutathione.	[68] Diabetes: [66,67] Cancer: [69,70]

3.5 List of Abbreviations

BRENDA = Braunschweig Enzyme Database

CPCHIVtat = cationic polymer possessing a cleavage site for HIV-1 protease

DDS = drug delivery system

DOX = doxorubicin

ECM = extracellular matrix

EPR = enhanced permeation and retention

ExPASy = Expert Protein Analysis System

MMP = matrix metalloproteinase

PDB = Protein Data Bank

PEG = poly(ethylene glycol)

S-FIL = step and flash imprint lithography

sPLA2 = secretory phospholipase A2

UniPROBE = Universal PBM Resource for Oligonucleotide Binding Evaluation

3.6 References

[1] P. Bawa, V. Pillay, Y.E. Choonara, L.C. du Toit, Stimuli-responsive polymers and their applications in drug delivery, Biomed Mater. 4 (2009) 022001.

[2] M. Caldorera-Moore, N.A. Peppas, Micro- and nanotechnologies for intelligent and responsive biomaterial-based medical systems, Adv Drug Deliv Rev. 61 (2009) 1391–1401.

[3] T. Miyata, T. Uragami, K. Nakamae, Biomolecule-sensitive hydrogels, Adv Drug Deliv Rev. 54 (2002) 79–98.

[4] M. Caldorera-Moore, N. Guimard, L. Shi, K. Roy, Designer nanoparticles: incorporating size, shape and triggered release into nanoscale drug carriers, Expert Opin Drug Deliv. 7 (2010) 479–495.

[5] S. Ganta, H. Devalapally, A. Shahiwala, M. Amiji, A review of stimuli-responsive nanocarriers for drug and gene delivery, J Control Release. 126 (2008) 187–204.

[6] A.R. Khare, N.A. Peppas, Release behavior of bioactive agents from pH-sensitive hydrogels, J Biomater Sci Polym Ed. 4 (1993) 275–289.

[7] R. Langer, N. Peppas, Advances in biomaterials, drug delivery, and bionanotechnology, AIChE Journal. 49 (2003) 2990–3006.

[8] D.W.P.M. Löwik, E.H.P. Leunissen, M. van den Heuvel, M.B. Hansen, J.C.M. van Hest, Stimulus responsive peptide based materials, Chem Soc Rev. 39 (2010) 3394–3412.

[9] F. Meng, W. Hennink, Z. Zhong, Reduction-sensitive polymers and bioconjugates for biomedical applications, Biomaterials. (2009).

[10] O. Onaca, R. Enea, D.W. Hughes, W. Meier, Stimuli-responsive polymersomes as nanocarriers for drug and gene delivery, Macromolecular Bioscience. 9 (2009) 129–139.

[11] Y. Qiu, K. Park, Environment-sensitive hydrogels for drug delivery, Adv Drug Deliv Rev. 53 (2001) 321–339.

[12] D. Mudhakir, H. Harashima, Learning from the viral journey: how to enter cells and how to overcome intracellular barriers to reach the nucleus, The AAPS Journal. 11 (2009) 65–77.

[13] C.W. Pouton, K.M. Wagstaff, D.M. Roth, G.W. Moseley, D.A. Jans, Targeted delivery to the nucleus, Adv Drug Deliv Rev. 59 (2007) 698–717.

[14] D. Putnam, C.A. Gentry, D.W. Pack, R. Langer, Polymer-based gene delivery with low cytotoxicity by a unique balance of side-chain termini, Proc Natl Acad Sci U S A. 98 (2001) 1200–1205.

[15] R.P. Shaikh, V. Pillay, Y.E. Choonara, L.C. du Toit, V.M.K. Ndesendo, P. Bawa, et al., A review of multi-responsive membranous systems for rate-modulated drug delivery, AAPS PharmSciTech. 11 (2010) 441–459.

[16] D. Gallardo, B. Skalsky, P. Kleinebudde, Controlled release solid dosage forms using combinations of (meth)acrylate copolymers, Pharm Dev Technol. 13 (2008) 413–423.

[17] F. Liu, A.W. Basit, A paradigm shift in enteric coating: achieving rapid release in the proximal small intestine of man, J Control Release. 147 (2010) 242–245.

[18] O. Boussif, F. Lezoualc'h, M.A. Zanta, M.D. Mergny, D. Scherman, B. Demeneix, et al., A versatile vector for gene and oligonucleotide transfer into cells in culture and in vivo: polyethylenimine, Proc Natl Acad Sci U S A. 92 (1995) 7297–7301.

[19] R.M. Sawant, J.P. Hurley, S. Salmaso, A. Kale, E. Tolcheva, T.S. Levchenko, et al., “SMART” drug delivery systems: double-targeted pH-responsive pharmaceutical nanocarriers, Bioconjug Chem. 17 (2006) 943–949.

[20] A.R. Khare, N.A. Peppas, Swelling/deswelling of anionic copolymer gels, Biomaterials. 16 (1995) 559–567.

[21] W. Gao, J. Chan, O.C. Farokhzad, pH-responsive Nanoparticles for Drug Delivery, Mol Pharm. (2010).

[22] J.-O. You, D.T. Auguste, Feedback-regulated paclitaxel delivery based on poly(N,N-dimethylaminoethyl methacrylate-co-2-hydroxyethyl methacrylate) nanoparticles, Biomaterials. 29 (2008) 1950–1957.

[23] R.E. Johns, M.E.H. El-Sayed, V. Bulmus, J. Cuschieri, R. Maier, A.S. Hoffman, et al., Mechanistic analysis of macrophage response to IRAK-1 gene knockdown by a smart polymer-antisense oligonucleotide therapeutic, J Biomater Sci Polym Ed. 19 (2008) 1333–1346.

[24] N. Murthy, J. Campbell, N. Fausto, A.S. Hoffman, P.S. Stayton, Bioinspired pH-responsive polymers for the intracellular delivery of biomolecular drugs, Bioconjug Chem. 14 (2003) 412–419.

[25] A.P. Griset, J. Walpole, R. Liu, A. Gaffey, Y.L. Colson, M.W. Grinstaff, Expansile nanoparticles: synthesis, characterization, and in vivo efficacy of an acid-responsive polymeric drug delivery system, J Am Chem Soc. 131 (2009) 2469–2471.

[26] Y. Wu, J.A. MacKay, J.R. McDaniel, A. Chilkoti, R.L. Clark, Fabrication of elastin-like polypeptide nanoparticles for drug delivery by electrospraying, Biomacromolecules. 10 (2009) 19–24.

[27] T.Z. Grove, C.O. Osuji, J.D. Forster, E.R. Dufresne, L. Regan, Stimuli-Responsive Smart Gels Realized via Modular Protein Design, J Am Chem Soc. 132 (2010) 14024–14026.

[28] D. Velasco, C. Elvira, J. San Román, New stimuli-responsive polymers derived from morpholine and pyrrolidine, J Mater Sci Mater Med. 19 (2008) 1453–1458.

[29] A. Wijaya, S.B. Schaffer, I.G. Pallares, K. Hamad-Schifferli, Selective release of multiple DNA oligonucleotides from gold nanorods, ACS Nano. 3 (2009) 80–86.

[30] X. Huang, I.H. El-Sayed, W. Qian, M.A. El-Sayed, Cancer cells assemble and align gold nanorods conjugated to antibodies to produce highly enhanced, sharp, and polarized surface Raman spectra: a potential cancer diagnostic marker, Nano Lett. 7 (2007) 1591–1597.

[31] P. Chen, S. Mwakwari, A. Oyelere, Gold nanoparticles: From nanomedicine to nanosensing, Nanotechnology, Science and Applications. 1 (2008) 45–66.

[32] L. Fass, Imaging and cancer: a review, Molecular Oncology. 2 (2008) 115–152.

[33] M. Ferrari, Cancer nanotechnology: opportunities and challenges, Nature Reviews Cancer. 5 (2005) 161–171.

[34] B. Sumer, J. Gao, Theranostic nanomedicine for cancer, Nanomedicine (Lond). 3 (2008) 137–140.

[35] N. Portney, M. Ozkan, Nano-oncology: drug delivery, imaging, and sensing, Analytical and Bioanalytical Chemistry. 384 (2006) 620–630.

[36] A. Akinc, W. Querbes, S. De, J. Qin, M. Frank-Kamenetsky, K.N. Jayaprakash, et al., Targeted delivery of RNAi therapeutics with endogenous and exogenous ligand-based mechanisms, Mol Ther. 18 (2010) 1357–1364.

[37] D.R. Elias, Z. Cheng, A. Tsourkas, An Intein-Mediated Site-Specific Click Conjugation Strategy for Improved Tumor Targeting of Nanoparticle Systems, Small. (2010).

[38] A. Fakhari, A. Baoum, T.J. Siahaan, K.B. Le, C. Berkland, Controlling ligand surface density optimizes nanoparticle binding to ICAM-1, J Pharm Sci. (2010).

[39] G. Sarfati, T. Dvir, M. Elkabetz, R.N. Apte, S. Cohen, Targeting of polymeric nanoparticles to lung metastases by surface-attachment of YIGSR peptide from laminin, Biomaterials. (2010).

[40] E.M. Rezler, D.R. Khan, J. Lauer-Fields, M. Cudic, D. Baronas-Lowell, G.B. Fields, Targeted drug delivery utilizing protein-like molecular architecture, J Am Chem Soc. 129 (2007) 4961–4972.

[41] R.E. Eliaz, F.C. Szoka, Liposome-encapsulated doxorubicin targeted to CD44: a strategy to kill CD44-overexpressing tumor cells, Cancer Res. 61 (2001) 2592–2601.

[42] A.E. Faassen, J.A. Schrager, D.J. Klein, T.R. Oegema, J.R. Couchman, J.B. McCarthy, A cell surface chondroitin sulfate proteoglycan, immunologically related to CD44, is involved in type I collagen-mediated melanoma cell motility and invasion, J Cell Biol. 116 (1992) 521–531.

[43] A.E. Faassen, D.L. Mooradian, R.T. Tranquillo, R.B. Dickinson, P.C. Letourneau, T.R. Oegema, et al., Cell surface CD44-related chondroitin sulfate proteoglycan is required for transforming growth factor-beta-stimulated mouse melanoma cell motility and invasive behavior on type I collagen, J Cell Sci. 105 (Pt 2) (1993) 501–511.

[44] J.W. Park, D.B. Kirpotin, K. Hong, R. Shalaby, Y. Shao, U.B. Nielsen, et al., Tumor targeting using anti-her2 immunoliposomes, J Control Release. 74 (2001) 95–113.

[45] X. Li, L. Ding, Y. Xu, Y. Wang, Q. Ping, Targeted delivery of doxorubicin using stealth liposomes modified with transferrin, Int J Pharm. 373 (2009) 116–123.

[46] E. Cukierman, D.R. Khan, The benefits and challenges associated with the use of drug delivery systems in cancer therapy, Biochem Pharmacol. 80 (2010) 762–770.

[47] Y.-K. Kim, J.-T. Kwon, J.Y. Choi, H.-L. Jiang, R. Arote, D. Jere, et al., Suppression of tumor growth in xenograft model mice by programmed cell death 4 gene delivery using folate-PEG-baculovirus, Cancer Gene Therapy. 17 (2010) 751–760.

[48] T.A. Yap, C.P. Carden, S.B. Kaye, Beyond chemotherapy: targeted therapies in ovarian cancer, Nature Reviews Cancer. 9 (2009) 167–181.

[49] T. Miyata, N. Asami, T. Uragami, A reversibly antigen-responsive hydrogel, Nature. 399 (1999) 766–769.

[50] T. Miyata, M. Jige, T. Nakaminami, T. Uragami, Tumor marker-responsive behavior of gels prepared by biomolecular imprinting, Proc Natl Acad Sci U S A. 103 (2006) 1190–1193.

[51] M.E. Byrne, J.Z. Hilt, N.A. Peppas, Recognitive biomimetic networks with moiety imprinting for intelligent drug delivery, J Biomed Mater Res A. 84 (2008) 137–147.

[52] C.L. Bayer, A.A. Konuk, N.A. Peppas, Development of a protein sensing device utilizing interactions between polyaniline and a polymer acid dopant, Biomed Microdevices. 12 (2010) 435–442.

[53] M.E. Byrne, K. Park, N.A. Peppas, Molecular imprinting within hydrogels, Adv Drug Deliv Rev. 54 (2002) 149–161.

[54] N.A. Peppas, P. Bures, W. Leobandung, H. Ichikawa, Hydrogels in pharmaceutical formulations, Eur J Pharm Biopharm. 50 (2000) 27–46.

[55] D.G. Vartak, R.A. Gemeinhart, Matrix metalloproteases: underutilized targets for drug delivery, Journal of Drug Targeting. 15 (2007) 1–20.

[56] A.S. Gobin, J.L. West, Val-ala-pro-gly, an elastin-derived non-integrin ligand: Smooth muscle cell adhesion and specificity, J Biomed Mater Res. (2003).

[57] A.H. Zisch, M.P. Lutolf, J.A. Hubbell, Biopolymeric delivery matrices for angiogenic growth factors, Cardiovasc Pathol. 12 (2003) 295–310.

[58] A.A. Aimetti, A.J. Machen, K.S. Anseth, Poly(ethylene glycol) hydrogels formed by thiol-ene photopolymerization for enzyme-responsive protein delivery, Biomaterials. 30 (2009) 6048–6054.

[59] L.C. Glangchai, M. Caldorera-Moore, L. Shi, K. Roy, Nanoimprint lithography based fabrication of shape-specific, enzymatically-triggered smart nanoparticles, J Control Release. 125 (2008) 263–272.

[60] J.R. Tauro, B.-S. Lee, S.S. Lateef, R.A. Gemeinhart, Matrix metalloprotease selective peptide substrates cleavage within hydrogel matrices for cancer chemotherapy activation, Peptides. 29 (2008) 1965–1973.

[61] D. Baram, G. Vaday, P. Salamon, I. Drucker, R. Hershkoviz, Y. Mekori, Human mast cells release metalloproteinase-9 on contact with activated T cells: juxtacrine regulation by TNF-{alpha}, The Journal of Immunology. 167 (2001) 4008–4016.

[62] J.L. Simpson, R.J. Scott, M.J. Boyle, P.G. Gibson, Differential proteolytic enzyme activity in eosinophilic and neutrophilic asthma, Am J Respir Crit Care Med. 172 (2005) 559–565.

[63] J.R. Tauro, R.A. Gemeinhart, Extracellular protease activation of chemotherapeutics from hydrogel matrices: a new paradigm for local chemotherapy, Mol Pharm. 2 (2005) 435–438.

[64] T. Tokatlian, C.T. Shrum, W.M. Kadoya, T. Segura, Protease degradable tethers for controlled and cell-mediated release of nanoparticles in 2- and 3-dimensions, Biomaterials. 31 (2010) 8072–8080.

[65] P.D. Thornton, A. Heise, Highly specific dual enzyme-mediated payload release from peptide-coated silica particles, J Am Chem Soc. 132 (2010) 2024–2028.

[66] K. Podual, F.J. Doyle, N.A. Peppas, Dynamic behavior of glucose oxidase-containing microparticles of poly(ethylene glycol)-grafted cationic hydrogels in an environment of changing pH, Biomaterials. 21 (2000) 1439–1450.

[67] K. Podual, F.J. Doyle, N.A. Peppas, Glucose-sensitivity of glucose oxidase-containing cationic copolymer hydrogels having poly(ethylene glycol) grafts, J Control Release. 67 (2000) 9–17.

[68] S.S. Satav, S. Bhat, S. Thayumanavan, Feedback regulated drug delivery vehicles: carbon dioxide responsive cationic hydrogels for antidote release, Biomacromolecules. 11 (2010) 1735–1740.

[69] I.A. Solsona, R.B. Smith, C. Livingstone, J. Davis, Metabolic mimics: thiol responsive drug release, J Colloid Interface Sci. 302 (2006) 698–701.

[70] G.K. Balendiran, R. Dabur, D. Fraser, The role of glutathione in cancer, Cell Biochem Funct. 22 (2004) 343–352.

[71] H.M. Berman, J. Westbrook, Z. Feng, G. Gilliland, T.N. Bhat, H. Weissig, et al., The Protein Data Bank, Nucleic Acids Res. 28 (2000) 235–242.

[72] A. Chang, M. Scheer, A. Grote, I. Schomburg, D. Schomburg, BRENDA, AMENDA and FRENDA the enzyme information system: new content and tools in 2009, Nucleic Acids Res. 37 (2009) D588–92.

[73] E. Gasteiger, A. Gattiker, C. Hoogland, I. Ivanyi, R.D. Appel, A. Bairoch, ExPASy: The proteomics server for in-depth protein knowledge and analysis, Nucleic Acids Res. 31 (2003) 3784–3788.

[74] D.E. Newburger, M.L. Bulyk, UniPROBE: an online database of protein binding microarray data on protein-DNA interactions, Nucleic Acids Res. 37 (2009) D77–82.

[75] W.-K. Fong, T. Hanley, B.J. Boyd, Stimuli responsive liquid crystals provide “on-demand” drug delivery in vitro and in vivo, J Control Release. 135 (2009) 218–226.

[76] S.M. Janib, A.S. Moses, J.A. MacKay, Imaging and drug delivery using theranostic nanoparticles, Adv Drug Deliv Rev. (2010).

[77] Y.-P. Ho, K.W. Leong, Quantum dot-based theranostics, Nanoscale. 2 (2010) 60–68.

[78] P. Debbage, W. Jaschke, Molecular imaging with nanoparticles: giant roles for dwarf actors, Histochem Cell Biol. 130 (2008) 845–875.

[79] S. Del Vecchio, A. Zannetti, R. Fonti, L. Pace, M. Salvatore, Nuclear imaging in cancer theranostics, The Quarterly Journal of Nuclear Medicine and Molecular Imaging : Official Publication of the Italian Association of Nuclear Medicine (AIMN) [and] the International Association of Radiopharmacology (IAR), [and] Section of the Society of Radiopharmaceutical Chemistry and Biology. 51 (2007) 152–163.

[80] F.J. Picard, M.G. Bergeron, Rapid molecular theranostics in infectious diseases, Drug Discov Today. 7 (2002) 1092–1101.

[81] I. Gilham, T. Rowland, Predictive medicine: Potential benefits from the integration of diagnostics and pharmaceuticals, Journal of Medical Marketing. (2001).

[82] S.K. Parks, J. Chiche, J. Pouysségur, pH control mechanisms of tumor survival and growth, J Cell Physiol. (2010).

[83] V. Pavet, M.M. Portal, J.C. Moulin, R. Herbrecht, H. Gronemeyer, Towards novel paradigms for cancer therapy, Oncogene. (2010).

[84] Y. Shen, H. Tang, M. Radosz, E. Van Kirk, W.J. Murdoch, pH-responsive nanoparticles for cancer drug delivery, Methods Mol Biol. 437 (2008) 183–216.

[85] Z.G. Gao, D.H. Lee, D.I. Kim, Y.H. Bae, Doxorubicin loaded pH-sensitive micelle targeting acidic extracellular pH of human ovarian A2780 tumor in mice, Journal of Drug Targeting. 13 (2005) 391–397.

[86] E.S. Lee, H.J. Shin, K. Na, Y.H. Bae, Poly(L-histidine)-PEG block copolymer micelles and pH-induced destabilization, J Control Release. 90 (2003) 363–374.

[87] J. Ko, K. Park, Y.-S. Kim, M.S. Kim, J.K. Han, K. Kim, et al., Tumoral acidic extracellular pH targeting of pH-responsive MPEG-poly(beta-amino ester) block copolymer micelles for cancer therapy, J Control Release. 123 (2007) 109–115.

[88] D.S.W. Benoit, S.M. Henry, A.D. Shubin, A.S. Hoffman, P.S. Stayton, pH-responsive polymeric sirna carriers sensitize multidrug resistant ovarian cancer cells to doxorubicin via knockdown of polo-like kinase 1, Mol Pharm. 7 (2010) 442–455.

[89] T.L. Andresen, S.S. Jensen, T. Kaasgaard, K. Jørgensen, Triggered activation and release of liposomal prodrugs and drugs in cancer tissue by secretory phospholipase A2, Current Drug Delivery. 2 (2005) 353–362.

[90] M.A. Gertz, New targets and treatments in multiple myeloma: Src family kinases as central regulators of disease progression, Leuk Lymphoma. 49 (2008) 2240–2245.

[91] J.R. Tauro, R.A. Gemeinhart, Matrix metalloprotease triggered delivery of cancer chemotherapeutics from hydrogel matrixes, Bioconjug Chem. 16 (2005) 1133–1139.

[92] T. Kaasgaard, T.L. Andresen, S.S. Jensen, R.O. Holte, L.T. Jensen, K. Jørgensen, Liposomes containing alkylated methotrexate analogues for phospholipase A(2) mediated tumor targeted drug delivery, Chem Phys Lipids. 157 (2009) 94–103.

[93] P.J. Pedersen, S.K. Adolph, A.K. Subramanian, A. Arouri, T.L. Andresen, O.G. Mouritsen, et al., Liposomal formulation of retinoids designed for enzyme triggered release, J Med Chem. 53 (2010) 3782–3792.

[94] T.J. Harris, G. von Maltzahn, M.E. Lord, J.-H. Park, A. Agrawal, D.-H. Min, et al., Protease-triggered unveiling of bioactive nanoparticles, Small. 4 (2008) 1307–1312.

[95] H. Hatakeyama, H. Akita, K. Kogure, M. Oishi, Y. Nagasaki, Y. Kihira, et al., Development of a novel systemic gene delivery system for cancer therapy with a tumor-specific cleavable PEG-lipid, Gene Ther. 14 (2007) 68–77.

[96] J.A. Moss, S. Stokols, M.S. Hixon, F.T. Ashley, J.Y. Chang, K.D. Janda, Solid-phase synthesis and kinetic characterization of fluorogenic enzyme-degradable hydrogel cross-linkers, Biomacromolecules. 7 (2006) 1011–1016.

[97] E.-F. Moustoifa, M.-A. Alouini, A. Salaün, T. Berthelot, A. Bartegi, S. Albenque-Rubio, et al., Novel cyclopeptides for the design of MMP directed delivery devices: a novel smart delivery paradigm, Pharm Res. 27 (2010) 1713–1721.

[98] J. Wang, In vivo glucose monitoring: towards “Sense and Act” feedback-loop individualized medical systems, Talanta. 75 (2008) 636–641.

[99] D. Asai, A. Tsuchiya, J.-H. Kang, K. Kawamura, J. Oishi, T. Mori, et al., Inflammatory cell-specific transgene expression system responding to Ikappa-B kinase beta activation, J Gene Med. 11 (2009) 624–632.

[100] P.J. Barnes, Immunology of asthma and chronic obstructive pulmonary disease, Nature Reviews Immunology. 8 (2008) 183–192.

[101] Y. Suzuki, M. Tanihara, Y. Nishimura, K. Suzuki, Y. Kakimaru, Y. Shimizu, A new drug delivery system with controlled release of antibiotic only in the presence of infection, J Biomed Mater Res. 42 (1998) 112–116.

[102] D. Neut, O.S. Kluin, B.J. Crielaard, H.C. van der Mei, H.J. Busscher, D.W. Grijpma, A biodegradable antibiotic delivery system based on poly-(trimethylene carbonate) for the treatment of osteomyelitis, Acta Orthop. 80 (2009) 514–519.

[103] D. Asai, M. Kuramoto, Y. Shoji, J.-H. Kang, K.B. Kodama, K. Kawamura, et al., Specific transgene expression in HIV-infected cells using protease-cleavable transcription regulator, J Control Release. 141 (2010) 52–61.

[104] A. Beyerle, A. Braun, O. Merkel, F. Koch, T. Kissel, T. Stoeger, Comparative in vivo study of poly(ethylene imine)/siRNA complexes for pulmonary delivery in mice, J Control Release. 151 (2011) 51–56.

Chapter 4: Development of Enzyme-Responsive Hydrogel Networks using Michael Addition Reactions

4.1 INTRODUCTION

This chapter focuses on the development of enzyme-responsive hydrogel networks that have been formed using Michael addition reactions (Specific Aim 1A). Hydrogel compositions were designed to consist of a combination of multi-armed or multi-branched polymer cross-linked with an enzyme-specific peptide sequence, as popularized by the Hubbell group [1-6]. For this specific Michael addition chemistry, the reactive groups were chosen to be acrylates and sulfhydryls [7]. Polymers explored were poly(ethylene glycol), or PEG, and chitosan. Peptides were designed to be sensitive to trypsin for cost-efficient proof-of-concept studies. The approach to the design of components and the feasibility studies carried out are laid out in Figure 4.1.

4.1.1 Stimuli-Responsive Hydrogel Networks

4.1.1.1 Currently available stimuli-responsive networks

Stimuli sensitive hydrogels have been developed as 'smart' drug delivery systems and biomimetic tissue engineering scaffolds to sense environmental changes and induce a structural change or degradation [2,8-17]. Temperature and pH sensitive hydrogels can be used for site-specific delivery. Biomolecule-sensitive hydrogels have been used to deliver drugs when in contact with glucose or specific antigens [11,13]. There are also hydrogels that are sensitive to light, magnetic field, and ultrasound [12,13]. However, physiologically site-specific responsive gels have not been incorporated for pulmonary drug delivery.

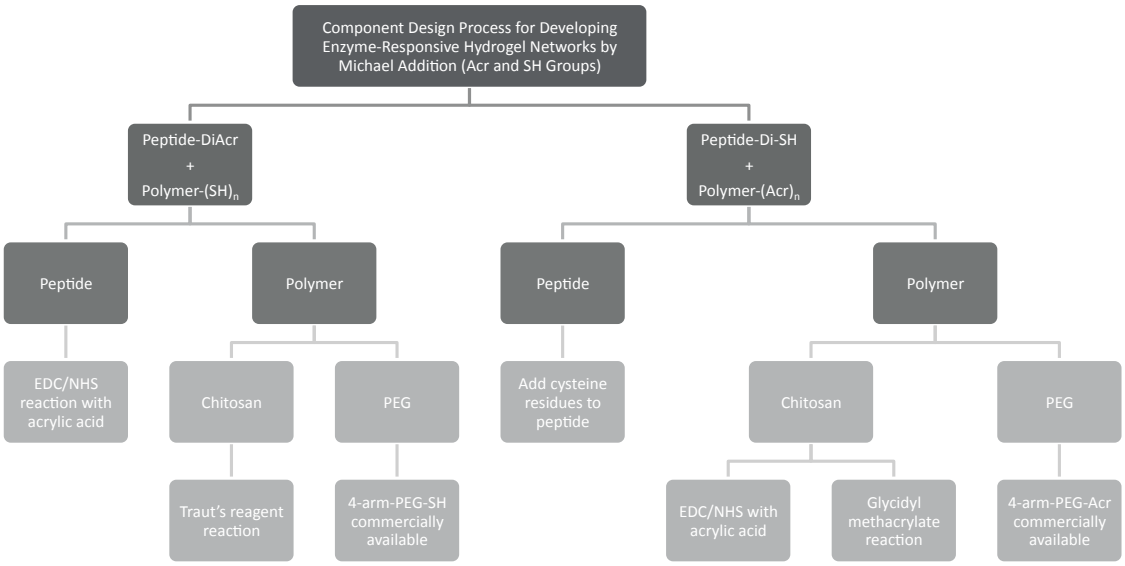

Figure 4.1 Approach to component design and feasibility studies in development of enzyme-responsive hydrogel networks

4.1.1.2 Enzyme-responsive networks

For a bolus dose at a target location, an enzymatically degradable polymer carrier could be advantageous. This is because enzymatic cleavage is highly specific and could be tailored for certain diseased tissues where specific enzymes are up regulated. A series of enzymatically degradable hydrogels, specifically designed to mimic the extracellular matrix (ECM) in tissue engineering applications, have been extensively reported [9,10,14]. These designs contain a peptide linkage either in the backbone of the polymer or as a cross-linking agent that is degraded by the presence of tissue-specific enzymes (e.g. collagenase, elastase or MMPs). A key relevant finding in these studies, reported by Hubbell and colleagues [1] was the highly specific enzyme-controlled release of recombinant human bone morphogenetic protein (rhBMP). West and co-workers [10] showed the differential degradation kinetics of these gels in the presence of various

concentrations of the peptide-specific enzymes (collagenase or elastase). Their results indicated that the hydrogels do not degrade in the absence of enzymes, while rapid degradation can be achieved by optimizing the enzyme concentrations. These studies demonstrate the possibility that similar peptide-based hydrogels could be used to control drug release from micro- and nanoparticle carriers.

4.1.2 Michael addition reactions

Polymeric delivery systems have exhibited the potential for controlled release and protection of protein therapeutics; however, ideal polymer systems for broad use with a wide variety of proteins are yet to be developed. Although the classic poly(lactide-co-glycolide) (PLGA) or polyanhydride-based systems have demonstrated suitable delivery characteristics, these systems may often cause protein denaturation due to the fabrication conditions, degradation characteristics or hydrophobicity [18-20]. A number of hydrogel materials have also been characterized as hydrophilic delivery systems, which greatly decreases the foreign body response as compared to hydrophobic materials. Typically, the protein and polymer are in the same solution, allowing the polymer network to form around the proteins. However, many of the proposed hydrogel networks are formed in a way such that the polymer reacts with the protein, or network formation requires initiation by radiation, UV light, or high temperatures that may also denature the protein [1-6,19,21].

Michael addition reactions for the formation of hydrogel networks with encapsulated proteins have been recently developed using reactions between acrylate and thiol groups on a number of different synthetic and natural polymers, including PEG, PVA, dextrans, hyaluronic acid, and chitosan [7,22]. This allows rapid initiation of

polymerization or cross-linking at physiological temperature and pH, and under aqueous conditions. Reactions between acrylate and thiol groups on the polymers occur much more quickly than with the chemical groups found on proteins, thus eliminating possible covalent modification of protein, which may hinder its release rate or bioactivity. Hydrogel swelling and degradation typically drive the release of protein, with variations in cross-linking density and molecular weights between cross-links offering tailor-ability in protein release rates [2,8-17,19-24].

As previously mentioned, the Michael addition reaction proceeds under mild conditions; it occurs in aqueous conditions at physiological temperature and pH, although a slightly basic pH will accelerate the reaction. Reactions are between a Michael donor, the nucleophile, and a Michael acceptor, the electrophile. Some other common Michael reactions occur with amines, vinyl-sulfones, and maleimides [7,11,13,21,25].

The Michael reaction used in this work is between a sulfhydryl and acrylate group. The slightly basic buffer creates a thiolate anion, which then reacts with the acrylate. For example, using a multi-armed polymer acrylate and a di-sulfhydryl peptide, this reaction yields a cross-linked network structure, or hydrogel network. In this case, the sulfhydryl group acts as the Michael donor, and the acrylate group is the Michael acceptor. The specific reaction scheme, as well as an illustration of the hydrogel cross-linking reaction, is shown in Figure 4.2.

4.1.3 Choice of Biocompatible Polymers

Two different polymers were chosen to evaluate in feasibility studies to form these enzyme-degradable hydrogel networks: chitosan and poly(ethylene glycol). Chitosan is a polysaccharide, and functional groups would need to be added as side

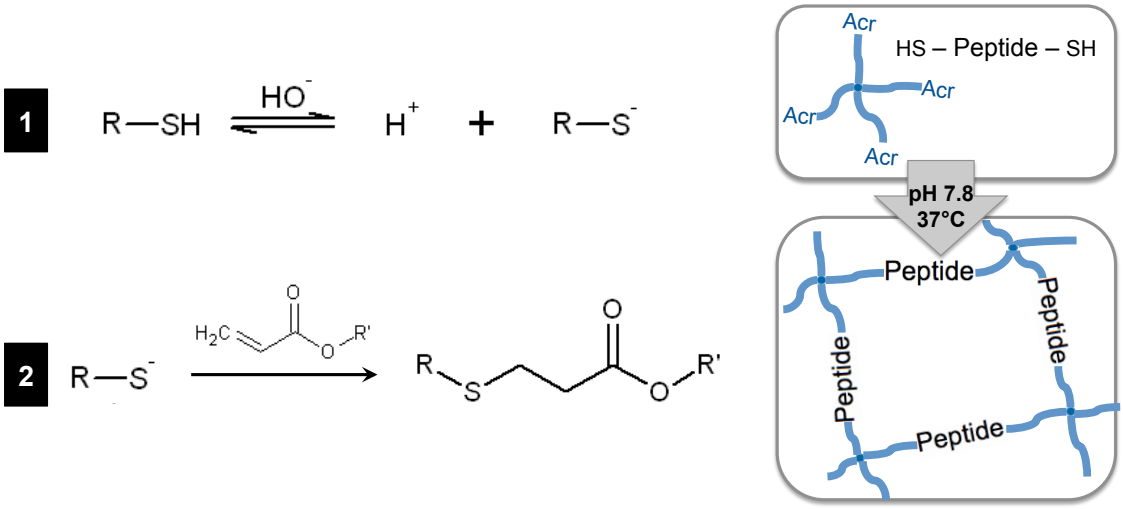

Figure 4.2 Michael addition reaction scheme and illustration of hydrogel network cross-linking

functional groups to the monomer units ("multi-branched" or "multi-functionalized"). Poly(ethylene glycol), or PEG, is commercially available in multi-armed, dendrimer-like configurations. The terminal groups of these multi-armed PEGs can be functionalized with a variety of reactive moieties. Figure 4.3 shows an illustrated schematic of the Michael addition cross-linking for the different types of polymers (multi-branched or multi-armed) used.

4.1.3.2 Chitosan

Chitosan is a biodegradable and biocompatible polysaccharide that is inexpensive and readily available. It is currently FDA approved for use as a haemostatic bandage due to rapid blood clotting capabilities. Chitosan has also been widely studied as a drug and gene delivery vehicle due to its mucoadhesive and cationic properties. It is comprised of β 1-4 linked units of glucosamine and N-acetyl glucosamine and has been shown to have

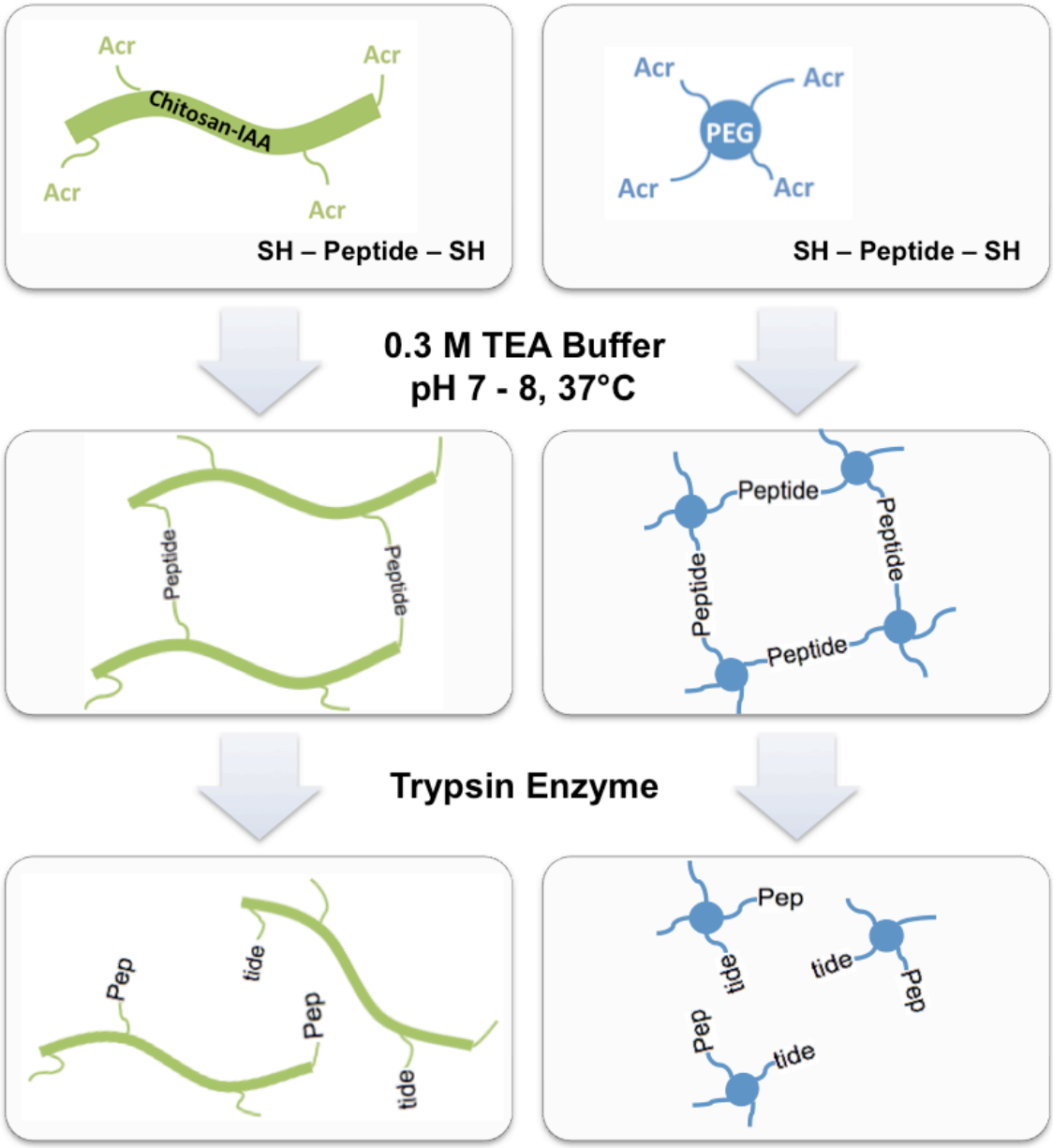

Figure 4.3 Schematic representing Michael addition based crosslinking of polymers and enzymatic degradation of the peptide

minimal cytotoxicity. Chitosan has been crosslinked into a number of hybrid hydrogels for encapsulation of various macromolecular drugs for oral, intranasal, and intravenous delivery. For the purposes of mucosal delivery, mucoadhesive and enhanced paracellular permeability properties of chitosan have been well established that could increase bioavailability of various drugs, while maintaining low cytotoxicity [12,13,22,26-37].

4.1.3.3 Poly(ethylene glycol)

Poly(ethylene glycol) has long been a staple biomaterial in drug delivery applications, both as a covalently-attached molecule, and as a hydrogel-based protective drug carrier. PEG is non-toxic, non-immunogenic, non-antigenic, hydrophilic, and FDA-approved [9,10,14,38,39]. Due to its widespread use in a number of biomaterial applications, it is widely available in a variety of molecular weights and a number of functionalized forms, including multi-armed PEGs, and acrylate or thiol-containing groups. PEG has been used in numerous hydrogels, especially with hybrid components, for applications in drug and contrast agent delivery and tissue engineering scaffolds [1,19,21,38,39].

4.2 Materials and Methods

4.2.1 Materials

Four-armed poly(ethylene glycol) acrylate with a molecular weight of approximately 10,000 kDa or 20,000 kDa was purchased from Laysan Bio (Arab, AL). Protasan (chitosan salt) was purchased from Novamatrix (Sandvika, Norway). Chitosan oligosaccharide lactate, trypsin from bovine pancreas (USP grade, >2500 USP units per mg), 2-carboxyethyl acrylate, acrylic acid, glycidyl methacrylate, and triethylamine were

purchased from Sigma-Aldrich (St. Louis, MO). EDC, Sulfo-NHS, and snakeskin dialysis tubing were purchased from Pierce/Thermo Fisher Scientific (Rockford, IL). Float-a-Lyzer dialysis tubes were purchased from Spectrum Labs (Rancho Dominguez, CA).

4.2.2 Design of enzyme-responsive peptide cross-linker

For this body of work, as a proof-of-concept, peptides that are sensitive to the enzyme trypsin were used for cost-efficiency. Trypsin cleaves non-specifically at the terminal carbon of the amino acids lysine and arginine, either of which may be incorporated into the peptide sequence in to provide specificity for degradation and release in response to trypsin. Varying sequence lengths may be used to vary the pore size of the resulting hydrogel, thus giving the option to tailor for different molecular weight peptide and protein drugs. In general, however, sequences were kept below 10 amino acids.

Two approaches were taken for the design of these peptide cross-linkers: (1) naturally-inspired peptide sequences, or (2) rationally-designed synthetic sequences. Naturally-inspired peptide sequences may offer improved biocompatibility, whereas rationally-designed sequences may be intelligently designed using the wealth of knowledge in enzyme/substrate bioinformatics databases.

4.2.2.1 Design of naturally-derived peptide sequences

For naturally-inspired peptide sequences, the human protein hemoglobin A (HbA) was used as the peptide design base. The protein was plotted on a Kyte-Doolittle/Hopp-Woods scale to determine regions of hydrophobicity and hydrophilicity. All hydrophobic

regions were removed from consideration, as hydrophobic sequences would be unlikely to easily incorporate into a hydrophilic hydrogel. Sequences were then run through a model protein cutter for trypsin [10,40], and those with the least specificity removed from consideration. Top candidates with a size range of 5-7 amino acids were then run through careful NCBI BLAST (National Center for Biotechnology Information Basic Local Alignment Search Tool) sequence analysis for exclusion of those bearing similarity to toxic and/or apoptotic peptide sequences. Remaining sequences were evaluated for primary amines (arginine, glutamine, lysine, and asparagine) for further bioconjugation of acrylate groups, or cysteine residues, which contain a sulfhydryl group.

4.2.2.2 Design of rationally-designed synthetic peptides

For rationally designed sequences, data was collected on trypsin activity and preferential cleavage sites using the BRaunshweig ENzyme Database (BRENDA) [18-20,41]. As previously mentioned, trypsin cleaves terminal to either arginine or lysine residues in a peptide/protein sequence. Glycine was used as spacer amino acids, due to its minimal steric hindrance, surrounding the trypsin cleavage site. Cysteine residues were added at the alpha and terminal residue sites to provide sulfhydryl reactive groups for the Michael addition cross-linking. Sequences were checked for hydrophilicity, using the Hopp-Woods and Kyte-Doolittle scales. Other optimization considerations could include (1) the use of arginine over lysine, because arginine is more effective at lowering the pKa of sulfhydryl groups, accelerating the cross-linking reaction, and (2) use of glutamic acid, which inhibits disulfide bond formation, maintaining stoichiometric ratios required for the reaction [7].

4.2.3 Synthesis of the peptide cross-linker

Peptide synthesis was performed at The University of Texas at Austin Institute for Cellular and Molecular Biology in the Protein Microanalysis Facility (Austin, TX) by custom peptide order. Following initial studies, custom peptide orders (up to one gram) were then obtained from CHI Scientific (Maynard, MA) at 95% purity, verified by mass spectrometry.

4.2.4 Confirmation of peptide cross-linker degradability

Trypsin digestion of the designed peptide sequences was confirmed by liquid chromatography-mass spectrometry (LC-MS) using an in-solution trypsin digestion protocol. Briefly, a 50 µl sample of 50 picomole/µl peptide in 100 mM ammonium bicarbonate at pH 8.5 was prepared for digestion. 0.1 µl of trypsin was dissolved in 1 mM HCl to a concentration of 1 mg/ml and added to the peptide solution. The mixture was then placed in an incubator on a rotator at 37°C, and samples were collected for HPLC and MALDI analysis at 2, 4, 6, and 12 hours to quantify digested fragments. A control group (without trypsin) was also analyzed for comparison.

4.2.5 Modification of peptide cross-linker with acrylate groups

Peptides for crosslinking with thiol polymers were QVRAHGK and KGHGKK. The di-acrylation of these peptides at the α-amine and terminal lysine amine was accomplished using EDC/Sulfo-NHS (1-Ethyl-3-[3-dimethylaminopropyl]carbodiimide hydrochloride; N-hydroxysulfosuccinimide) chemistry. First, 25mg of peptide was dissolved into 2mL de-ionized water. A four to eight molar excess of acrylic acid, EDC, and Sulfo-NHS was reacted to create an amine reactive NHS-ester-acrylate. The reaction

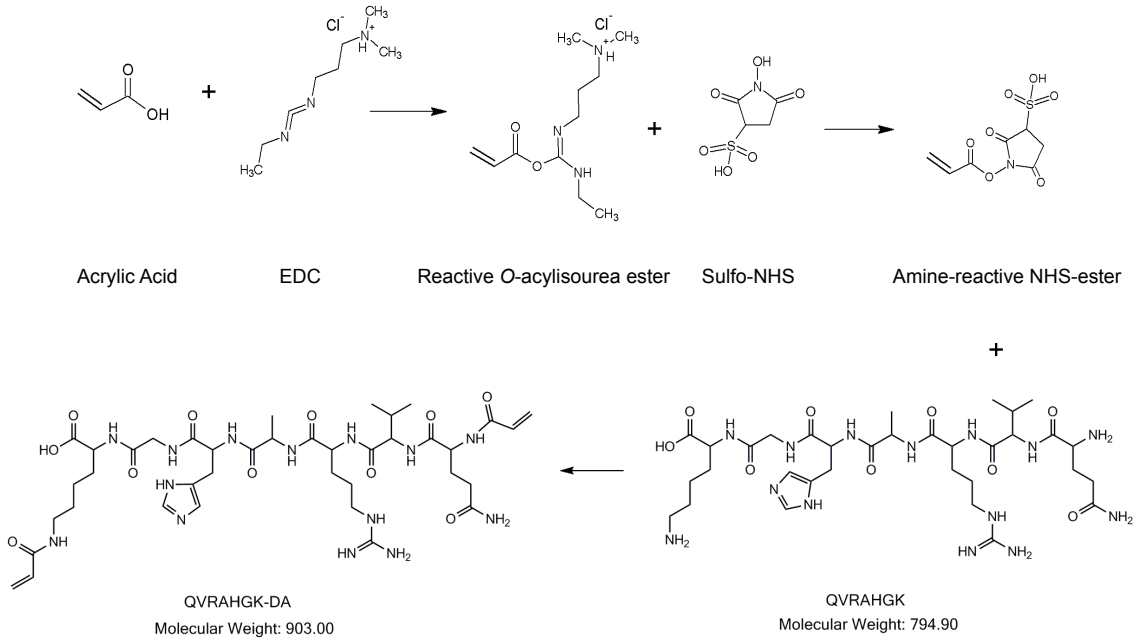

Figure 4.4 Reaction scheme for acrylation of amine-containing peptide (QVRAHGK) using EDC/NHS chemistry (top half of image courtesy of Mary Caldorera-Moore)

was run for 2 hrs at room temperature while stirring, then titrated up to the pKa of the target amine, added to the peptide solution, and reacted for 2 hrs at room temperature while stirring. The solution was subsequently dialyzed for 48 hours in de-ionized water using a 500 MW cutoff Float-a-Lyzer dialysis tube, followed by snap freezing, lyophilization, and ^{1}H NMR analysis to evaluate degree of acrylation.

4.2.6 Modification of chitosan with acrylate groups by EDC/NHS chemistry

The grafting of acrylate groups to chitosan was carried out using EDC and Sulfo-NHS (1-Ethyl-3-[3-dimethylaminopropyl]carbodiimide hydrochloride; N-hydroxysulfosuccinimide) chemistry with acrylic acid and/or 2-carboxyethyl acrylate.

Both acrylic acid and 2-carboxyethyl acrylate contain carboxyl groups, which may be grafted onto the primary amine groups of chitosan (de-acetylated). Briefly, chitosan was dissolved in 80-100 ml deionized water and pH adjusted to 4.75. Acrylic acid or Carboxyethyl acrylate (1.5 mL) was added to EDC and Sulfo-NHS to create an amine reactive NHS-ester with an acrylate group. Reaction components were mixed at varying molar ratios. The reaction was run for 2 hours at room temperature while stirring, added to the chitosan, and allowed to react for 4-8 hours at room temperature (in the dark) while stirring. Finally, dialysis was performed using snakeskin dialysis tubing for 24 hours with the following cycles: 3 times for 2 hours against 5 mM HCl buffer, followed by 3 cycles of 6 hours in length against de-ionized water. Dialyzed product was lyophilized to remove water. Acrylate substitution was confirmed and percent degree of substitution (DS) was determined using NMR [22].

4.2.7 Modification of chitosan with acrylate groups using glycidyl methacrylate

Chitosan was modified with methacrylate groups by reaction with glycidyl methacrylate and triethylamine, in which the hydroxyl group on the chitosan monomer units are reacted (both acetylated and de-acetylated monomer). Figure 4.5 shows the reaction scheme and procedure. Briefly, chitosan was dissolved into a solution of up to 40% acetone at a concentration of 10 mg/mL by high-speed vortexing, and allowed to stir for an additional hour. A 20 M excess of triethylamine was then added to the solution and allowed to react for two hours while stirring, followed by addition of 20 M excess of glycidyl methacylate, which was reacted for 24 hours with stirring. The resulting solution was then placed on dialysis (snakeskin dialysis tubing) over 48 hours against three washes of 5mM HCl and three washes of de-ionized water. The sample was then snap

frozen in liquid nitrogen, lyophilized for 48 hours, and then analyzed by ^{1}H NMR to confirm the degree of substitution.

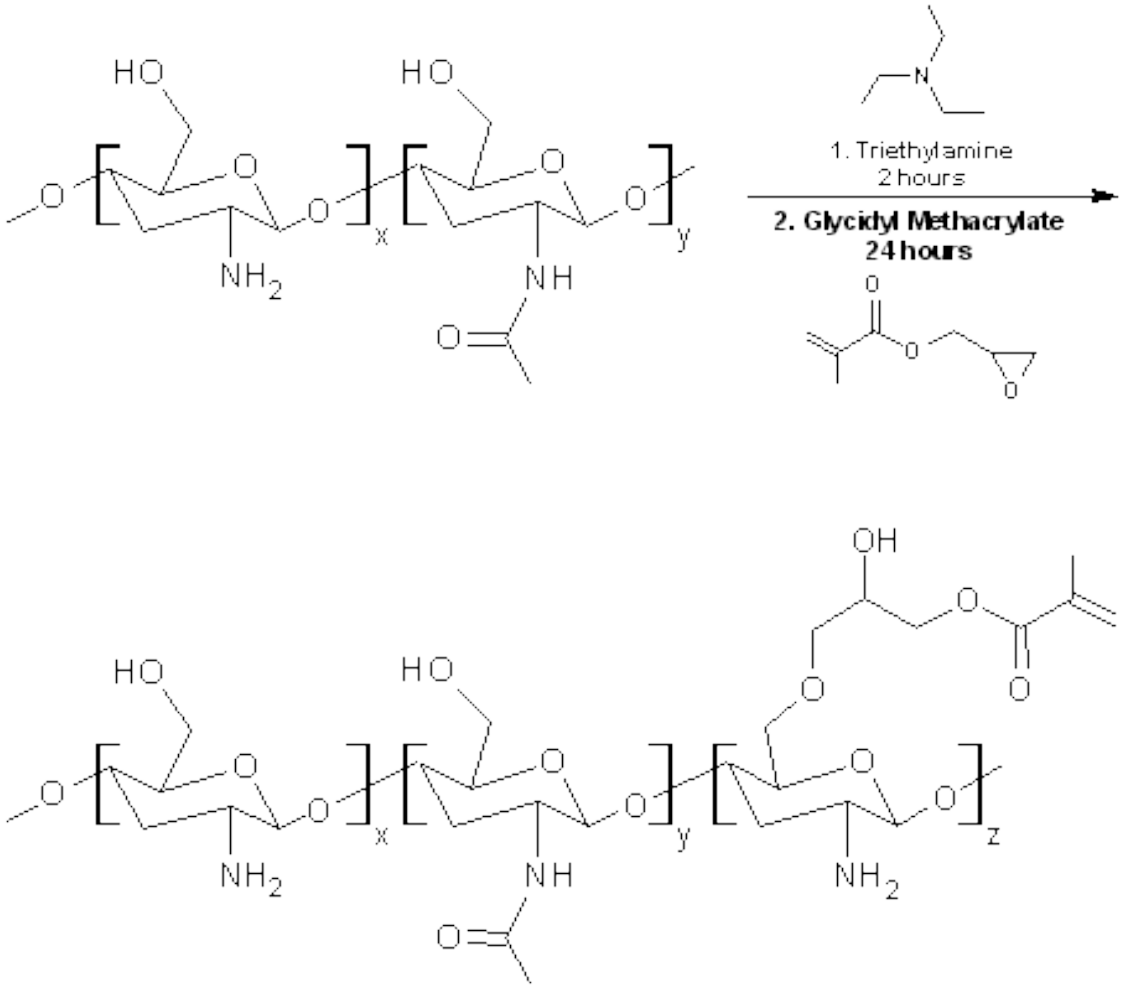

Figure 4.5 Reaction scheme for conjugation of methacrylate groups to chitosan by reaction with triethylamine and glycidyl methacrylate

4.2.8 Michael addition cross-linking of polymer with enzymatically-responsive peptides

In order to crosslink the polymer with the enzymatically-responsive peptide, a Michael's addition reaction between acrylate and sulfhydryl groups was employed. Multi-armed polymers with acrylate groups and peptides with sulfhydryl groups were dissolved separately in 0.3 molar triethanolamine (TEA) buffers, or 1X phosphate buffered saline (PBS), ranging from pH 7.4 to 8.15. Solutions were then combined in a 1:1 acrylate to sulfhydryl ratio in varying concentrations and incubated at 37°C to react. Varying concentrations of polymer and peptide were explored, and expressed as a total combined percent weight by volume:

$$\text{Hydrogel } \%\ {}^{w}\!/_{v} = \frac{(\text{weight of polymer, grams}) + (\text{weight of peptide, grams})}{\text{milliliter of solution}} \times 100\%$$

4.3 Results and Discussion

4.3.1 Design of enzyme-responsive peptide cross-linker

4.3.1.1 Design of naturally-derived peptides

Peptide sequences derived from human hemoglobin subunits were analyzed for trypsin responsiveness, hydrophillicity, and functional groups on terminal amino acids. The sequences were then subjected to BLAST analysis for detrimental physiological impacts. The sequences found to suit all these requirements were QVRAHGK (glutamine-valine-arginine-alanine-histidine-glycine-lysine) and KGHGKK (lysine-glycine-histidine-glycine-lysine-lysine). These peptides have amine terminal groups that may be modified with acrylate groups, as described earlier, such that they may be used to cross-link sulfhydryl-containing polymers into hydrogels.

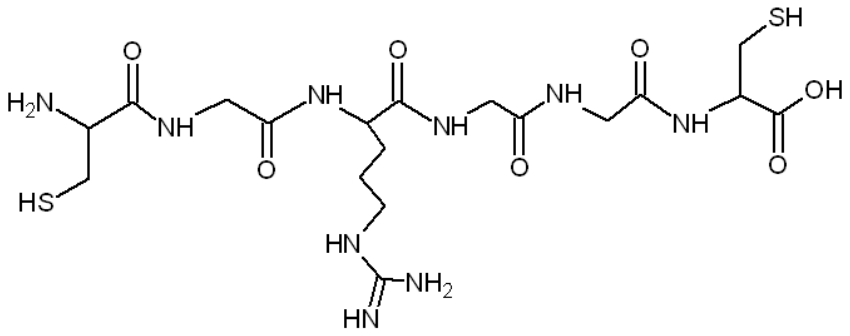

Figure 4.6 Chemical structure of CGRGGC peptide

4.3.1.2 Design of rationally-designed synthetic peptides

A second set of peptide sequences, containing terminal cysteine residues (for sulfhydryl groups) for Michael-addition cross-linking, were also designed for trypsin responsiveness, least steric hindrance surrounding the trypsin cleavage site, hydrophillicity, functional groups on terminal amino acids, and BLAST analysis. The sequences that met all the conditions were CGRGGC (cysteine-glycine-arginine-glycine-glycine-cysteine, Figure 4.6) and CGKGGC (cysteine-glycine-lysine-glycine-glycine-cysteine).

4.3.2 Confirmation of peptide cross-linker degradability

Results for the digestion of the QVRAHGK sequence after 12 hours are shown in Figure 4.7. Analysis of the control group shows the peak fractions are primarily composed of the un-digested peptide (795 Da and 398 x 2 = 796 Da for doubly-charged peptide). The trypsin-digested group exhibits peak fractions primarily composed of QVRA, QVR, and K fragments (429 Da, 355 Da, and 149 Da, respectively), confirming predicted degradation.

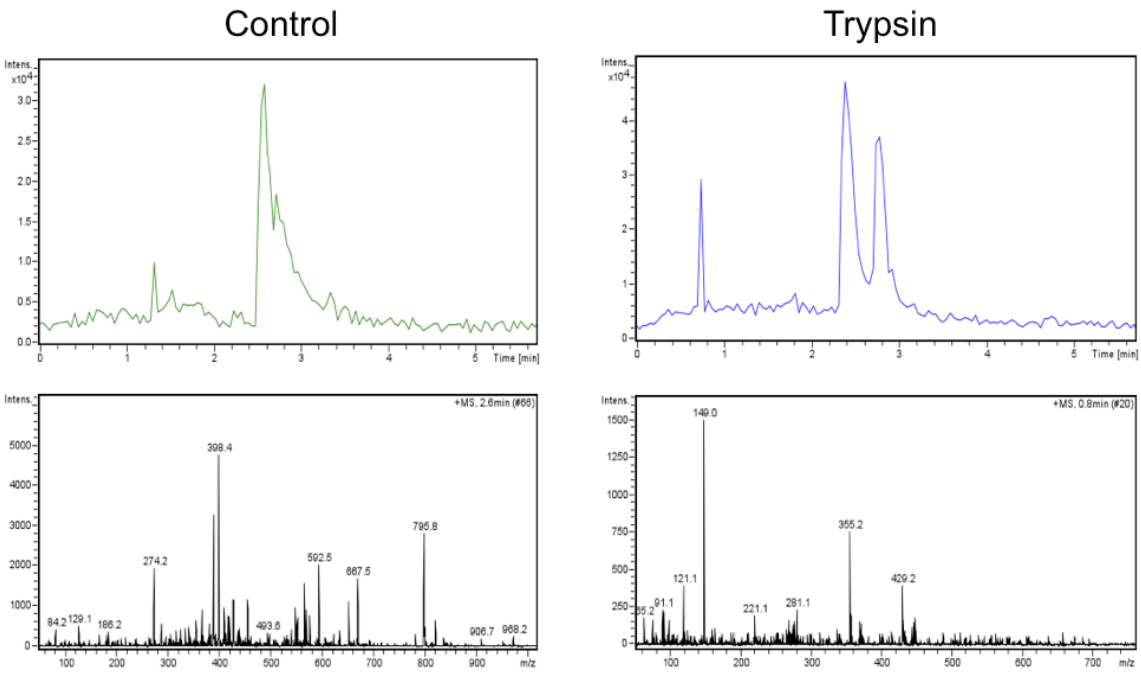

Figure 4.7 Digestion of QVRAHGK peptide by trypsin confirmed by HPLC.

4.3.3 Modification of peptide cross-linkers with acrylate groups

Di-acrylation of both peptides was achieved, as indicated by the ^{1}H NMR spectra shown in Figure 4.8. However, despite pH-based optimization (towards pKa of targeted amines) and varying molar ratios, the highest di-acrylation achieved was a degree of substitution (average) up to 1.75. This indicates that a significant portion of peptide had only one acrylate substitution, which would affect hydrogel cross-linking. Another possible reaction scheme would involve the side chain primary amines on the center arginine/lysine (trypsin cleavage site) being modified with acrylate groups. This is problematic in that it may prevent full cleavage of the hydrogel by trypsin.

With these results, it became apparent that the most feasible pathway to continue was to use cysteine-containing peptides (with sulfhydryl groups) to react with acrylated polymers. Thus, successful peptide synthesis would result in two readily available sulfhydryl groups per peptide, without the need for further modification (as well as peptide loss through modification and purification).

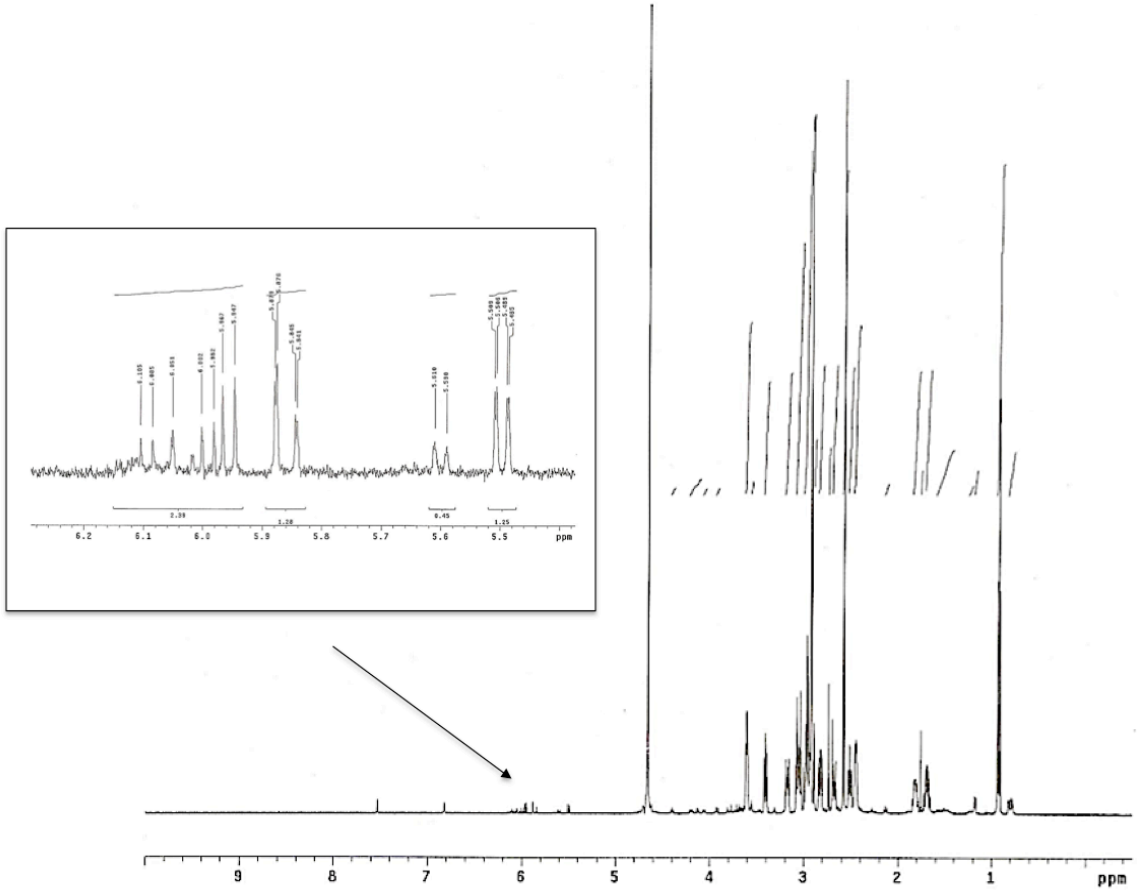

Figure 4.8 NMR spectra for di-acrylated QVRAHGK peptide (acrylate groups magnified within the inset figure)

4.3.4 Modification of chitosan with acrylate groups by EDC/NHS chemistry

Addition of acrylate groups to chitosan, carried out using EDC/NHS chemistry, was successful, as verified by a sample ^{1}H NMR shown in Figure 4.9. However, the presence of several other unexplained peaks, despite careful dialysis and methodically varying molar ratios in the reaction, indicated the presence of other side reactions and polymerizations. This method was therefore not continued, and other methods (namely, glycidyl methacrylation of chitosan) were explored.

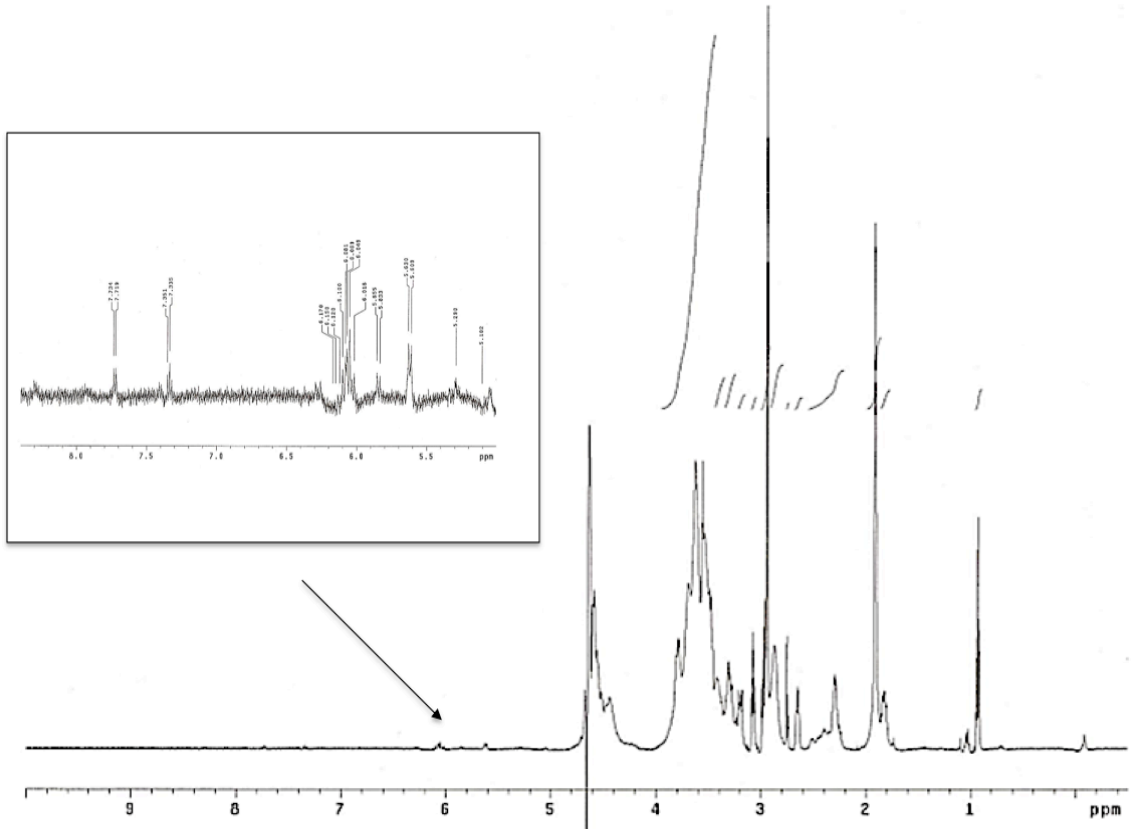

Figure 4.9 ^{1}H NMR spectra for chitosan modified with acrylate groups by EDC/NHS chemistry (magnified spectra shown in inset window)

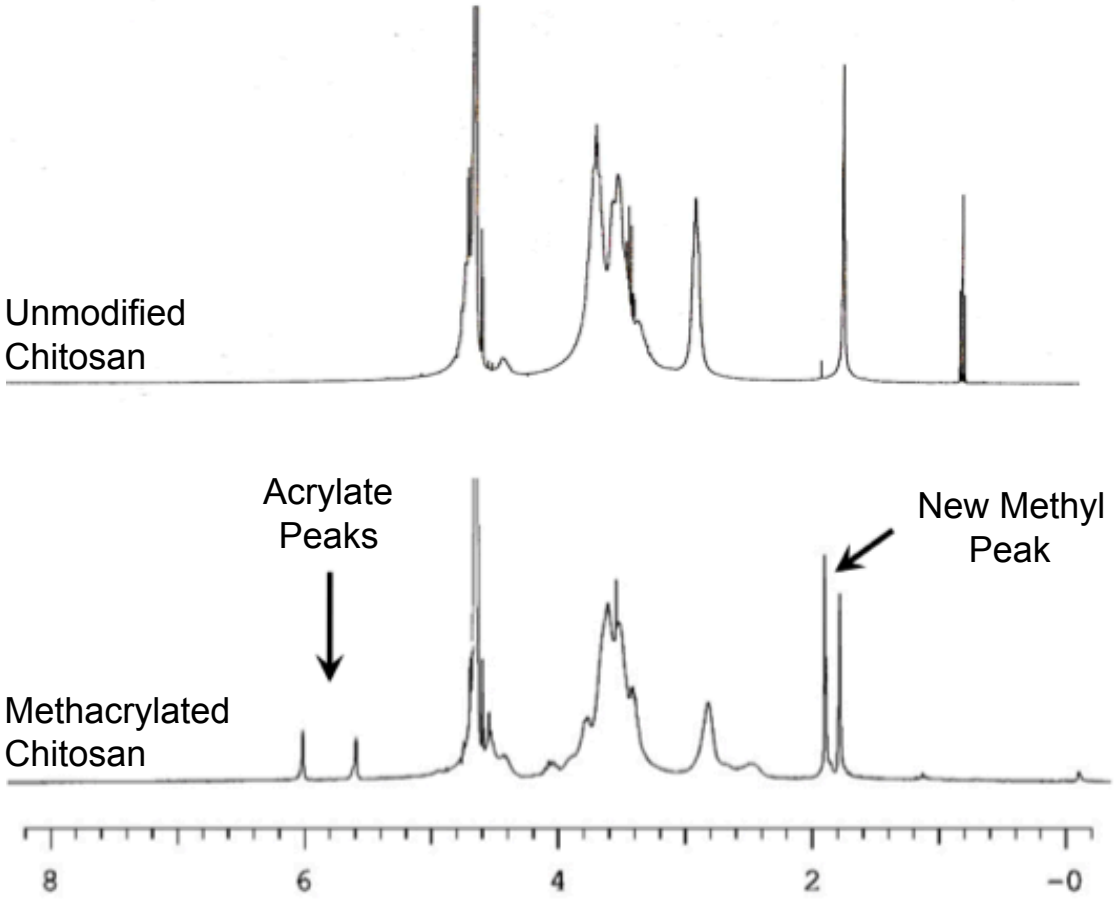

Figure 4.10 ^{1}H NMR spectra for chitosan modified with methacrylate groups by reaction with triethylamine and glycidyl methacrylate

4.3.5 Modification of chitosan with glycidyl methacrylate

As discussed above, another method for modification of chitosan with acrylate groups, to produce cleaner products, was desired. A new modification scheme for the methacrylation of chitosan, using triethylamine and glycidyl methacrylate, was developed based on methacrylation schmes for hyaluronic acid [42]. With this reaction, the methacrylate group is added onto the hydroxyl group, rather than amine groups. This

allows for the possibility of greater degrees of substitution, as every chitosan monomer subunit contains a hydroxyl group. In contrast, the presence of primary amines on chitosan (for EDC/NHS reaction) depends on the degree of deacetylation of the chitosan (from chitin).

Using this protocol, degrees of substitution up to 21% were achieved, as was confirmed by ^{1}H NMR. Figure 4.10 displays the NMR spectra of unmodified chitosan in contrast with the methacrylated chitosan spectra below. Methacrylate peaks are clearly visible in the 5.5-6.5 ppm range.

4.3.6 Michael addition cross-linking of polymer with enzymatically-responsive peptides

Gel formation between CGRGGC and 4-arm-PEG-acrylate was observed within 15 minutes in all samples in TEA buffer. TEA buffered samples in the range of pH 7.6 and higher began forming gels at room temperature, prior to putting into the incubator. However, the samples remained incubated overnight to ensure complete reaction. Samples in PBS primarily formed loose or inconsistent gels, and were not used. Figure 4.11 shows a sample of these hydrogels formed in 0.3M TEA buffer at pH 8.15. Little to no gel was formed in 2-8% w/v, loose gels formed in 10-12% w/v, and stiffer gels formed at 14-20% w/v.

Gel formation between CGRGGC and methacrylated chitosan was wholly unsuccessful, with only loose and inconsistent gels being formed. In large part, the issue was that the methacrylated chitosan proved difficult to dissolve into solution. Chitosan is already quite viscous and difficult to work with, and the addition of methyl groups likely resulted in even greater hydrophobicity. The chitosan portion of this project was therefore not continued.

Preliminary characterization studies of 20, 40, 60, and 80% (w/v) gels composed of PEG-4-Acr (MW 20kDa) and CGRGGC peptide showed that the gels did not completely hydrolytically degrade until days 5, 9, 9, and 11, respectively, when left in PBS pH 7.4 at 37°C (Figure 4.12).

Higher percent composition gels displayed the greatest structural integrity, longest time before hydrolytic degradation, and tightest theoretical network (to maintain drug encapsulation), while still displaying high swelling behavior. Gels of 80% composition, though possible to make, had practical issues in handling and synthesis, due to the high viscosity of precursor solutions. Therefore, moving forward, 60% w/v composition hydrogels were chosen to move forward into the particle synthesis phase of Aim 1.

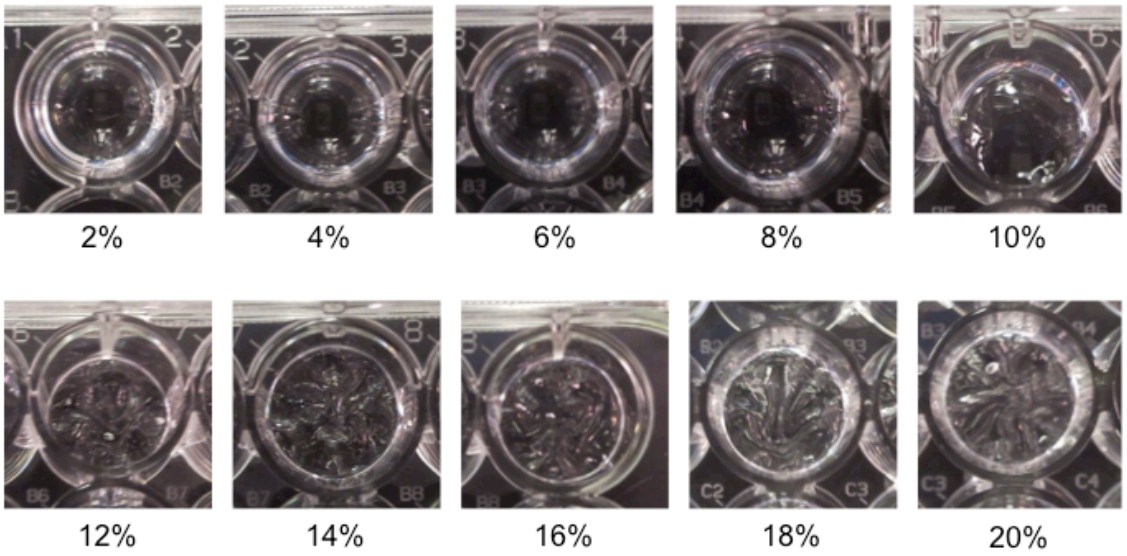

Figure 4.11 Bulk enzymatically-degradable microgels formed by Michael addition between PEG-4-Acr and CGRGGC peptide of various percent weight by volume composition

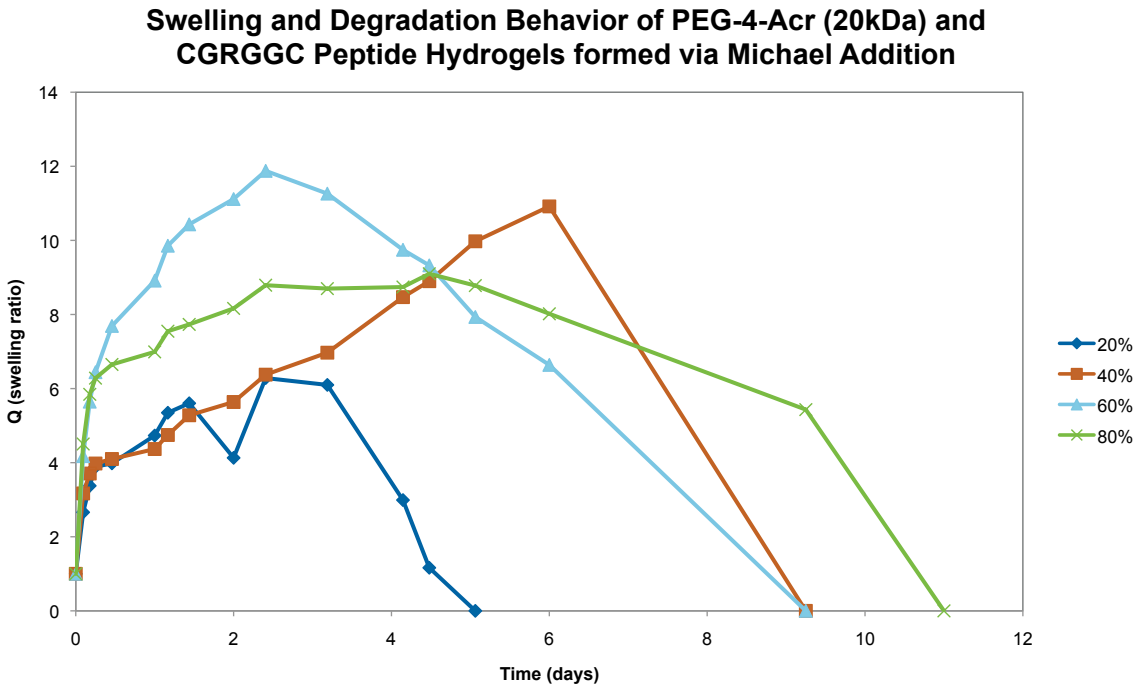

Figure 4.12 Swelling and degradation behavior of PEG-4-Acr and CGRGGC peptide hydrogels formed via Michael addition

4.4 CONCLUSIONS

Through the series of experiments shown here, it was concluded that the optimized hydrogel composition moving forward into Aim 1B would consist of the following:

- 4-arm Poly(ethylene glycol) acrylate
- CGRGGC peptide
- 60% w/v gel composition
- 0.3M triethanolamine buffer at pH 7.6 or higher

4.5 REFERENCES

[1] M.P. Lutolf, F.E. Weber, H.G. Schmoekel, J.C. Schense, T. Kohler, R. Müller, et al., Repair of bone defects using synthetic mimetics of collagenous extracellular matrices, Nat Biotechnol. 21 (2003) 513–518.

[2] M. Lutolf, J.A. Hubbell, Synthesis and physicochemical characterization of end-linked poly(ethylene glycol)-co-peptide hydrogels formed by Michael-type addition, Biomacromolecules. 4 (2003) 713–722.

[3] M.P. Lutolf, J.L. Lauer-Fields, H.G. Schmoekel, A.T. Metters, F.E. Weber, G.B. Fields, et al., Synthetic matrix metalloproteinase-sensitive hydrogels for the conduction of tissue regeneration: engineering cell-invasion characteristics, Proc Natl Acad Sci U S A. 100 (2003) 5413–5418.

[4] M. Lutolf, N. Tirelli, S. Cerritelli, L. Cavalli, J.A. Hubbell, Systematic modulation of Michael-type reactivity of thiols through the use of charged amino acids, Bioconjug Chem. 12 (2001) 1051–1056.

[5] J. Patterson, J.A. Hubbell, Enhanced proteolytic degradation of molecularly engineered PEG hydrogels in response to MMP-1 and MMP-2, Biomaterials. 31 (2010) 7836–7845.

[6] J. Patterson, J.A. Hubbell, SPARC-derived protease substrates to enhance the plasmin sensitivity of molecularly engineered PEG hydrogels, Biomaterials. 32 (2011) 1301–1310.

[7] B. Mather, K. Viswanathan, K. Miller, T. Long, Michael addition reactions in macromolecular design for emerging technologies, Prog Polym Sci. 31 (2006) 487–531.

[8] M. Ehrbar, A. Metters, P. Zammaretti, J.A. Hubbell, A.H. Zisch, Endothelial cell proliferation and progenitor maturation by fibrin-bound VEGF variants with

differential susceptibilities to local cellular activity, J Control Release. 101 (2005) 93–109.

[9] A.S. Gobin, J.L. West, Cell migration through defined, synthetic ECM analogs, Faseb J. 16 (2002) 751–753.

[10] B.K. Mann, A.S. Gobin, A.T. Tsai, R.H. Schmedlen, J.L. West, Smooth muscle cell growth in photopolymerized hydrogels with cell adhesive and proteolytically degradable domains: synthetic ECM analogs for tissue engineering, Biomaterials. 22 (2001) 3045–3051.

[11] T. Miyata, T. Uragami, K. Nakamae, Biomolecule-sensitive hydrogels, Adv Drug Deliv Rev. 54 (2002) 79–98.

[12] N.A. Peppas, P. Bures, W. Leobandung, H. Ichikawa, Hydrogels in pharmaceutical formulations, Eur J Pharm Biopharm. 50 (2000) 27–46.

[13] Y. Qiu, K. Park, Environment-sensitive hydrogels for drug delivery, Adv Drug Deliv Rev. 53 (2001) 321–339.

[14] D. Seliktar, A.H. Zisch, M.P. Lutolf, J.L. Wrana, J.A. Hubbell, MMP-2 sensitive, VEGF-bearing bioactive hydrogels for promotion of vascular healing, J Biomed Mater Res A. 68 (2004) 704–716.

[15] L. Urech, A.G. Bittermann, J.A. Hubbell, H. Hall, Mechanical properties, proteolytic degradability and biological modifications affect angiogenic process extension into native and modified fibrin matrices in vitro, Biomaterials. 26 (2005) 1369–1379.

[16] B.-S. Kim, S.W. Park, P.T. Hammond, Hydrogen-bonding layer-by-layer-assembled biodegradable polymeric micelles as drug delivery vehicles from surfaces, ACS Nano. 2 (2008) 386–392.

[17] M. Xiong, M. Forrest, A. Karls, G. Kwon, Biotin-Triggered Release of Poly (ethylene glycol)– Avidin from Biotinylated Polyethylenimine …, Bioconjug Chem. (2007).

[18] M. Ehrbar, S.C. Rizzi, R.G. Schoenmakers, B.S. Miguel, J.A. Hubbell, F.E. Weber, et al., Biomolecular hydrogels formed and degraded via site-specific enzymatic reactions, Biomacromolecules. 8 (2007) 3000–3007.

[19] D.L. Elbert, A.B. Pratt, M.P. Lutolf, S. Halstenberg, J.A. Hubbell, Protein delivery from materials formed by self-selective conjugate addition reactions, J Control Release. 76 (2001) 11–25.

[20] S.K. Hahn, J.S. Kim, T. Shimobouji, Injectable hyaluronic acid microhydrogels for controlled release formulation of erythropoietin, J Biomed Mater Res A. 80 (2007) 916–924.

[21] A. Metters, J.A. Hubbell, Network formation and degradation behavior of hydrogels formed by Michael-type addition reactions, Biomacromolecules. 6 (2005) 290–301.

[22] M.-S. Kim, Y.-J. Choi, I. Noh, G. Tae, Synthesis and characterization of in situ chitosan-based hydrogel via grafting of carboxyethyl acrylate, J Biomed Mater Res A. 83 (2007) 674–682.

[23] D.P. Huynh, M.K. Nguyen, B.S. Pi, M.S. Kim, S.Y. Chae, K.C. Lee, et al., Functionalized injectable hydrogels for controlled insulin delivery, Biomaterials. 29 (2008) 2527–2534.

[24] C. He, S.W. Kim, D.S. Lee, In situ gelling stimuli-sensitive block copolymer hydrogels for drug delivery, J Control Release. 127 (2008) 189–207.

[25] B.N. Naidu, M.E. Sorenson, T.P. Connolly, Y. Ueda, Michael addition of amines and thiols to dehydroalanine amides: a remarkable rate acceleration in water, J Org Chem. 68 (2003) 10098–10102.

[26] J. Shim, Y. Nho, Preparation of poly (acrylic acid)-chitosan hydrogels by gamma irradiation and in vitro drug release, Journal of Applied Polymer Science. (2003).

[27] M. George, T. Abraham, Polyionic hydrocolloids for the intestinal delivery of protein drugs: Alginate and chitosan—a review, J Control Release. (2006).

[28] J. Grant, M. Blicker, M. Piquette-Miller, C. Allen, Hybrid films from blends of chitosan and egg phosphatidylcholine for localized delivery of …, J Pharm Sci. (2005).

[29] D. Lee, W. Zhang, S. Shirley, X. Kong, G. Hellermann, Thiolated Chitosan/DNA Nanocomplexes Exhibit Enhanced and Sustained Gene Delivery, Pharm Res. (2007).

[30] H. Mao, K. Roy, Chitosan-DNA nanoparticles as gene carriers - synthesis characterization and transfection efficiency, J Control Release. (2001) 23.

[31] K. Roy, H. Mao, S. Huang, Oral gene delivery with chitosan-DNA nanoparticles generates immunologic protection in a murine model of peanut allergy, Nature Medicine. 5 (1999) 5.

[32] N. Schipper, K. Vårum, P. Artursson, Chitosans as absorption enhancers for poorly absorbable drugs. 1: Influence of molecular weight and degree of acetylation on drug transport across human intestinal epithelial (Caco-2) cells, Pharm Res. 13 (1996) 1686–1692.

[33] N. Schipper, S. Olsson, J. Hoogstraate, A. deBoer, K. Vårum, P. Artursson, Chitosans as absorption enhancers for poorly absorbable drugs 2: mechanism of absorption enhancement, Pharm Res. 14 (1997) 923–929.

[34] N. Schipper, K. Vårum, P. Stenberg, G. Ocklind, H. Lennernäs, P. Artursson, Chitosans as absorption enhancers of poorly absorbable drugs 3: Influence of mucus on absorption enhancement, Eur J Pharm Sci. 8 (1999) 335–343.

[35] H. Ta, C. Dass, D. Dunstan, Injectable chitosan hydrogels for localised cancer therapy, J Control Release. (2008).

[36] L. Verestiuc, O. Nastasescu, E. Barbu, I. Sarvaiya, K.L. Green, J. Tsibouklis, Functionalized chitosan/NIPAM (HEMA) hybrid polymer networks as inserts for ocular drug delivery: Synthesis,in vitro assessment, andin vivo evaluation, J Biomed Mater Res A. 77A (2006) 726–735.

[37] M.R. Rekha, C.P. Sharma, Synthesis and evaluation of lauryl succinyl chitosan particles towards oral insulin delivery and absorption, J Control Release. 135 (2009) 144–151.

[38] N.A. Peppas, K.B. Keys, M. Torres-Lugo, A.M. Lowman, Poly(ethylene glycol)-containing hydrogels in drug delivery, J Control Release. 62 (1999) 81–87.

[39] F.M. Veronese, G. Pasut, PEGylation, successful approach to drug delivery, Drug Discov Today. 10 (2005) 1451–1458.

[40] E. Gasteiger, A. Gattiker, C. Hoogland, I. Ivanyi, R.D. Appel, A. Bairoch, ExPASy: The proteomics server for in-depth protein knowledge and analysis, Nucleic Acids Res. 31 (2003) 3784–3788.

[41] A. Chang, M. Scheer, A. Grote, I. Schomburg, D. Schomburg, BRENDA, AMENDA and FRENDA the enzyme information system: new content and tools in 2009, Nucleic Acids Res. 37 (2009) D588–92.

[42] S. Suri, C.E. Schmidt, Cell-laden hydrogel constructs of hyaluronic acid, collagen, and laminin for neural tissue engineering, Tissue Engineering Part A. 16 (2010) 1703–1716.

Chapter 5: Development of the Michael Addition During Emulsion (MADE) Method for Fabricating Enzyme-Responsive Microgels

5.1 INTRODUCTION

As described in the preceding chapters, enzymatically-degradable hydrogels offer several engineered material advantages over other types of polymers used in drug delivery today. Furthermore, the ability to perform polymerization cross-linking of these types of hydrogels under mild conditions, using a Michael addition cross-linking reaction, makes these materials ideal candidates for next generation drug vehicles. The ability to scale this hydrogel synthesis method down to create microgels would be a significant step forward in the development of disease-responsive carriers for biologic drugs delivered via non-invasive routes.

This chapter consists of a collection of preliminary data from feasibility and optimization studies on several particle synthesis methods, from cryomilling to molding, before arriving at the optimized Michael Addition During Emulsion (MADE) synthesis method. In-depth characterization of the microgels is discussed in the following chapter.

5.1.1 Design Criteria

Taking several of the same criteria from the previous chapter, the design criteria for the microgel synthesis method included:

- optimum Michael addition reaction conditions (physiological pH and temperature)
- maintain bioactivity of biologic drugs using mild manufacturing techniques.

However, several new criteria were also considered in order to create the ideal particle synthesis method:

- size range of approximately 1-5 μm
- efficient recovery after synthesis
- low residual volume or material loss during synthesis
- stability and shelf life
- high-throughput
- high encapsulation efficiency
- low cost for start-up and continuous operation.

5.1.2 Context and Perspective

When work on this portion of the project began, it was not clear that the ultimate use of these particles would be for pulmonary drug delivery. It was first determined that feasibility studies should be done to see if hydrogel microparticles could be formed using Michael addition chemistry, and in what size range. Other primary uses considered, besides pulmonary delivery, included oral delivery of proteins and responsive release of growth factors in tissue engineering systems. Therefore, many of the methods for forming particles discussed throughout this chapter were not ideal methods to fabricate particles in the 1-5 micron range (optimal aerodynamic range). Additionally, many of these methods were developed and tested concurrently, until one clear "winner" began to emerge. At that point, all time and resources were diverted to development in that area.

5.2 Materials and Methods

5.2.1 Materials

Peptide sequence QVRAHGK was custom synthesized by the University of Texas at Austin, Institute for Cellular and Molecular Biology, Protein Microanalysis Facility (Austin, TX). Peptide sequence CGRGGC was custom synthesized by CHI Scientific (Maynard, MA). All 4-arm PEG products were purchased from Laysan Bio (Arab, AL). Trypsin from bovine pancreas and paraffin oil was purchased from Sigma Aldrich (St. Louis, MO). All other reagents were of at least USP or biological grade, and were purchased from either Sigma Aldrich (St. Louis, MO) or Thermo Fisher Scientific (Waltham, MA).

5.2.2 Trial and Error: Other Particle Synthesis Methods

5.2.2.1 Micron Mesh Molding

Hydrogel pre-cursor solution consisting of 20% total w/v of 4-arm poly(ethylene glycol) sulfhydryl (PEG-4-SH, 20kDa molecular weight) and di-acrylated QVRAHGK (or PEG di-acrylate, 3400 Da molecular weight) peptide was spread onto a glass slide into a thin layer. A nylon mesh screen with a 64 μm pore size was then pressed onto the thin polymer solution. The set-up was placed inside a humidity chamber at 37°C for 4 hours or overnight. The resulting patterned hydrogel particles, affixed to the slide, were then viewed under the microscope. Particles were removed from the slide by scraping, and any leftover residual layer was broken up to release the particles by stirring in de-ionized water for several hours.

5.2.2.2 Mortar and Pestle Grinding Under Liquid Nitrogen

Hydrogels were made by combining 4-arm poly(ethylene glycol) acrylate (PEG-4-Acr, 20 kDa molecular weight) with CGRGGC peptide in 0.3M TEA buffer at pH 8.15 at a 20% w/v composition. The mixture was incubated at 37°C for four hours. The resulting hydrogel was then removed from the reaction vessel, placed in a mortar, and submerged in liquid nitrogen until frozen through (about 1 minute). A pestle was used to crush the hydrogel for approximately 3 minutes, replenishing liquid nitrogen about once per minute. The resulting crushed hydrogel particles were recovered from the mortar using 3ml of 1% poly(vinyl alcohol), or PVA, in de-ionized water. The use of liquid nitrogen was required make the hydrogel brittle enough to break apart.

5.2.2.3 Cryogenic Milling

Hydrogels (500 mg each) were pre-prepared as above in section 5.2.2.2 . The resulting gels were cut into ¼ inch pieces, snap frozen in liquid nitrogen, and lyophilized for 48 hours. Using a SPEX Sample Prep (Metuchen, NJ) 6870 Freezer/Mill, the following cycles were programmed and run:

- 10 minute pre-cooling in liquid nitrogen
- 2 minute milling at a rate of 10 cycles per second (20 impacts per second)
- 2 minute re-cooling
- Repeated for 8 cycles

The chamber and impactor were then placed in a 37°C water bath for 1 hour to equilibrate in temperature, avoiding condensation when opening the chamber. Resulting particles were then collected from the milling chamber. One additional optional step was to place the sample on an orbital shaker for 48 hours to break up clumps.

5.2.2.4 Reactive Spray Drying

Peptide-crosslinked microparticles will be obtained by spraying the macromer precursor solutions through the nozzle (0.7 mm diameter) of a spray dryer (co-current flow type) model Mini Spray Dryer Büchi B-191 (Büchi Labortechnik AG, Flawil, Switzerland) as mentioned elsewhere62,63. In spray drying, the inlet air temperature with the polymer spray is usually around 100°C, which is intended to quickly evaporate off all water in the particles. However, we want to ensure protection of the peptide and model drug IFN-β from high temperature denaturation; thus a cooler injection temperature of 60°C is proposed and will be optimized. The conditions of the spray-drying process will involve following parameters: inlet air temperature 60°C; outlet air temperature 60°C; pump ratio 13%; aspirator ratio 73%; flow control 400/600 l/h and spray rate of feed about 8 ml/min. Following parameters will be extensively optimized in the process: crosslinking density (% w/v), effect of solution pH (7-8.5), air flow speed, and temperature. We hypothesize that Spray dryer temperature at 60°C should allow for quick formation of microparticles and also quickly dry them to prevent any aggregation in the collection chamber. The dried (or semi-dried) microparticles will be harvested from the apparatus collector and kept under vacuum for 24-48 hours at room temperature for complete drying.

5.2.2.5 Handheld Nebulization

As a proof-of-concept, microparticle fabrication, using the 4 arm PEG-SH and the acrylated peptide was performed using a Valois handheld nasal-spray type nebulizer. Briefly, 200µl of polymer and peptide in 0.3M TEA buffer at pH 8.15 was fed into the nebulizer inlet. The solution was sprayed onto a clean hydrophobic surface at 37°C, or a

shallow bath of warm paraffin oil, allowed to react for 3 hours, vacuum-dried overnight, and harvested using a scraper.

5.2.3 Michael Addition During Emulsion (MADE) Method for Microgel Synthesis

5.2.3.1 Choice of Surfactants

Several surfactants were tested out in the course of this study to determine which worked best with different types of emulsions. Surfactants included poly(vinyl alcohol) and several in the Brij, Tween, and Span family.

Several surfactant combination recipes were also used. For the water-in-paraffin oil emulsion, a hydrophilic-lipophilic balance (HLB) ranging from four to six was desired [1,2]. To determine concentrations of each component surfactant, the following equation was solved for each combination:

$$\text{HLB of surfactant mixture} = \Sigma \chi_s \times \text{HLB}_s$$

where χ_s is the weight fraction of each surfactant, and HLB_s is its corresponding HLB. Apart from varying the HLB and surfactant combinations, different percent compositions of surfactant in the emulsion were also considered, ranging from 0.01% to 3%.

Surfactant mixtures were eliminated using a method adopted by Fisher and Peppas [3]. Briefly, the stability of test emulsions, consisting of 0.3M TEA buffer and paraffin oil, were observed under light microscopy (40x). Following homogenization, a sample of the emulsion was placed on a glass slide with a coverslip and observed. If a high incidence of droplet coalescence was observed within 1 minute, the emulsion was considered unstable.

5.2.3.2 Choice of Emulsion Oil

Two types of "oil," or organic, solvents were considered for the emulsion process: (1) evaporative, or (2) viscous, non-evaporative. Namely, dichloromethane (DCM) was chosen as an evaporative "oil" to facilitate the removal of the oil phase after the emulsion. On the other hand, evaporative organic solvents tend to have low viscosities, and it was postulated that a viscous oil could contribute towards stabilizing the emulsion. Therefore, paraffin oil was chosen as the viscous, non-evaporative oil. A ratio of 15 mL oil to 100 μL water/aqeous phase was set and maintained for all experiments (15 mL is the minimum operating volume for a 50 mL Corning® centrifuge tube with the particular homogenizer used).

5.2.3.3 Other Optimization Parameters

Aside from varying the surfactant composition and emulsion oil, other parameters for optimization included the pH of reaction buffer (0.3M TEA), homogenization speed, and washing steps.

5.2.3.4 MADE Basic Protocol

Equimolar amounts (sulfhydryl:acrylate) of peptide and PEG-4-acr were dissolved separately into 0.3 M triethanolamine buffer to a total combined concentration of 60% (w/v), in a total volume of 100 μL. The two solutions were combined, mixed, and added to 15 mL of paraffin oil with varying surfactant combinations and concentrations. The entire mixture was then immersed in a hot water bath at 40–45 °C and homogenized for 3 min at 3000-5000 rpm using a Polytron PT 3100 homogenizer. The resulting

surfactant-stabilized water-in-oil emulsion was incubated for at least 2 hours at 37 °C to allow the cross-linking reaction to complete, forming solid, cross-linked, micro-sized hydrogels (microgels). Thus, as the reaction proceeds, the mixture becomes a suspension of solid microgels in oil, rather than an emulsion. These microgels were removed from oil, residual surfactant, and un-reacted material by a series of centrifugal washes with fresh oil and water. Briefly, microgels were centrifuged at 10,000×g for 20 min, supernatant discarded, re-suspended in de-ionized water, and vortexed. The process was repeated three times, with the final re-suspension in either de-ionized water, phosphate buffered saline, or 100 mM ammonium bicarbonate (depending on the buffer required for various assays).

5.2.4 Microgel Degradation

Hydrogel microparticles were allowed to re-hydrate in 40mM ammonium bicarbonate in a 37°C incubator for one hour (if previously dried). 100 µL of 1 mg/mL Trypsin (in 1mM hydrochloric acid) was added to hydrogel particles in 900 µL ammonium bicarbonate for a final solution of 90% 40mM ammonium bicarbonate and 10% hydrochloric acid (final concentration of 0.1 mg/mL Trypsin), and placed in a 37°C incubator with shaking. Control samples without enzyme contained the same ratio of ammonium bicarbonate/hydrocholoric acid solution. Samples were observed at various time points for particle degradation.

5.3 Results and Discussion

5.3.1 Trial and Error: Other Methods

5.3.1.1 Micron Mesh Molding

Hydrogels were successfully molded into micron-scale features, as shown in Figure 5.1. Figure 5.2 displays the trypsin-mediated degradation of these microparticle features on the slides after only two hours. Particles remain affixed to the slide surface in these images. Using this method, the particles would often remain interconnected due to a

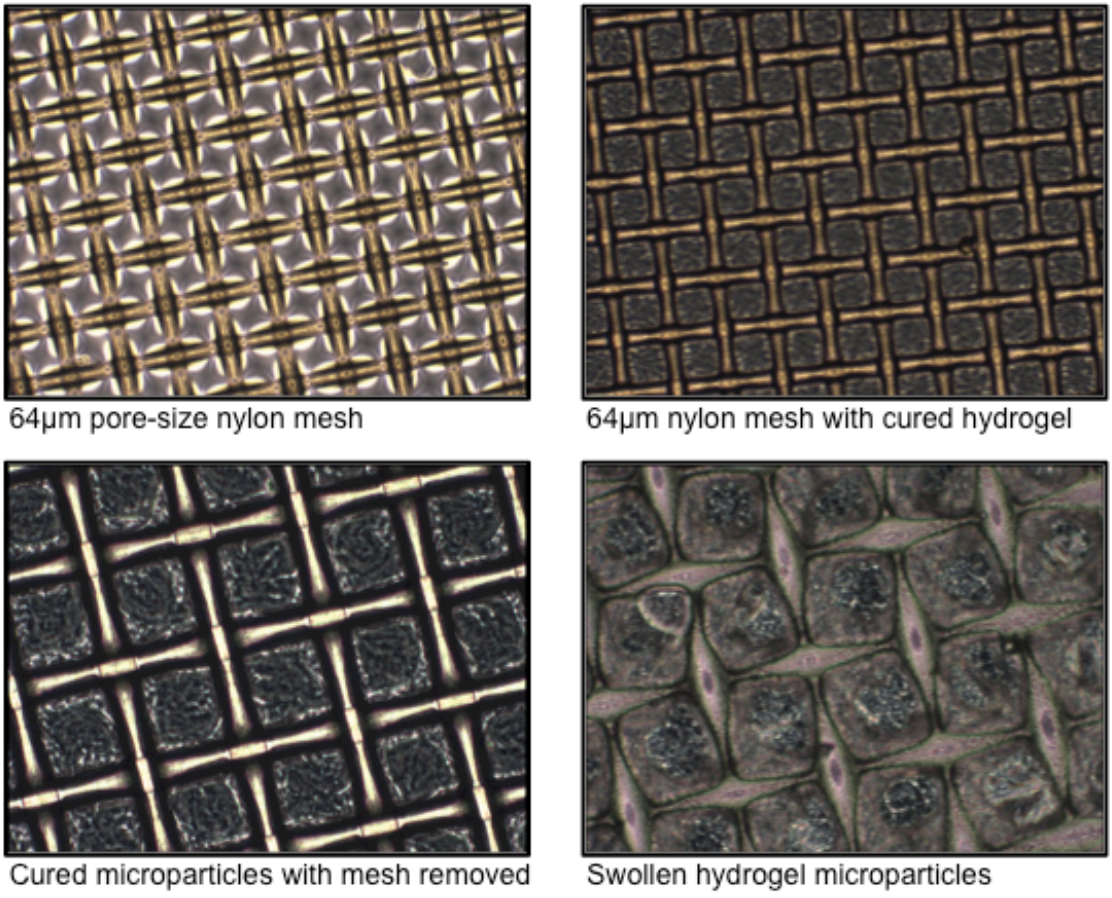

Figure 5.1 PEG hydrogel microparticles formed by the micron mesh patterning press method

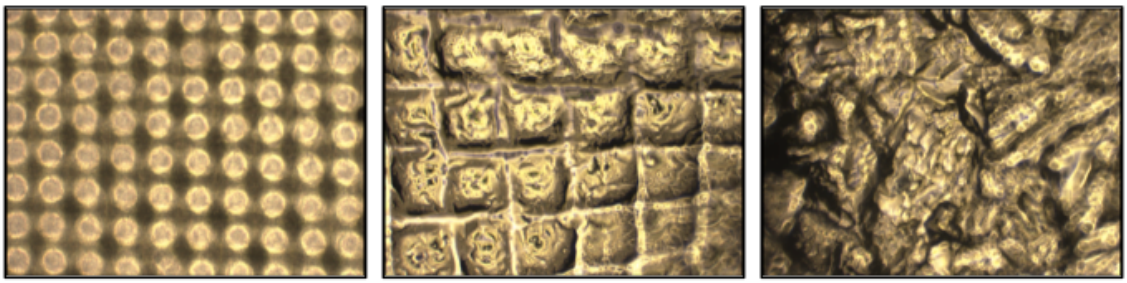

Unswollen microparticles on slide at initial time point, before exposure to trypsin. Focus is on top plane of microparticles.

Swollen microparticles on slide after one hour of trypsin exposure. Surface degradation is apparent on each particle.

Swollen microparticles on slide after two hours of trypsin exposure. Particle degradation is apparent.

Figure 5.2 Trypsin-mediated degradation of PEG-QVRAHGK hydrogel microparticles formed by the micron mesh patterning press method

residual polymer layer, which could be somewhat broken up through high-speed vortexing or stirring, though not entirely.

5.3.1.2 Mortar and Pestle Grinding Under Liquid Nitrogen

Particles were observed via light microscropy of the recovered samples, as shown in Figure 5.3. The method, however, proved to be quite variable, difficult to work with, and posed a significant safety hazard (even with cryo gloves). Moreover, when the particles collected were subject to trypsin degradation, there was no observable change after 24 hours exposure. This method was, therefore, not pursued any further.

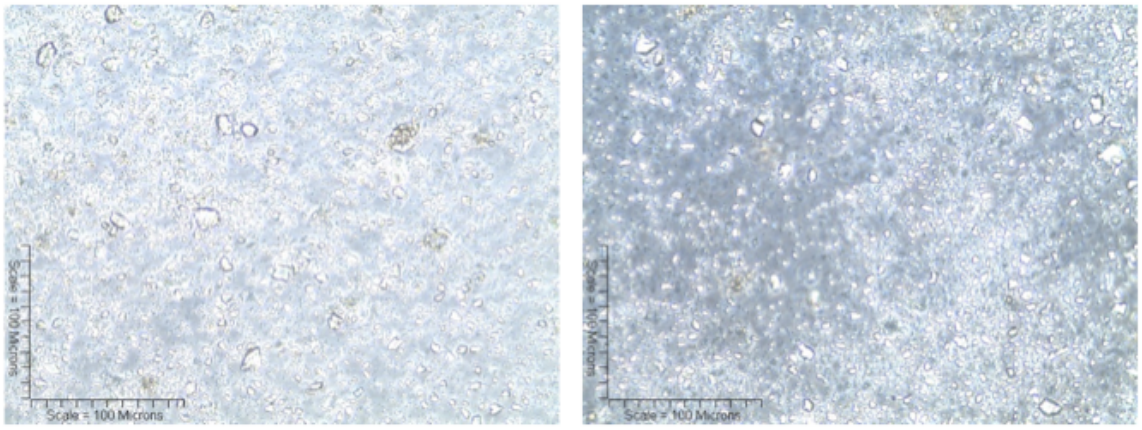

Figure 5.3 Particles formed by mortar and pestle grinding of frozen PEG-CGRGGC hydrogel

5.3.1.3 Cryogenic Milling

As was mentioned in section 5.2.2.2 , shattering of the hydrogel required low temperatures, as the hydrogel material was quite soft and pliable at room temperature (low T_g). Therefore, cryogenic milling (cryomilling) was explored rather than other traditional milling methods. The cryomilling technique was able to produce a fine, free flowing powder, as can be seen in Figure 5.4. These particles, however, faced the same difficulty observed with the mortar and pestle grinding; the particles were not observed to degrade by trypsin within 24 hours. This method was, therefore, not explored further.

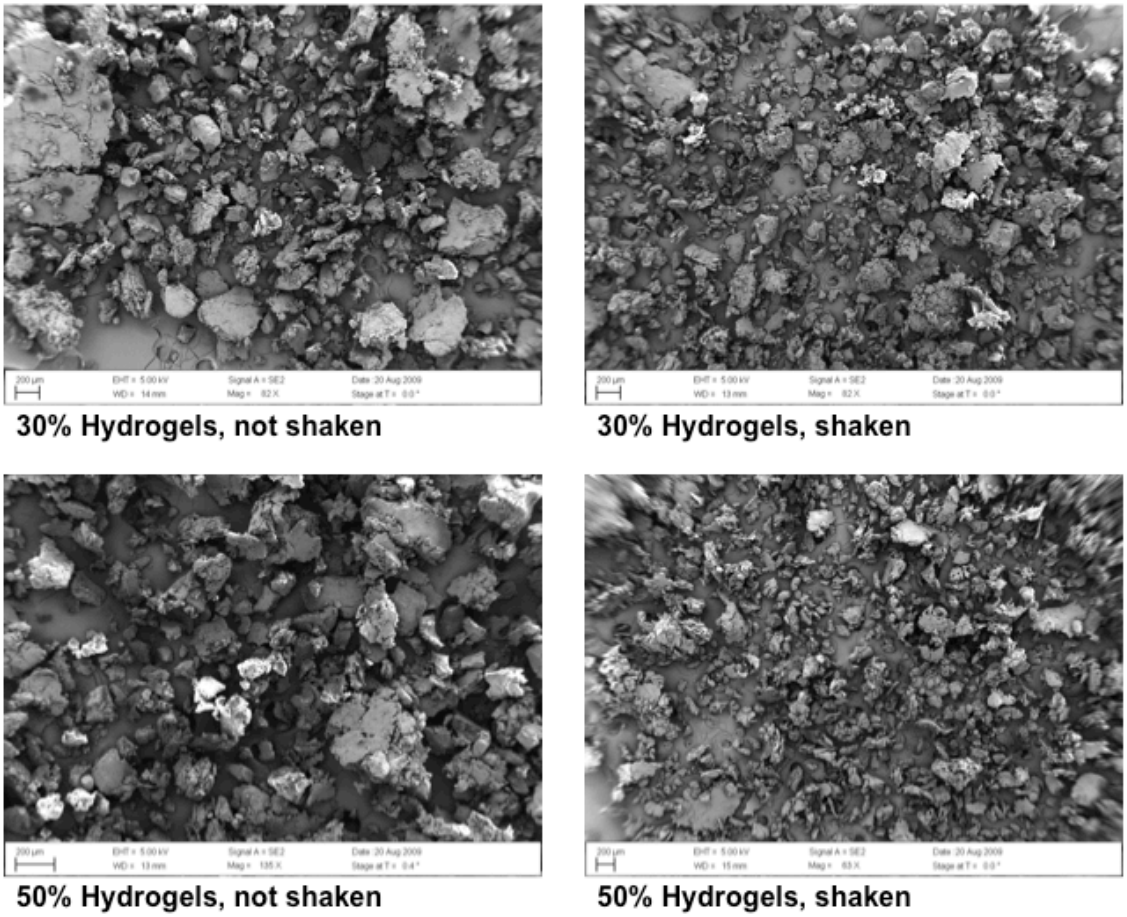

Figure 5.4 Scanning electron microscope images of cryomilled PEG-CGRGGC hydrogel particles

5.3.1.4 Handheld Nebulization

The particles sprayed onto a hydrophobic surface were on the scale of 500-1000 μm, were flat and discoidal in shape, and had air-pocket features. Visual observation of particles in solution by optical microscope revealed complete particle degradation by 40 minutes. Figure 5.5 shows particle degradation at 0 and 30 minutes.

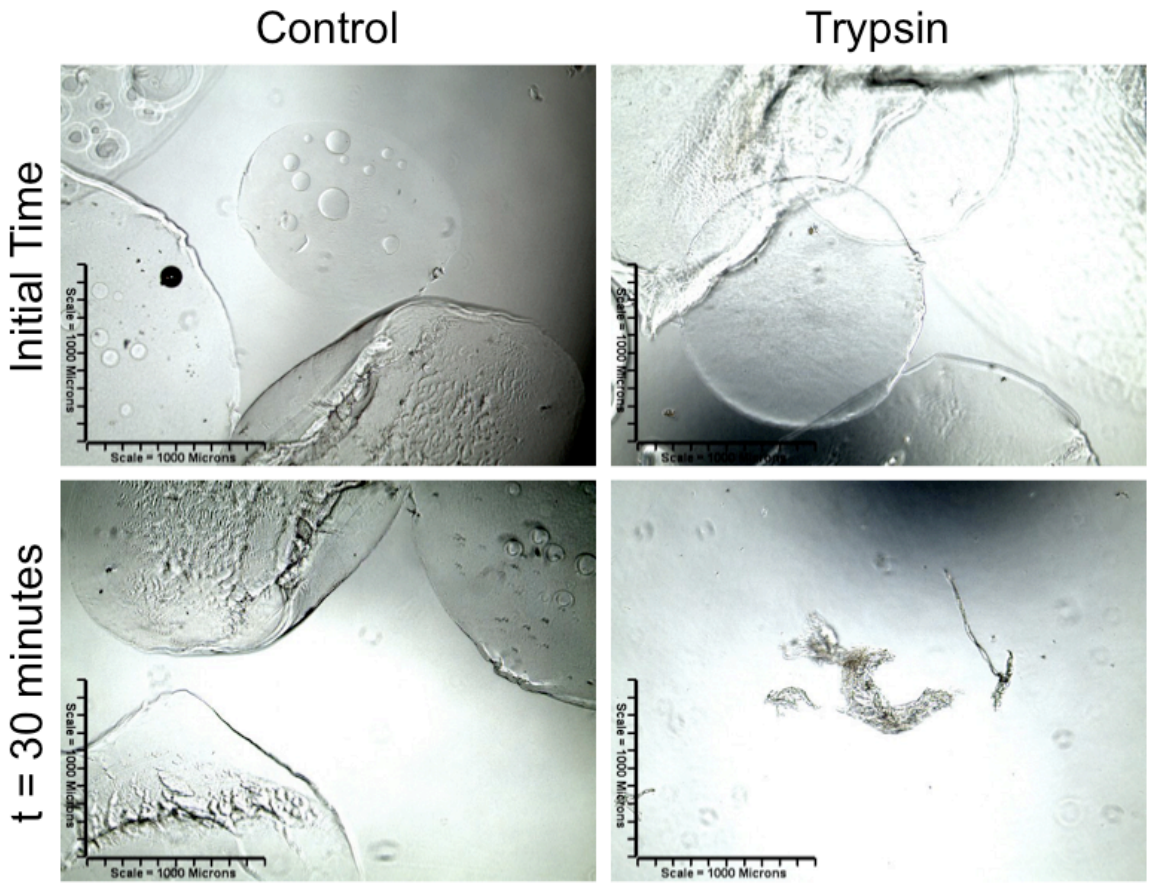

Figure 5.5 Trypsin-driven degradation of enzymatically-responsive hydrogel particles formed by nebulization. Control group remains intact, whereas Trypsin group is degraded after 30 minutes.

5.3.1.5 Other Methods

Other ideas and set-ups explored for feasibility included set-up of a microfluidic syringe pump system and preliminary studies into reactive spray drying [4]. The microfluidic syringe pump system consisted of a double-barreled syringe, individually loaded with precursor polymer solution, which would mix together in the mixing tip. Another line was introduced into the system to maintain a flow of paraffin oil. The

syringe pump would slowly pump micro-droplets of polymer solution into the oil, which would collect in a heated vessel with paraffin oil. Ultimately, the system proved to be too slow and low-throughput to continue developing in comparison to other methods.

An attempt at "reactive spray drying" [4] was carried out using PEG-4-Acr and PEG-DA, suspended in 70% ethanol/30% 0.3M TEA pH 8.15. Using a Mini Spray Dryer Büchi B-191 (Büchi Labortechnik AG, Flawil, Switzerland), the following conditions were attempted in order to achieve an outlet temperature near the optimum reaction temperature:

- Rate 2 mL/min, Inlet 70°C, Outlet 40°C
- Rate 2 mL/min, Inlet 100°C, Outlet 55°C
- Rate 5 mL/min, Inlet 100°C, Outlet 50°C

All of these runs resulted in a sprayed coating of PEG film in the collection chamber, which may have been a reacted PEG hydrogel film, or simply a PEG film, as the melting point of PEG is approximately between 45-50°C (depending on molecular weight). No further runs were attempted.

5.3.2 Michael Addition During Emulsion (MADE) Method for Microgel Synthesis

Microgels were successfully formed using a variety of conditions, as described in section 5.2.3 . A sampling of microgel images formed using various emulsion oils and surfactants is shown in Figure 5.6. When using DCM as the emulsion oil, it was observed that the microgels did not seem to be fully formed, and there was an abundance of leftover unreacted monomer. This likely was due to the evaporative cooling of DCM after the emulsion process. Emulsions carried out using viscous, non-evaporative paraffin oil were all well-formed, discrete particles. Furthermore, these microgels (PEG-CGRGGC

microgels with 0.01% Brij 30 with paraffin oil) were verified to undergo trypsin-mediated degradation, depicted in Figure 5.7. This preliminary work indicated that the Michael Addition During Emulsion (MADE) method for microgel synthesis could be further optimized and fine-tuned to produce enzymatically-degradable microgels within the desired range of 1-5 μm.

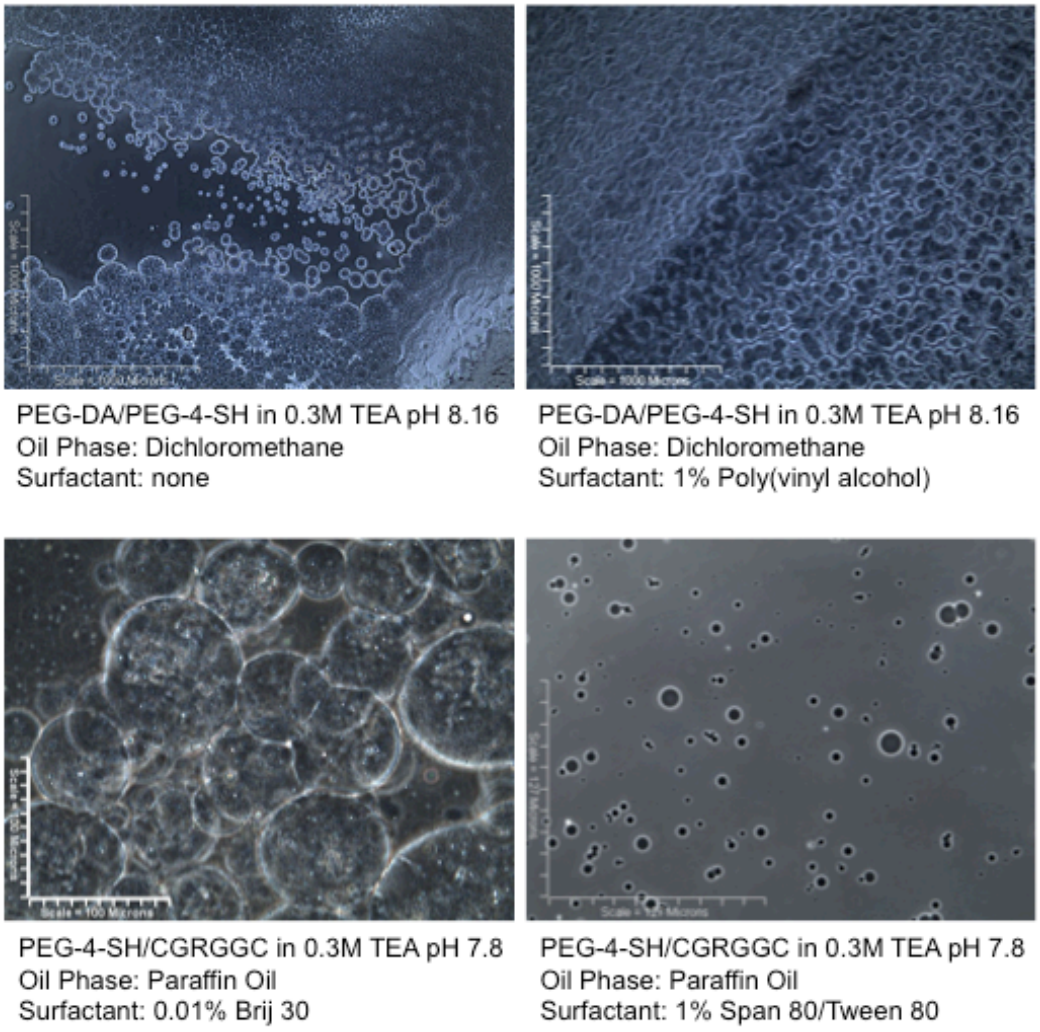

Figure 5.6 Light microscrope images of microgels formed under varying conditions by the MADE method

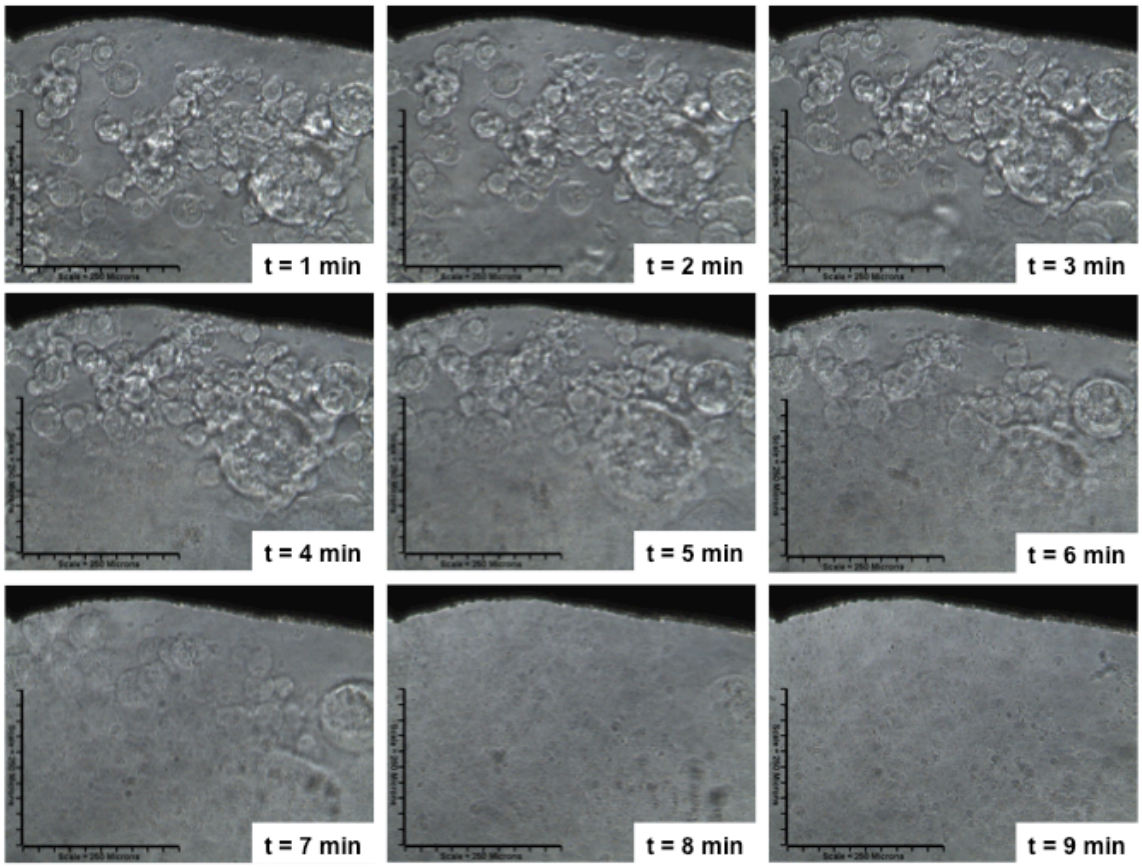

Figure 5.7 Trypsin-mediated degradation of PEG-CGRGGC microgels synthesized using the MADE method

5.3.2.2 Emulsion Optimization to Tune Microgel Size

Parameters to optimize microgel size included homogenization speed, time, and surfactant concentration. Homogenization time beyond three minutes was not observed to affect microgel size. Immersion of the vessel in a 40-45°C hot water bath, rather than at room temperature, during the emulsion process was visually observed under light microscopy to minimize microgel agglomerates (microgels that cross-linked together),

although this point was not further studied beyond visual observation. Homogenization speeds up to 5000 RPM did not appear to significantly affect microgel size as compared to 3000 RPM (Figure 5.8).

The surfactant cocktail was found to be the most critical parameter in changing microgel size. Several surfactants and combinations were evaluated to identify those that provided the longest droplet stability time, as previously described [3]. Out of the many surfactant combinations adopted here, an HLB value of five using a combination of Span 80 and Tween 80 was deemed the most stable and uniform. Although other combinations in the HLB range from five to six were also fairly stable, those with an HLB value of five were the most uniform. Furthermore, although use of Brij 30 also was successful in creating stabilized emulsions, groups of agglomerated droplets were observed in Brij 30 samples, which were not observed in others. Varying the percent concentration of surfactant in emulsion did produce the expected shift in particle size distribution, as seen in Figure 5.8. However, microgel batches with 3% surfactant required more extensive washing than those of lower percentages. The final optimized surfactant cocktail was found to be a combination of Span 80 and Tween 80, in a mixture ratio to achieve an HLB of five, at a concentration of 1% volume by volume of surfactant in paraffin oil. The final optimized homogenization conditions were a three minute homogenization time at 3000 RPM while immersed in a 40-45°C hot water bath.

Parameters to optimize Michael addition cross-linking included buffer, pH, and reaction temperature. PEG-4-acr and peptide were combined in equimolar concentrations, adjusted for PEG-4-acr degree of acrylate substitution and the percent purity of PEG and peptide. The chosen buffer was 0.3M triethanolamine, as previously reported in the literature [5-7], although a pH of 7.8 was used, rather than a pH of 8.0. Gelation is observed to occur within seconds, even at room temperature, and a more basic pH

increases the reaction rate [8]. Using a slightly less basic pH 7.8 buffer allowed for more time to uniformly mix the combined polymer/peptide solution, using pipette aspiration, and transfer to the emulsion vessel before gelation prohibited pipetting of the solution. PBS from pH 7.0 to 8.4 was also evaluated for suitability, but it was observed that the triethanolamine buffer yielded an overall faster reaction time. The incubation temperature after emulsion was kept at 37°C in order to minimize any temperature-related denaturing of encapsulated biologics. Lastly, in order to minimize disulfide bond formation, the reaction buffer was not added to the peptide until immediately before mixing with the PEG-4-acr solution.

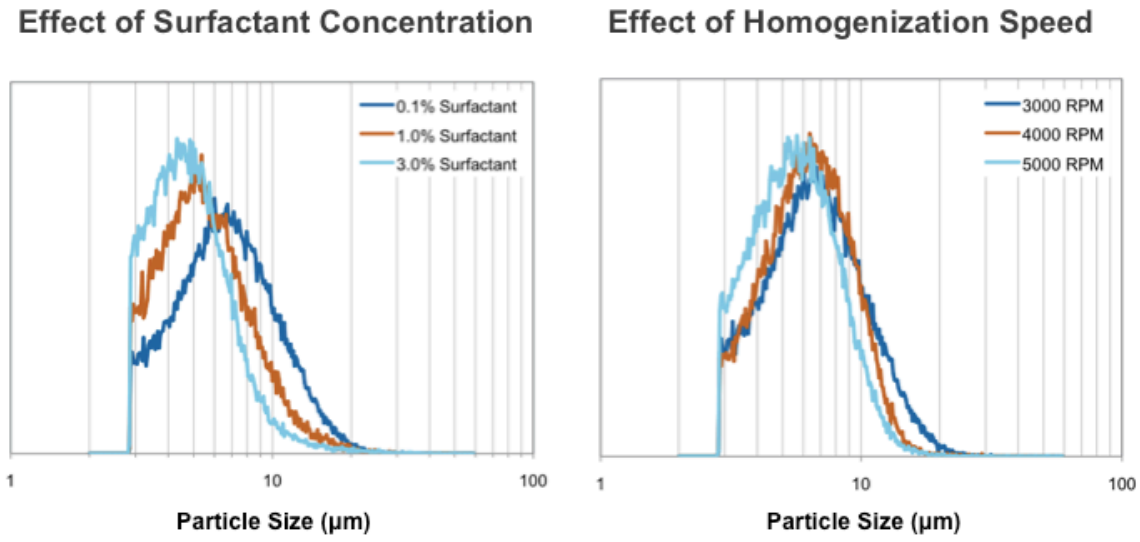

Figure 5.8 The effect of surfactant concentration and homogenization speed on MADE-fabricated microgel particle sizes

5.3.2.3 Final Adopted Protocol for MADE Method

An illustration depicting the basic steps in the MADE method is shown in Figure 5.9. Adapted from P. Wanakule, et. al. [9]: Equimolar amounts (sulfhydryl:acrylate) of di-sulfhydryl peptide and PEG-4-acr (10 kDa) were dissolved separately into 0.3 M triethanolamine buffer at pH 7.8 to a total combined concentration of 60% (w/v), in a total volume of 100 μL. The two solutions were combined, mixed, and added to 15 mL of paraffin oil with 1% (v/v) surfactant (Span 80/Tween 80 combination to achieve an HLB=5). The entire mixture was then immersed in a hot water bath at 40–45 °C and homogenized for 3 min at 3000 rpm using a Polytron PT 3100 homogenizer. The resulting surfactant-stabilized water-in-oil emulsion was incubated for at least 2 h at 37 °C to allow the cross-linking reaction to complete, forming solid, cross-linked, micro-sized hydrogels (microgels). Thus, as the reaction proceeds, the mixture becomes a suspension of solid microgels in oil, rather than an emulsion. These microgels were removed from oil, residual surfactant, and un-reacted material by a series of centrifugal washes with fresh oil and water. Briefly, microgels were centrifuged at 10,000×g for 20 min, supernatant discarded, re-suspended in de-ionized water, and vortexed. The process was repeated three times, with the final re-suspension in either deionized water, phosphate buffered saline, or 100 mM ammonium bicarbonate (depending on the buffer required for various assays).

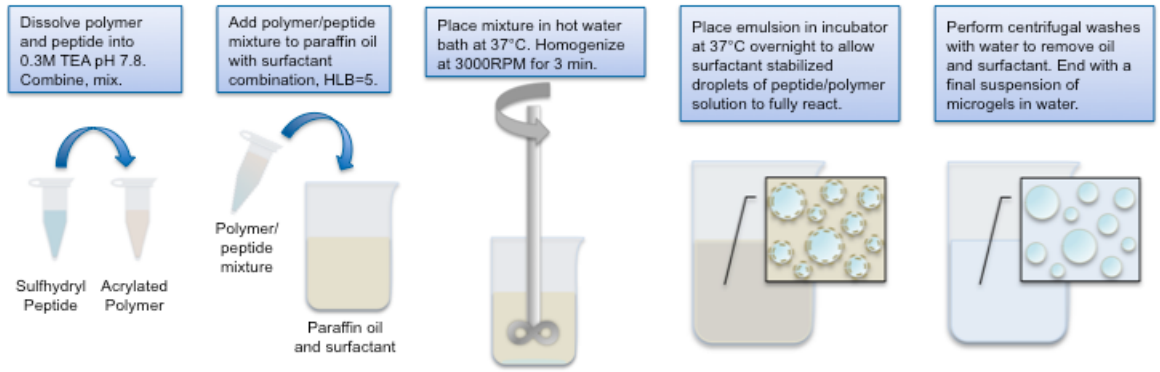

Figure 5.9 Illustration depicting basic steps in the MADE method

5.4 Conclusions

In this chapter, a variety of particle synthesis methods, using Michael addition cross-linked hydrogels, were explored in order to develop the most high-throughput and cost-effective fabrication method, while maintaining mild fabrication conditions. Out of all methods explored, the MADE synthesis method emerged as the clear choice for continued study and use. Preliminary data demonstrated that the microgels could be formed in the desired size range of 1-5 μm, and also maintain enzyme-responsiveness. Further characterization of these microgels is discussed in the following chapters.

5.5 References

[1] M. Bermejo, I. Gonzalez-Alvarez, M.G. Alvarez, V.G. Casabo, J. Price, G.L. Amidon, Computer Aided Learning in Biopharmacy, in: INTED2009 Proceedings, IATED, Valencia, Spain, 2009: pp. 2923–2926.

[2] D.L. Elbert, Liquid-liquid two-phase systems for the production of porous hydrogels and hydrogel microspheres for biomedical applications: A tutorial review, Acta Biomaterialia. 7 (2011) 31–56.

[3] O.Z. Fisher, N.A. Peppas, Polybasic Nanomatrices Prepared by UV-Initiated Photopolymerization, Macromolecules. 42 (2009) 3391–3398.

[4] S.K. Hahn, J.S. Kim, T. Shimobouji, Injectable hyaluronic acid microhydrogels for controlled release formulation of erythropoietin, J Biomed Mater Res A. 80 (2007) 916–924.

[5] A. Singh, S. Suri, K. Roy, In-situ crosslinking hydrogels for combinatorial delivery of chemokines and siRNA-DNA carrying microparticles to dendritic cells, Biomaterials. 30 (2009) 5187–5200.

[6] M. Ehrbar, S.C. Rizzi, R.G. Schoenmakers, B.S. Miguel, J.A. Hubbell, F.E. Weber, et al., Biomolecular hydrogels formed and degraded via site-specific enzymatic reactions, Biomacromolecules. 8 (2007) 3000–3007.

[7] M.P. Lutolf, F.E. Weber, H.G. Schmoekel, J.C. Schense, T. Kohler, R. Müller, et al., Repair of bone defects using synthetic mimetics of collagenous extracellular matrices, Nat Biotechnol. 21 (2003) 513–518.

[8] B. Mather, K. Viswanathan, K. Miller, T. Long, Michael addition reactions in macromolecular design for emerging technologies, Prog Polym Sci. 31 (2006) 487–531.

[9] P. Wanakule, G.W. Liu, A.T. Fleury, K. Roy, Nano-inside-micro: Disease-responsive microgels with encapsulated nanoparticles for intracellular drug delivery to the deep lung, J Control Release. 162 (2012) 429–437.

Chapter 6: *In Vitro* Characterization of Microgels Fabricated using the MADE Method

[This chapter was adapted, with permission[**], from P. Wanakule, G.W. Liu, A.T. Fleury, K. Roy[††], Nano-inside-micro: Disease-responsive microgels with encapsulated nanoparticles for intracellular drug delivery to the deep lung, J Control Release. 162 (2012) 429–437.]

6.1 INTRODUCTION

In recent years, there has been increasing interest in developing systems for the controlled delivery of therapeutic molecules to the lungs, especially to intracellular targets in the deep lung. Pulmonary drug delivery has great potential for both local and systemic treatments, especially with newly emerging biologic drugs, such as proteins, peptides and nucleic acids. Aside from its attractiveness as a non-invasive route of administration, delivery via pulmonary inhalation offers several advantages, including a large surface area with high vascularization for drug absorption, thin epithelial layer, low enzymatic activity, and avoidance of first-pass metabolism [1-3].

Despite the many advantages, there exists several design challenges to achieve efficient and effective delivery of biologic drugs inside cells of the deep lung. The

[**] Copyright 2012 From Nano-inside-micro: Disesase-responsive microgels with encapsulated nanoparticles for intracellular drug delivery to the deep lung, by P. Wanakule et al. Reproduced by permission of Elsevier Limited. Elsevier Limited retains the copyright for all text, figures, and tables reproduced here.

[††] Statement of co-author contribution: This chapter was written by Prinda Wanakule, with editorial and content assistance by Krishnendu Roy (research supervisor). All results, methods, and ideas described in this chapter are original works by Prinda Wanakule, with assistance in the laboratory by undergraduate student Gary W. Liu and Masters student Asha T. Fleury.

established range for optimal aerodynamic particle diameter to achieve efficient deep lung deposition (following inhalation) is between 0.5-5μm [1,2,4]. Significant fractions of particles with aerodynamic diameters (d_a) <0.5μm may fail to deposit, and are exhaled, whereas particles >5μm tend to deposit in the mouth and throat [1,2,4]. However, the rate of particle clearance by alveolar macrophages is especially high in this optimum aerodynamic diameter range [5-7]. To avoid this rapid clearance, particles must typically have a geometric diameter (d_g) >6μm [4,6], and have hydrophilic, rather than hydrophobic, surface chemistry [5,7]. In addition, drugs that are targeted to intracellular pathways and molecules, such as siRNA, DNA or intracellularly-targeted proteins or peptides, often require nanoscale carriers <0.2μm to improve mucus penetration [8] and cellular uptake in airway epithelial cells [9,10]. These conflicting requirements make for a complex design space where the ideal carrier should be $0.5<d_a<5$μm during inhalation, have a d_g >6μm following lung deposition, and d_g<0.2μm to penetrate the mucus and deliver drugs intracellularly. Additionally, due to the non-uniform distribution and presentation of pathologies in the lungs, it should also be beneficial for pulmonary drug carriers to incorporate pathophysiologically-triggered drug release mechanisms to minimize non-specific side effects on normal cells [11,12].

To address these challenges, we have developed an innovative nanoparticle-in-microgel delivery system comprised of swellable, peptide-cross-linked microgel-carriers encapsulating therapeutic drugs and nanoparticles. These carriers were fabricated using a novel method of Michael addition during (water-in-oil) emulsion (MADE). This new method avoids exposure to UV, high temperatures, or organic solvents, all of which could potentially denature biologic drugs [13]. Here we report the potential of this nanoparticle-in-microgel system as inhalable carriers with (a) optimal aerodynamic diameter, (b) ability to avoid rapid clearance by alveolar macrophages (c) high

drug/nanoparticle loading efficiency and (d) efficient triggered release in response to disease-specific enzymes. In this study, we use trypsin as a convenient model enzyme to trigger the drug release, although the system could be tailored in the future for various disease-specific enzymes, including matrix metalloproteinases, cathepsins, etc. [11].

The Amiji group has previously reported a gelatin-poly(caprolactone)-based nanoparticle-in-microparticle system for oral delivery of plasmid DNA [14]. Edwards and colleagues have reported porous, micron-sized structures assembled from nanoparticles for pulmonary delivery [15]. Bawendi, Fukumura and co-workers have also reported a 10nm-QD-in-100nm-gelatin particle construct for efficient penetration into tumor tissue, which releases the QDs (quantum dots) upon exposure to matrix metalloproteinases [16]. In addition, a swellable hydrogel particle for pulmonary delivery has been recently described [4], and peptide-containing hydrogels have long been used for extracellular matrix mimicking scaffolds [17,18], with few reports on their application in drug delivery [19,20]. However, a swellable, multi-tiered two-stage system that incorporates all the design barriers for intracellular deep lung delivery for biologic drugs has not been introduced. The nanoparticle-in-microgel system described here could have a significant impact in pulmonary delivery of biologics by increasing deep lung deposition, avoiding clearance by alveolar macrophages and delivering therapeutics intracellularly in response to disease-specific stimuli.

6.2 MATERIALS AND METHODS

6.2.1 Materials

Four-arm-poly(ethylene glycol)-acrylate-10kDa (PEG-4-acr) was obtained from Laysan Bio (Arab, AL). The peptide sequence, CGRGGC (cysteine-glycine-arginine-

glycine-glycine-cysteine), was specifically designed in lab to have high specificity for trypsin [21,22], then custom synthesized by CHI Scientific (Maynard, MA). All other chemicals and reagents were purchased from Sigma Aldrich (St. Louis, MO) unless otherwise specified. Cell lines used in this study were purchased from ATCC® (Manassas, VA), and included A549 human lung epithelial cells (CCL-185™), HEK 293 human embryonic kidney cells (CRL-1573™), and RAW 264.7 mouse monocytes/macrophages (TIB-71™). Cells were cultured according to recommendations by ATCC® for each cell line.

6.2.2 Synthesis of enzymatically-degradable microgels

Enzymatically-degradable microgels were synthesized using a newly developed method of Michael addition cross-linking during water-in-oil emulsion (MADE), wherein the cross-linking occurs through a Michael-addition reaction within surfactant stabilized aqueous droplets to form microgels. Equimolar amounts (sulfhydryl:acrylate) of the trypsin sensitive di-sulfhydryl peptide (CGRGGC) and PEG-4-acr were dissolved separately into 0.3M triethanolamine buffer at pH 7.8 to a total combined concentration of 60% (w/v), in a total volume of 100µl. The two solutions were combined, mixed, and added to 15mL of paraffin oil with 1% (v/v) surfactant (Span 80/Tween 80 combination to achieve an HLB=5). The entire mixture was then immersed in a hot water bath at 40-45°C and homogenized for three minutes at 3000 RPM using a Polytron PT 3100 homogenizer. The resulting surfactant-stabilized water-in-oil emulsion was incubated for at least two hours at 37°C to allow the cross-linking reaction to complete, forming solid, cross-linked, micro-sized hydrogels (microgels). Thus, as the reaction proceeds, the mixture becomes a suspension of solid microgels in oil, rather than an emulsion. The

microgels were removed from oil, residual surfactant, and un-reacted material by a series of centrifugal washes with fresh oil and water. Briefly, microgels were centrifuged at 10,000xg for 20 minutes, supernatant discarded, re-suspended in deionized water, and vortexed. The process was repeated three times, with the final re-suspension in either deionized water, phosphate buffered saline or 100mM ammonium bicarbonate (depending on the buffer required for various assays).

6.2.3 Encapsulation of nanoparticles and biologics within microgels

Nanoparticles and biologics were simply mixed into the PEG-4-acr in 0.3M triethanolamine buffer solution to achieve encapsulation within microgels. All other steps were as described in the previous section. Encapsulated nanoparticles included 20nm and 40nm FluoSpheres (Invitrogen, Carlsbad, CA), and 200nm PEI-modified PLGA nanoparticles (produced in lab [23-27]). Encapsulated biologics included Alexa Fluor® 594 labeled IgG and Lambda DNA (Invitrogen, Carlsbad, CA).

6.2.4 Microgel sizing and characterization

6.2.4.1 Size and morphology

Microgels were sized using a Malvern Zen1600 Zetasizer (Malvern Instruments Ltd., Worcestershire, United Kingdom) in water (swollen state) or paraffin oil (relaxed state). Particle size and distribution were obtained from the accompanying instrument software.

To observe morphology, the microgels were dried at low vacuum for 48 hours, or lyophilized for 24 hours, and analyzed via SEM. They were also imaged under light microscopy during the hydrolytic degradation studies (detailed in section 6.3.2) and

analyzed using the ImageJ particle analysis toolkit (public domain image processing and analysis software from the National Institutes of Health) for sizing.

Cryo SEM was used to analyze the internal porous structure of the microgels. A drop of microgel suspension in water was added onto the sample holder, flash frozen in liquid nitrogen, and fractured open to reveal cross-section using a scalpel. The sample was transferred (EM VCT-100 vacuum cryo transfer system, Leica Microsystems, Weitzlar, Germany), sputter coated (Bal-Tec/Leica Med 20), and imaged (Zeiss Supra 40 VP Scanning Electron Microscope with cryo stage) at low temperature and high vacuum. Three batches of microgels were prepared and analyzed.

6.2.4.2 Density and aerodynamic diameter

Microgel density was determined by centrifugation into discrete sucrose gradients of known density, based on the premise that the microgels will come to rest in a solution of matching density after adequate centrifugation time. 40%, 30%, 20%, and 10% (w/v) sucrose solutions were prepared, and 2mL of each solution was carefully layered (highest to lowest density) in a centrifuge tube in order to maintain a discrete interface between each. 2mL of microgel suspension in water was then carefully added to the top of the gradient, and the set-up was centrifuged at 10,000xg for 20 minutes. Each gradient layer was then collected from the base of the tube using 2mL serological pipets, and sized using a Malvern Zen1600 Zetasizer. Refractive indices were adjusted accordingly for each sucrose layer. The microgel density and z-average size was then used to calculate the aerodynamic diameter of the microgels as detailed in the results section.

6.2.4.3 Swelling properties

The extent of particle crosslinking (which determines degradation and release rate of encapsulated drugs or nanoparticles) was assessed through swelling studies in PBS (pH 7.4). Specifically, 100mg of microgels were allowed to swell for 24 hours in 15 ml PBS with continuous rocking in a 37°C incubator. After 24 hours, swollen microgels were collected on filter paper (0.47μm pore) to remove surface water and placed in a pre-weighed vial (W_v). The weight of the swollen microgels and vial were recorded ($W_{s,v}$). Microgels were then lyophilized for 24 hours and dry weight was recorded ($W_{d,v}$). Accordingly, the fold swelling ratio (S) was calculated as:

$$S = \frac{W_{s,v} - W_{d,v}}{W_{d,v} - W_v}$$

6.2.5 Verification of enzyme-triggered degradation

CGRGGC-peptide-crosslinked, trypsin-sensitive microgels were studied in the presence or absence of trypsin using time-lapse video from a Zeiss Axiovert microscope fitted with a Ti:S laser optical trap. A dilute microgel suspension was prepared in trypsin digestion buffer (10% 1mM HCl, 90% 100mM NH_4HCO_3) and a single microgel was optically trapped and held stationary in the focal plane for the duration of the study. Trypsin (325 U/mL; high concentration to reduce required trapping time) was added and the sample was observed for 10 minutes while comparing to control particles without enzyme.

6.2.6 Enzyme-triggered release of nanoparticles and biologics

Microgels with encapsulated nanoparticles or biologics were allowed to swell for 24 hours in trypsin digestion buffer and exposed to physiologically relevant levels of enzyme (10-16.5 USP U/mL; no enzyme in control samples) [28]. At each time point, the samples were centrifuged at 10,000xg for 20 minutes, and the supernatant was collected for analysis in a BioTek Synergy SIAFRTD plate reader (BioTek Instruments, Inc., Winooski, VT). New samples, which were all aliquotted at the beginning of the study, were used for each time point. One aliquot was quickly degraded by trypsin at 0.1 mg/mL and read in a plate reader to determine encapsulation level, which was set as the 100% release value to compare with experimental samples. All experiments were conducted using commercially available fluorescently labeled molecules or nanoparticles, with the exception of lambda DNA, which was fluorescently labeled post-release using the Quant-iT^{TM} PicoGreen dsDNA Assay Kit (Invitrogen, Carlsbad, CA), following manufacturer protocols.

6.2.7 Hydrolysis-mediated release of nanoparticles

Microgels with encapsulated 40nm Dark Red (ex/em 660/680) FluoSpheres® or Alexa Fluor® 594 labeled IgG were loaded into hanging cell culture inserts with a 0.4μm filter size (EMD Millipore Millicell, Billerica, MA), then placed into 24-well ultra low attachment cell culture plates (Corning® Costar®, Corning, NY). Approximately 3mg of microgels were loaded per well in a total volume of 1.5mL PBS (inside and outside of insert). The entire set-up was wrapped in parafilm and plastic wrap, and placed on a rocker in a 37°C incubator for 20 days, or until readings reached a plateau, after which the experiment was terminated. Using this setup, intact microgels remain inside of the cell culture inserts, whereas released nanoparticles are free to diffuse out of the insert,

and into the well plate. At various time points, fluid from the well (outside of the insert) was sampled for fluorescence measurements using a BioTek plate reader, to measure cumulative release of nanoparticles from microgels. Wells were replenished to maintain a volume of 1.5mL PBS.

6.2.8 Cytotoxicity

Using the MTS Assay (Promega, Fitchburg, WI), cytotoxicity of intact microgels, trypsin-degraded microgels, and un-reacted PEG-4-acr and CGRGGC peptide were tested on A549 human lung epithelial cells and HEK 293 human embryonic kidney cells. High polymer doses of 0.5 mg/mL or 1.0 mg/mL were used for these studies (approximately 4350 and 8700 microgels per cell, respectively). The un-reacted condition contained PEG-4-acr and peptide in equivalent amounts that would be used to synthesize microgels to a total weight of 0.5 and 1.0 mg/mL. 8000 cells were seeded into a 96 well plate with 100μL of media and incubated at 37°C for 24 hours prior to the addition of the microgels and various component conditions. After 6, 24, and 48 hours exposure, media was discarded, 100μL of fresh media and 20μL of MTS reagent was added to each well, incubated for 25 minutes, and the absorbance was read at 490nm using a BioTek plate reader.

6.2.9 *In vitro* microgel uptake studies

The potential for clearance by alveolar macrophages was evaluated though macrophage uptake studies both qualitatively by confocal microscopy, and quantitatively using flow cytometry analysis. 20nm-sized Dark Red (ex/em 660/680) FluoSpheres® were encapsulated within the microgels for use as a fluorescent tracer. Uptake of

microgels was compared relative to uptake of 1μm-sized Orange (ex/em 540/560) FluoSpheres (Invitrogen, Carlsbad, CA) as a positive control.

For confocal microscopy, 2 x 10^6 RAW 264.7 mouse monocytes/macrophages were seeded into a 6-well plate with a poly-L-lysine coated microscope coverslip at the base. At various time points after particle incubation (15, 30 minutes, 1, 2, 12, and 24 hours), the cells were fixed and stained according to the manufacturer instructions using DAPI nucleic acid stain and Texas Red-X labeled phalloidin (Invitrogen, Carlsbad, CA). The coverslips were then mounted onto glass slides and imaged on a Leica SP2 AOBS Confocal Microscope (Leica Microsystems).

For flow cytometry analysis, 5 x 10^4 macrophages were seeded per well in a 24-well plate. Along with an untreated control sample, cells were treated with 1μm Orange FluoSpheres, 20nm Dark Red encapsulated FluoSpheres encapsulated inside microgels, and 20nm Dark Red FluoSpheres alone (for a signal comparison). After 2 hours, cells were washed and agitated six times with PBS to remove free particles, gently removed using a cell scraper, and re-suspended in PBS. Analysis was carried out on an Accuri C6 flow cytometer (Becton, Dickinson and Company, Franklin Lakes, NJ) using FL2 for 1μm Orange FluoSpheres and FL4 for both 20nm Dark Red FluoSpheres encapsulated in microgels and naked 20nm Dark Red FluoSpheres. An untreated control was used to establish baseline autofluorescence.

6.3 RESULTS AND DISCUSSION

6.3.1 PEG-peptide microgels can be efficiently synthesized using the MADE method

Microgels were formed by the newly developed Michael addition during (water-in-oil) emulsion (MADE) process, which offers the advantages of large batch size and

simple manufacturing under mild conditions. Typical batches studied here consisted of 60mg combined total weight of PEG-4-acr and CGRGGC peptide in 100µl of reaction buffer, giving a final 60% weight by volume percent hydrogel (w/v). Weight percentages higher than 60% were difficult to solubilize, and thus, were not explored further. Lower polymer weight percentages were also achieved using the MADE method, but were not explored in this study. After washing, typical microgel recovery was ~75% of the initial polymer weight.

Parameters to optimize microgel size included homogenization speed, time, and surfactant concentration. Homogenization time beyond three minutes was not observed to affect microgel size. Immersion of the vessel in a 40-45°C hot water bath, rather than at room temperature, during the emulsion process was observed (under light microscopy) to minimize microgel aggregation. Homogenization speeds up to 5000 RPM did not affect microgel size as compared to 3000 RPM (data not shown). The surfactant cocktail was found to be the most critical parameter in changing microgel size. Several surfactants and combinations were evaluated to identify those that provided the longest droplet stability time, as previously described [29]. The final optimized surfactant cocktail was found to be a combination of Span 80 and Tween 80, in a mixture ratio to achieve a hydrophile lipophile balance (HLB) of 5, at a concentration of 1% v/v of surfactant in paraffin oil. The final optimized condition for synthesis involved a three minute homogenization time at 3000 RPM while immersed in a 40-45°C water bath.

Parameters to optimize Michael addition cross-linking included buffer, pH, and reaction temperature. PEG-4-acr and peptide were combined in equimolar concentrations, adjusted for degree of acrylate substitution and the percent purity of PEG and peptide. The chosen buffer was 0.3M triethanolamine, as previously reported in the literature [27,30,31], although a pH of 7.8 was used, rather than a pH of 8.0. Gelation

was observed to occur within seconds, even at room temperature, and a more basic pH increased the reaction rate [32]. Using a slightly less basic pH of 7.8 allowed for more time to uniformly mix the combined polymer/peptide solution, using pipette aspiration, and transfer to the emulsion vessel before gelation prohibited pipetting of the solution. PBS from pH 7.0 to 8.4 was also evaluated for suitability, but it was observed that the triethanolamine buffer yielded an overall faster reaction time. The incubation temperature after emulsion was kept at 37°C in order to minimize any temperature-related denaturing of encapsulated biologics. Lastly, in order to minimize inter-peptide disulfide bond formation, the reaction buffer was not added to the peptide until immediately before mixing with the PEG-4-acr solution.

Microgel morphologies in different hydration states were observed under SEM (dry), cryo SEM (wet, frozen) and light microscopy (wet), as shown in Figure 6.1 (page 142). In contrast to the smooth and spherical morphology observed under wet conditions, lyophilized microgels (Figure 6.1A), although mostly spherical, had a wrinkled surface. This was likely due to the high vacuum collapsing the internal porous structure, consistent with hydrogel microstructure. When drying the samples under low pressure with a bench top Nalgene vacuum chamber, microgels retained their smooth spherical surface (Figure 6.1B). Cryo SEM was performed on a swollen suspension of microgels in water to observe the surface architecture, internal morphology, as well as size in the wet, swollen state. As shown in Figure 6.1C, cryo SEM revealed a porous internal network structure, indicating successful Michael addition-type cross-linking to form hydrogel microparticles within an emulsion droplet. This is further evidenced by the swelling and hydrolytic degradation behavior observed over time. The fold swelling ratio of the microgels across three separate batches was found to be 17.683±4.8394 (average ±

standard deviation), indicating the microgels are able to absorb approximately 18 times their dry weight in water.

6.3.2 Microgel sizes are within the optimum range for deep lung delivery by inhalation

In order to achieve effective delivery via pulmonary inhalation, the aerodynamic diameter of a particle should be in the range of 0.5-5μm [1,2,4]. The aerodynamic diameter (d_a) is dependent on the physical diameter, shape, and density of the particle. For a spherical particle, this is given by the equation

$$d_a = \rho^{0.5} d_g$$

where ρ is the density and d_g is the geometric diameter [1]. Previous groups have shown success in pulmonary delivery using large porous particles, with larger geometric diameters, but low densities [15,33,34]. Given the highly porous nature of hydrogels, we theorized that microgels would have a low density while maintaining a larger geometric diameter, capable of carrying a higher drug payload.

Due to the dynamic changes in microgel sizes based on states of hydration, microgels were sized while still in oil (relaxed state), immediately after washing into water, and at various time points afterwards to observe swelling and degradation behavior. Microgels had an average geometric diameter of 1.660±1.362μm in the relaxed state (in oil, Malvern Zetasizer). Immediately after washing into water, the average geometric diameter was 1.893±2.729μm (in water, Malvern Zetasizer).

Michael addition reactions between PEG-4-acrylate and sulfhydryl groups result in the formation of a hydrolytically degradable ester bond [13,32]. Slow hydrolytic

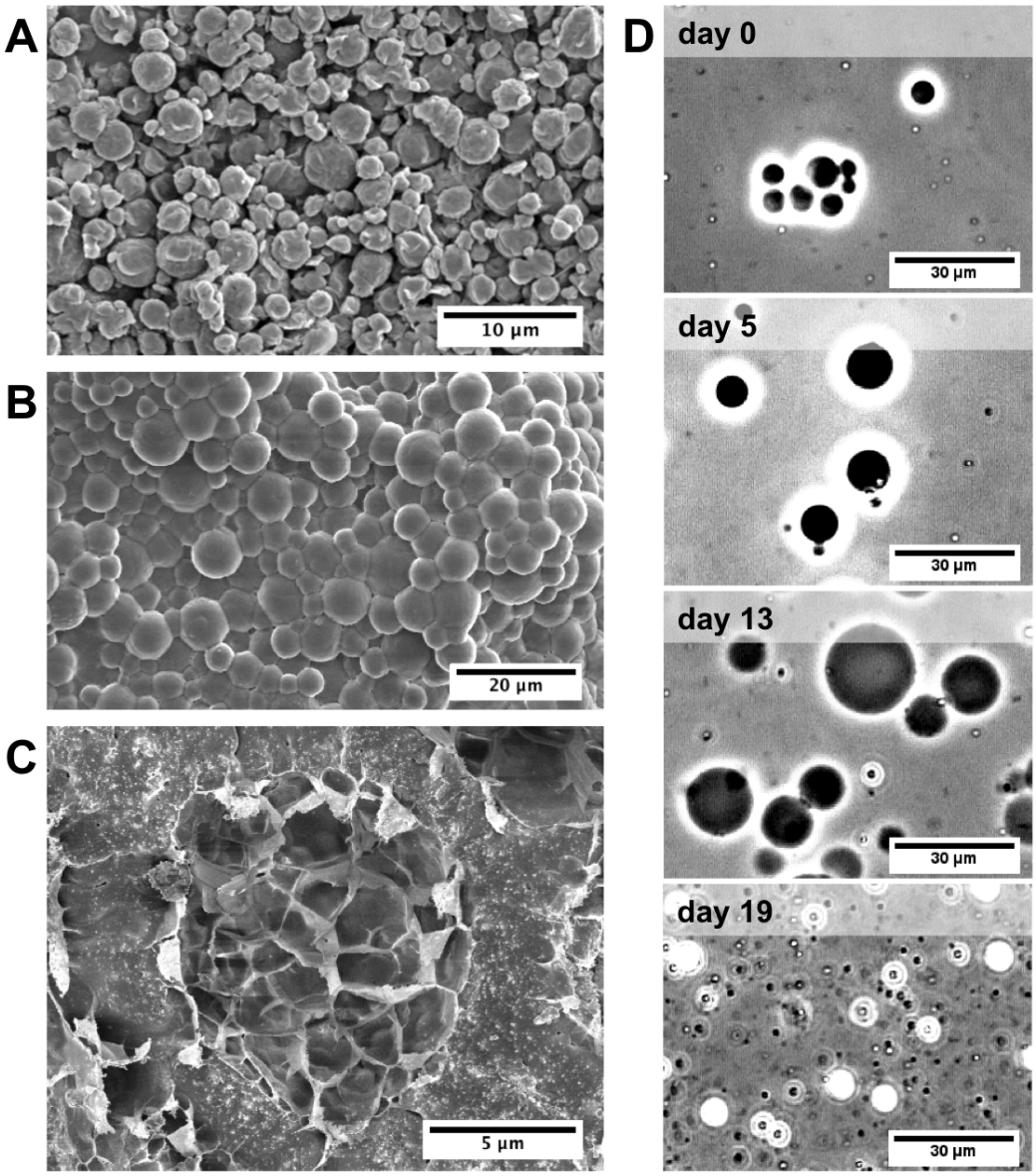

Figure 6.1 Microscopy of microgels in different states of hydration, swelling, and degradation.
(A) SEM image of microgels after 24 hours lyophilization, scale bar = 10µm.
(B) SEM image of microgels after 48 hours in a low-pressure vacuum chamber, scale bar = 20µm.
(C) Cryo SEM image of a single microgel frozen in water and fractured open under liquid nitrogen to reveal porous cross-section, scale bar = 5µm.
(D) Light microscope images of microgels in water, showing swelling and degradation changes over 19 days in PBS at 37°C, scale bars = 30µm.

degradation of the particles was desired to provide an eventual clearance mechanism (further discussed in section 6.3.5).

To determine rates of hydrolytic degradation, microgels were kept in PBS in a 37°C incubator on a rotator. During the hydrolytic degradation process, microgels exhibited increasing transparency, and thus, changes in refractive index (RI). RI is a key parameter in dynamic light scattering (DLS) methods [35] and thus DLS could not be used to monitor particle size over time. Instead geometric measurements were taken using microscopy images and analyzed using the ImageJ particle analysis software. The gels were sampled and observed out to day 19 (Figure 6.1D), however, geometric diameters were measured only to day 13. Past this time point, microgels became too transparent to apply an accurate contrast threshold for the analysis function. From day 15 through experiment termination at day 19 only debris (<0.1μm) could be found in the samples. The geometric diameters are summarized in Table 6.1 (page 144), and were taken as an average across three separate batches of microgels ± standard error. For each time point, 30 images were analyzed (10 per batch), resulting in average of approximately 2250 particles analyzed per time point.

Our data indicates that after the washing step, the microgels begin to swell and have slightly increased size. By 24 hours after washing, the microgels have increased in size to >6μm, the size targeted to avoid macrophage uptake. The time required to swell to >6μm may prove problematic in avoiding alveolar macrophage uptake. Thus, to determine if this had an effect on uptake, we evaluated macrophage uptake at shorter time points (section 6.3.5).

Table 6.1 Microgel Characterization: Size, Swelling, and Degradation

	Geometric Diameter (mean ± standard error)	Suspension Medium	Measurement Method
Relaxed	1.660±1.362 μm	Paraffin oil	DLS
Washed	1.893±2.729 μm	D.I. water	DLS
Day 1	6.269±0.9148 μm	PBS	ImageJ
Day 2	7.321±0.4725μm	PBS	ImageJ
Day 3	8.179±2.872 μm	PBS	ImageJ
Day 4	7.350±2.162 μm	PBS	ImageJ
Day 5	7.816±1.883 μm	PBS	ImageJ
Day 7	7.433±1.035 μm	PBS	ImageJ
Day 9	10.76±3.165 μm	PBS	ImageJ
Day 11	9.922±1.385 μm	PBS	ImageJ
Day 13	9.604±3.139 μm	PBS	ImageJ

In order to determine microgel densities in the hydrated state, microgels were centrifuged into discrete sucrose gradients [36]. Interestingly, the average geometric diameters of microgels varied across sucrose layers, although the majority of particles were visually observed to settle into the 0, 10, and 20% layers. Theoretical aerodynamic diameters were calculated for each fraction, and ranged from 0.3146-5.824μm. Fractionated geometric diameters, densities, and aerodynamic diameters are summarized in Table 6.2 (page 145), taken as an average across three separate batches.

The 10% sucrose fraction accumulated the majority of larger-sized microgels, resulting in an aerodynamic diameter of 5.824μm. However, the microgels in the

Table 6.2 Microgel Characterization: Density and Theoretical Aerodynamic Diameter

Sucrose Fraction	Geometric Diameter	Density	Theoretical Aerodynamic Diameter
40%	0.2901 μm	1.1764 g/cc	0.3146 μm
30%	1.338 μm	1.1270 g/cc	1.420 μm
20%	3.527 μm	1.0810 g/cc	3.667 μm
10%	5.717 μm	1.0381 g/cc	5.824 μm
0%	1.890 μm	0.9982 g/cc	1.889 μm
Overall*	4.694 μm	1.0497 g/cc	4.809 μm

**Corresponds to overall average normalized by the concentration of microgels in each fraction.*

remaining fractions had aerodynamic diameters well within the desired range, conferring their suitability for use as a pulmonary drug carrier system. The overall values across the entire distribution were determined by normalizing to the concentration of microgels in each fraction. This normalized theoretical aerodynamic diameter, 4.809μm over the entire population, is sufficiently within the desirable range for efficient deep lung delivery.

Microgel aerodynamic diameters were not characterized using the Next Generation Impactor or Anderson Cascade Impactor systems, as the primary purpose of this study was to show the development and characterization of this disease-responsive microgel system. Future work will include formulation development of these microgels for use in existing pulmonary delivery devices, such as dry powder inhalers (DPIs), nebulizers, and pressurized metered dose inhalers (pMDIs). Due to the potential of hydrolytic degradation of the microgels during wet storage and administration, we speculate that dry powder formulations would be most suitable for stability and shelf life.

The actual aerodynamic diameter will depend on the device and formulation, and will thus be the subject of future study.

6.3.3 Microgels are a versatile therapeutic carrier system, capable of encapsulating various biologics and nanoparticles

We were able to successfully encapsulate a wide variety of nanoparticles and biologics, including proteins and nucleotides, within the microgels (Figure 6.2, page 147). Encapsulation was achieved by simply adding the nanoparticle or biologic to the pre-cursor PEG-4-acr in 0.3M triethanolamine buffer solution, mixing uniformly using pipette aspiration, and combining with the peptide solution just prior to emulsion. Up to 20μg of IgG and 859μg of nanoparticles were encapsulated per mg of PEG/peptide. An important consideration is the solubility of the biologic or dispersability of the nanoparticle in the polymer solution, including whether or not it is lipophilic, and thus, more likely to associate with the paraffin oil phase during the emulsion process.

6.3.4 Microgels rapidly degrade and release biologics and nanoparticles in response to varying levels of enzyme while efficiently retaining encapsulants in the absence of the enzyme

The use of optical trapping techniques [37] provided a means to capture, view, and track the same microgel as it is being exposed to enzyme over time. Microgels that had settled onto the surface of a slide were captured and optically pulled up into suspension, such that the reaction would be isotropic, and unhindered by the surface of the slide. Reviewing the time-lapse images, select time points of which are shown in Figure 6.3A (page 151), we were able to observe the various stages of enzyme-mediated degradation. The entire time-lapse sequence is provided in the online version of the

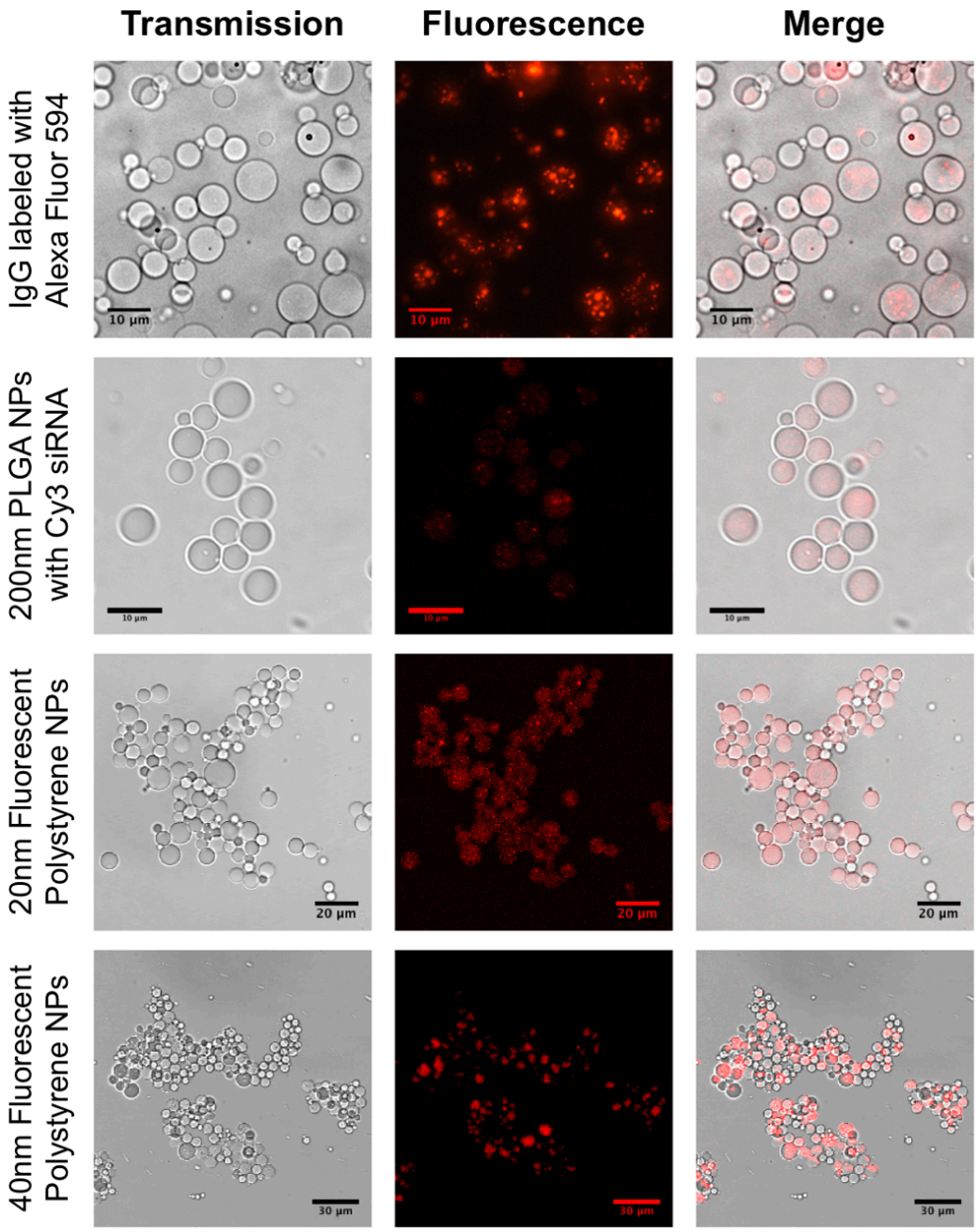

Figure 6.2 Bright field and fluorescence images of microgels with various fluorescent compounds encapsulated, including IgG-labeled with Alexa Fluor® 594, 200nm PLGA nanoparticles with surface loaded Cy3-labeled siRNA, 20nm and 40nm fluorescent polystyrene nanoparticles (FluoSpheres®). Top row to bottom row consecutively, scale bars = 10µm, 10µm, 20µm, 30µm. Up to 20µg of IgG and 859µg of nanoparticles were encapsulated per mg of PEG/peptide.

published article [38]. As the enzyme cleaves the peptide cross-links, the particle initially begins to swell, which is consistent with increased swelling capacity seen in similar hydrogels of lower cross-linking density [18]. At this point, we postulate that the enzyme is able to further penetrate into the microgel, resulting in rapid bulk-type erosion. Degradation is accelerated due to the nature of the network structure, and remaining fragmented components freely dissolve into solution.

Enzyme-mediated release studies were demonstrated with the encapsulation and enzyme-triggered release of fluorescently labeled IgG antibody, lambda DNA, and 20nm fluorescent polystyrene nanoparticles (Dark Red FluoSpheres®) in separate experiments. Figure 6.3B (page 151) provides a visual confirmation of the release of encapsulated fluorescent IgG, correlating to microgel degradation, over time.

Figure 6.4A (page 152) quantitatively shows the cumulative release of 20nm polystyrene nanoparticles, lambda DNA, and IgG over time in response to enzyme after an 18-24 hour swelling period at 37°C. The time at which trypsin was added is denoted in the figure. A trypsin concentration of 10-16.25 USP U/mL was used, a level well below normal physiological ranges [28]. A burst release for all encapsulated compounds was observed within 30 minutes of enzyme addition, demonstrating the ability to exhibit a rapid response to low levels of enzyme. Anomalous decreases seen in cumulative release may be attributed to the experimental method, in which each of the time points collected are from different samples, although originating from the same batch. In order to avoid a misleading multi-phase release in response to supplemented enzyme, the trypsin was not refreshed or supplemented for the duration of the experiment. Thus, the study was terminated after eight hours, before the IgG sample could reach 100% release. The overall trend, however, is clear.

It appears that the nanoparticles are released at a higher rate than both the IgG and DNA in the trypsin-mediated release study. This is likely an artifact of the assay method, in which the particles must be centrifuged in order to sample the supernatant. The centrifugation process may deform soft materials, such as hydrogels, resulting in a force-mediated release. To test this, we also performed long-term diffusion/hydrolysis-mediated release studies using cell culture insert filters, without the use of enzyme or centrifugation, as described in section 6.2.7 . Figure 6.4B (page 152) shows the diffusion/hydrolysis-mediated release of nanoparticles and IgG over a period of 17-20 days. It is apparent that the IgG is released to a greater extent during this period, likely due to a combination of diffusion and hydrolysis. It is also interesting to note that there is a spike in the release of both IgG and nanoparticles around day 12, which corresponds to the rapid change in hydrolytic degradation at this same time point, presented in Figure 6.1D (page 142).

Given that the hydrodynamic radius of the 20-40nm particles lies between the hydrodynamic radii of IgG (~5nm) [39] and lambda DNA (130-300nm, depending on conformation) [40,41], hydrodynamic size is not the only predictor of release. It is possible that large macromolecules, such as DNA and IgG, can potentially entangle with the hydrogel network structure, which allows them to more easily be retained during centrifugation, but results in a diffusion-driven release during the first ten days. Nanoparticles, on the other hand, may be entrapped within the pores seen in Figure 6.1C (page 142). When exposed to high centrifugal force (10,000xg), the microgel may be deformed such that the nanoparticles are released from these "pockets." Without any applied force, the nanoparticles are effectively retained by the microgels.

The rate of diffusion-mediated release, of IgG for example, may be easily tuned by changing the cross-linking density, wherein a tighter cross-linking density (with a

higher % polymer weight by volume composition) will result in slower diffusion. The four-armed PEG used in this study had a molecular weight of 10kDa per arm. Increasing the number of branches on the polymer, using a 6- or 8-arm PEG for instance, and/or using a lower molecular weight polymer could also reduce the rate of diffusion.

We do not expect there to be significant effects on bioactivity of the drug due to the mild fabrication conditions, as similar systems have been used to encapsulate cells and growth factors within bulk hydrogels for tissue engineering [42-44]. However, one important consideration that warrants discussion is the ability of the trigger enzyme to degrade not only the microgel, but also any encapsulated proteins or peptides. For this study, we used trypsin as a cost-efficient model enzyme in these proof-of-concept studies. Trypsin is able to cleave amino acid sequences terminal to arginine and lysine residues [21], meaning that it may not be a viable trigger for delivery of many protein or peptide drugs. However, there are a host of other enzymes that are up-regulated in diseases that require much more sequence specificity, including matrix metalloproteinases and cathepsins [11]. It may then be unlikely that the trigger enzyme could degrade an encapsulated protein. This could be further improved by optimizing the cross-linker peptide sequence to have greater specificity and quicker degradation by the enzyme of interest (k_{cat}) [42]. In moving towards a disease-specific system, the enzymatic activity of the trigger enzyme on any encapsulated protein or peptide must be considered, and a cross-linker peptide should be designed accordingly. This does not pose a significant challenge, especially with the increasing prevalence and sophistication of bioinformatics tools and databases to predict enzyme-substrate activities [21,22]. Moreover, as we are specifically using protease triggers (enzymes that digest proteins), this is of less concern for other biologics (DNA, RNA) and nanoparticles.

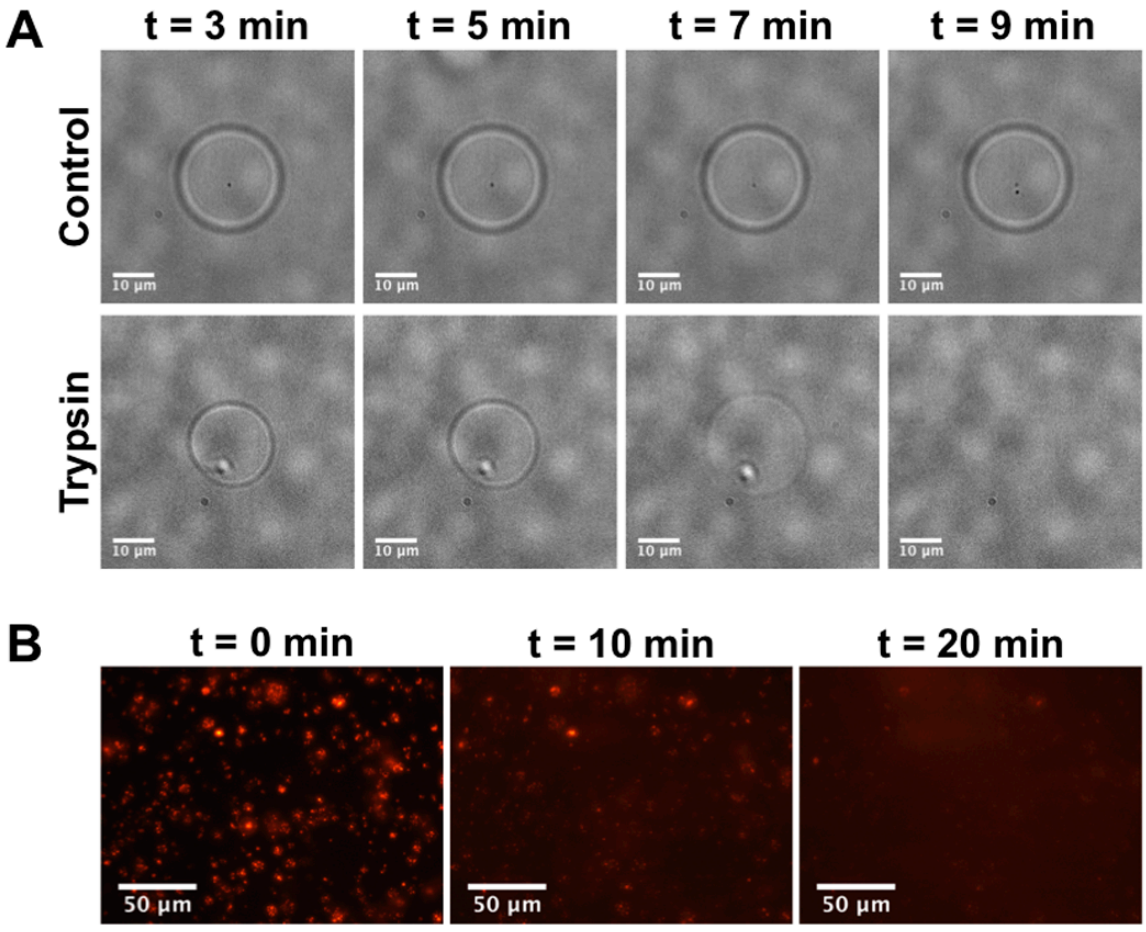

Figure 6.3 Microgel degradation and release of encapsulated compounds in response to enzyme exposure by microscopy.
(A) Light microscopy of a single microgel captured by optical trapping techniques, exposed to trypsin enzyme over time to view isotropic enzyme-responsive degradation in comparison to a control sample; 325 U/mL trypsin. All scale bars = 10µm. A video of the time-lapse degradation is provided in the web version of [38].
(B) Fluorescent microscopy of IgG releasing from microgels at 325 U/mL trypsin. All scale bars = 50µm.

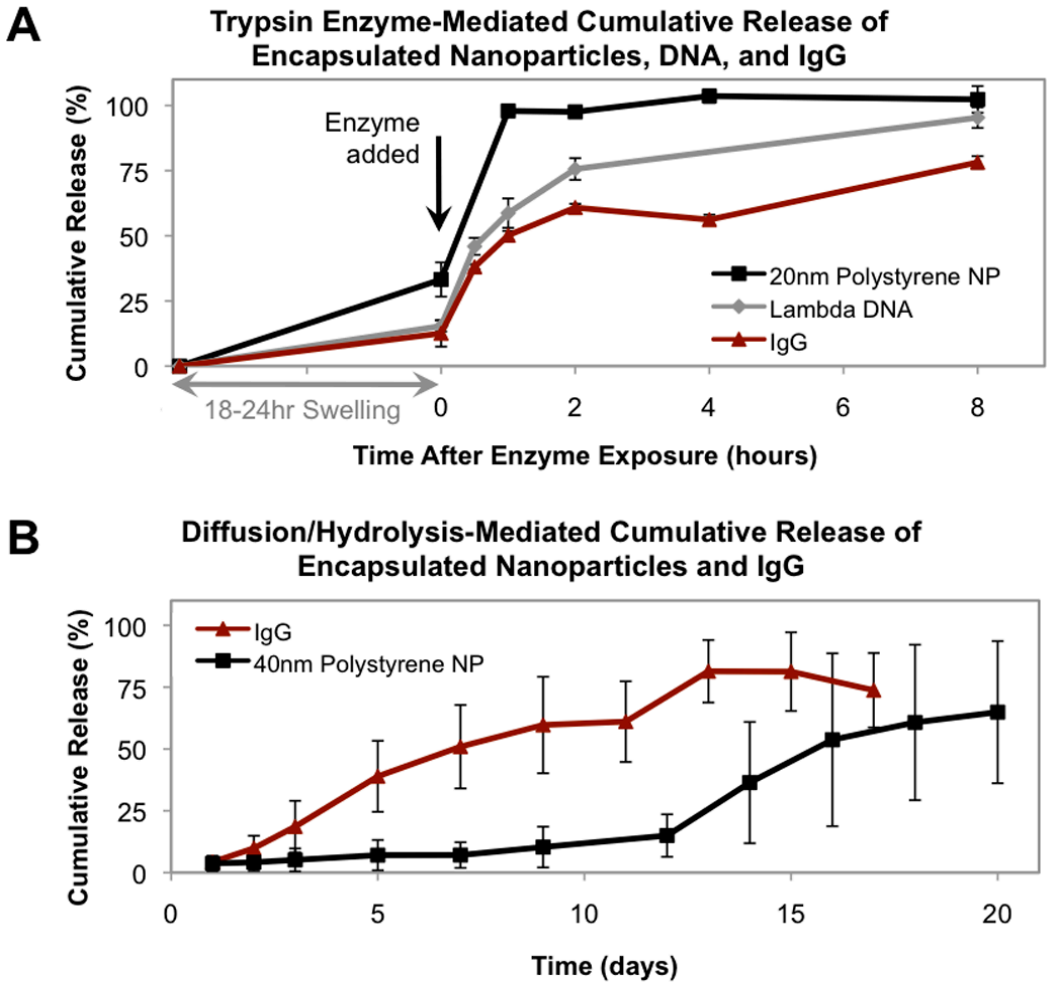

Figure 6.4 Microgel degradation and release of encapsulated compounds in response to or absence of enzyme, by quantitative fluorometric assays.
(A) Cumulative release of encapsulated 20nm Dark Red FluoSpheres®, lambda DNA, and Alexa Fluor® 594 IgG from microgels in response to enzyme exposure. Rapid release of all encapsulated compounds is observed at physiologically relevant concentrations of 10-16.25 U/mL trypsin. Trypsin was added after an 18-24 hour equilibrium swelling period. All error bars are plotted, but may be obscured by data markers.
(B) Cumulative release of encapsulated 40nm Dark Red FluoSpheres® and Alexa Fluor® 594 IgG from microgels due to hydrolysis and/or diffusion. Nanoparticles are more effectively retained within the microgels than IgG, which may be related to hydrodynamic radius and/or hydrogel network entanglement. An increase in release of both IgG and nanoparticles is seen around day 12, which correlates to the rapid hydrolytic degradation seen during the same time frame in Figure 6.1D.

6.3.5 Microgels exhibit minimal cytotoxicity and evade clearance by macrophages

Microgel toxicity was tested on two epithelial cell lines, A549 human lung epithelial cells and HEK 293 human embryonic kidney epithelial cells, using the MTS assay. Microgels, trypsin-degraded microgels, and un-reacted PEG-4-acr and CGRGGC peptide (equivalent levels to microgel condition) at doses of 0.5 and 1.0 mg/mL were tested at 6, 24, and 48 hours. The doses correspond to approximately 4350 and 8700 microgels per cell, respectively, which are high enough doses to completely blanket the cells. Significant cytotoxicity was determined by an F-test for equal or unequal variances ($p<0.05$), followed by a two-tailed t-test (equal or unequal variances depending on F-test result, $p<0.01$). There was no significant difference in A549 or HEK 293 cell viability at high doses of 0.5 and 1.0 mg/mL of microgels over all time points, as compared to untreated control samples. At 48 hours and a dose of 0.5 mg/mL, there was a significant difference ($p=0.005$) between the untreated control and the degraded microgel condition. This may be attributed to the extended presence of trypsin in the culture, which was required to degrade the microgels. This significance was not observed in the higher dose of 1.0 mg/mL of degraded microgels at any time point, nor was it observed in conditions with un-reacted PEG-4-acr and CGRGGC peptide at any time point. Overall, the data indicates that the microgels, and their components, are not significantly cytotoxic at extremely high doses over several time points. The complete data set is shown in Figure 6.5 (page 154).

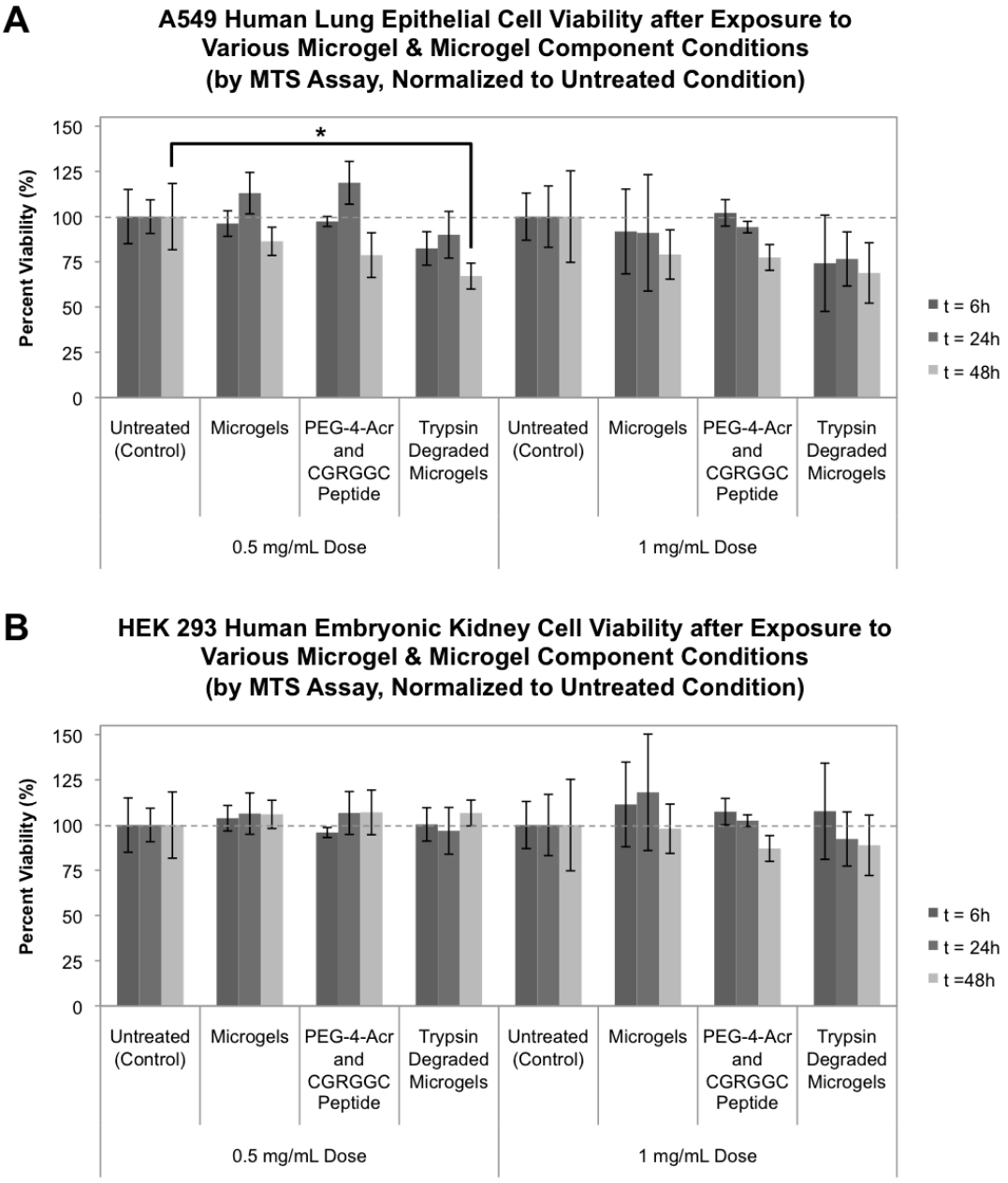

Figure 6.5 *In vitro* cytotoxicity of microgels on multiple cell lines.
Percent viability of (A) A549 human lung epithelial and (B) HEK 293 human embryonic kidney cells following exposure to microgels and microgel components for 6, 24, and 48 hours. Cell numbers are normalized to untreated control samples for each time point, with a dotted line denoting 100% viability. *The only significant difference found in cell viability across all conditions and time points was for trypsin-degraded microgels after 48 hours exposure in A549 cells, denoted in (A), where p=0.005.

A potential issue with long-term controlled release particulate systems for pulmonary delivery is the rapid clearance of particles by alveolar macrophages. Macrophages begin taking up inhaled micron-sized particulates in a span of minutes, thus negating the effects of slow or controlled drug release particle formulations [4-7]. We theorized that the swelling behavior and hydrophilicity of the microgels, coupled with the stealth characteristics of PEG, would result in a decreased amount of microgel clearance as compared to 1μm fluorescent polystyrene microparticles (1μm-MP Positive Control), used as a positive control. In order to fluorescently trace microgels, 20nm fluorescent polystyrene nanoparticles were encapsulated within the microgels (Microgel-with-20nm-NP). Due to the particle size differences between the 1μm-MP Positive Control and microgels, dosages were matched by weight (28μg per well, 50,000 cells per well). Free fluorescent polystyrene nanoparticles were also delivered as a comparative control (Free-20nm-NP), and were matched to microgels by number of nanoparticles-encapsulated-in-microgels and number of nanoparticles per cell (2.12×10^5 nanoparticles per cell). The amount of Free-20nm-NP and Microgels-with-20nm-NP were experimentally matched using standard curves of fluorescence versus concentration. Flow cytometry data for 1μm-MP Positive Control (ex/em 540/560) were collected in the FL2 channel, and data for Microgel-with-20nm-NP and Free-20nm-NP (ex/em 660/680) were collected in the FL4 channel. Using the fluorescence intensity of the untreated cells, a very tight gate was applied (depicted as a vertical dotted line in Figure 6.6, page 157) as a threshold on fluorescence intensity for positive uptake of particles.

As can be seen in Figure 6.6 (page 157) and Figure 6.7B (page 158), 94.1% of the cell population has already taken up the hydrophobic polystyrene 1μm-MP Positive Control sample after only 2 hours, and 99.7% after 24 hours. In comparison, Microgel-

with-20nm-NP uptake was quantified as only 12.1% after two hours, and 11.8% after 24 hours. This was also visually confirmed by confocal microscopy, shown in Figure 6.7 (page 158). Effectively, this data supports the conclusion that the hydrophilic and swellable microgels may offer improved retention over hydrophobic polymer particles for long-term controlled drug release in the lungs by avoiding macrophage uptake in the short- and long-term. As shown in section 6.3.2 , microgels required up to 24 hours to reach the theoretical size to avoid macrophage uptake (>6μm). Freshly synthesized, pre-swollen microgels were used for this study, indicating that other factors than size, perhaps the hydrophilic and/or PEG "stealth" characteristic, are involved. Whether the hydrophilicity, swelling, or PEG composition plays a greater role in this macrophage avoidance must be further studied to draw final conclusions, and will be used to improve future microgel design.

With regards to long-term treatment with an un-clearable particle, it may be dangerous to receive repeat chronic dosages, thereby increasing particle accumulation in the lungs over time. This proposed microgel system, however, contains a hydrolytically degradable ester bond in the cross-link, which was shown to degrade over a time period of approximately two weeks (section 6.3.2).

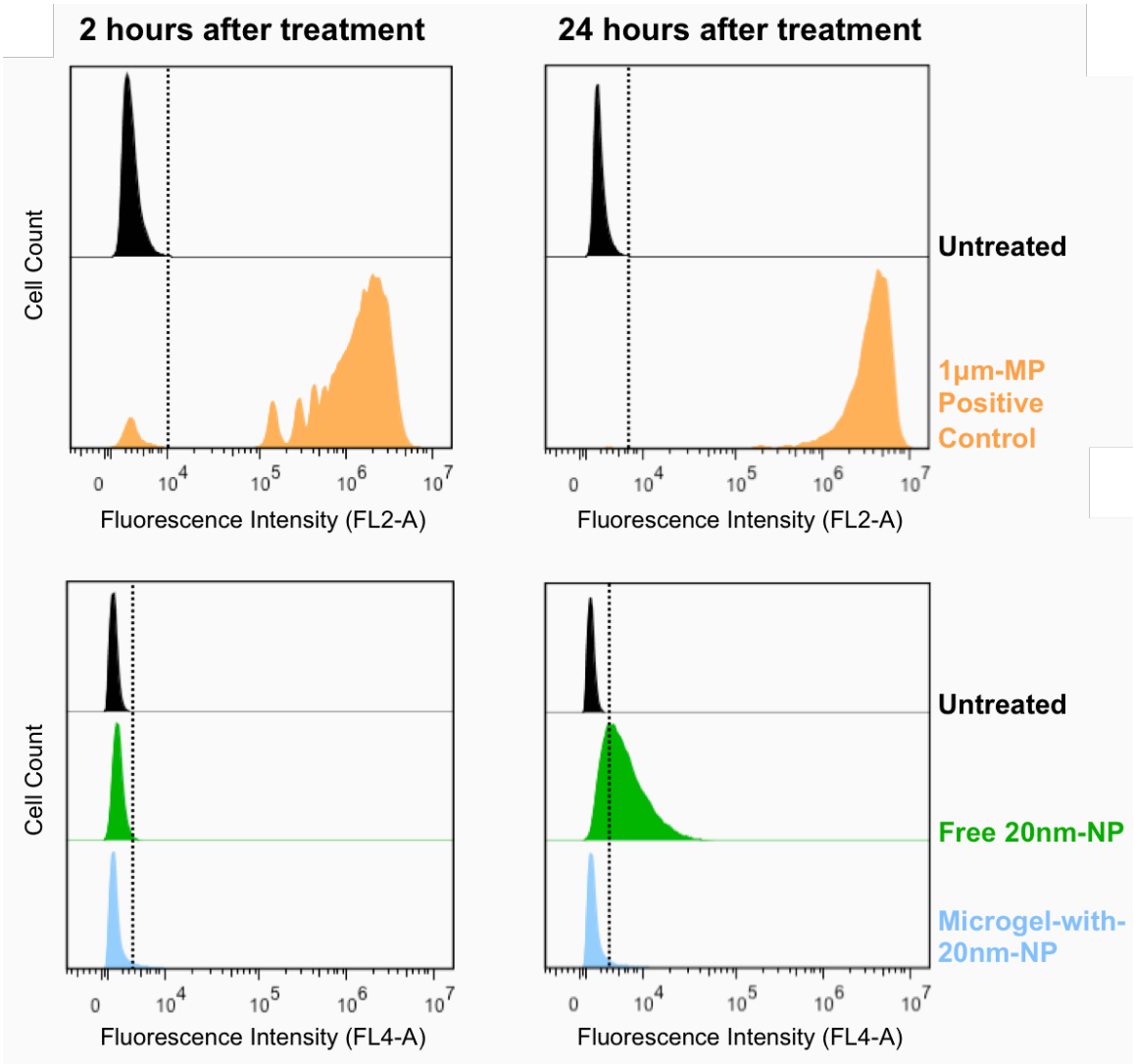

Figure 6.6 Microgels exhibit reduced uptake and clearance by macrophages in comparison to polystyrene particles, by flow cytometry. Flow cytometry histograms comparing fluorescence intensity of untreated cells to those that have taken up 1µm fluorescent polystyrene microparticles as a positive control (1µm-MP Positive Control), free 20nm fluorescent polystyrene nanoparticles (Free-20nm-NP), and 20nm fluorescent polystyrene nanoparticles encapsulated in microgels (Microgel-with-20nm-NP). Free-20nm-NP and Microgel-with-20nm-NP have the same nanoparticle dosage by number of nanoparticles. The 1µm-MP Positive Control and Microgel-with-20nm-NP groups have the same dosage by weight. Typical results are shown representing three experimental repeats, and are taken from a gated population of at least 10,000 RAW 264.7 macrophages.

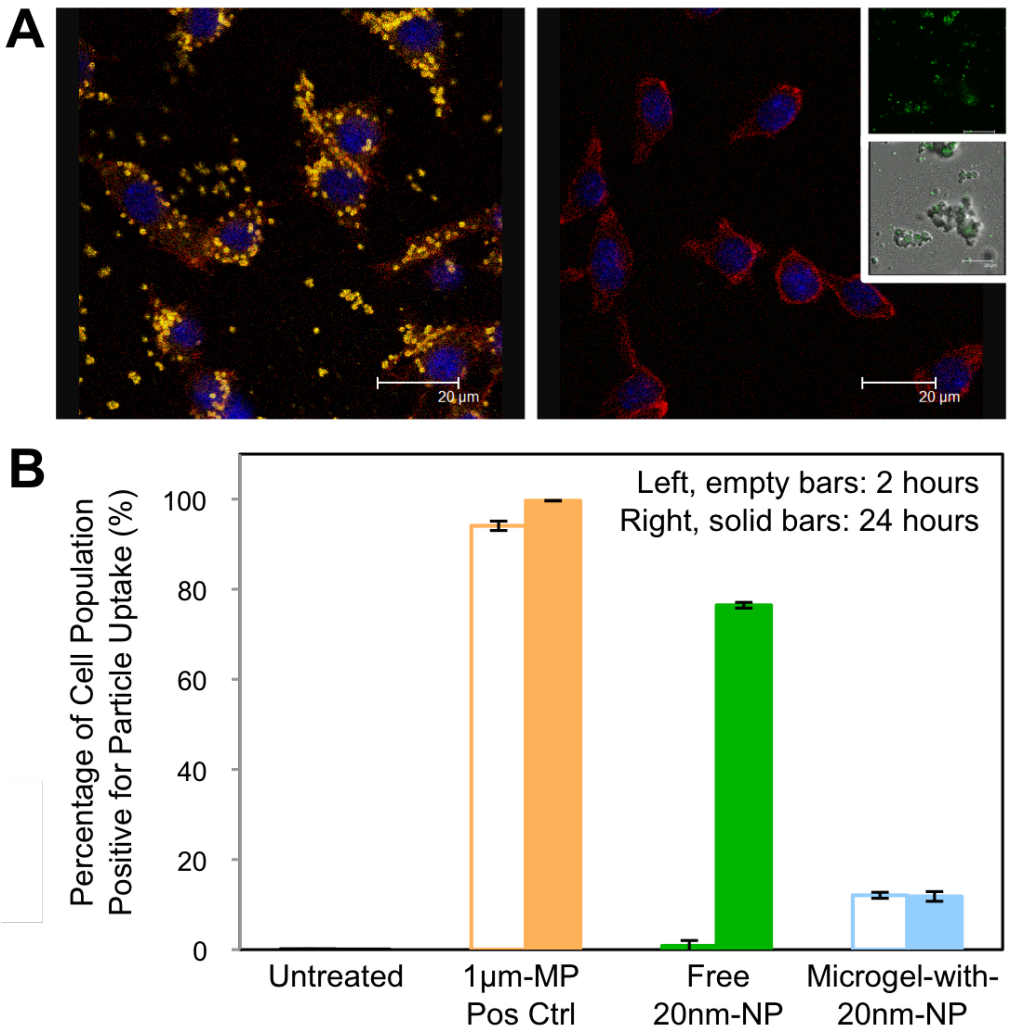

Figure 6.7 Microgels exhibit reduced uptake and clearance by macrophages in comparison to polystyrene particles, by microscopy and flow cytometry. (A) Confocal microscopy of RAW 264.7 macrophages after one hour of incubation with 1µm-MP Positive Control at left, and Microgel-with-20nm-NP at right. Cell nuclei are stained with DAPI in blue, and actin cytoskeletal protein is stained with phalloidin in red; 1µm-MP Positive Control particles are shown in orange; Microgel-with-20nm-NP are shown in green at inset. No uptake of microgels was observed. Scale bars = 20µm.
(B) Percentage of RAW 264.7 macrophage cell population positive for particle uptake after two and 24 hours, by flow cytometry analysis of at least 10,000 cells representing three repeats. Cells were considered positive for uptake if their fluorescence intensity was increased and shifted past an applied gated threshold on the untreated population, depicted by a vertical dashed line in (A).

6.4 CONCLUSIONS

Here, we have discussed the many challenges to achieving effective delivery of biologic drugs inside cells to the deep lung, and the design of a new platform drug delivery system to overcome them. In considering these challenges, the following criteria were considered:

a. Reduced exposure to fabrication conditions that may denature biologic drugs
b. Aerodynamic diameter between 0.5 and 5μm to achieve deep lung deposition
c. Geometric diameter greater than 6μm and hydrophilic surface chemistry to avoid rapid clearance by alveolar macrophages
d. Nanoscale sizes, less than 0.2μm, for mucus penetration and intracellular delivery
e. Disease-responsive drug release mechanism to improve targeting to diseased tissue for non-uniform lung diseases, thereby reducing side effects.

Regarding (a), we have introduced a new MADE fabrication method, which produces aqueous microgels by employing a Michael addition cross-linking during water-in-oil emulsion at physiological temperature and pH, without exposure to organic solvents. The microgels were shown to have geometric and theoretical aerodynamic diameters within the required range to achieve deep lung deposition, 0.5-5μm (b). As the microgels are inherently micro-sized hydrogels, they exhibit hydrogel swelling behavior. After 24 hours of swelling in PBS, the microgels swelled to a geometric diameter greater than 6μm. It was noted, however, that the required swelling time was longer than expected, leaving a question of whether or not they could avoid macrophage clearance in the short term (c). Nonetheless, macrophage uptake studies with freshly synthesized

microgels (pre-swelling) were able to effectively avoid macrophage uptake at both two and 24 hours, indicating greater potential for retention of this controlled release system in the lungs.

Concerning (d), we demonstrated the versatility to encapsulate various types of biologics (DNA, siRNA, and proteins) and nanoparticles (20nm to 200nm). In future work, encapsulated nanoparticles could be further engineered to have improved mucosal penetration, uptake, and endosomal escape, if desired. Lastly, we successfully incorporated a disease-triggered release mechanism into the microgels, in the form of enzyme-specific peptide cross-linkers. The microgels exhibited rapid release of biologics and nanoparticles in response to enzyme and the ability to retain drug in the absence of enzyme. In future iterations of this microgel system, the peptide cross-linker may be easily interchanged for one customized to a highly specific, disease up-regulated protease, thus providing the disease-responsive drug release mechanism (e).

Overall, the microgel delivery system has successfully met all design criteria laid out in (a-e), showing great potential as a versatile disease-responsive system for pulmonary delivery of biologic drugs. Future work will involve formulation optimization for existing, non-invasive, pulmonary delivery devices, such as DPIs, pMDIs, or nebulizers. Other future studies will include *in vivo* biodistribution, efficacy, and significance of disease-responsive drug release triggers in reducing side effects.

6.5 REFERENCES

[1] D.A. Edwards, C. Dunbar, Bioengineering of therapeutic aerosols, Annu Rev Biomed Eng. 4 (2002) 93–107.

[2] Y.-J. Son, J.T. McConville, Advancements in dry powder delivery to the lung, Drug Dev Ind Pharm. 34 (2008) 948–959.

[3] G. Pilcer, K. Amighi, Formulation strategy and use of excipients in pulmonary drug delivery, Int J Pharm. 392 (2010) 1–19.

[4] I.M. El-Sherbiny, S. McGill, H.D.C. Smyth, Swellable microparticles as carriers for sustained pulmonary drug delivery, J Pharm Sci. 99 (2010) 2343–2356.

[5] F. Ahsan, I.P. Rivas, M.A. Khan, A.I. Torres Suarez, Targeting to macrophages: role of physicochemical properties of particulate carriers--liposomes and microspheres--on the phagocytosis by macrophages, J Control Release. 79 (2002) 29–40.

[6] J.A. Champion, A. Walker, S. Mitragotri, Role of Particle Size in Phagocytosis of Polymeric Microspheres, Pharm Res. 25 (2008) 1815–1821.

[7] K. Makino, N. Yamamoto, K. Higuchi, N. Harada, H. Ohshima, H. Terada, Phagocytic uptake of polystyrene microspheres by alveolar macrophages: effects of the size and surface properties of the microspheres, Colloids Surf B Biointerfaces. 27 (2003) 33–39.

[8] S.K. Lai, Y.-Y. Wang, J. Hanes, Mucus-penetrating nanoparticles for drug and gene delivery to mucosal tissues, Adv Drug Deliv Rev. 61 (2009) 158–171.

[9] J.C. Sung, B.L. Pulliam, D.A. Edwards, Nanoparticles for drug delivery to the lungs, Trends Biotechnol. 25 (2007) 563–570.

[10] E. Rytting, J. Nguyen, X. Wang, T. Kissel, Biodegradable polymeric nanocarriers for pulmonary drug delivery, Expert Opin Drug Deliv. 5 (2008) 629–639.

[11] P. Wanakule, K. Roy, Disease-responsive drug delivery: the next generation of smart delivery devices, Curr Drug Metab. 13 (2012) 42–49.

[12] M. Caldorera-Moore, N. Guimard, L. Shi, K. Roy, Designer nanoparticles: incorporating size, shape and triggered release into nanoscale drug carriers, Expert Opin Drug Deliv. 7 (2010) 479–495.

[13] D.L. Elbert, A.B. Pratt, M.P. Lutolf, S. Halstenberg, J.A. Hubbell, Protein delivery from materials formed by self-selective conjugate addition reactions, J Control Release. 76 (2001) 11–25.

[14] M.D. Bhavsar, M.M. Amiji, Development of novel biodegradable polymeric nanoparticles-in-microsphere formulation for local plasmid DNA delivery in the gastrointestinal tract, AAPS PharmSciTech. 9 (2008) 288–294.

[15] N. Tsapis, D. Bennett, B. Jackson, D.A. Weitz, D.A. Edwards, Trojan particles: large porous carriers of nanoparticles for drug delivery, Proc Natl Acad Sci U S A. 99 (2002) 12001–12005.

[16] C. Wong, T. Stylianopoulos, J. Cui, J. Martin, V.P. Chauhan, W. Jiang, et al., Multistage nanoparticle delivery system for deep penetration into tumor tissue, Proc Natl Acad Sci U S A. 108 (2011) 2426–2431.

[17] S. Kim, E.H. Chung, M. Gilbert, K.E. Healy, Synthetic MMP-13 degradable ECMs based on poly(N-isopropylacrylamide-co-acrylic acid) semi-interpenetrating polymer networks. I. Degradation and cell migration, J Biomed Mater Res A. 75 (2005) 73–88.

[18] A. Metters, J.A. Hubbell, Network formation and degradation behavior of hydrogels formed by Michael-type addition reactions, Biomacromolecules. 6 (2005) 290–301.

[19] Y. Qiu, K. Park, Environment-sensitive hydrogels for drug delivery, Adv Drug Deliv Rev. 53 (2001) 321–339.

[20] A.A. Aimetti, A.J. Machen, K.S. Anseth, Poly(ethylene glycol) hydrogels formed by thiol-ene photopolymerization for enzyme-responsive protein delivery, Biomaterials. 30 (2009) 6048–6054.

[21] A. Chang, M. Scheer, A. Grote, I. Schomburg, D. Schomburg, BRENDA, AMENDA and FRENDA the enzyme information system: new content and tools in 2009, Nucleic Acids Res. 37 (2009) D588–92.

[22] E. Gasteiger, A. Gattiker, C. Hoogland, I. Ivanyi, R.D. Appel, A. Bairoch, ExPASy: The proteomics server for in-depth protein knowledge and analysis, Nucleic Acids Res. 31 (2003) 3784–3788.

[23] Y.-S. Chen, R.G. Alany, S.A. Young, C.R. Green, I.D. Rupenthal, In vitro release characteristics and cellular uptake of poly(D,L-lactic-co-glycolic acid) nanoparticles for topical delivery of antisense oligodeoxynucleotides, Drug Deliv. 18 (2011) 493–501.

[24] S.P. Kasturi, I. Skountzou, R.A. Albrecht, D. Koutsonanos, T. Hua, H.I. Nakaya, et al., Programming the magnitude and persistence of antibody responses with innate immunity, Nature. 470 (2011) 543–547.

[25] S.K. Sahoo, W. Ma, V. Labhasetwar, Efficacy of transferrin-conjugated paclitaxel-loaded nanoparticles in a murine model of prostate cancer, International Journal of Cancer. 112 (2004) 335–340.

[26] A. Singh, H. Nie, B. Ghosn, H. Qin, L.W. Kwak, K. Roy, Efficient modulation of T-cell response by dual-mode, single-carrier delivery of cytokine-targeted siRNA and DNA vaccine to antigen-presenting cells, Mol Ther. 16 (2008) 2011–2021.

[27] A. Singh, S. Suri, K. Roy, In-situ crosslinking hydrogels for combinatorial delivery of chemokines and siRNA-DNA carrying microparticles to dendritic cells, Biomaterials. 30 (2009) 5187–5200.

[28] A. Pusztai, G. Grant, S. Bardocz, K. Baintner, E. Gelencsér, S.W. Ewen, Both free and complexed trypsin inhibitors stimulate pancreatic secretion and change duodenal enzyme levels, Am. J. Physiol. 272 (1997) G340–50.

[29] O.Z. Fisher, N.A. Peppas, Polybasic Nanomatrices Prepared by UV-Initiated Photopolymerization, Macromolecules. 42 (2009) 3391–3398.

[30] M. Ehrbar, S.C. Rizzi, R.G. Schoenmakers, B.S. Miguel, J.A. Hubbell, F.E. Weber, et al., Biomolecular hydrogels formed and degraded via site-specific enzymatic reactions, Biomacromolecules. 8 (2007) 3000–3007.

[31] M.P. Lutolf, F.E. Weber, H.G. Schmoekel, J.C. Schense, T. Kohler, R. Müller, et al., Repair of bone defects using synthetic mimetics of collagenous extracellular matrices, Nat Biotechnol. 21 (2003) 513–518.

[32] B. Mather, K. Viswanathan, K. Miller, T. Long, Michael addition reactions in macromolecular design for emerging technologies, Prog Polym Sci. 31 (2006) 487–531.

[33] K. Hadinoto, P. Phanapavudhikul, Z. Kewu, R.B.H. Tan, Dry powder aerosol delivery of large hollow nanoparticulate aggregates as prospective carriers of nanoparticulate drugs: effects of phospholipids, Int J Pharm. 333 (2007) 187–198.

[34] K. Hadinoto, K. Zhu, R.B.H. Tan, Drug release study of large hollow nanoparticulate aggregates carrier particles for pulmonary delivery, Int J Pharm. 341 (2007) 195–206.

[35] Y. Liu, P. Daum, The effect of refractive index on size distributions and light scattering coefficients derived from optical particle counters, J Aerosol Sci. 31 (2000) 945–957.

[36] C. Vauthier, C. Schmidt, P. Couvreur, Measurement of the density of polymeric nanoparticulate drug carriers by isopycnic centrifugation, J Nanopart Res. (1999).

[37] D.G. Grier, A revolution in optical manipulation, Nature. 424 (2003) 810–816.

[38] P. Wanakule, G.W. Liu, A.T. Fleury, K. Roy, Nano-inside-micro: Disease-responsive microgels with encapsulated nanoparticles for intracellular drug delivery to the deep lung, J Control Release. 162 (2012) 429–437.

[39] J.K. Armstrong, R.B. Wenby, H.J. Meiselman, T.C. Fisher, The Hydrodynamic Radii of Macromolecules and Their Effect on Red Blood Cell Aggregation, Biophys J. 87 (2004) 4259–4270.

[40] R.S. Dias, J. Innerlohinger, O. Glatter, M.G. Miguel, B. Lindman, Coil–Globule Transition of DNA Molecules Induced by Cationic Surfactants: A Dynamic Light Scattering Study, J. Phys. Chem. B. 109 (2005) 10458–10463.

[41] H. Oana, K. Tsumoto, Y. Yoshikawa, K. Yoshikawa, Folding transition of large DNA completely inhibits the action of a restriction endonuclease as revealed by single-chain observation, FEBS Lett. 530 (2002) 143–146.

[42] J. Patterson, J.A. Hubbell, Enhanced proteolytic degradation of molecularly engineered PEG hydrogels in response to MMP-1 and MMP-2, Biomaterials. 31 (2010) 7836–7845.

[43] J. Patterson, J.A. Hubbell, SPARC-derived protease substrates to enhance the plasmin sensitivity of molecularly engineered PEG hydrogels, Biomaterials. 32 (2011) 1301–1310.

[44] M.P. Lutolf, J.L. Lauer-Fields, H.G. Schmoekel, A.T. Metters, F.E. Weber, G.B. Fields, et al., Synthetic matrix metalloproteinase-sensitive hydrogels for the conduction of tissue regeneration: engineering cell-invasion characteristics, Proc Natl Acad Sci U S A. 100 (2003) 5413–5418.

Chapter 7: In Vivo Pulmonary Distribution and Clearance of Microgels

7.1 Introduction

As discussed in the previous chapter (Chapter 6), in the development of controlled release systems for pulmonary delivery, an important design consideration is the ability of the system to avoid the rapid clearance by alveolar macrophages [1,2]. In other words, a controlled release particle must reside in the pulmonary space sufficiently long enough to allow for its controlled release mechanism to take place, whether it is sustained and long-term release of drug, or until an environmental trigger causes the release of drug; both of these release mechanisms are applicable to the work presented in this dissertation. The majority of polymer particles are cleared from the rodent pulmonary space within 1-3 days [3-5]. The goal of the study presented here was to determine if the *in vitro* data

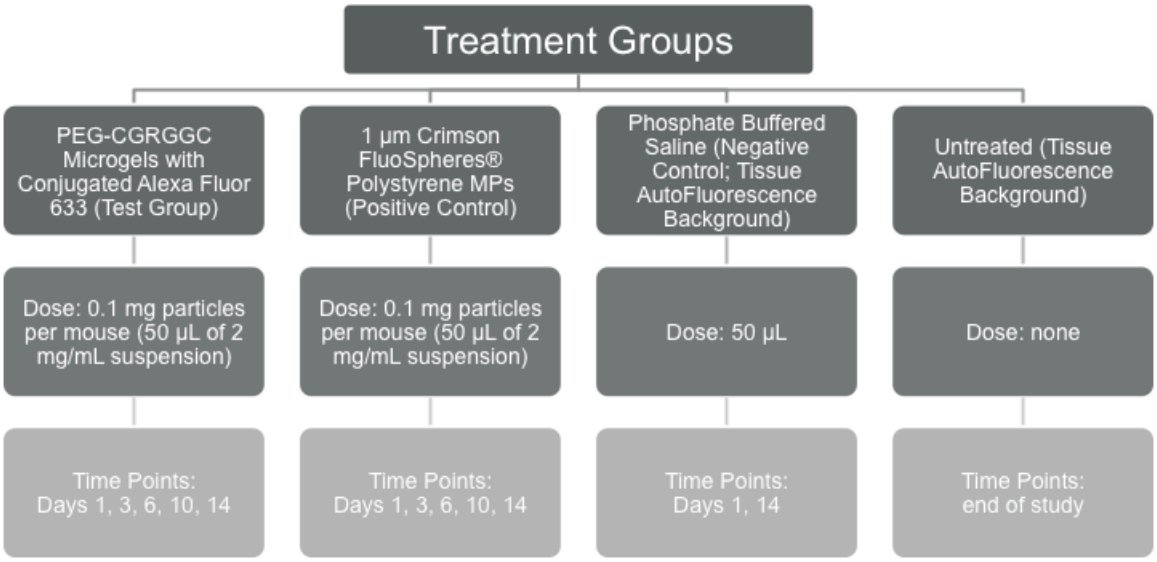

Figure 7.1 *In Vivo* Pulmonary Distribution and Clearance of Microgels: Study Groups

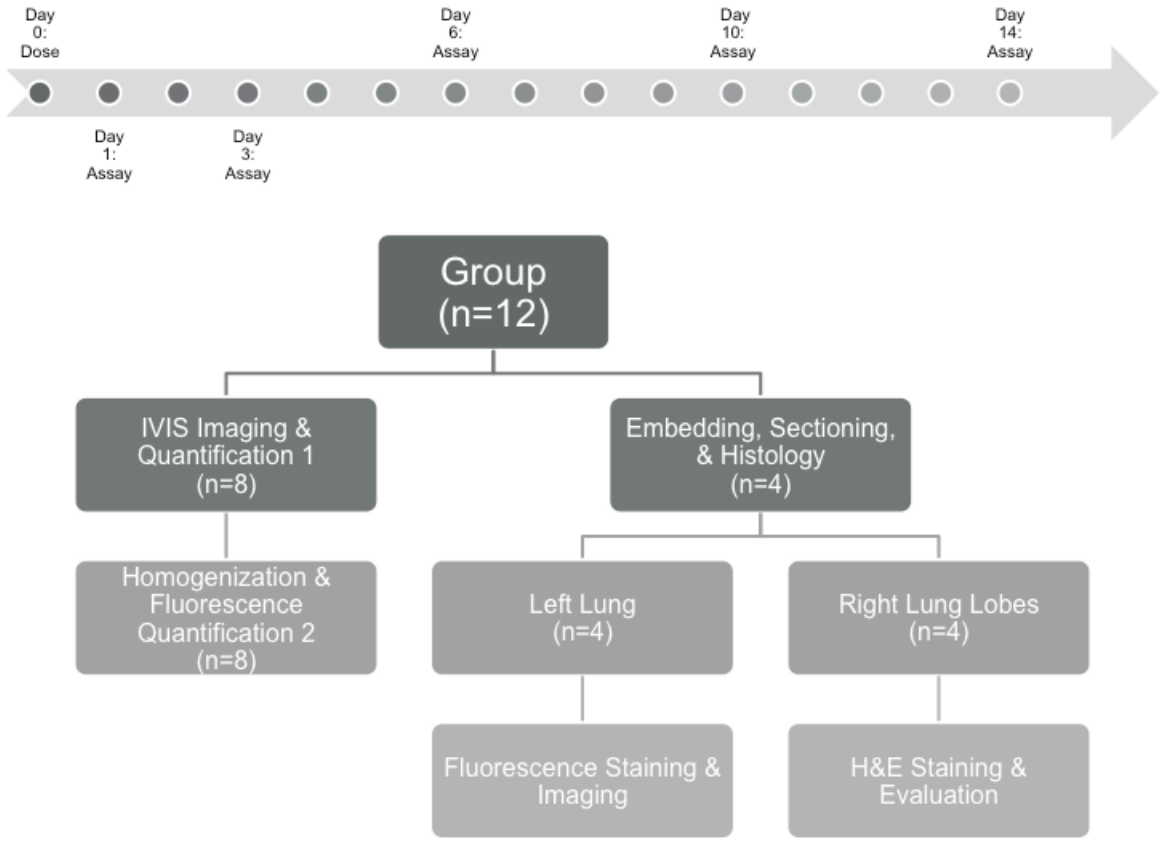

Figure 7.2 *In Vivo* Pulmonary Distribution and Clearance of Microgels: Timeline and Sample Assays

from Chapter 6, which indicated that the PEG-CGRGGC microgels are better able to avoid macrophage clearance than polystyrene particles, was significant enough to prolong the residence time of microgels in the murine lung *in vivo*.

For the purposes of this study, microgels were directly introduced into mouse lungs using a Penn-Century MicroSprayer device, commonly used to deliver test formulations to rodents *in vivo* [3,6-9]. Polystyrene microparticles were also used as a positive control for comparison. The amount of particles remaining in the lungs at days 1, 3, 6, 10, and 14 were determined using IVIS (*In Vivo* Imaging System) imaging, as well

fluorescence measurements from lung homogenates. The IVIS images also provided a means to view the distribution of particles in the lungs. The study groups, timeline and assays performed are illustrated in Figure 7.1 and Figure 7.2, respectively.

7.2 MATERIALS AND METHODS

7.2.1 Materials

Alexa Fluor ® 633 Carboxylic Acid Succinimidyl Ester (AF633-SE) and 1 μm Crimson (excitation/emission 625/645) FluoSpheres® were purchased from Life Technologies (Carlsbad, CA). Float-a-Lyzer dialysis tubes were purchased from Spectrum Labs (Rancho Dominguez, CA). The microsprayer assembly, including the FMJ-250 High Pressure Syringe and Model IA-1C (1.25 inch, for mouse) MicroSprayer® tip, was purchased from Penn-Century, Inc. (Wyndmoor, PA). The Model LS-2 Small Animal Laryngoscope and Mouse Intubation Platform were also purchased from Penn-Century, Inc. Nylon suture thread and 20 gauge x 1 inch intravenous catheters were purchased from Thermo Fisher Scientific (Hampton, New Hampshire). Paraformaldehyde (dry powder) was purchased from Sigma-Aldrich (St. Louis, MO).

7.2.2 Conjugation of Fluorescent Probe to Microgels

The direct and covalent incorporation of fluorescent probes on microgels was carried out by bioconjugation of AF633-SE, which contains a carboxylic acid group, onto the peptide sequence CGRGGC, which contains primary amines. The reaction was carried out according to manufacturer instructions at a pH favorable for conjugation at the alpha amine, rather than the side chain amines. Following the reaction, the product

was dialyzed to remove side products and un-reacted materials for at least three dialysis changes in one liter of de-ionized water for four to six hours each. The product was snap frozen in liquid nitrogen and lyophilized for 48-72 hours, then stored under nitrogen gas at -20°C until used. Fluorescently labeled microgels were synthesized using the MADE method (as described in Chapter 5), substituting in a ratio of one fluorescently tagged peptide per five un-tagged peptides.

7.2.3 Animal Strains, Care, and Use

All experiments were approved by the University of Texas at Austin Institutional Animal Care and Usage Committee (IACUC), and all new procedures were developed with careful consultation with clinical veterinarians. All mice used in this study were 8-10 week old female BALB/c mice from Jackson Laboratories (Bar Harbor, ME), weighing approximately 20 grams each. Prior to study assays, all animals were kept on a modified alfalfa-free diet for at least seven days to reduce tissue and food autofluorescence (Teklad Global Rodent Diet 2014, Harlan Laboratories, Indianapolis, IN) in IVIS images.

7.2.4 Mouse Endotracheal Intubation and Intrapulmonary Aerosol Delivery of Particles using a Penn-Century MicroSprayer Device

Both control fluorescent polystyrene particles and microgels were delivered using a Penn-Century MicroSprayer device designed for use in mice. This procedure has been significantly modified from the method given by Bivas-Benita, et. al. [8], through several practice administrations in mice post-mortem to reduce incidence of tracheal perforation and mortality. Primary deviations include the orientation of the mouse to improve

operator's ergonomic posture, as well as introduction of a flexible intubation tube (20 gauge catheter) to serve as a "guide" to insert the MicroSprayer needle tip, minimizing incidence of trauma. As such, a detailed protocol, including images, for this procedure is given in Appendix A. A procedure record and monitoring worksheet to facilitate recordkeeping for monitoring and recovery is also provided in Appendix B. Prior to loading into the MicroSprayer, all particle suspensions were filtered through a 36 μm mesh, to prevent the sprayer tip from clogging.

Mice were anesthetized using an intraperitoneal (IP) injection of Ketamine (800-100mg/kg) and Xylazine (10-20mg/kg). Anesthetized mice were kept on heating pads until recovery, except during intubation and dose delivery. The intubation platform was placed at a 20-degree angle, at eye level with the operator (seated). After approximately 5-10 minutes, the depth of anesthesia was determined using a toe pinch to the back foot. When the mouse was no longer responsive to toe-pinch, it was placed on the intubation platform in the prone position (ventral side down), with the upper incisors hooked over the wire. The entire body of the mouse was then aligned and straightened.

The mouth was gently opened using blunt forceps, held open with a lighted laryngoscope, and the tongue was pulled to the side. The epiglottis is opened to reveal the vocal cords, and the tapered end of a 20 gauge x 1 inch catheter is inserted into the trachea to intubate the mouse. The catheter should be initially angled downwards, then parallel to the intubation platform. With proper alignment, little to no resistance should be felt. To facilitate use with the Penn-Century MicroSprayer needle, accommodating the bend in the needle, a slit along the female Luer hub of the catheter must be cleanly cut prior to use (using a cut-off wheel of a Dremmel, or other similar device); see Appendix A for details and an image.

At this point, the laryngoscope can be removed and both hands may be dedicated to operation of the MicroSprayer. The needle tip of the MicroSprayer is then inserted into the catheter, until the bend of the needle reaches the opening of the mouth. The aerosol is then quickly delivered, and both catheter and MicroSprayer are quickly removed. Correct intubation and delivery will be signified by rapid breaths, which should return to baseline within 1-2 minutes. The mouse is allowed to recover to baseline normal breathing on the intubation platform before it is moved into a cage, on a heating pad, for recovery from anesthesia.

7.2.5 IVIS Imaging of Mouse Lungs and Image Analysis

Mice were euthanized at days 1, 3, 6, 10, and 14 after particle delivery with an intraperitoneal injection of sodium pentobarbital (200 mg/kg Euthasol), followed by cervical dislocation. Trachea, lungs, heart, and thymus were excised en block. The heart and thymus, along with any other remaining connective tissue, were then carefully removed from the lungs. The lungs and trachea were rinsed with PBS and then placed in a 12-well plate with 1 mL of PBS on ice.

Lungs were placed on the flat underside of a black polypropylene 96-well plate (intended for fluorescence measurements) to facilitate later removal. It was found that lungs placed directly on black imaging paper tend to stick and are difficult to remove. The lungs were carefully arranged such that each lobe was layed out and visible. Fluorescent images of the lungs were then acquired using an IVIS Spectrum (Caliper Life Sciences, PerkinElmer, Waltham, MA) using the settings in Table 7.1.

Table 7.1 IVIS Imaging Settings

Parameters		Setting
Constant	Pixel Width	1
	Pixel Height	1
	Binning Factor	4 (small)
	Image Units	Counts
	f Number	2
	Field of View	13.2 (C)
	Excitation Filter	605
	Emission Filter	660
Varied (sequence)	Exposure	0.01 seconds
		0.05 seconds
		0.10 seconds
		0.25 seconds
		0.50 seconds
		0.75 seconds
		1.00 seconds
		1.50 seconds
		2.00 seconds

Quantitative data was collected using the IVIS Living Image software using the following steps:

1. Set units to radiance (photons)
2. Draw regions of interest (ROIs) around each lung
3. Measure ROIs in radiance (photons)
4. Export data into Microsoft Excel
5. Data with saturated pixels cannot be used.

The quantitative data was then analyzed and graphed in Microsoft Excel to determine if any trends or significant changes in clearance rates between particle groups could be established. The background fluorescence was determined from untreated lungs, and subtracted from the data set.

7.2.6 Tissue Homogenization and Fluorescence Quantification

7.2.6.1 FluoSpheres Fluorescent Polystyrene Particles

Following IVIS imaging, the lungs were carefully trimmed to remove the trachea and any other remaining connective tissue, and then minced into small pieces (< 0.5 centimeters) using dissection scissors. They were then suspended in 3 milliliters of tissue lysis buffer (50 mM Tris-HCl, 150 mM NaCl, 0.1% Triton-X 100) and homogenized for one minute, or until completely homogenized. To dissolve and extract fluorescence from the 1 μm Crimson FluoSpheres® polystyrene microparticles, three milliliters of xylene was added. The sample was then capped, parafilmed, and allowed to rotate at room temperature for three days (time point determined from preliminary studies for assay validation). After removing from the rotator, the sample was centrifuged at RCF 3220 at 4°C for five minutes to allow separation of the xylene and aqueous phases. Sample

aliquots of 100 µl were taken from the (top) xylene phase and read in a fluorescence plate reader at an excitation/emission of 645/680. Readings were quantified by comparison with standard curves.

7.2.6.2 AF633-Conjugated Microgels

The same protocol as above (section 7.2.6.1) was used to homogenize mouse lungs. However, to dissolve and extract fluorescence from the AF633-conjugated microgels, the (trypsin-degradable) microgels were digested in trypsin solution for 72 hours at 37°C. After removing from the rotator, 1 mL aliquots were removed into 1.7 mL centrifuge tubes, and cell lysate was centrifuged out at 21,100xg. Sample aliquots of 100 µl were taken and read in a fluorescence plate reader at an excitation/emission of 645/680. Readings were quantified by comparison with standard curves.

7.3 RESULTS AND DISCUSSION

7.3.1 IVIS Imaging

7.3.1.1 Troubleshooting

The primary advantage to using an IVIS imaging system to track and quantify particle clearance and distribution was in the ability to perform live imaging on the experimental subjects, such that the same set of dosed mice could be followed throughout the time course of the study. In addition to being able to view the fluorescence distribution of particles, the IVIS Living Image software also contains analysis functions in which fluorescence intensity could be quantified.

In practice, however, this system proved to be unrealistic for deep tissue fluorescence quantification (of the lung). Several preliminary studies were conducted in

an attempt to develop an experimental protocol that would follow the same set of dosed mice throughout the time course (live imaging). All recommended best practices from the manufacturer were followed, including:

- Modification to an alfalfa-free diet, for at least seven days, to reduce gut and tissue autofluorescence
- Use of near-infrared fluorescent probes
- Removal of fur using a depilatory to reduce scattering
- Imaging in various orientations
- Trial with both epifluorescence (surface) and transillumination (deep) imaging settings.

The variation of all these parameters produced no reliable fluorescent signal from the lungs under epifluorescence. Although transillumination would perhaps be more applicable, the in-practice imaging time was approximately one hour per mouse, which prevented its further use. One other option would have been to make use of specialized fluorescent probes for IVIS, but such probes were cost-prohibitive at the time of study. Therefore, different sets of mice were used for each time point, and the dosing and delivery was divided across multiple days for practicality and time limitations.

7.3.1.2 Fluorescence Quantification from IVIS Images

Raw data was originally collected in radiance, or photons, and the total flux (photons per second) from each region of interest was calculated and averaged as a total flux per lung. Background fluorescence was subtracted using the average from untreated control lungs. This data was then normalized as a percentage to the total flux at Day 1 in order to display the total remaining as a percentage of Day 1. Although IVIS imaging

settings were kept constant from day-to-day measurements (see Table 7.1), quantified data had anomalous changes in signal intensities. The data, from an exposure time of 0.5 seconds, is plotted in Figure 7.3. Data cannot be quantified from images with saturated pixels, which was the case for Day 6 images at all exposure times, as well as for all FluoSpheres (polystyrene positive control). Therefore, those points are not plotted or shown.

As can be seen in Figure 7.3, the Day 3 time point shows less microgel remaining as compared to Day 10, despite both of these time points having small error bars. The unexplainable low fluorescence at Day 3, followed by an increase at Day 10, was also seen in the FluoSphere data (not shown). Therefore, it was concluded that the quantified fluorescence was somewhat unreliable, and would not be determined by IVIS analysis.

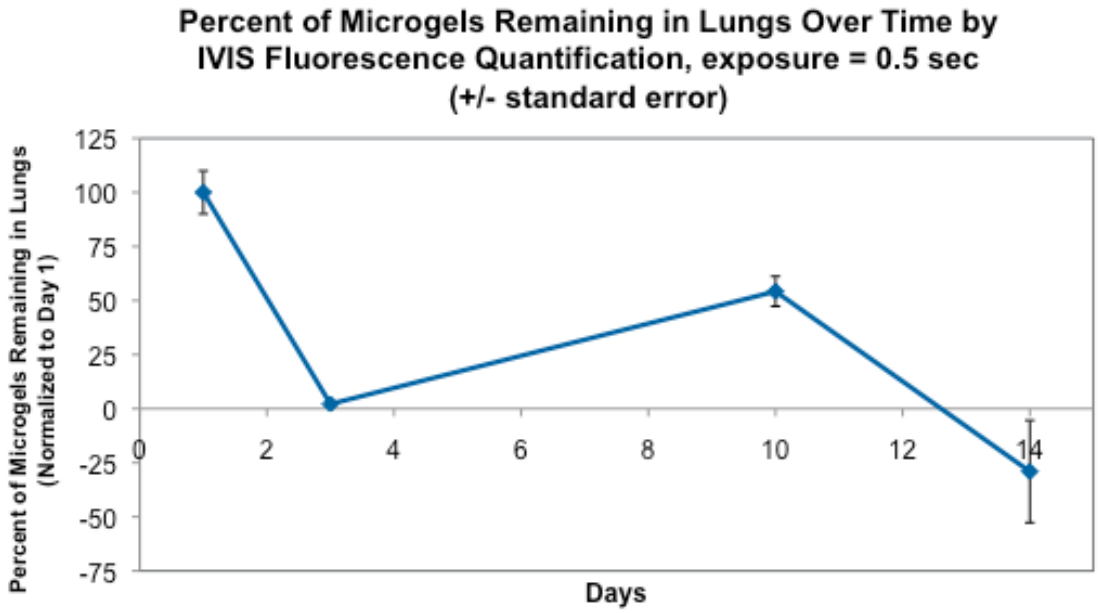

Figure 7.3 Percent of Microgels Remaining in Lungs Over Time by IVIS Fluorescence Quantification

7.3.1.3 Pulmonary Distribution

Despite the unresolved issues with IVIS imaging discussed in sections 7.3.1.1 and 7.3.1.2 , the use of IVIS imaging post mortem on extracted lung samples was still useful for visualizing the pulmonary distribution of both polystyrene particles and microgels throughout the time points. Figure 7.4 shows the IVIS images of the extracted mouse lungs from the polystyrene group at all time points (days 1, 3, 6, 10, 14), using an exposure of 0.01 seconds. Figure 7.5 shows the IVIS images of the extracted mouse lungs from the microgel group at all time points, using an exposure of 0.5 seconds.

Observing the images, it may be seen that both polystyrene particles and microgels exhibit uniform distribution throughout the upper and lower airways. Some allowance for directed delivery into one lobe over another may be attributed to the method of delivery, which would be a result of a delivery point past the carina (first bifurcation). The absence of fluorescence in one lung of the polystyrene group indicates an error in delivery method, which likely resulted from intubation into the esophagus rather than the trachea. None of these outliers were discounted from analysis, however, in order to account for the probability of mis-delivery into the esophagus for all time points.

One final interesting trend, seen in the day 14 image of the microgel group (Figure 7.5), is that day 14 lungs are generally free of any fluorescent trace, save for one out of eight samples. This is of special significance when recalling that the microgels undergo hydrolytic degradation around day 11. It was postulated that the hydrolytic degradation would serve as a fail-safe mechanism to promote clearance of the microgels from the lungs, thereby preventing long-term accumulation from multiple and frequent doses. This data, though not conclusive, is enough to warrant further study of the exact clearance mechanism.

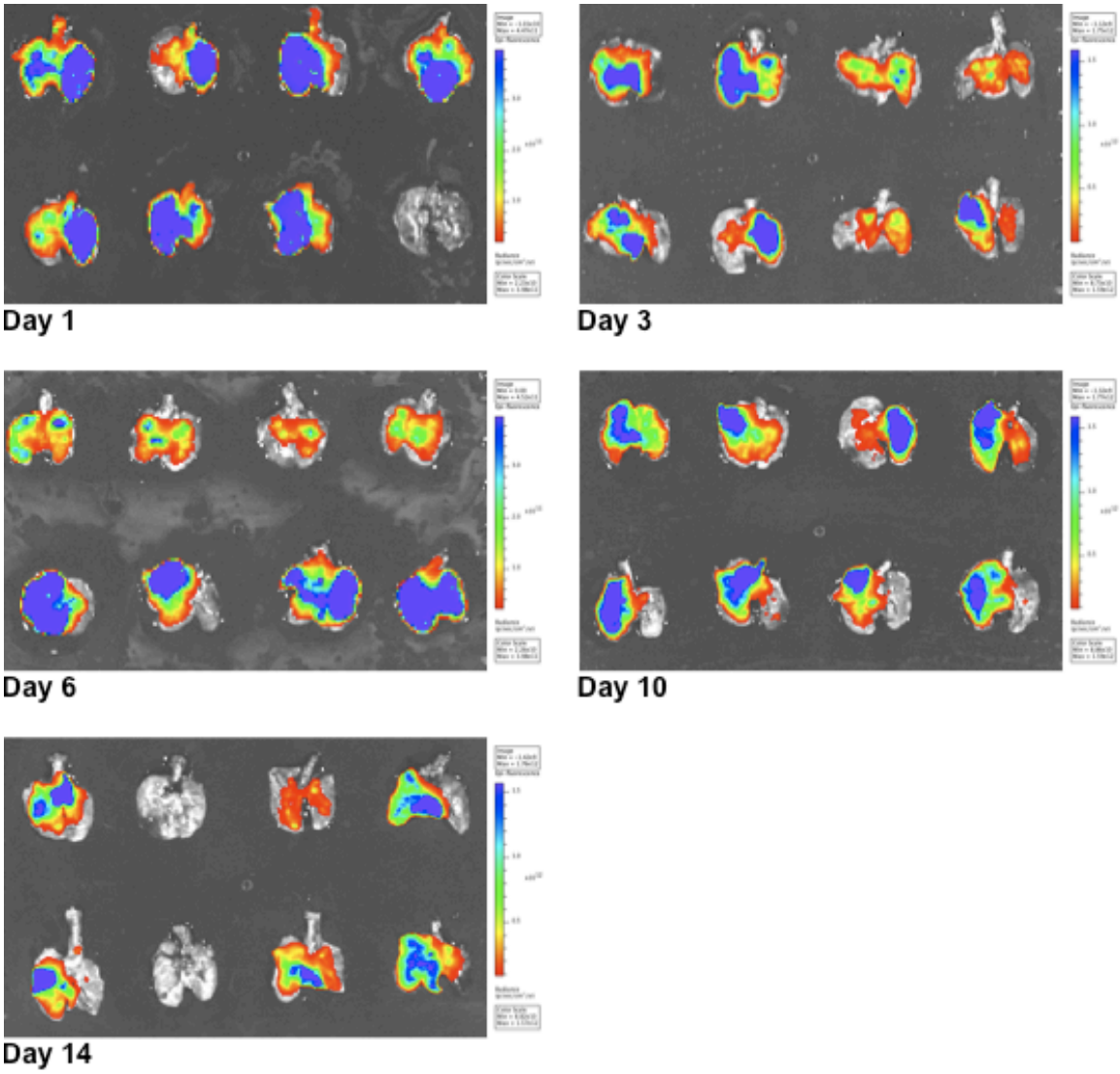

Figure 7.4 IVIS Images of Extracted Lungs from Mice Dosed with 1µm Fluorescent Polystyrene Particles

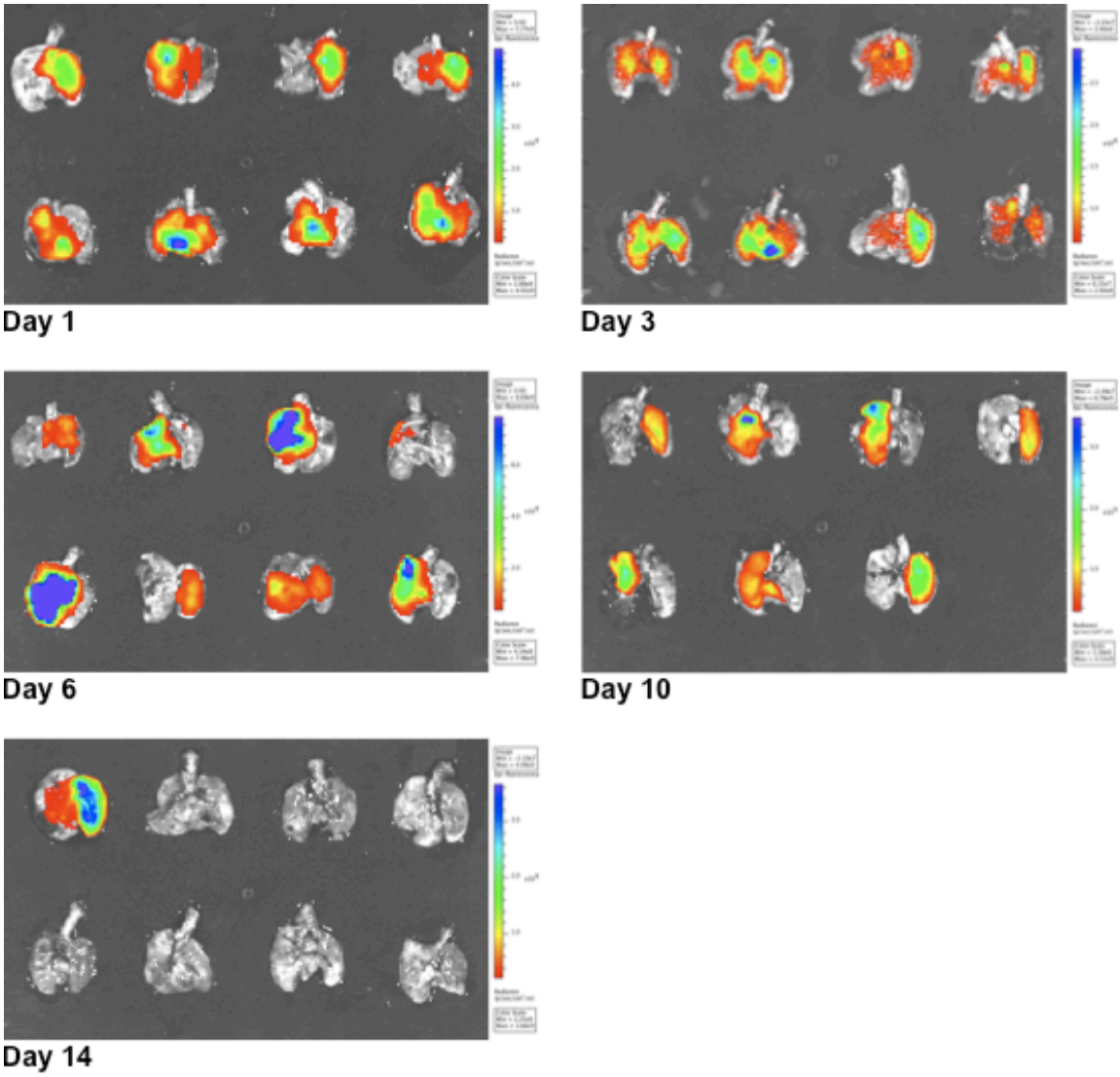

Figure 7.5 IVIS Images of Extracted Lungs from Mice Dosed with AF633 Microgels

7.3.2 Fluorescence Quantification from Tissue Homogenates

In addition to IVIS imaging, the same lung samples from each group were homogenized and analyzed for total levels of fluorescence at each time point. These samples were compared as a percentage of the initial dose of 0.1 mg (both microgels and polystyrene particles). Standard curves were made using untreated homogenized lung tissue for background autofluorescence.

Figure 7.6 displays both the dot plots (which shows the entire distribution of each data set) and average percent of particles remaining for each time point, for microgels (top) and FluoSpheres fluorescent polystyrene particles (bottom). Figure 7.7 displays the average of the data set for both microgels and polystyrene microparticles graphed together for comparison, as a percentage of the initial dose.

The FluoSpheres polystyrene microparticles are cleared very rapidly from the lungs, as was seen in Chapter 6 *in vitro* data. By day 1, approximately 70% of FluoSpheres have already been cleared from the lungs, and continues to decrease over day 3 and day 6, when somewhat of a baseline level of 15% remaining has been reached. The initial rapid clearance over day 1 is likely primarily due to macrophage clearance, as has been observed in the literature [4,5]. The slower, secondary clearance mechanism is likely due to mucociliary clearance. Furthermore, the data from the polystyrene microparticles, as a positive control, agrees with that seen in the literature for polymer particles in general [3,4], validating the method of assay.

In contrast to the polystyrene particles, the microgels exhibit significantly less clearance over the first day, with over 85% of microgels still remaining in the lungs at day 1. This again correlates very well with *in vitro* macrophage uptake data seen in Chapter 6. Again, like the FluoSpheres, levels of microgel remaining in the lungs continues to decrease over day 3 and day 6, down to approximately 45% remaining at day

6. In context, this is very significant in that the amount of microgels remaining at day 6 is greater than the amount of FluoSpheres remaining at day 1.

However, the data at day 14 is greatly deviates from the trend seen in the other time points in that the fluorescent signal has actually increased to greater than the initial dose (~135%). When viewing the dot plot for that data set (Figure 7.6), the entire data set displays a marked increase in fluorescence, so it is not due to averaging with an included extreme outlier. Furthermore, this data does not agree with the IVIS images seen for microgels at day 14 (Figure 7.5). Several possible explanations exist, though none of which have been validated conclusively as of yet. It is possible that the microgel samples weighed out for dosing to the day 14 set of mice were weighed out incorrectly, at least twice as much as for other groups. The IVIS data does not support this, however, and it cannot be determined now, after the fact. This would also mean that the data from other time points must also be discounted from analysis. Another explanation is sample contamination during homogenization, which again, cannot be determined after the fact. Lastly, it may be possible that the Alexa Fluor 633, when conjugated to an intact microgel, exhibits some level of fluorescent signal quenching. However, due to the trypsin degradation step in the assay, it must mean that the fluorescent signal is quenched in trypsin-degraded microgels, as well, or that hydrolytically degraded microgels can somehow boost the fluorescent signal. This theory is not supported by any previous data, however, but should be tested *in vitro* at the very least.

Despite the anomalous data from day 14, this data set hints towards a significant difference in microgel clearance as compared to polystyrene microparticle clearance. This study should be repeated in the future, with some minor changes in method to prevent any of the possible errors explained here.

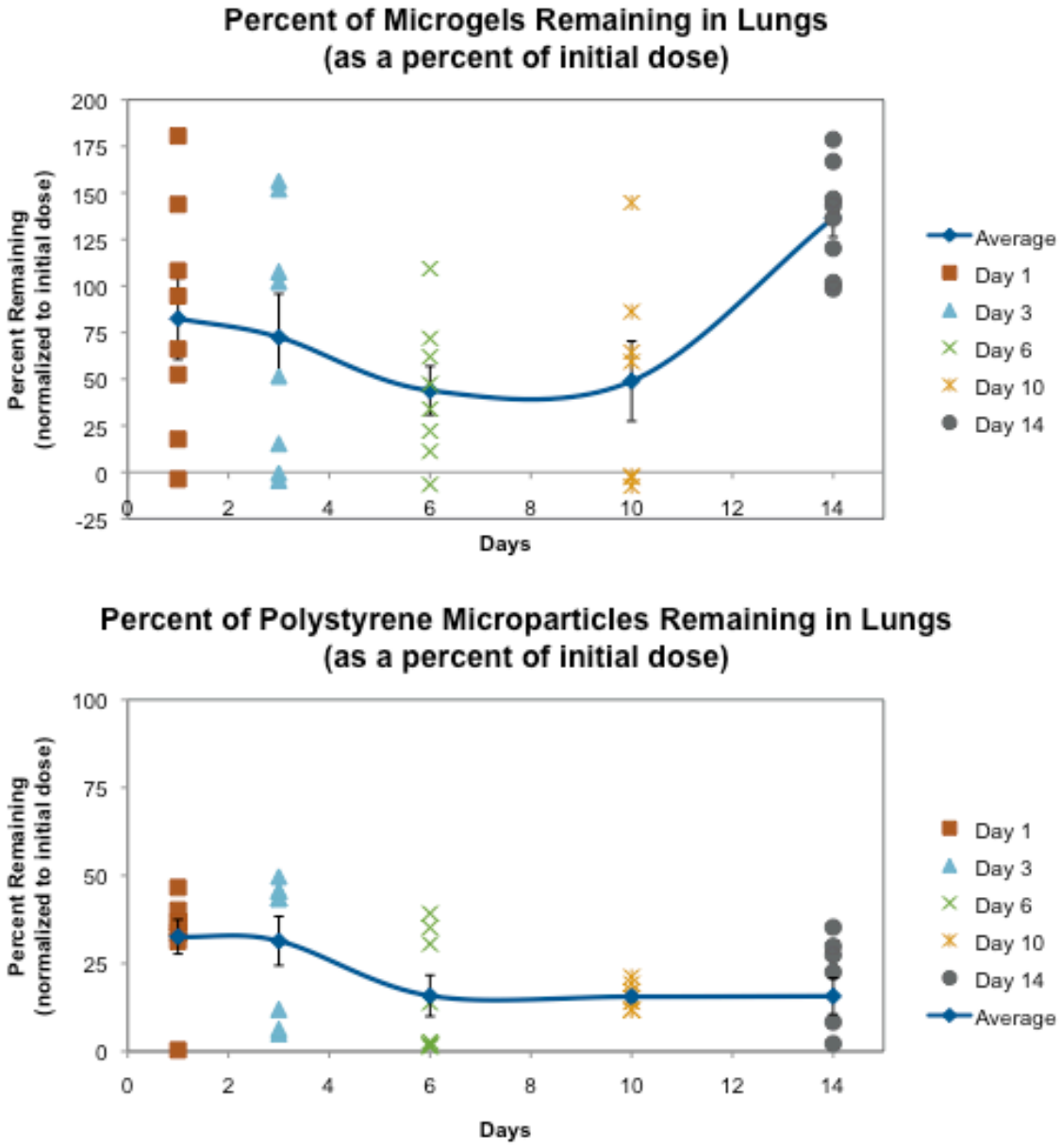

Figure 7.6 Percent of Microgels and Polystyrene Microparticles Remaining in Lungs over Time by Fluorescence Quantification from Tissue Homogenates

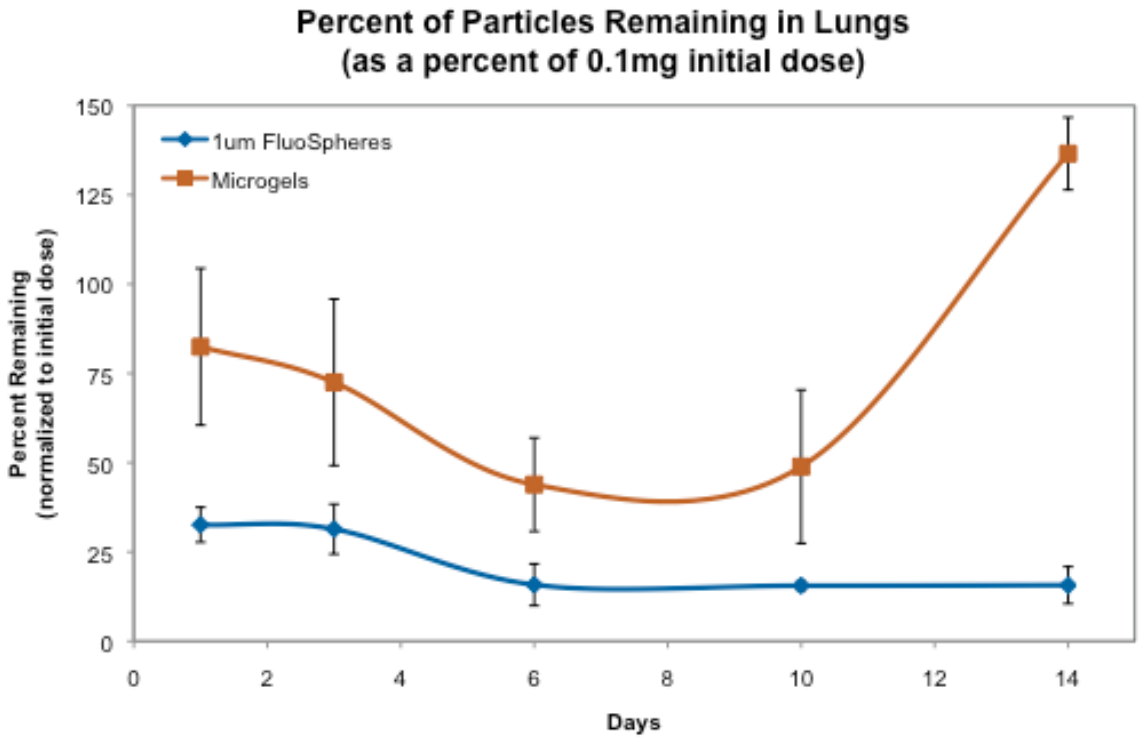

Figure 7.7 Comparison of Percent of Particles Remaining in Lungs over Time by Fluorescence Quantification from Tissue Homogenates

7.4 CONCLUSIONS

In this chapter, the *in vivo* performance of the microgels was studied in comparison to fluorescent polystyrene microparticles in terms of pulmonary distribution and clearance patterns over a two week time period. In the realization of this study, a new method of intratracheal intubation and aerosol delivery was developed and modified from previously published methods [8] in order to minimize incidence of trauma or tracheal perforation. The pulmonary distribution of microgels and polystyrene particles was monitored via IVIS fluorescent images of extracted mouse lungs post mortem, indicating successful delivery to the deep lung. Unfortunately, quantification of particles remaining

using the IVIS analysis software was ultimately unreliable and unsuccessful. However, the clearance pattern of the particles was successfully quantified by measuring fluorescence from lung tissue homogenate. The clearance of fluorescent polystyrene particles measured was well in agreement with that published in the literature [4], showing approximately 70% of particles cleared from the lungs within the first day. In contrast, only about 15% of microgels were cleared from lungs at this same time point, and at day 6, 40% of microgels were still remaining in lungs in comparison to only 15% of polystyrene particles. Microgel data at day 14 could not be explained, however, but hinted towards significant differences in clearance mechanisms between microgels and polystyrene microparticles. Collectively, this data presents clues in understanding how to affect the particle clearance patterns from the lungs, and should be repeated in the future.

7.5 REFERENCES

[1] I.M. El-Sherbiny, S. McGill, H.D.C. Smyth, Swellable microparticles as carriers for sustained pulmonary drug delivery, J Pharm Sci. 99 (2010) 2343–2356.

[2] P. Wanakule, G.W. Liu, A.T. Fleury, K. Roy, Nano-inside-micro: Disease-responsive microgels with encapsulated nanoparticles for intracellular drug delivery to the deep lung, J Control Release. 162 (2012) 429–437.

[3] B. Patel, V. Gupta, F. Ahsan, PEG–PLGA based large porous particles for pulmonary delivery of a highly soluble drug, low molecular weight heparin, J Control Release. 162 (2012) 310–320.

[4] W.G. Kreyling, M. Semmler-Behnke, S. Takenaka, W. Möller, Differences in the Biokinetics of Inhaled Nano- versus Micrometer-Sized Particles, Acc Chem Res. (2012).

[5] M. Geiser, W.G. Kreyling, Deposition and biokinetics of inhaled nanoparticles, Part Fibre Toxicol. 7 (2010) 2.

[6] M. Wygrecka, P. Markart, C. Ruppert, K. Petri, K.T. Preissner, W. Seeger, et al., Cellular origin of pro-coagulant and (anti)-fibrinolytic factors in bleomycin-injured lungs, Eur Respir J. 29 (2007) 1105–1114.

[7] J. Lee, Y.J. Oh, S.K. Lee, K.Y. Lee, Facile control of porous structures of polymer microspheres using an osmotic agent for pulmonary delivery, J Control Release. 146 (2010) 61–67.

[8] M. Bivas-Benita, R. Zwier, H.E. Junginger, G. Borchard, Non-invasive pulmonary aerosol delivery in mice by the endotracheal route, Eur J Pharm Biopharm. 61 (2005) 214–218.

[9] K. Hirose, A. Marui, Y. Arai, T. Kushibiki, Y. Kimura, H. Sakaguchi, et al., Novel approach with intratracheal administration of microgelatin hydrogel microspheres incorporating basic fibroblast growth factor for rescue of rats with monocrotaline-induced pulmonary hypertension, J Thorac Cardiovasc Surg. 136 (2008) 1250–1256.

Chapter 8: Conclusions and Future Directions

8.1 Research Summary

The objective of this dissertation work was to develop an enzyme-responsive platform drug delivery system for the delivery of biologic drugs through the pulmonary route. In the design of this system, the fragile nature of these biologic drugs was considered throughout the development of a hydrogel microparticle, or microgel, manufacturing process. The enzyme-responsiveness of the system was made easily adaptable through the incorporation of peptide sequences, although as a proof of concept, the trypsin-responsive pentapeptide CGRGGC was used throughout this work. These enzyme-responsive hydrogel microparticles were then evaluated *in vitro*, and preliminary *in vivo* studies were performed.

In **Chapter 1**, the concept of a disease-responsive hydrogel microparticle for pulmonary delivery was introduced, as well as the many design challenges that are currently limiting the potential of polymer particle-based pulmonary vehicles for controlled drug release. Chief among them is that the ideal sizes for uniform and deep lung distribution are also the sizes which are most observed to be rapidly cleared by alveolar macrophages. The rationale for utilizing enzyme-responsive systems was also discussed, as well as the need for developing new carriers for the emerging class of biologic drugs.

Chapter 4 extensively discussed the various biomaterials that were studied for incorporation into the microgel system. This chapter also included background material on the Michael addition reaction between sulfhydryl and acrylate groups, as well as the modification of polymers to incorporate these reactive groups. Work on peptide

bioconjugation chemistry was also covered in this chapter. Finally, optimal hydrogel ingredients, ratios, and reaction buffers were determined in this chapter. The final composition to move forward with was a 60% combined weight by volume hydrogel consisting of a four-arm poly(ethylene) glycol acrylate cross-linked with the CGRGGC peptide in 0.3 molar triethanolamine buffer.

In the next chapter, **Chapter 5**, the newly developed PEG-CGRGGC hydrogel material was scaled down to microparticle scale through the trial of various particle synthesis methods. Various particle synthesis methods included mesh molding, grinding, cryomilling, emulsions, and more. The method that best preserved the desired material properties was an emulsion method. This chapter then details the development and optimization of the Michael Addition During water-in-oil Emulsion, or MADE, process to produce the microgels.

Chapter 6 covers the extensive *in vitro* characterization of these PEG-CGRGGC microgels. These studies included hydrogel swelling and hydrolytic degradation studies, as well as enzyme-mediated degradation studies. Microgels were confirmed to undergo rapid trypsin-mediated degradation. In swelling studies, the microgels were shown to swell over the course of 10 days, and begin undergoing hydrolytic degradation thereafter. The density and aerodynamic diameter of the microgels was also determined to be within the appropriate range of inhalation and deep lung delivery.

A number of biologic drug candidates were successfully encapsulated within the microgels, including proteins, DNA, siRNA, and nanoparticles of different sizes. The release of these encapsulated model drugs was also studied in the presence or absence of enzyme. The microgels exhibited a rapid release of drug upon enzyme exposure, while also displaying efficient retention of the drug without enzyme. In diffusion/hydrolysis-driven release studies, proteins were shown to slowly diffuse out over the course of 11

days before undergoing rapid hydrolysis. Nanoparticles, however, were efficiently retained until the point of hydrolytic degradation, around day 12.

The microgels were also evaluated for cellular interactions *in vitro* in this same chapter, and were found to exhibit no significant cytotoxicity with multiple cell lines. Of special interest was the interaction of microgels with RAW 264.7 macrophages in comparison to polystyrene particles. It was found that the microgels principally avoided uptake by macrophages over short (2 hours) and long (24 hours) time points, whereas polystyrene particles were rapidly taken up within both time courses. This avoidance of macrophage uptake implicated that the microgels may have improved residence time in the lungs, which may in turn improve its performance as a controlled release system for pulmonary delivery over other polymer particles.

Given the promising *in vitro* performance of microgels, the pulmonary distribution and clearance of microgels were then studied with preliminary *in vivo* experiments using BALB/c mice, discussed in **Chapter 7**. Overall, the microgels exhibited on par performance in terms of pulmonary distribution to the lower airways as compared with 1 μm polystyrene particles, as confirmed by IVIS (*In Vivo* Imaging System) studies. The clearance of the microgels over the course of two weeks was also studied and quantified in comparison to the same polystyrene particles. Similar to the *in vitro* data, the polystyrene particles were rapidly cleared (~70%) within the first day, whereas only about 20% of microgels were cleared in the same time span. Following the study out to day 10, only ~15% of polystyrene particles remain in the pulmonary space, whereas just under 50% of microgels are still remaining. Although this study needs to be repeated with some modification, it provided compelling evidence for the improved retention and performance of the microgels as a pulmonary controlled release vehicle.

However, as mentioned, further study should be done, as will be described in the next section.

8.2 FUTURE WORK

8.2.1 Repeated Pulmonary Distribution, Clearance, and Toxicity

As described in **Chapter 7**, promising preliminary data was presented that provided evidence for modified clearance patterns of microgels over other polymer particles. This study should be further repeated, and complementing data should be gathered both from IVIS studies, as well as homogenate-based fluorescent quantification. In addition to only the lung distribution being studied, full biodistribution and biokinetic studies should also be performed. Biokinetic analysis during microgel clearance should elucidate the primary mechanisms of microgel clearance as macrophage clearance, mucociliary clearance, or a combination of both. Along with biodistribution and biokinetics, the systemic toxicity and immunological response should be evaluated using cytokine-based assays and pulmonary edema. It may also be prudent to repeat studies in a rat model instead of a mouse model, as is commonly reported.

8.2.2 *In Vivo* Disease-Triggered Drug Release

One major theme of this work was the concept of disease-triggered drug release using enzyme-specific peptide sequences. Although the enzyme-triggered drug release was extensively characterized *in vitro* in **Chapter 6**, this concept was not tested *in vivo*. In order to test this system *in vivo*, a disease-model with up regulated enzyme expression in the lungs should be used for comparison of drug release with healthy control groups. Some viable candidates for disease models that are currently being considered include an

ovalbumin-based airway allergy model, in which levels of matrix metalloproteinase-9 (MMP-9) are expressed by mast cells in the pulmonary epithelial space [1,2], and bleomycin-induced pulmonary fibrosis model, in which levels of matrix metalloproteinase-2 (MMP-2) are over expressed in the airways[3-6]. Peptide sequences for both of these enzymes have already been well studied and incorporated into similar Michael addition hydrogels [7,8], one of which has already been successfully incorporated into the system described in this work (data not shown).

8.3 CONCLUSIONS

The development of enzymatically-degradable hydrogel microparticles, as well as the development of methods to synthesize them, has provided the opportunity to make a significant impact on controlled release pulmonary drug delivery systems for biologic drugs. The Michael addition chemistry used here is especially suitable for biologic drugs, which may be denatured by traditional manufacturing methods, and is easily accomplished using cysteine-containing peptide sequences to cross-link commercially available biopolymers, without the need for bioconjugation or modification. This polymer chemistry was successfully scaled into microparticle synthesis via the newly developed MADE microgel synthesis method. Microgels synthesized using this method reproducibly exhibit enzyme-mediated degradation and release of encapsulated protein, DNA, and nanoparticles, and efficient retention without enzyme. Both *in vitro* and *in vivo* experiments provide evidence for modified retention and clearance of these microgels in the pulmonary space, with significant implications for design of future pulmonary controlled delivery systems. Collectively, the work in this dissertation has followed the conception, development, and evaluation of disease-triggered hydrogel microparticles for

pulmonary delivery, supporting the future realization of non-invasive, dynamic and disease-responsive delivery systems for the emerging class of biologic drugs.

8.4 REFERENCES

[1] J.L. Simpson, R.J. Scott, M.J. Boyle, P.G. Gibson, Differential proteolytic enzyme activity in eosinophilic and neutrophilic asthma, Am J Respir Crit Care Med. 172 (2005) 559–565.

[2] D. Baram, G. Vaday, P. Salamon, I. Drucker, R. Hershkoviz, Y. Mekori, Human mast cells release metalloproteinase-9 on contact with activated T cells: juxtacrine regulation by TNF-{alpha}, The Journal of Immunology. 167 (2001) 4008–4016.

[3] T. Okuma, Y. Terasaki, K. Kaikita, H. Kobayashi, W.A. Kuziel, M. Kawasuji, et al., C-C chemokine receptor 2 (CCR2) deficiency improves bleomycin-induced pulmonary fibrosis by attenuation of both macrophage infiltration and production of macrophage-derived matrix metalloproteinases, J. Pathol. 204 (2004) 594–604.

[4] T. Yaguchi, Y. Fukuda, M. Ishizaki, N. Yamanaka, Immunohistochemical and gelatin zymography studies for matrix metalloproteinases in bleomycin-induced pulmonary fibrosis, Pathol. Int. 48 (1998) 954–963.

[5] T. Hayashi, W.G. Stetler-Stevenson, M.V. Fleming, N. Fishback, M.N. Koss, L.A. Liotta, et al., Immunohistochemical study of metalloproteinases and their tissue inhibitors in the lungs of patients with diffuse alveolar damage and idiopathic pulmonary fibrosis, Am J Pathol. 149 (1996) 1241–1256.

[6] M. Corbel, S. Caulet-Maugendre, N. Germain, S. Molet, V. Lagente, E. Boichot, Inhibition of bleomycin-induced pulmonary fibrosis in mice by the matrix metalloproteinase inhibitor batimastat, J. Pathol. 193 (2001) 538–545.

[7] J. Patterson, J.A. Hubbell, Enhanced proteolytic degradation of molecularly engineered PEG hydrogels in response to MMP-1 and MMP-2, Biomaterials. 31 (2010) 7836–7845.

[8] J. Patterson, J.A. Hubbell, SPARC-derived protease substrates to enhance the plasmin sensitivity of molecularly engineered PEG hydrogels, Biomaterials. 32 (2011) 1301–1310.

Appendix A: Detailed Protocol and Visual Instructions for Mouse Endotracheal Intubation and Intrapulmonary Aerosol Delivery of Particles using a Penn-Century MicroSprayer Device

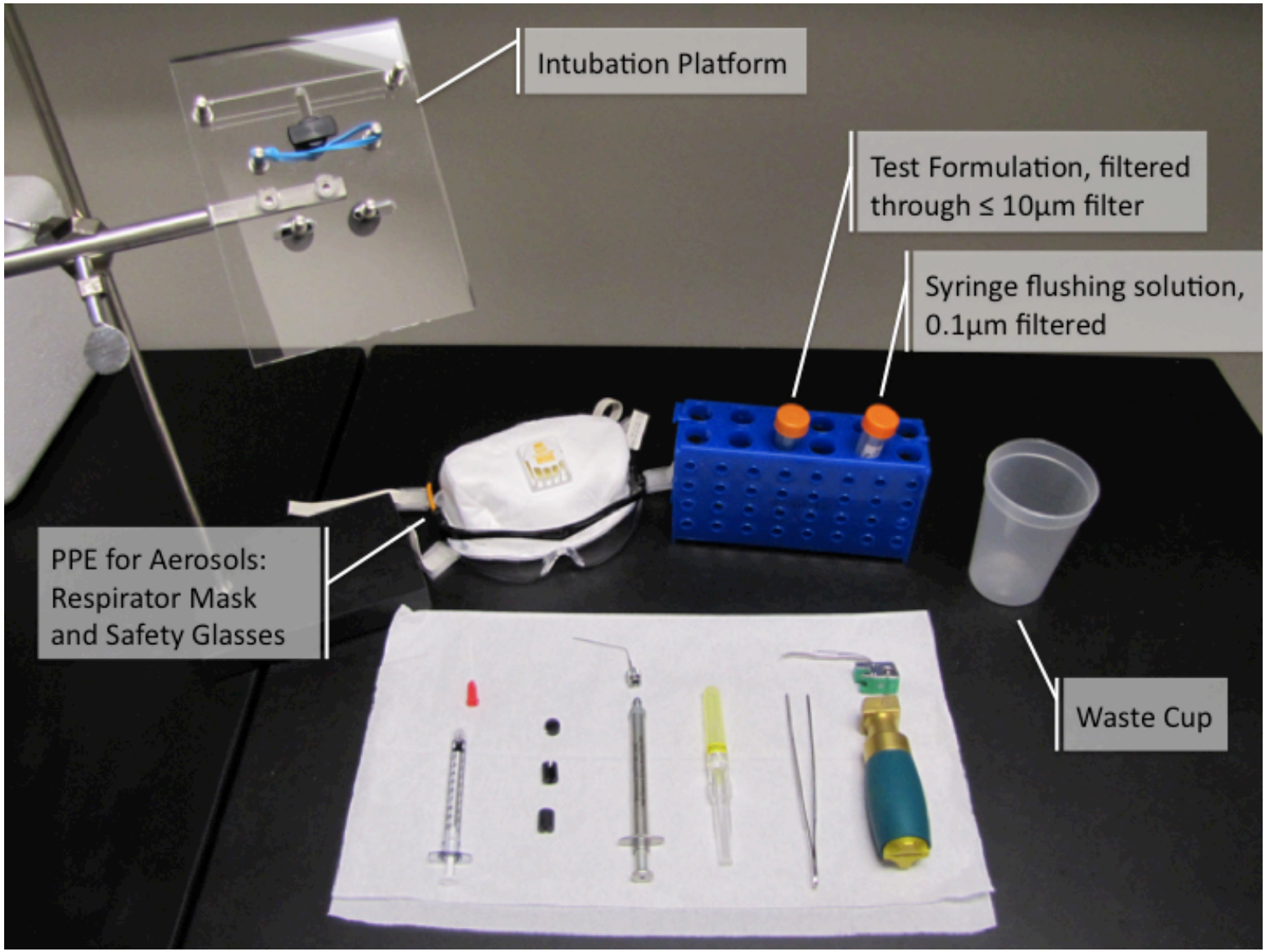
Intubation Platform
Test Formulation, filtered through ≤ 10µm filter
Syringe flushing solution, 0.1µm filtered
PPE for Aerosols: Respirator Mask and Safety Glasses
Waste Cup

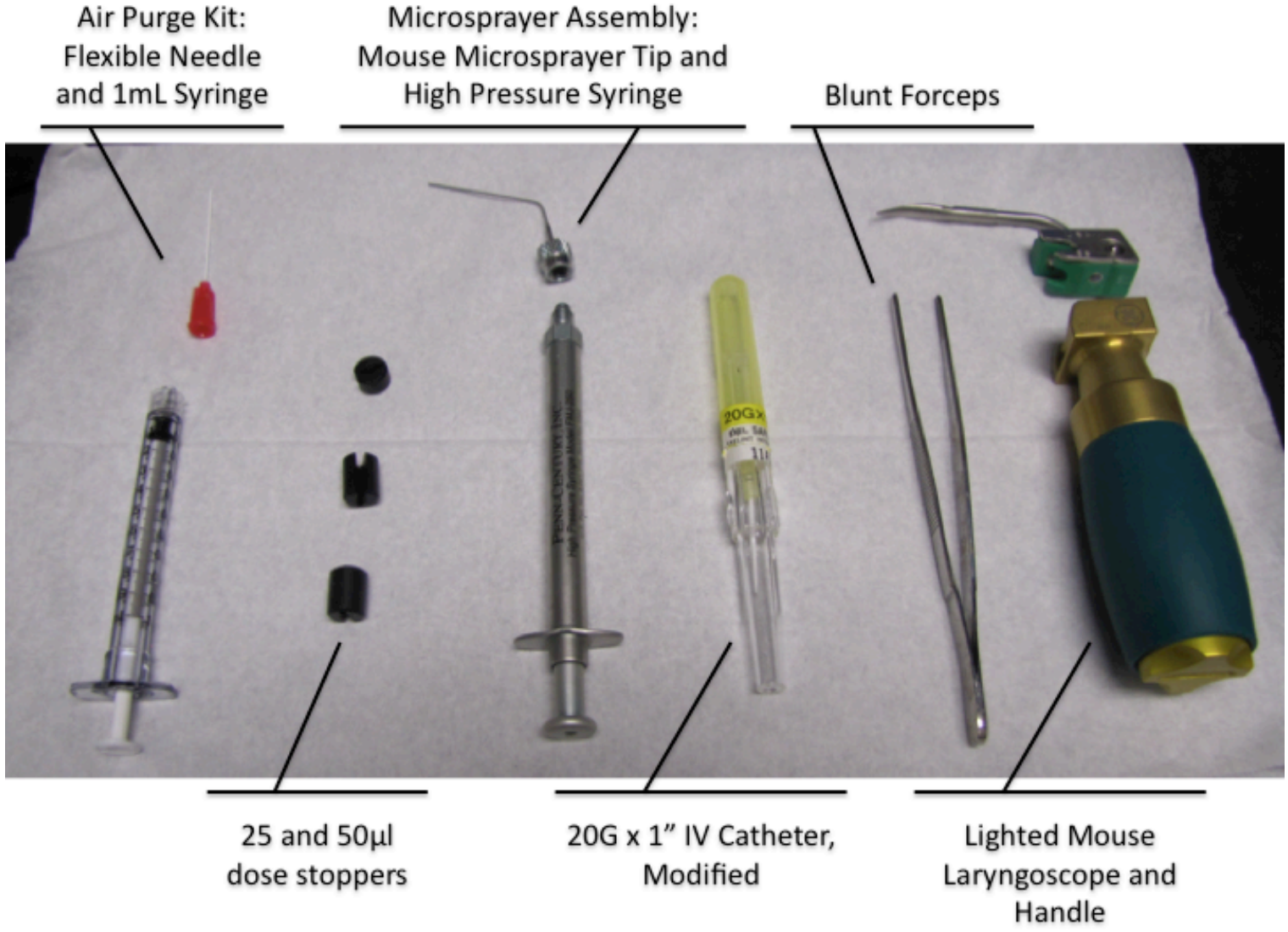
Air Purge Kit:
Flexible Needle
and 1mL Syringe
Microsprayer Assembly:
Mouse Microsprayer Tip and
High Pressure Syringe
Blunt Forceps
25 and 50µl
dose stoppers
20G x 1" IV Catheter,
Modified
Lighted Mouse
Laryngoscope and
Handle

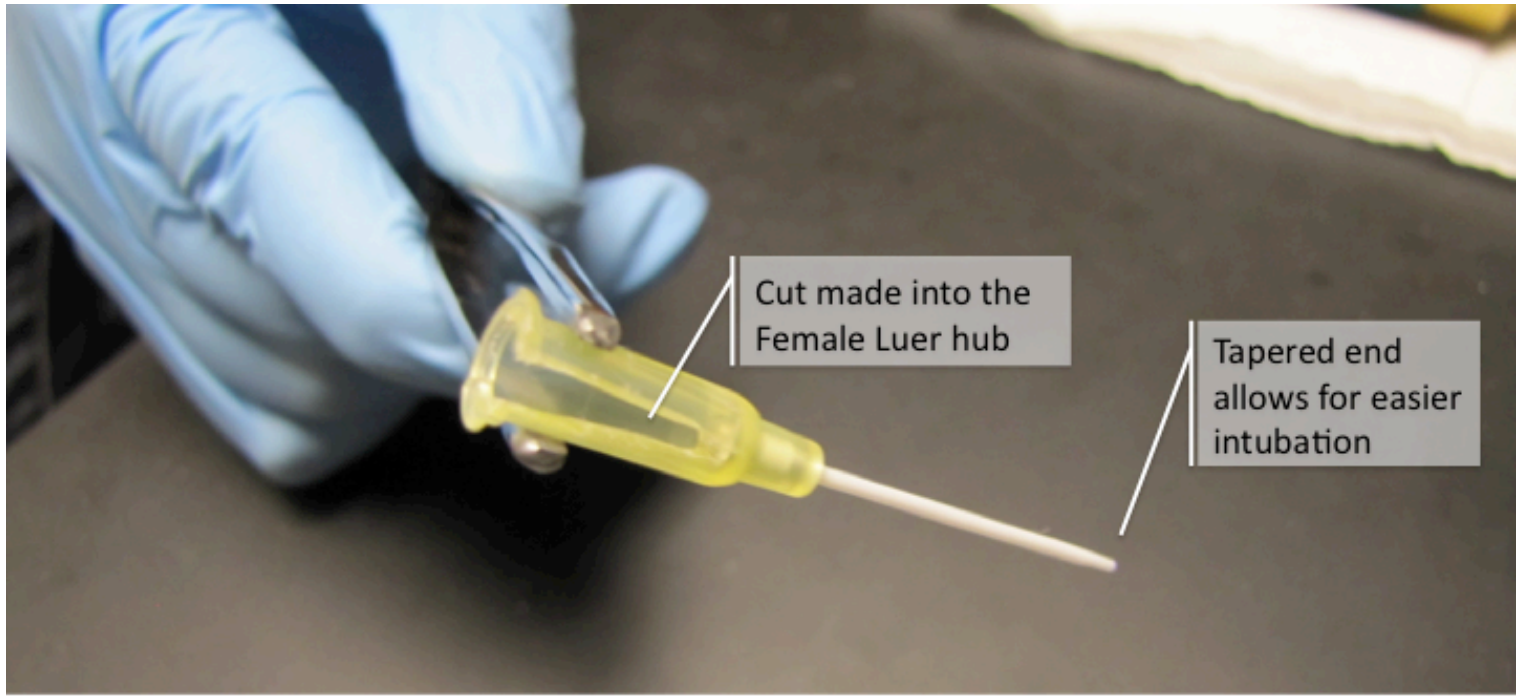

- The IV needle is discarded, as only the catheter component is needed
- A cut has been made along the Female Luer portion of the catheter using a Dremel with Cut-Off Wheel
  - This cut is needed to allow full insertion of the microsprayer needle, accommodating its bend
  - The Luer-Lok wings were left intact
  - Rough edges were filed away

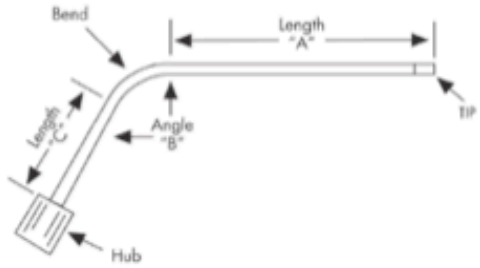

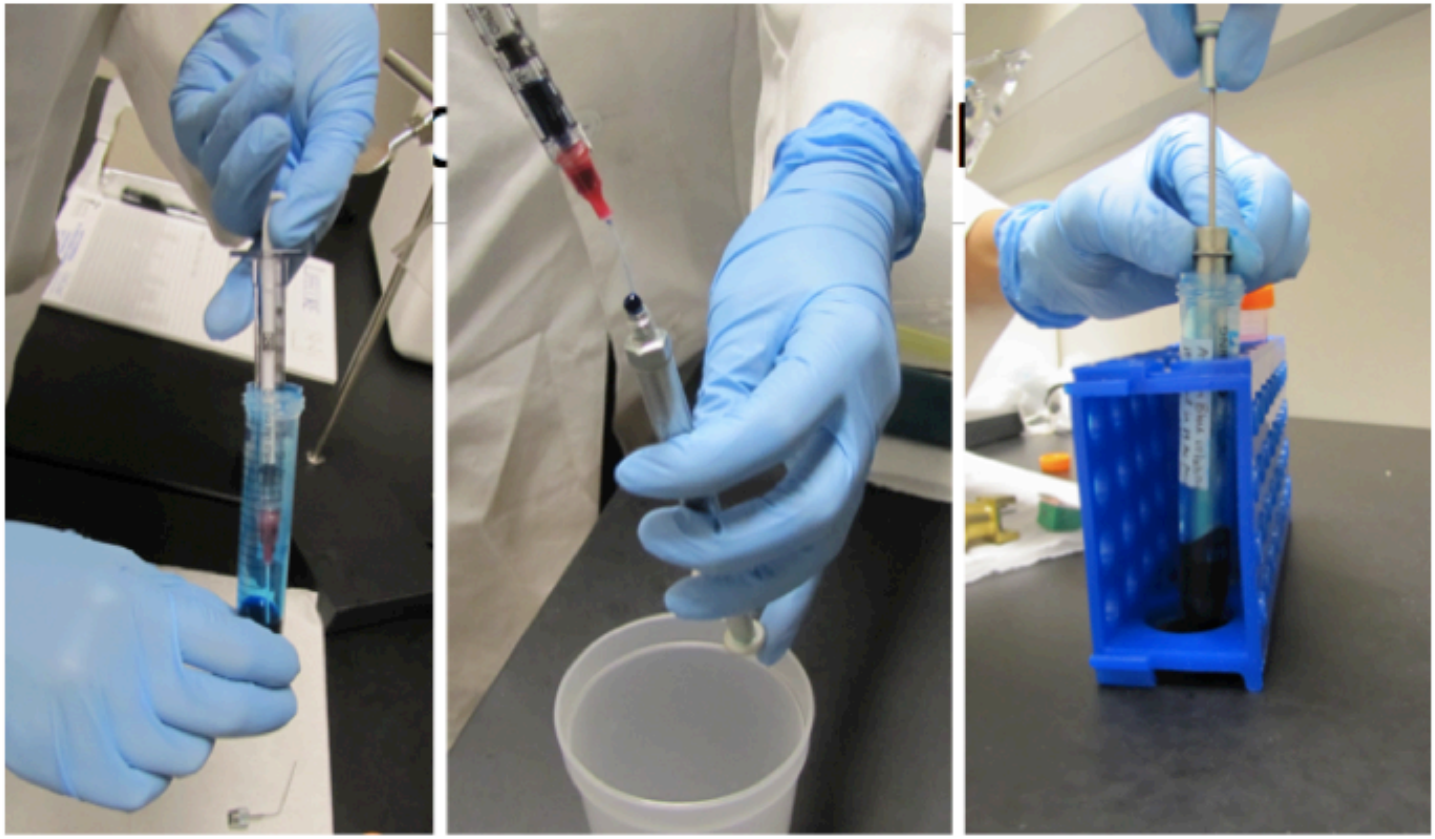

Use the air purge kit to begin filling the microsprayer. Any air bubbles within the microsprayer assembly will disrupt the aerosol plume.

- Draw the solution into the air purge needle and syringe
- With the microsprayer syringe plunger closed (and without the sprayer tip), insert the flexible needle tip into the syringe until it hits the end of the plunger
- Inject solution into the syringe continuously as you draw out the air purge kit, leaving a drop of solution on the end of the syringe
- Immerse the syringe into the solution and draw back on the plunger to fill the syringe

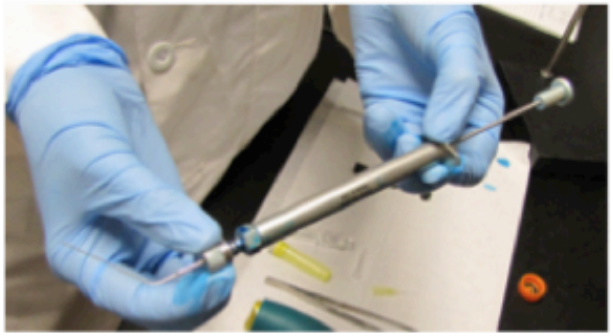

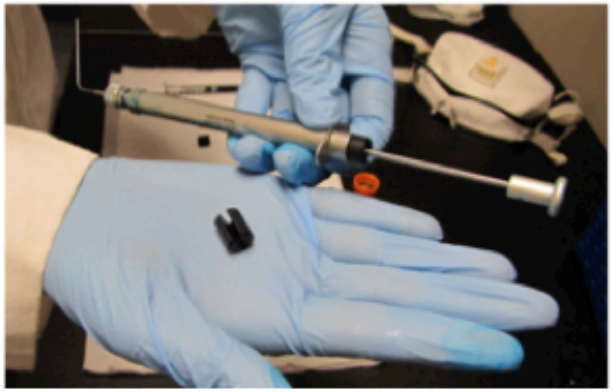

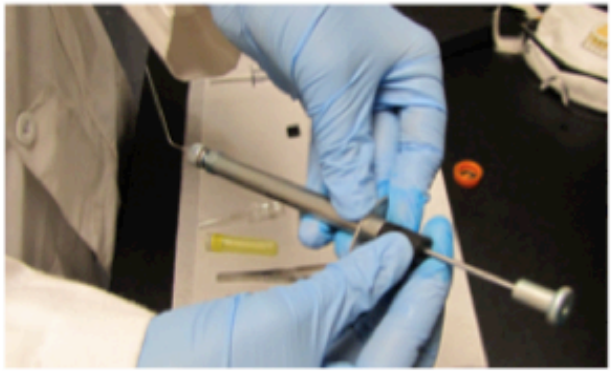

- Attach the microsprayer tip to the syringe
- Use the appropriate dose stoppers to provide the correct dose measurements
  - Placing an extra 25µl stopper at the base of the syringe helps to ensure quality aerosol plume, in case there are air bubbles within the syringe
- Spray excess solution into the waste cup

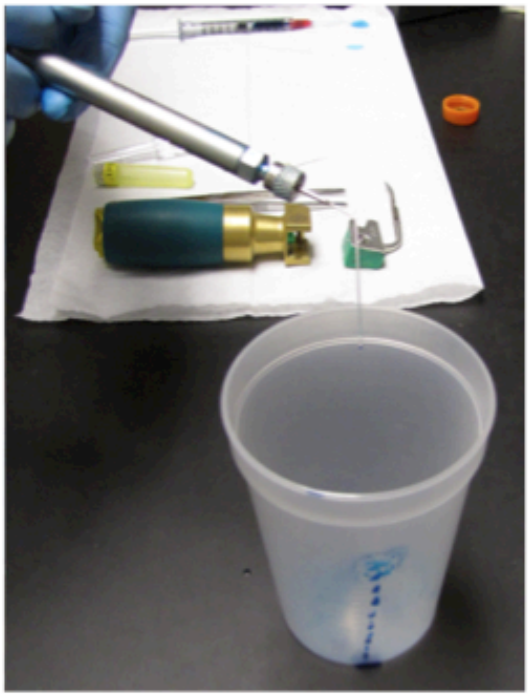

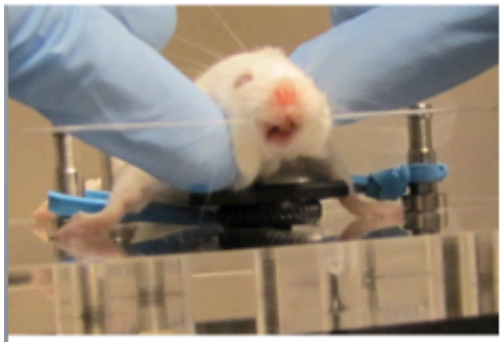

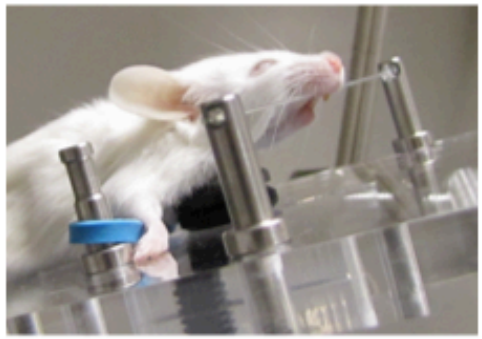

- The mouse is placed under anesthesia and assessed using the toe-pinch response
  - Anesthesia: Intraperitoneal injection of Ketamine (800-100mg/kg) and Xylazine (10-20mg/kg)
  - Approximately 5-10min until ready for procedure
- The intubation platform is placed at a 20-degree angle, depending on operator height and comfort
- When the mouse is no longer responsive to a toe-pinch, it is placed on the intubation platform in the prone position, with the upper incisors hooked over the wire
- The entire body of the mouse is straightened

Pull out the tongue with the forceps, and draw it to either side of the lower incisors to keep it out of the way.

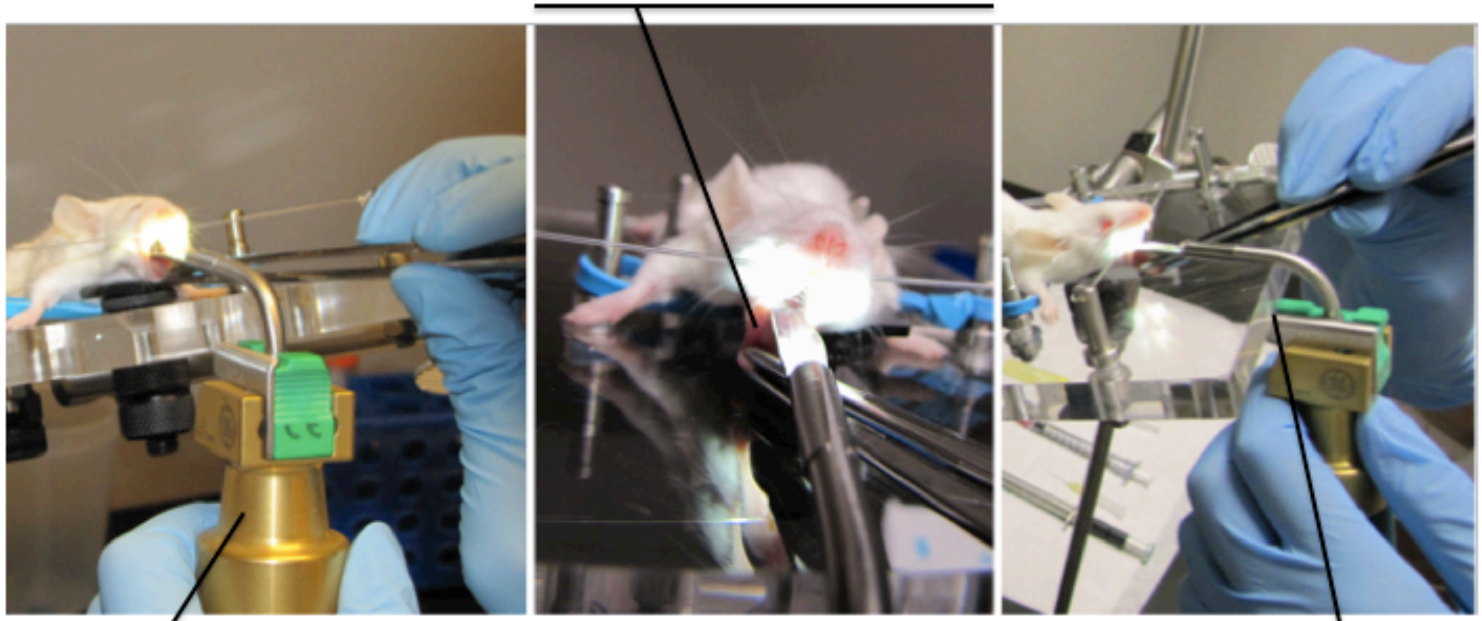

Hold the laryngoscope is in the non-dominant hand. Gently open the mouth using the tweezers, and keeping it open with the laryngoscope.

Notice that the edge of the platform prevents the laryngoscope blade from fully inserting into the mouth, preventing trauma.

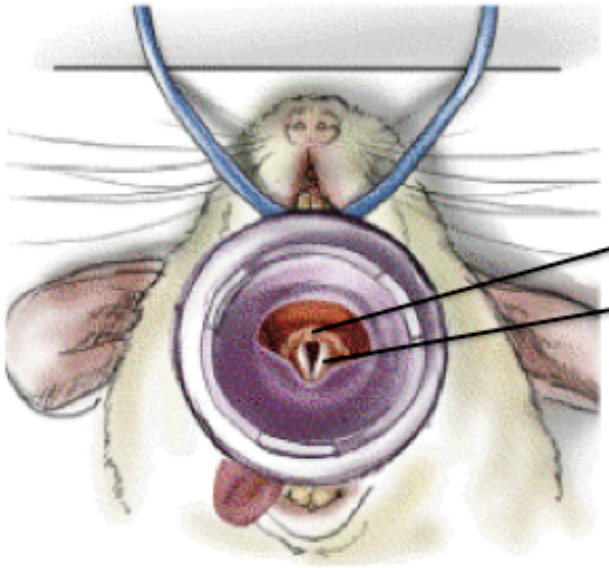

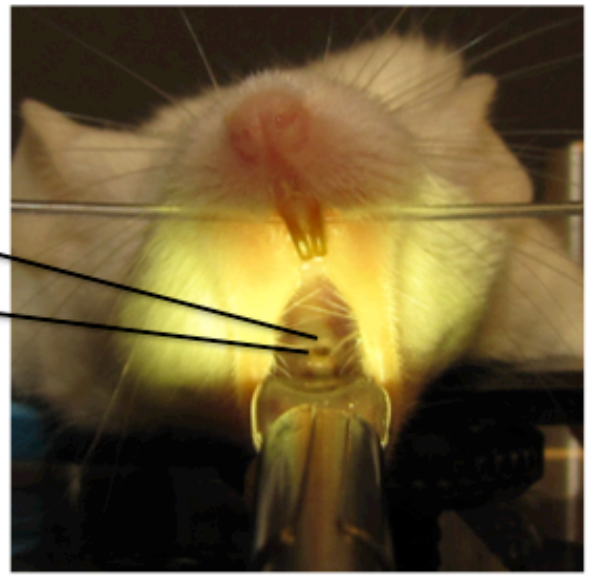

- These structures may not be readily visible, as the epiglottis may be covering them. If you probe at the white-colored area, you will be able to lift the epiglottis up and out of the way.
- The opening of the trachea is just between the vocal cords. The vocal cords will look like they are "blinking" as the mouth breathes.
- Once you see the opening, gently tease the end of the catheter through.
- Angle the tip downwards and parallel with the body of the mouse as you insert the catheter, and it should glide in with no resistance.

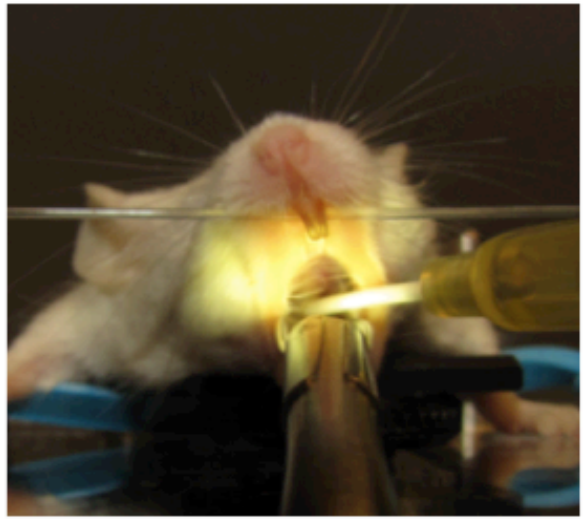

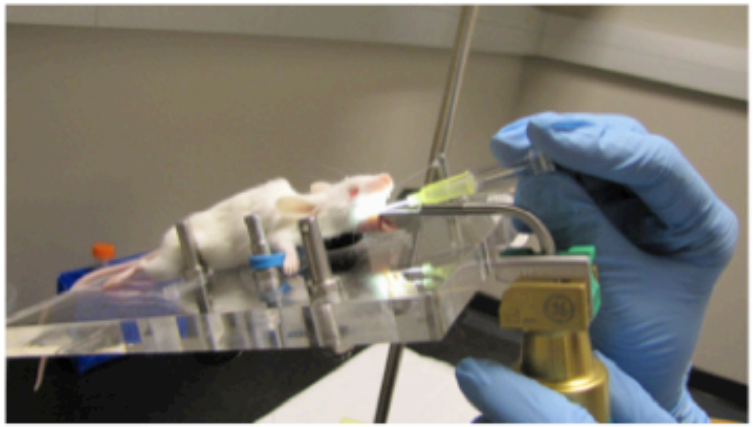

- Once the catheter is fully inserted, the laryngoscope may be removed.
- Insert the microsprayer through the catheter, using both hands to keep steady.
- It should be fully inserted so that the bend of the needle goes through the cut in the side of the catheter hub.
- Once fully inserted, deliver the aerosol, and quickly remove both the catheter and microsprayer.

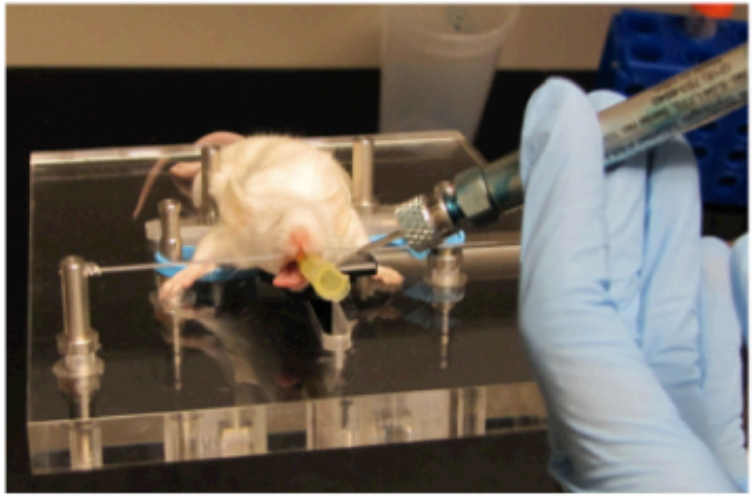

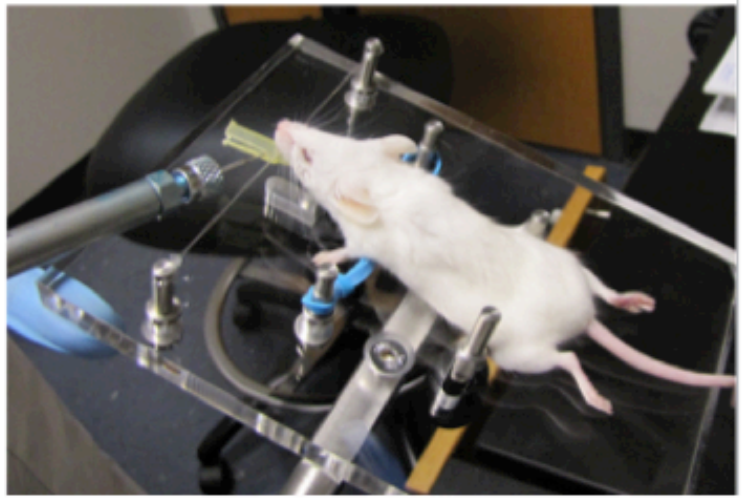

Response and Recovery

- Typically, the respiration rate will increase, and the mouse may be heard wheezing or squeaking.
- Respiration should slow down and return to normal anywhere from 1 - 15 minutes.
- Once the breathing has returned to normal, leave the mouse on the platform for an additional minute before returning to the cage (on top of a heating pad and paper towel) for recovery from anesthesia (~30 min).

Appendix B: Pulmonary Procedure Record and Monitoring Worksheet

Murine Pulmonary Procedure Record & Monitoring Worksheet Date: _____

Group Description: _____ Mouse #: _____

Mouse ID: _____ Weight: _____

Anesthesia:

Substance(s):

☐ Ketamine/Xylazine Combo

☐ Other _____

Dose: _____

Route:

☐ IP ☐ IV ☐ Inhalation

☐ Other _____

Time Administered: _____

Time Regained Consciousness: _____

Time Fully Recovered: _____

Additional Notes:

Procedure(s):

☐ 20G catheter intubation

☐ Penn-Century Microspray

Dose (vol & conc): _____

Spray Time: _____

1-min Recovery Start Time: _____

☐ Other _____

Procedure Reaction & Recovery Notes:

Euthanasia (if ahead of time point):

Date: _____ Time: _____

Method:

☐ Euthasol IP, cervical dislocation

☐ Other _____

Reason:

Glossary

Abbreviations and Acronyms

^{1}H NMR	proton nuclear magnetic resonance
Acr	acrylate
BRENDA	Braunschweig Enzyme Database
CGKGGC	cysteine-glycine-lysine-glycine-glycine-cysteine
CGRGGC	cysteine-glycine-arginine-glycine-glycine-cysteine
CPCHIVtat	cationic polymer possessing a cleavage site for HIV-1 protease
Da	Dalton
DDS	drug delivery system
DI H_2O	de-ionized water
DNA	deoxyribonucleic acid
DOX	doxorubicin
ECM	extracellular matrix
EDC	1-Ethyl-3-[3-dimethylaminopropyl]carbodimide Hydrochloride
EPR	enhanced permeation and retention
ExPASy	Expert Protein Analysis System
FBS	fetal bovine serum
FDA	Food and Drug Administration
HEK	human embryonic kidney
HLB	hydrophilic-lipophilic balance
kDa	kilo Dalton
KGHGKK	lysine-glycine-histidine-glycine-lysine-lysine

MADE	Michael addition during emulsion
MMP	matrix metalloproteinase
MW	molecular weight
NHS	*N*-hydroxysuccinimide
NMR	nuclear magnetic resonance
PBS	phosphate buffered saline
PDB	Protein Data Bank
PEG	poly(ethylene glycol)
PEG-4-Acr	four arm poly(ethylene glycol) acrylate
PEG-DA	poly(ethylene glycol) diacrylate
PVA	poly(vinyl alcohol)
QVRAHGK	glutamine-valine-arginine-alanine-histidine-glycine-lysine
RCF	relative centrifugal force
S-FIL	step and flash imprint lithography
SEM	scanning electron microscopy
siRNA	short interfering ribonucleic acid
sPLA2	secretory phospholipase A2
Sulfo-NHS	*N*-hydroxysulfosuccinimide
TEA	triethanolamine
UniPROBE	Universal PBM Resource for Oligonucleotide Binding Evaluation
UV	ultraviolet
w/v	weight by volume, percent

Bibliography

Ahsan, F., Rivas, I. P., Khan, M. A., & Torres Suarez, A. I. (2002). Targeting to macrophages: role of physicochemical properties of particulate carriers--liposomes and microspheres--on the phagocytosis by macrophages. *Journal of Controlled Release*, *79*(1-3), 29–40.

Aimetti, A. A., Machen, A. J., & Anseth, K. S. (2009). Poly(ethylene glycol) hydrogels formed by thiol-ene photopolymerization for enzyme-responsive protein delivery. *Biomaterials*, *30*(30), 6048–6054. doi:10.1016/j.biomaterials.2009.07.043

Akinc, A., Querbes, W., De, S., Qin, J., Frank-Kamenetsky, M., Jayaprakash, K. N., Jayaraman, M., et al. (2010). Targeted delivery of RNAi therapeutics with endogenous and exogenous ligand-based mechanisms. *Molecular Therapy*, *18*(7), 1357–1364. doi:10.1038/mt.2010.85

Andresen, T. L., Jensen, S. S., Kaasgaard, T., & Jørgensen, K. (2005). Triggered activation and release of liposomal prodrugs and drugs in cancer tissue by secretory phospholipase A2. *Current Drug Delivery*, *2*(4), 353–362.

Annabi, N., Nichol, J. W., Zhong, X., Ji, C., Koshy, S., Khademhosseini, A., & Dehghani, F. (2010). Controlling the porosity and microarchitecture of hydrogels for tissue engineering. *Tissue engineering Part B, Reviews*, *16*(4), 371–383. doi:10.1089/ten.TEB.2009.0639

Armstrong, J. K., Wenby, R. B., Meiselman, H. J., & Fisher, T. C. (2004). The Hydrodynamic Radii of Macromolecules and Their Effect on Red Blood Cell

Aggregation. *Biophysical Journal*, *87*(6), 4259–4270. doi:10.1529/biophysj.104.047746

Arrighi, I., Mark, S., Alvisi, M., Rechenberg, von, B., Hubbell, J. A., & Schense, J. C. (2009). Bone healing induced by local delivery of an engineered parathyroid hormone prodrug. *Biomaterials*, *30*(9), 1763–1771. doi:10.1016/j.biomaterials.2008.12.023

Asai, D., Kuramoto, M., Shoji, Y., Kang, J.-H., Kodama, K. B., Kawamura, K., Mori, T., et al. (2010). Specific transgene expression in HIV-infected cells using protease-cleavable transcription regulator. *Journal of Controlled Release*, *141*(1), 52–61. doi:10.1016/j.jconrel.2009.08.025

Asai, D., Tsuchiya, A., Kang, J.-H., Kawamura, K., Oishi, J., Mori, T., Niidome, T., et al. (2009). Inflammatory cell-specific transgene expression system responding to Ikappa-B kinase beta activation. *The journal of gene medicine*, *11*(7), 624–632. doi:10.1002/jgm.1342

Athanasiou, K. A., Agrawal, C. M., Barber, F. A., & Burkhart, S. S. (1998). Orthopaedic applications for PLA-PGA biodegradable polymers. *Arthroscopy : the journal of arthroscopic & related surgery : official publication of the Arthroscopy Association of North America and the International Arthroscopy Association*, *14*(7), 726–737.

Baeza, A., Izquierdo-Barba, I., & Vallet-Regí, M. (2010). Biotinylation of silicon-doped hydroxyapatite: a new approach to protein fixation for bone tissue regeneration. *Acta biomaterialia*, *6*(3), 743–749. doi:10.1016/j.actbio.2009.09.004

Balendiran, G. K., Dabur, R., & Fraser, D. (2004). The role of glutathione in cancer. *Cell biochemistry and function*, *22*(6), 343–352. doi:10.1002/cbf.1149

Baram, D., Vaday, G., Salamon, P., Drucker, I., Hershkoviz, R., & Mekori, Y. (2001). Human mast cells release metalloproteinase-9 on contact with activated T cells: juxtacrine regulation by TNF-{alpha}. *The Journal of Immunology*, *167*, 4008–4016.

Barnes, P. J. (2008). Immunology of asthma and chronic obstructive pulmonary disease. *Nature Reviews Immunology*, *8*(3), 183–192. doi:10.1038/nri2254

Bawa, P., Pillay, V., Choonara, Y. E., & Toit, du, L. C. (2009). Stimuli-responsive polymers and their applications in drug delivery. *Biomedical materials (Bristol, England)*, *4*(2), 022001. doi:10.1088/1748-6041/4/2/022001

Bayer, C. L., Konuk, A. A., & Peppas, N. A. (2010). Development of a protein sensing device utilizing interactions between polyaniline and a polymer acid dopant. *Biomedical microdevices*, *12*(3), 435–442. doi:10.1007/s10544-010-9400-y

Benoit, D. S. W., & Anseth, K. S. (2005). Heparin functionalized PEG gels that modulate protein adsorption for hMSC adhesion and differentiation. *Acta biomaterialia*, *1*(4), 461–470. doi:10.1016/j.actbio.2005.03.002

Benoit, D. S. W., Durney, A. R., & Anseth, K. S. (2007). The effect of heparin-functionalized PEG hydrogels on three-dimensional human mesenchymal stem cell osteogenic differentiation. *Biomaterials*, *28*(1), 66–77. doi:10.1016/j.biomaterials.2006.08.033

Benoit, D. S. W., Henry, S. M., Shubin, A. D., Hoffman, A. S., & Stayton, P. S. (2010). pH-responsive polymeric sirna carriers sensitize multidrug resistant ovarian cancer cells to doxorubicin via knockdown of polo-like kinase 1. *Molecular Pharmaceutics*, *7*(2), 442–455. doi:10.1021/mp9002255

Berman, H. M., Westbrook, J., Feng, Z., Gilliland, G., Bhat, T. N., Weissig, H., Shindyalov, I. N., et al. (2000). The Protein Data Bank. *Nucleic acids research*, *28*(1), 235–242.

Bermejo, M., Gonzalez-Alvarez, I., Alvarez, M. G., Casabo, V. G., Price, J., & Amidon, G. L. (2009). Computer Aided Learning in Biopharmacy (pp. 2923–2926). Presented at the INTED2009 Proceedings, Valencia, Spain: IATED.

Beyerle, A., Braun, A., Merkel, O., Koch, F., Kissel, T., & Stoeger, T. (2011). Comparative in vivo study of poly(ethylene imine)/siRNA complexes for pulmonary delivery in mice. *Journal of Controlled Release*, *151*(1), 51–56. doi:10.1016/j.jconrel.2010.12.017

Bhavsar, M. D., & Amiji, M. M. (2008). Development of novel biodegradable polymeric nanoparticles-in-microsphere formulation for local plasmid DNA delivery in the gastrointestinal tract. *AAPS PharmSciTech*, *9*(1), 288–294. doi:10.1208/s12249-007-9021-9

Biondi, M., Ungaro, F., Quaglia, F., & Netti, P. A. (2008). Controlled drug delivery in tissue engineering. *Advanced Drug Delivery Reviews*, *60*(2), 229–242. doi:10.1016/j.addr.2007.08.038

Bivas-Benita, M., Zwier, R., Junginger, H. E., & Borchard, G. (2005). Non-invasive pulmonary aerosol delivery in mice by the endotracheal route. *European Journal of Pharmaceutics and Biopharmaceutics*, *61*(3), 214–218. doi:10.1016/j.ejpb.2005.04.009

Boontheekul, T., & Mooney, D. J. (2003). Protein-based signaling systems in tissue engineering. *Current opinion in biotechnology*, *14*(5), 559–565.

Boussif, O., Lezoualc'h, F., Zanta, M. A., Mergny, M. D., Scherman, D., Demeneix, B., & Behr, J. P. (1995). A versatile vector for gene and oligonucleotide transfer into

cells in culture and in vivo: polyethylenimine. *Proceedings of the National Academy of Sciences of the United States of America*, *92*(16), 7297–7301.

Brunner, A., Mäder, K., & Göpferich, A. (1999). pH and osmotic pressure inside biodegradable microspheres during erosion. *Pharmaceutical Research*, *16*(6), 847–853.

Byrne, M. E., Hilt, J. Z., & Peppas, N. A. (2008). Recognitive biomimetic networks with moiety imprinting for intelligent drug delivery. *Journal of Biomedical Materials Research Part A*, *84*(1), 137–147. doi:10.1002/jbm.a.31443

Byrne, M. E., Park, K., & Peppas, N. A. (2002). Molecular imprinting within hydrogels. *Advanced Drug Delivery Reviews*, *54*(1), 149–161.

Caldorera-Moore, M., & Peppas, N. A. (2009). Micro- and nanotechnologies for intelligent and responsive biomaterial-based medical systems. *Advanced Drug Delivery Reviews*, *61*(15), 1391–1401. doi:10.1016/j.addr.2009.09.002

Caldorera-Moore, M., Guimard, N., Shi, L., & Roy, K. (2010). Designer nanoparticles: incorporating size, shape and triggered release into nanoscale drug carriers. *Expert Opinion on Drug Delivery*, *7*(4), 479–495. doi:10.1517/17425240903579971

Cao, Y., & Langer, R. (2008). A review of Judah Folkman's remarkable achievements in biomedicine. *Proceedings of the National Academy of Sciences of the United States of America*, *105*(36), 13203.

Champion, J. A., Walker, A., & Mitragotri, S. (2008). Role of Particle Size in Phagocytosis of Polymeric Microspheres. *Pharmaceutical Research*, *25*(8), 1815–1821. doi:10.1007/s11095-008-9562-y

Chang, A., Scheer, M., Grote, A., Schomburg, I., & Schomburg, D. (2009). BRENDA, AMENDA and FRENDA the enzyme information system: new content and tools

in 2009. *Nucleic acids research*, *37*(Database issue), D588–92. doi:10.1093/nar/gkn820

Chen, P., Mwakwari, S., & Oyelere, A. (2008). Gold nanoparticles: From nanomedicine to nanosensing. *Nanotechnology, Science and Applications*, *1*, 45–66.

Chen, Y.-S., Alany, R. G., Young, S. A., Green, C. R., & Rupenthal, I. D. (2011). In vitro release characteristics and cellular uptake of poly(D,L-lactic-co-glycolic acid) nanoparticles for topical delivery of antisense oligodeoxynucleotides. *Drug delivery*, *18*(7), 493–501. doi:10.3109/10717544.2011.589088

Chintala, S. K., Miller, R. R., & McDevitt, C. A. (1995). Role of heparan sulfate in the terminal differentiation of growth plate chondrocytes. *Archives of biochemistry and biophysics*, *316*(1), 227–234. doi:10.1006/abbi.1995.1032

Chiu, L. L. Y., & Radisic, M. (2010). Scaffolds with covalently immobilized VEGF and Angiopoietin-1 for vascularization of engineered tissues. *Biomaterials*, *31*(2), 226–241. doi:10.1016/j.biomaterials.2009.09.039

Clapper, J. D., Pearce, M. E., Guymon, C. A., & Salem, A. K. (2008). Biotinylated biodegradable nanotemplated hydrogel networks for cell interactive applications. *Biomacromolecules*, *9*(4), 1188–1194. doi:10.1021/bm701176j

Conference, E. S. F. B. C., Franklyn Williams, D., & Society for Biomaterials, E. (1987). Definitions in biomaterials: proceedings of a consensus conference of the European Society for Biomaterials, Chester, England, March 3-5, 1986, 72.

Corbel, M., Caulet-Maugendre, S., Germain, N., Molet, S., Lagente, V., & Boichot, E. (2001). Inhibition of bleomycin-induced pulmonary fibrosis in mice by the matrix metalloproteinase inhibitor batimastat. *The Journal of pathology*, *193*(4), 538–545. doi:10.1002/path.826

Cukierman, E., & Khan, D. R. (2010). The benefits and challenges associated with the use of drug delivery systems in cancer therapy. *Biochemical pharmacology*, *80*(5), 762–770. doi:10.1016/j.bcp.2010.04.020

Darcan-Nicolaisen, Y., Meinicke, H., Fels, G., Hegend, O., Haberland, A., Kühl, A., Loddenkemper, C., et al. (2009). Small interfering RNA against transcription factor STAT6 inhibits allergic airway inflammation and hyperreactivity in mice. *Journal of immunology (Baltimore, Md : 1950)*, *182*(12), 7501–7508. doi:10.4049/jimmunol.0713433

Debbage, P., & Jaschke, W. (2008). Molecular imaging with nanoparticles: giant roles for dwarf actors. *Histochemistry and cell biology*, *130*(5), 845–875. doi:10.1007/s00418-008-0511-y

Del Vecchio, S., Zannetti, A., Fonti, R., Pace, L., & Salvatore, M. (2007). Nuclear imaging in cancer theranostics. *The quarterly journal of nuclear medicine and molecular imaging : official publication of the Italian Association of Nuclear Medicine (AIMN) [and] the International Association of Radiopharmacology (IAR), [and] Section of the Society of Radiopharmaceutica*, *51*(2), 152–163.

Dias, R. S., Innerlohinger, J., Glatter, O., Miguel, M. G., & Lindman, B. (2005). Coil–Globule Transition of DNA Molecules Induced by Cationic Surfactants: A Dynamic Light Scattering Study. *The Journal of Physical Chemistry B*, *109*(20), 10458–10463. doi:10.1021/jp0444464

Drinnan, C. T., Zhang, G., Alexander, M. A., Pulido, A. S., & Suggs, L. J. (2010). Multimodal release of transforming growth factor-β1 and the BB isoform of platelet derived growth factor from PEGylated fibrin gels. *Journal of Controlled Release*, *147*(2), 180–186. doi:10.1016/j.jconrel.2010.03.026

Edwards, D. A., & Dunbar, C. (2002). Bioengineering of therapeutic aerosols. *Annual Review of Biomedical Engineering*, *4*, 93–107. doi:10.1146/annurev.bioeng.4.100101.132311

Ehrbar, M., Metters, A., Zammaretti, P., Hubbell, J. A., & Zisch, A. H. (2005). Endothelial cell proliferation and progenitor maturation by fibrin-bound VEGF variants with differential susceptibilities to local cellular activity. *Journal of Controlled Release*, *101*(1-3), 93–109. doi:10.1016/j.jconrel.2004.07.018

Ehrbar, M., Rizzi, S. C., Schoenmakers, R. G., Miguel, B. S., Hubbell, J. A., Weber, F. E., & Lutolf, M. P. (2007). Biomolecular hydrogels formed and degraded via site-specific enzymatic reactions. *Biomacromolecules*, *8*(10), 3000–3007. doi:10.1021/bm070228f

Ehrbar, M., Zeisberger, S. M., Raeber, G. P., Hubbell, J. A., Schnell, C., & Zisch, A. H. (2008). The role of actively released fibrin-conjugated VEGF for VEGF receptor 2 gene activation and the enhancement of angiogenesis. *Biomaterials*, *29*(11), 1720–1729. doi:10.1016/j.biomaterials.2007.12.002

El-Sherbiny, I. M., McGill, S., & Smyth, H. D. C. (2010). Swellable microparticles as carriers for sustained pulmonary drug delivery. *Journal of Pharmaceutical Sciences*, *99*(5), 2343–2356. doi:10.1002/jps.22003

Elbert, D. L. (2011). Liquid-liquid two-phase systems for the production of porous hydrogels and hydrogel microspheres for biomedical applications: A tutorial review. *Acta biomaterialia*, *7*(1), 31–56. doi:10.1016/j.actbio.2010.07.028

Elbert, D. L., Pratt, A. B., Lutolf, M. P., Halstenberg, S., & Hubbell, J. A. (2001). Protein delivery from materials formed by self-selective conjugate addition reactions. *Journal of Controlled Release*, *76*(1-2), 11–25.

Elias, D. R., Cheng, Z., & Tsourkas, A. (2010). An Intein-Mediated Site-Specific Click Conjugation Strategy for Improved Tumor Targeting of Nanoparticle Systems. *Small*. doi:10.1002/smll.201001095

Eliason, J. F. (2001). Pegylated cytokines: potential application in immunotherapy of cancer. *BioDrugs : clinical immunotherapeutics, biopharmaceuticals and gene therapy*, *15*(11), 705–711.

Eliaz, R. E., & Szoka, F. C. (2001). Liposome-encapsulated doxorubicin targeted to CD44: a strategy to kill CD44-overexpressing tumor cells. *Cancer research*, *61*(6), 2592–2601.

Faassen, A. E., Mooradian, D. L., Tranquillo, R. T., Dickinson, R. B., Letourneau, P. C., Oegema, T. R., & McCarthy, J. B. (1993). Cell surface CD44-related chondroitin sulfate proteoglycan is required for transforming growth factor-beta-stimulated mouse melanoma cell motility and invasive behavior on type I collagen. *Journal of cell science*, *105 (Pt 2)*, 501–511.

Faassen, A. E., Schrager, J. A., Klein, D. J., Oegema, T. R., Couchman, J. R., & McCarthy, J. B. (1992). A cell surface chondroitin sulfate proteoglycan, immunologically related to CD44, is involved in type I collagen-mediated melanoma cell motility and invasion. *The Journal of cell biology*, *116*(2), 521–531.

Fakhari, A., Baoum, A., Siahaan, T. J., Le, K. B., & Berkland, C. (2010). Controlling ligand surface density optimizes nanoparticle binding to ICAM-1. *Journal of Pharmaceutical Sciences*. doi:10.1002/jps.22342

Fass, L. (2008). Imaging and cancer: a review. *Molecular Oncology*, *2*(2), 115–152.

Ferrari, M. (2005). Cancer nanotechnology: opportunities and challenges. *Nature Reviews Cancer*, *5*(3), 161–171.

Fisher, J. P., Mikos, A. G., & D Bronzino, J. (2007). *Tissue Engineering*.

Fisher, O. Z., & Peppas, N. A. (2009). Polybasic Nanomatrices Prepared by UV-Initiated Photopolymerization. *Macromolecules*, *42*(9), 3391–3398. doi:10.1021/ma801966r

Fisher, O. Z., Khademhosseini, A., Langer, R., & Peppas, N. A. (2010). Bioinspired materials for controlling stem cell fate. *Accounts of Chemical Research*, *43*(3), 419–428. doi:10.1021/ar900226q

Fong, W.-K., Hanley, T., & Boyd, B. J. (2009). Stimuli responsive liquid crystals provide "on-demand" drug delivery in vitro and in vivo. *Journal of Controlled Release*, *135*(3), 218–226. doi:10.1016/j.jconrel.2009.01.009

Fu, K., Pack, D. W., Klibanov, A. M., & Langer, R. (2000). Visual evidence of acidic environment within degrading poly(lactic-co-glycolic acid) (PLGA) microspheres. *Pharmaceutical Research*, *17*(1), 100–106.

Gaffney, J., Matou-Nasri, S., Grau-Olivares, M., & Slevin, M. (2010). Therapeutic applications of hyaluronan. *Molecular bioSystems*, *6*(3), 437–443. doi:10.1039/b910552m

Gallardo, D., Skalsky, B., & Kleinebudde, P. (2008). Controlled release solid dosage forms using combinations of (meth)acrylate copolymers. *Pharmaceutical development and technology*, *13*(5), 413–423. doi:10.1080/10837450802202098

Ganta, S., Devalapally, H., Shahiwala, A., & Amiji, M. (2008). A review of stimuli-responsive nanocarriers for drug and gene delivery. *Journal of Controlled Release*, *126*(3), 187–204. doi:10.1016/j.jconrel.2007.12.017

Gao, W., Chan, J., & Farokhzad, O. C. (2010). pH-responsive Nanoparticles for Drug Delivery. *Molecular Pharmaceutics*. doi:10.1021/mp100253e

Gao, Z. G., Lee, D. H., Kim, D. I., & Bae, Y. H. (2005). Doxorubicin loaded pH-sensitive micelle targeting acidic extracellular pH of human ovarian A2780 tumor in mice. *Journal of drug targeting*, *13*(7), 391–397. doi:10.1080/10611860500376741

Garcia-Contreras, L., Fiegel, J., Telko, M. J., Elbert, K., Hawi, A., Thomas, M., VerBerkmoes, J., et al. (2007). Inhaled large porous particles of capreomycin for treatment of tuberculosis in a guinea pig model. *Antimicrobial agents and chemotherapy*, *51*(8), 2830–2836. doi:10.1128/AAC.01164-06

Gasteiger, E., Gattiker, A., Hoogland, C., Ivanyi, I., Appel, R. D., & Bairoch, A. (2003). ExPASy: The proteomics server for in-depth protein knowledge and analysis. *Nucleic acids research*, *31*(13), 3784–3788.

Gavenis, K., Schneider, U., Groll, J., & Schmidt-Rohlfing, B. (2010). BMP-7-loaded PGLA microspheres as a new delivery system for the cultivation of human chondrocytes in a collagen type I gel: the common nude mouse model. *The International journal of artificial organs*, *33*(1), 45–53.

Geiser, M., & Kreyling, W. G. (2010). Deposition and biokinetics of inhaled nanoparticles. *Particle and fibre toxicology*, *7*, 2. doi:10.1186/1743-8977-7-2

George, M., & Abraham, T. (2006). Polyionic hydrocolloids for the intestinal delivery of protein drugs: Alginate and chitosan—a review. *Journal of Controlled Release*.

Gertz, M. A. (2008). New targets and treatments in multiple myeloma: Src family kinases as central regulators of disease progression. *Leukemia & lymphoma*, *49*(12), 2240–2245. doi:10.1080/10428190802475311

Ghosn, B., Kasturi, S. P., & Roy, K. (2008). Enhancing polysaccharide-mediated delivery of nucleic acids through functionalization with secondary and tertiary amines. *Current Topics in Medicinal Chemistry*, *8*(4), 331–340.

Gilham, I., & Rowland, T. (2001). Predictive medicine: Potential benefits from the integration of diagnostics and pharmaceuticals. *Journal of Medical Marketing*.

Glangchai, L. C., Caldorera-Moore, M., Shi, L., & Roy, K. (2008). Nanoimprint lithography based fabrication of shape-specific, enzymatically-triggered smart nanoparticles. *Journal of Controlled Release*, *125*(3), 263–272. doi:10.1016/j.jconrel.2007.10.021

Gobin, A. S., & West, J. L. (2002). Cell migration through defined, synthetic ECM analogs. *The FASEB Journal: Official Publication of the Federation of American Societies for Experimental Biology*, *16*(7), 751–753. doi:10.1096/fj.01-0759fje

Gobin, A. S., & West, J. L. (2003). Val-ala-pro-gly, an elastin-derived non-integrin ligand: Smooth muscle cell adhesion and specificity. *Journal of Biomedical Materials Research*.

Gombotz, W. R., & Pettit, D. K. (1995). Biodegradable polymers for protein and peptide drug delivery. *Bioconjugate Chemistry*, *6*(4), 332–351.

Göpferich, A. (1996). Mechanisms of polymer degradation and erosion. *Biomaterials*, *17*(2), 103–114.

Grant, J., Blicker, M., Piquette-Miller, M., & Allen, C. (2005). Hybrid films from blends of chitosan and egg phosphatidylcholine for localized delivery of …. *Journal of Pharmaceutical Sciences*.

Grier, D. G. (2003). A revolution in optical manipulation. *Nature*, *424*(6950), 810–816. doi:10.1038/nature01935

Griset, A. P., Walpole, J., Liu, R., Gaffey, A., Colson, Y. L., & Grinstaff, M. W. (2009). Expansile nanoparticles: synthesis, characterization, and in vivo efficacy of an acid-responsive polymeric drug delivery system. *Journal of the American Chemical Society*, *131*(7), 2469–2471. doi:10.1021/ja807416t

Grove, T. Z., Osuji, C. O., Forster, J. D., Dufresne, E. R., & Regan, L. (2010). Stimuli-Responsive Smart Gels Realized via Modular Protein Design. *Journal of the American Chemical Society*, *132*(40), 14024–14026. doi:10.1021/ja106619w

Guo, X., Park, H., Young, S., Kretlow, J. D., van den Beucken, J. J., Baggett, L. S., Tabata, Y., et al. (2010). Repair of osteochondral defects with biodegradable hydrogel composites encapsulating marrow mesenchymal stem cells in a rabbit model. *Acta biomaterialia*, *6*(1), 39–47. doi:10.1016/j.actbio.2009.07.041

Hadinoto, K., Phanapavudhikul, P., Kewu, Z., & Tan, R. B. H. (2007a). Dry powder aerosol delivery of large hollow nanoparticulate aggregates as prospective carriers of nanoparticulate drugs: effects of phospholipids. *International Journal of Pharmaceutics*, *333*(1-2), 187–198. doi:10.1016/j.ijpharm.2006.10.009

Hadinoto, K., Zhu, K., & Tan, R. B. H. (2007b). Drug release study of large hollow nanoparticulate aggregates carrier particles for pulmonary delivery. *International Journal of Pharmaceutics*, *341*(1-2), 195–206. doi:10.1016/j.ijpharm.2007.03.035

Hahn, S. K., Kim, J. S., & Shimobouji, T. (2007). Injectable hyaluronic acid microhydrogels for controlled release formulation of erythropoietin. *Journal of Biomedical Materials Research Part A*, *80*(4), 916–924. doi:10.1002/jbm.a.30997

Haller, M. F., & Saltzman, W. M. (1998). Nerve growth factor delivery systems. *Journal of Controlled Release*, *53*(1-3), 1–6.

Harris, T. J., Maltzahn, von, G., Lord, M. E., Park, J.-H., Agrawal, A., Min, D.-H., Sailor, M. J., et al. (2008). Protease-triggered unveiling of bioactive nanoparticles. *Small*, *4*(9), 1307–1312. doi:10.1002/smll.200701319

Hatakeyama, H., Akita, H., Kogure, K., Oishi, M., Nagasaki, Y., Kihira, Y., Ueno, M., et al. (2007). Development of a novel systemic gene delivery system for cancer

therapy with a tumor-specific cleavable PEG-lipid. *Gene Therapy*, *14*(1), 68–77. doi:10.1038/sj.gt.3302843

Hayashi, T., Stetler-Stevenson, W. G., Fleming, M. V., Fishback, N., Koss, M. N., Liotta, L. A., Ferrans, V. J., et al. (1996). Immunohistochemical study of metalloproteinases and their tissue inhibitors in the lungs of patients with diffuse alveolar damage and idiopathic pulmonary fibrosis. *The American journal of pathology*, *149*(4), 1241–1256.

He, C., Kim, S. W., & Lee, D. S. (2008). In situ gelling stimuli-sensitive block copolymer hydrogels for drug delivery. *Journal of Controlled Release*, *127*(3), 189–207. doi:10.1016/j.jconrel.2008.01.005

Heller, J. (1985). Controlled drug release from poly(ortho esters). *Annals of the New York Academy of Sciences*, *446*, 51–66.

Helm, C.-L. E., Fleury, M. E., Zisch, A. H., Boschetti, F., & Swartz, M. A. (2005). Synergy between interstitial flow and VEGF directs capillary morphogenesis in vitro through a gradient amplification mechanism. *Proceedings of the National Academy of Sciences of the United States of America*, *102*(44), 15779–15784. doi:10.1073/pnas.0503681102

Helm, C.-L. E., Zisch, A., & Swartz, M. A. (2007). Engineered blood and lymphatic capillaries in 3-D VEGF-fibrin-collagen matrices with interstitial flow. *Biotechnology and bioengineering*, *96*(1), 167–176. doi:10.1002/bit.21185

Hern, D., & Hubbell, J. A. (1998). Incorporation of adhesion peptides into nonadhesive hydrogels useful for tissue resurfacing. *Journal of Biomedical Materials Research*.

Hirose, K., Marui, A., Arai, Y., Kushibiki, T., Kimura, Y., Sakaguchi, H., Yuang, H., et al. (2008). Novel approach with intratracheal administration of microgelatin

hydrogel microspheres incorporating basic fibroblast growth factor for rescue of rats with monocrotaline-induced pulmonary hypertension. *The Journal of thoracic and cardiovascular surgery*, *136*(5), 1250–1256. doi:10.1016/j.jtcvs.2008.05.038

Ho, Y.-P., & Leong, K. W. (2010). Quantum dot-based theranostics. *Nanoscale*, *2*(1), 60–68. doi:10.1039/b9nr00178f

Huang, X., El-Sayed, I. H., Qian, W., & El-Sayed, M. A. (2007). Cancer cells assemble and align gold nanorods conjugated to antibodies to produce highly enhanced, sharp, and polarized surface Raman spectra: a potential cancer diagnostic marker. *Nano Letters*, *7*(6), 1591–1597. doi:10.1021/nl070472c

Huynh, D. P., Nguyen, M. K., Pi, B. S., Kim, M. S., Chae, S. Y., Lee, K. C., Kim, B. S., et al. (2008). Functionalized injectable hydrogels for controlled insulin delivery. *Biomaterials*, *29*(16), 2527–2534. doi:10.1016/j.biomaterials.2008.02.016

Ikada, Y., & Tabata, Y. (1998). Protein release from gelatin matrices. *Advanced Drug Delivery Reviews*, *31*(3), 287–301.

Inoue, A., Takahashi, K. A., Arai, Y., Tonomura, H., Sakao, K., Saito, M., Fujioka, M., et al. (2006). The therapeutic effects of basic fibroblast growth factor contained in gelatin hydrogel microspheres on experimental osteoarthritis in the rabbit knee. *Arthritis and rheumatism*, *54*(1), 264–270. doi:10.1002/art.21561

Jain, J. P., Modi, S., Domb, A. J., & Kumar, N. (2005). Role of polyanhydrides as localized drug carriers. *Journal of Controlled Release*, *103*(3), 541–563. doi:10.1016/j.jconrel.2004.12.021

Janib, S. M., Moses, A. S., & MacKay, J. A. (2010). Imaging and drug delivery using theranostic nanoparticles. *Advanced Drug Delivery Reviews*. doi:10.1016/j.addr.2010.08.004

Ji, Y., Xu, G. P., Zhang, Z. P., Xia, J. J., Yan, J. L., & Pan, S. H. (2010). BMP-2/PLGA delayed-release microspheres composite graft, selection of bone particulate diameters, and prevention of aseptic inflammation for bone tissue engineering. *Annals of biomedical engineering*, *38*(3), 632–639. doi:10.1007/s10439-009-9888-6

Jia, X., & Kiick, K. L. (2009). Hybrid multicomponent hydrogels for tissue engineering. *Macromolecular Bioscience*, *9*(2), 140–156. doi:10.1002/mabi.200800284

Jiang, X., Dai, H., Leong, K. W., Goh, S.-H., Mao, H.-Q., & Yang, Y.-Y. (2006). Chitosan-g-PEG/DNA complexes deliver gene to the rat liver via intrabiliary and intraportal infusions. *The journal of gene medicine*, *8*(4), 477–487. doi:10.1002/jgm.868

Johns, R. E., El-Sayed, M. E. H., Bulmus, V., Cuschieri, J., Maier, R., Hoffman, A. S., & Stayton, P. S. (2008). Mechanistic analysis of macrophage response to IRAK-1 gene knockdown by a smart polymer-antisense oligonucleotide therapeutic. *Journal of Biomaterials Science, Polymer Edition*, *19*(10), 1333–1346. doi:10.1163/156856208786052326

Kaasgaard, T., Andresen, T. L., Jensen, S. S., Holte, R. O., Jensen, L. T., & Jørgensen, K. (2009). Liposomes containing alkylated methotrexate analogues for phospholipase A(2) mediated tumor targeted drug delivery. *Chemistry and physics of lipids*, *157*(2), 94–103. doi:10.1016/j.chemphyslip.2008.11.005

Kadiyala, I., Loo, Y., Roy, K., Rice, J., & Leong, K. W. (2010). Transport of chitosan-DNA nanoparticles in human intestinal M-cell model versus normal intestinal enterocytes. *European Journal of Pharmaceutical Sciences*, *39*(1-3), 103–109. doi:10.1016/j.ejps.2009.11.002

Kasturi, S. P., Sachaphibulkij, K., & Roy, K. (2005). Covalent conjugation of polyethyleneimine on biodegradable microparticles for delivery of plasmid DNA vaccines. *Biomaterials*, *26*(32), 6375–6385. doi:10.1016/j.biomaterials.2005.03.043

Kasturi, S. P., Skountzou, I., Albrecht, R. A., Koutsonanos, D., Hua, T., Nakaya, H. I., Ravindran, R., et al. (2011). Programming the magnitude and persistence of antibody responses with innate immunity. *Nature*, *470*(7335), 543–547. doi:10.1038/nature09737

Katas, H., & Alpar, H. O. (2006). Development and characterisation of chitosan nanoparticles for siRNA delivery. *Journal of Controlled Release*, *115*(2), 216–225. doi:10.1016/j.jconrel.2006.07.021

Kempen, D. H. R., Lu, L., Hefferan, T. E., Creemers, L. B., Maran, A., Classic, K. L., Dhert, W. J. A., et al. (2008). Retention of in vitro and in vivo BMP-2 bioactivities in sustained delivery vehicles for bone tissue engineering. *Biomaterials*, *29*(22), 3245–3252. doi:10.1016/j.biomaterials.2008.04.031

Khare, A. R., & Peppas, N. A. (1993). Release behavior of bioactive agents from pH-sensitive hydrogels. *Journal of Biomaterials Science, Polymer Edition*, *4*(3), 275–289.

Khare, A. R., & Peppas, N. A. (1995). Swelling/deswelling of anionic copolymer gels. *Biomaterials*, *16*(7), 559–567.

Kiick, K. L. (2008). Peptide- and protein-mediated assembly of heparinized hydrogels. *Soft Matter*, *4*, 29–37. doi:10.1039/b711319f

Kim, B.-S., Park, S. W., & Hammond, P. T. (2008). Hydrogen-bonding layer-by-layer-assembled biodegradable polymeric micelles as drug delivery vehicles from surfaces. *ACS nano*, *2*(2), 386–392. doi:10.1021/nn700408z

Kim, M.-S., Choi, Y.-J., Noh, I., & Tae, G. (2007). Synthesis and characterization of in situ chitosan-based hydrogel via grafting of carboxyethyl acrylate. *Journal of Biomedical Materials Research Part A*, *83*(3), 674–682. doi:10.1002/jbm.a.31278

Kim, S., Chung, E. H., Gilbert, M., & Healy, K. E. (2005). Synthetic MMP-13 degradable ECMs based on poly(N-isopropylacrylamide-co-acrylic acid) semi-interpenetrating polymer networks. I. Degradation and cell migration. *Journal of Biomedical Materials Research Part A*, *75*(1), 73–88. doi:10.1002/jbm.a.30375

Kim, Y.-K., Kwon, J.-T., Choi, J. Y., Jiang, H.-L., Arote, R., Jere, D., Je, Y. H., et al. (2010). Suppression of tumor growth in xenograft model mice by programmed cell death 4 gene delivery using folate-PEG-baculovirus. *Cancer Gene Therapy*, *17*(11), 751–760. doi:10.1038/cgt.2010.28

Klein, T. J., Malda, J., Sah, R. L., & Hutmacher, D. W. (2009). Tissue engineering of articular cartilage with biomimetic zones. *Tissue engineering Part B, Reviews*, *15*(2), 143–157. doi:10.1089/ten.TEB.2008.0563

Ko, J., Park, K., Kim, Y.-S., Kim, M. S., Han, J. K., Kim, K., Park, R.-W., et al. (2007). Tumoral acidic extracellular pH targeting of pH-responsive MPEG-poly(beta-amino ester) block copolymer micelles for cancer therapy. *Journal of Controlled Release*, *123*(2), 109–115. doi:10.1016/j.jconrel.2007.07.012

Kreyling, W. G., Semmler-Behnke, M., Takenaka, S., & Möller, W. (2012). Differences in the Biokinetics of Inhaled Nano- versus Micrometer-Sized Particles. *Accounts of Chemical Research*. doi:10.1021/ar300043r

Kumar, M., Behera, A. K., Lockey, R. F., Zhang, J., Bhullar, G., La Cruz, De, C. P., Chen, L.-C., et al. (2002). Intranasal gene transfer by chitosan-DNA nanospheres protects BALB/c mice against acute respiratory syncytial virus infection. *Human gene therapy*, *13*(12), 1415–1425. doi:10.1089/10430340260185058

Lai, S. K., Wang, Y.-Y., & Hanes, J. (2009). Mucus-penetrating nanoparticles for drug and gene delivery to mucosal tissues. *Advanced Drug Delivery Reviews*, *61*(2), 158–171. doi:10.1016/j.addr.2008.11.002

Langer, R., & Peppas, N. (2003). Advances in biomaterials, drug delivery, and bionanotechnology. *AIChE Journal*, *49*(12), 2990–3006.

Langer, R., & Vacanti, J. P. (1993). Tissue engineering. *Science*, *260*(5110), 920–926.

Lee, D., Zhang, W., Shirley, S., Kong, X., & Hellermann, G. (2007). Thiolated Chitosan/DNA Nanocomplexes Exhibit Enhanced and Sustained Gene Delivery. *Pharmaceutical Research*.

Lee, E. S., Shin, H. J., Na, K., & Bae, Y. H. (2003). Poly(L-histidine)-PEG block copolymer micelles and pH-induced destabilization. *Journal of Controlled Release*, *90*(3), 363–374.

Lee, J., Oh, Y. J., Lee, S. K., & Lee, K. Y. (2010). Facile control of porous structures of polymer microspheres using an osmotic agent for pulmonary delivery. *Journal of Controlled Release*, *146*(1), 61–67. doi:10.1016/j.jconrel.2010.05.026

Lee, M., Li, W., Siu, R. K., Whang, J., Zhang, X., Soo, C., Ting, K., et al. (2009). Biomimetic apatite-coated alginate/chitosan microparticles as osteogenic protein carriers. *Biomaterials*, *30*(30), 6094–6101. doi:10.1016/j.biomaterials.2009.07.046

Leslie-Barbick, J. E., Moon, J. J., & West, J. L. (2009). Covalently-immobilized vascular endothelial growth factor promotes endothelial cell tubulogenesis in poly(ethylene glycol) diacrylate hydrogels. *Journal of Biomaterials Science, Polymer Edition*, *20*(12), 1763–1779. doi:10.1163/156856208X386381

Li, B., Yoshii, T., Hafeman, A. E., Nyman, J. S., Wenke, J. C., & Guelcher, S. A. (2009a). The effects of rhBMP-2 released from biodegradable

polyurethane/microsphere composite scaffolds on new bone formation in rat femora. *Biomaterials*, *30*(35), 6768–6779. doi:10.1016/j.biomaterials.2009.08.038

Li, L., Okada, H., Takemura, G., Esaki, M., Kobayashi, H., Kanamori, H., Kawamura, I., et al. (2009b). Sustained release of erythropoietin using biodegradable gelatin hydrogel microspheres persistently improves lower leg ischemia. *Journal of the American College of Cardiology*, *53*(25), 2378–2388. doi:10.1016/j.jacc.2009.02.056

Li, X., Ding, L., Xu, Y., Wang, Y., & Ping, Q. (2009c). Targeted delivery of doxorubicin using stealth liposomes modified with transferrin. *International Journal of Pharmaceutics*, *373*(1-2), 116–123. doi:10.1016/j.ijpharm.2009.01.023

Lin, C.-C., & Anseth, K. S. (2009). PEG hydrogels for the controlled release of biomolecules in regenerative medicine. *Pharmaceutical Research*, *26*(3), 631–643. doi:10.1007/s11095-008-9801-2

Liu, F., & Basit, A. W. (2010). A paradigm shift in enteric coating: achieving rapid release in the proximal small intestine of man. *Journal of Controlled Release*, *147*(2), 242–245. doi:10.1016/j.jconrel.2010.07.105

Liu, X., Howard, K. A., Dong, M., Andersen, M. Ø., Rahbek, U. L., Johnsen, M. G., Hansen, O. C., et al. (2007). The influence of polymeric properties on chitosan/siRNA nanoparticle formulation and gene silencing. *Biomaterials*, *28*(6), 1280–1288. doi:10.1016/j.biomaterials.2006.11.004

Liu, Y., & Daum, P. (2000). The effect of refractive index on size distributions and light scattering coefficients derived from optical particle counters. *Journal of Aerosol Science*, *31*(8), 945–957.

Losi, P., Briganti, E., Magera, A., Spiller, D., Ristori, C., Battolla, B., Balderi, M., et al. (2010). Tissue response to poly(ether)urethane-polydimethylsiloxane-fibrin

composite scaffolds for controlled delivery of pro-angiogenic growth factors. *Biomaterials*, *31*(20), 5336–5344. doi:10.1016/j.biomaterials.2010.03.033

Löwik, D. W. P. M., Leunissen, E. H. P., van den Heuvel, M., Hansen, M. B., & van Hest, J. C. M. (2010). Stimulus responsive peptide based materials. *Chemical Society reviews*, *39*(9), 3394–3412. doi:10.1039/b914342b

Lucke, A., Kiermaier, J., & Göpferich, A. (2002). Peptide acylation by poly(alpha-hydroxy esters). *Pharmaceutical Research*, *19*(2), 175–181.

Lustig, S., & Peppas, N. (1988). Solute diffusion in swollen membranes. IX. Scaling laws for solute diffusion in gels. *Journal of Applied Polymer Science*, *36*(4), 735–747.

Lutolf, M. P., Lauer-Fields, J. L., Schmoekel, H. G., Metters, A. T., Weber, F. E., Fields, G. B., & Hubbell, J. A. (2003a). Synthetic matrix metalloproteinase-sensitive hydrogels for the conduction of tissue regeneration: engineering cell-invasion characteristics. *Proceedings of the National Academy of Sciences of the United States of America*, *100*(9), 5413–5418. doi:10.1073/pnas.0737381100

Lutolf, M. P., Weber, F. E., Schmoekel, H. G., Schense, J. C., Kohler, T., Müller, R., & Hubbell, J. A. (2003b). Repair of bone defects using synthetic mimetics of collagenous extracellular matrices. *Nature Biotechnology*, *21*(5), 513–518. doi:10.1038/nbt818

Lutolf, M., & Hubbell, J. A. (2003). Synthesis and physicochemical characterization of end-linked poly(ethylene glycol)-co-peptide hydrogels formed by Michael-type addition. *Biomacromolecules*, *4*(3), 713–722.

Lutolf, M., Tirelli, N., Cerritelli, S., Cavalli, L., & Hubbell, J. A. (2001). Systematic modulation of Michael-type reactivity of thiols through the use of charged amino acids. *Bioconjugate Chemistry*, *12*(6), 1051–1056.

Makino, K., Yamamoto, N., Higuchi, K., Harada, N., Ohshima, H., & Terada, H. (2003). Phagocytic uptake of polystyrene microspheres by alveolar macrophages: effects of the size and surface properties of the microspheres. *Colloids and surfaces B, Biointerfaces*, *27*(1), 33–39.

Mann, B. K., Gobin, A. S., Tsai, A. T., Schmedlen, R. H., & West, J. L. (2001). Smooth muscle cell growth in photopolymerized hydrogels with cell adhesive and proteolytically degradable domains: synthetic ECM analogs for tissue engineering. *Biomaterials*, *22*(22), 3045–3051.

Manning, M. C., Chou, D. K., Murphy, B. M., Payne, R. W., & Katayama, D. S. (2010). Stability of protein pharmaceuticals: an update. *Pharmaceutical Research*, *27*(4), 544–575. doi:10.1007/s11095-009-0045-6

Manning, M. C., Patel, K., & Borchardt, R. T. (1989). Stability of protein pharmaceuticals. *Pharmaceutical Research*, *6*(11), 903–918.

Mao, H., & Roy, K. (2001). Chitosan-DNA nanoparticles as gene carriers - synthesis characterization and transfection efficiency. *Journal of Controlled Release*, 23.

Mapili, G., Lu, Y., Chen, S., & Roy, K. (2005). Laser-layered microfabrication of spatially patterned functionalized tissue-engineering scaffolds. *Journal of Biomedical Materials Research Part B, Applied Biomaterials*, *75*(2), 414–424. doi:10.1002/jbm.b.30325

Mather, B., Viswanathan, K., Miller, K., & Long, T. (2006). Michael addition reactions in macromolecular design for emerging technologies. *Progress In Polymer Science*, *31*(5), 487–531.

Maxwell, D. J., Hicks, B. C., Parsons, S., & Sakiyama-Elbert, S. E. (2005). Development of rationally designed affinity-based drug delivery systems. *Acta biomaterialia*, *1*(1), 101–113. doi:10.1016/j.actbio.2004.09.002

McGonigle, J. S., Tae, G., Stayton, P. S., Hoffman, A. S., & Scatena, M. (2008). Heparin-regulated delivery of osteoprotegerin promotes vascularization of implanted hydrogels. *Journal of Biomaterials Science, Polymer Edition*, *19*(8), 1021–1034. doi:10.1163/156856208784909381

Meng, F., Hennink, W., & Zhong, Z. (2009). Reduction-sensitive polymers and bioconjugates for biomedical applications. *Biomaterials*.

Metters, A., & Hubbell, J. A. (2005). Network formation and degradation behavior of hydrogels formed by Michael-type addition reactions. *Biomacromolecules*, *6*(1), 290–301. doi:10.1021/bm049607o

Miyata, T., Asami, N., & Uragami, T. (1999). A reversibly antigen-responsive hydrogel. *Nature*, *399*(6738), 766–769. doi:10.1038/21619

Miyata, T., Jige, M., Nakaminami, T., & Uragami, T. (2006). Tumor marker-responsive behavior of gels prepared by biomolecular imprinting. *Proceedings of the National Academy of Sciences of the United States of America*, *103*(5), 1190–1193. doi:10.1073/pnas.0506786103

Miyata, T., Uragami, T., & Nakamae, K. (2002). Biomolecule-sensitive hydrogels. *Advanced Drug Delivery Reviews*, *54*(1), 79–98.

Mohamed, F., & van der Walle, C. F. (2008). Engineering biodegradable polyester particles with specific drug targeting and drug release properties. *Journal of Pharmaceutical Sciences*, *97*(1), 71–87. doi:10.1002/jps.21082

Molineux, G. (2002). Pegylation: engineering improved pharmaceuticals for enhanced therapy. *Cancer treatment reviews*, *28 Suppl A*, 13–16.

Molineux, G. (2003). Pegylation: engineering improved biopharmaceuticals for oncology. *Pharmacotherapy*, *23*(8 Pt 2), 3S–8S.

Moss, J. A., Stokols, S., Hixon, M. S., Ashley, F. T., Chang, J. Y., & Janda, K. D. (2006). Solid-phase synthesis and kinetic characterization of fluorogenic enzyme-degradable hydrogel cross-linkers. *Biomacromolecules*, *7*(4), 1011–1016. doi:10.1021/bm051001s

Moustoifa, E.-F., Alouini, M.-A., Salaün, A., Berthelot, T., Bartegi, A., Albenque-Rubio, S., & Déléris, G. (2010). Novel cyclopeptides for the design of MMP directed delivery devices: a novel smart delivery paradigm. *Pharmaceutical Research*, *27*(8), 1713–1721. doi:10.1007/s11095-010-0164-0

Moya, M. L., Cheng, M.-H., Huang, J.-J., Francis-Sedlak, M. E., Kao, S.-W., Opara, E. C., & Brey, E. M. (2010a). The effect of FGF-1 loaded alginate microbeads on neovascularization and adipogenesis in a vascular pedicle model of adipose tissue engineering. *Biomaterials*, *31*(10), 2816–2826. doi:10.1016/j.biomaterials.2009.12.053

Moya, M. L., Garfinkel, M. R., Liu, X., Lucas, S., Opara, E. C., Greisler, H. P., & Brey, E. M. (2010b). Fibroblast growth factor-1 (FGF-1) loaded microbeads enhance local capillary neovascularization. *The Journal of surgical research*, *160*(2), 208–212. doi:10.1016/j.jss.2009.06.003

Mudhakir, D., & Harashima, H. (2009). Learning from the viral journey: how to enter cells and how to overcome intracellular barriers to reach the nucleus. *The AAPS Journal*, *11*(1), 65–77. doi:10.1208/s12248-009-9080-9

Murthy, N., Campbell, J., Fausto, N., Hoffman, A. S., & Stayton, P. S. (2003). Bioinspired pH-responsive polymers for the intracellular delivery of biomolecular drugs. *Bioconjugate Chemistry*, *14*(2), 412–419. doi:10.1021/bc020056d

Nagai, N., Kumasaka, N., Kawashima, T., Kaji, H., Nishizawa, M., & Abe, T. (2010). Preparation and characterization of collagen microspheres for sustained release of

VEGF. *Journal of materials science Materials in medicine*, *21*(6), 1891–1898. doi:10.1007/s10856-010-4054-0

Naidu, B. N., Sorenson, M. E., Connolly, T. P., & Ueda, Y. (2003). Michael addition of amines and thiols to dehydroalanine amides: a remarkable rate acceleration in water. *The Journal of organic chemistry*, *68*(26), 10098–10102. doi:10.1021/jo034762z

Neut, D., Kluin, O. S., Crielaard, B. J., van der Mei, H. C., Busscher, H. J., & Grijpma, D. W. (2009). A biodegradable antibiotic delivery system based on poly-(trimethylene carbonate) for the treatment of osteomyelitis. *Acta orthopaedica*, *80*(5), 514–519. doi:10.3109/17453670903350040

Newburger, D. E., & Bulyk, M. L. (2009). UniPROBE: an online database of protein binding microarray data on protein-DNA interactions. *Nucleic acids research*, *37*(Database issue), D77–82. doi:10.1093/nar/gkn660

Nie, T., Baldwin, A., Yamaguchi, N., & Kiick, K. L. (2007). Production of heparin-functionalized hydrogels for the development of responsive and controlled growth factor delivery systems. *Journal of Controlled Release*, *122*(3), 287–296. doi:10.1016/j.jconrel.2007.04.019

Nomi, M., Atala, A., Coppi, P. D., & Soker, S. (2002). Principals of neovascularization for tissue engineering. *Molecular aspects of medicine*, *23*(6), 463–483.

Oana, H., Tsumoto, K., Yoshikawa, Y., & Yoshikawa, K. (2002). Folding transition of large DNA completely inhibits the action of a restriction endonuclease as revealed by single-chain observation. *FEBS letters*, *530*(1-3), 143–146.

Okuma, T., Terasaki, Y., Kaikita, K., Kobayashi, H., Kuziel, W. A., Kawasuji, M., & Takeya, M. (2004). C-C chemokine receptor 2 (CCR2) deficiency improves bleomycin-induced pulmonary fibrosis by attenuation of both macrophage

infiltration and production of macrophage-derived matrix metalloproteinases. *The Journal of pathology*, *204*(5), 594–604. doi:10.1002/path.1667

Onaca, O., Enea, R., Hughes, D. W., & Meier, W. (2009). Stimuli-responsive polymersomes as nanocarriers for drug and gene delivery. *Macromolecular Bioscience*, *9*(2), 129–139. doi:10.1002/mabi.200800248

Ozeki, M., & Tabata, Y. (2006). Interaction of hepatocyte growth factor with gelatin as the carrier material. *Journal of Biomaterials Science, Polymer Edition*, *17*(1-2), 163–175.

Park, J. W., Kirpotin, D. B., Hong, K., Shalaby, R., Shao, Y., Nielsen, U. B., Marks, J. D., et al. (2001). Tumor targeting using anti-her2 immunoliposomes. *Journal of Controlled Release*, *74*(1-3), 95–113.

Parks, S. K., Chiche, J., & Pouysségur, J. (2010). pH control mechanisms of tumor survival and growth. *Journal of cellular physiology*. doi:10.1002/jcp.22400

Patel, B., Gupta, V., & Ahsan, F. (2012). PEG–PLGA based large porous particles for pulmonary delivery of a highly soluble drug, low molecular weight heparin. *Journal of Controlled Release*, *162*(2), 310–320. doi:10.1016/j.jconrel.2012.07.003

Patterson, J., & Hubbell, J. A. (2010). Enhanced proteolytic degradation of molecularly engineered PEG hydrogels in response to MMP-1 and MMP-2. *Biomaterials*, *31*(30), 7836–7845. doi:10.1016/j.biomaterials.2010.06.061

Patterson, J., & Hubbell, J. A. (2011). SPARC-derived protease substrates to enhance the plasmin sensitivity of molecularly engineered PEG hydrogels. *Biomaterials*, *32*(5), 1301–1310. doi:10.1016/j.biomaterials.2010.10.016

Pavet, V., Portal, M. M., Moulin, J. C., Herbrecht, R., & Gronemeyer, H. (2010). Towards novel paradigms for cancer therapy. *Oncogene*. doi:10.1038/onc.2010.460

Pedersen, P. J., Adolph, S. K., Subramanian, A. K., Arouri, A., Andresen, T. L., Mouritsen, O. G., Madsen, R., et al. (2010). Liposomal formulation of retinoids designed for enzyme triggered release. *Journal of medicinal chemistry*, *53*(9), 3782–3792. doi:10.1021/jm100190c

Peppas, N. A., Bures, P., Leobandung, W., & Ichikawa, H. (2000). Hydrogels in pharmaceutical formulations. *European Journal of Pharmaceutics and Biopharmaceutics*, *50*(1), 27–46.

Peppas, N. A., Keys, K. B., Torres-Lugo, M., & Lowman, A. M. (1999). Poly(ethylene glycol)-containing hydrogels in drug delivery. *Journal of Controlled Release*, *62*(1-2), 81–87.

Pfister, L. A., Papaloïzos, M., Merkle, H. P., & Gander, B. (2007). Nerve conduits and growth factor delivery in peripheral nerve repair. *Journal of the peripheral nervous system : JPNS*, *12*(2), 65–82. doi:10.1111/j.1529-8027.2007.00125.x

Picard, F. J., & Bergeron, M. G. (2002). Rapid molecular theranostics in infectious diseases. *Drug Discovery Today*, *7*(21), 1092–1101.

Pieper, J. S., Hafmans, T., van Wachem, P. B., van Luyn, M. J. A., Brouwer, L. A., Veerkamp, J. H., & van Kuppevelt, T. H. (2002). Loading of collagen-heparan sulfate matrices with bFGF promotes angiogenesis and tissue generation in rats. *Journal of Biomedical Materials Research*, *62*(2), 185–194. doi:10.1002/jbm.10267

Pilcer, G., & Amighi, K. (2010). Formulation strategy and use of excipients in pulmonary drug delivery. *International Journal of Pharmaceutics*, *392*(1-2), 1–19. doi:10.1016/j.ijpharm.2010.03.017

Podual, K., Doyle, F. J., & Peppas, N. A. (2000a). Dynamic behavior of glucose oxidase-containing microparticles of poly(ethylene glycol)-grafted cationic hydrogels in an environment of changing pH. *Biomaterials*, *21*(14), 1439–1450.

Podual, K., Doyle, F. J., & Peppas, N. A. (2000b). Glucose-sensitivity of glucose oxidase-containing cationic copolymer hydrogels having poly(ethylene glycol) grafts. *Journal of Controlled Release*, *67*(1), 9–17.

Portney, N., & Ozkan, M. (2006). Nano-oncology: drug delivery, imaging, and sensing. *Analytical and Bioanalytical Chemistry*, *384*(3), 620–630.

Pouton, C. W., Wagstaff, K. M., Roth, D. M., Moseley, G. W., & Jans, D. A. (2007). Targeted delivery to the nucleus. *Advanced Drug Delivery Reviews*, *59*(8), 698–717. doi:10.1016/j.addr.2007.06.010

Pusztai, A., Grant, G., Bardocz, S., Baintner, K., Gelencsér, E., & Ewen, S. W. (1997). Both free and complexed trypsin inhibitors stimulate pancreatic secretion and change duodenal enzyme levels. *The American journal of physiology*, *272*(2 Pt 1), G340–50.

Putnam, D., Gentry, C. A., Pack, D. W., & Langer, R. (2001). Polymer-based gene delivery with low cytotoxicity by a unique balance of side-chain termini. *Proceedings of the National Academy of Sciences of the United States of America*, *98*(3), 1200–1205. doi:10.1073/pnas.031577698

Qiu, Y., & Park, K. (2001). Environment-sensitive hydrogels for drug delivery. *Advanced Drug Delivery Reviews*, *53*(3), 321–339.

Rekha, M. R., & Sharma, C. P. (2009). Synthesis and evaluation of lauryl succinyl chitosan particles towards oral insulin delivery and absorption. *Journal of Controlled Release*, *135*(2), 144–151. doi:10.1016/j.jconrel.2009.01.011

Rezler, E. M., Khan, D. R., Lauer-Fields, J., Cudic, M., Baronas-Lowell, D., & Fields, G. B. (2007). Targeted drug delivery utilizing protein-like molecular architecture. *Journal of the American Chemical Society*, *129*(16), 4961–4972. doi:10.1021/ja066929m

Roberts, M. J., Bentley, M. D., & Harris, J. M. (2002). Chemistry for peptide and protein PEGylation. *Advanced Drug Delivery Reviews*, *54*(4), 459–476.

Robinson, S. N., & Talmadge, J. E. (2002). Sustained release of growth factors. *In vivo (Athens, Greece)*, *16*(6), 535–540.

Roy, K., Mao, H., & Huang, S. (1999). Oral gene delivery with chitosan-DNA nanoparticles generates immunologic protection in a murine model of peanut allergy. *Nature Medicine*, *5*(4), 5.

Rytting, E., Nguyen, J., Wang, X., & Kissel, T. (2008). Biodegradable polymeric nanocarriers for pulmonary drug delivery. *Expert Opinion on Drug Delivery*, *5*(6), 629–639. doi:10.1517/17425247.5.6.629

Sahoo, S. K., Ma, W., & Labhasetwar, V. (2004). Efficacy of transferrin-conjugated paclitaxel-loaded nanoparticles in a murine model of prostate cancer. *International Journal of Cancer*, *112*(2), 335–340. doi:10.1002/ijc.20405

Sakiyama-Elbert, S. E., & Hubbell, J. A. (2000). Controlled release of nerve growth factor from a heparin-containing fibrin-based cell ingrowth matrix. *Journal of Controlled Release*, *69*(1), 149–158.

Saltzman, W. M., & Baldwin, S. (1998). Materials for protein delivery in tissue engineering. *Advanced Drug Delivery Reviews*, *33*(1-2), 71–86.

Saltzman, W. M., & Olbricht, W. L. (2002). Building drug delivery into tissue engineering. *Nature Reviews Drug discovery*, *1*(3), 177–186.

Sano, A., Hojo, T., Maeda, M., & Fujioka, K. (1998). Protein release from collagen matrices. *Advanced Drug Delivery Reviews*, *31*(3), 247–266.

Sarfati, G., Dvir, T., Elkabetz, M., Apte, R. N., & Cohen, S. (2010). Targeting of polymeric nanoparticles to lung metastases by surface-attachment of YIGSR peptide from laminin. *Biomaterials*. doi:10.1016/j.biomaterials.2010.09.014

Sasaki, N., Minami, T., Yamada, K., Yamada, H., Inoue, Y., Kobayashi, M., & Tabata, Y. (2008). In vivo effects of intra-articular injection of gelatin hydrogen microspheres containing basic fibroblast growth factor on experimentally induced defects in third metacarpal bones of horses. *American journal of veterinary research*, *69*(12), 1555–1559. doi:10.2460/ajvr.69.12.1555

Satav, S. S., Bhat, S., & Thayumanavan, S. (2010). Feedback regulated drug delivery vehicles: carbon dioxide responsive cationic hydrogels for antidote release. *Biomacromolecules*, *11*(7), 1735–1740. doi:10.1021/bm1005454

Sato, H. (2002). Enzymatic procedure for site-specific pegylation of proteins. *Advanced Drug Delivery Reviews*, *54*(4), 487–504.

Sawant, R. M., Hurley, J. P., Salmaso, S., Kale, A., Tolcheva, E., Levchenko, T. S., & Torchilin, V. P. (2006). "SMART" drug delivery systems: double-targeted pH-responsive pharmaceutical nanocarriers. *Bioconjugate Chemistry*, *17*(4), 943–949. doi:10.1021/bc060080h

Sánchez, A., Tobío, M., González, L., Fabra, A., & Alonso, M. J. (2003). Biodegradable micro- and nanoparticles as long-term delivery vehicles for interferon-alpha. *European Journal of Pharmaceutical Sciences*, *18*(3-4), 221–229.

Schipper, N., Olsson, S., Hoogstraate, J., deBoer, A., Vårum, K., & Artursson, P. (1997). Chitosans as absorption enhancers for poorly absorbable drugs 2: mechanism of absorption enhancement. *Pharmaceutical Research*, *14*(7), 923–929.

Schipper, N., Vårum, K., & Artursson, P. (1996). Chitosans as absorption enhancers for poorly absorbable drugs. 1: Influence of molecular weight and degree of acetylation on drug transport across human intestinal epithelial (Caco-2) cells. *Pharmaceutical Research*, *13*(11), 1686–1692.

Schipper, N., Vårum, K., Stenberg, P., Ocklind, G., Lennernäs, H., & Artursson, P. (1999). Chitosans as absorption enhancers of poorly absorbable drugs 3: Influence of mucus on absorption enhancement. *European Journal of Pharmaceutical Sciences*, *8*(4), 335–343.

Scott, E. A., Nichols, M. D., Kuntz-Willits, R., & Elbert, D. L. (2010). Modular scaffolds assembled around living cells using poly(ethylene glycol) microspheres with macroporation via a non-cytotoxic porogen. *Acta biomaterialia*, *6*(1), 29–38. doi:10.1016/j.actbio.2009.07.009

Seeherman, H. J., Archambault, J. M., Rodeo, S. A., Turner, A. S., Zekas, L., D'Augusta, D., Li, X. J., et al. (2008). rhBMP-12 accelerates healing of rotator cuff repairs in a sheep model. *The Journal of bone and joint surgery American volume*, *90*(10), 2206–2219. doi:10.2106/JBJS.G.00742

Seeherman, H. J., Li, X. J., Bouxsein, M. L., & Wozney, J. M. (2010). rhBMP-2 induces transient bone resorption followed by bone formation in a nonhuman primate core-defect model. *The Journal of bone and joint surgery American volume*, *92*(2), 411–426. doi:10.2106/JBJS.H.01732

Seeherman, H., & Wozney, J. M. (2005). Delivery of bone morphogenetic proteins for orthopedic tissue regeneration. *Cytokine & growth factor reviews*, *16*(3), 329–345. doi:10.1016/j.cytogfr.2005.05.001

Seeherman, H., Li, R., Bouxsein, M., Kim, H., Li, X. J., Smith-Adaline, E. A., Aiolova, M., et al. (2006). rhBMP-2/calcium phosphate matrix accelerates osteotomy-site healing in a nonhuman primate model at multiple treatment times and concentrations. *The Journal of bone and joint surgery American volume*, *88*(1), 144–160. doi:10.2106/JBJS.D.02453

Segura, T., Anderson, B. C., Chung, P. H., Webber, R. E., Shull, K. R., & Shea, L. D. (2005). Crosslinked hyaluronic acid hydrogels: a strategy to functionalize and pattern. *Biomaterials*, *26*(4), 359–371. doi:10.1016/j.biomaterials.2004.02.067

Seliktar, D., Zisch, A. H., Lutolf, M. P., Wrana, J. L., & Hubbell, J. A. (2004). MMP-2 sensitive, VEGF-bearing bioactive hydrogels for promotion of vascular healing. *Journal of Biomedical Materials Research Part A*, *68*(4), 704–716. doi:10.1002/jbm.a.20091

Shaikh, R. P., Pillay, V., Choonara, Y. E., Toit, du, L. C., Ndesendo, V. M. K., Bawa, P., & Cooppan, S. (2010). A review of multi-responsive membranous systems for rate-modulated drug delivery. *AAPS PharmSciTech*, *11*(1), 441–459. doi:10.1208/s12249-010-9403-2

Shen, Y., Tang, H., Radosz, M., Van Kirk, E., & Murdoch, W. J. (2008). pH-responsive nanoparticles for cancer drug delivery. *Methods in molecular biology (Clifton, NJ)*, *437*, 183–216. doi:10.1007/978-1-59745-210-6_10

Shim, J., & Nho, Y. (2003). Preparation of poly (acrylic acid)-chitosan hydrogels by gamma irradiation and in vitro drug release. *Journal of Applied Polymer Science*.

Sierra, D. H. (1993). Fibrin sealant adhesive systems: a review of their chemistry, material properties and clinical applications. *Journal of biomaterials applications*, *7*(4), 309–352.

Simpson, J. L., Scott, R. J., Boyle, M. J., & Gibson, P. G. (2005). Differential proteolytic enzyme activity in eosinophilic and neutrophilic asthma. *American Journal of Respiratory and Critical Care Medicine*, *172*(5), 559–565. doi:10.1164/rccm.200503-369OC

Singh, A., Nie, H., Ghosn, B., Qin, H., Kwak, L. W., & Roy, K. (2008). Efficient modulation of T-cell response by dual-mode, single-carrier delivery of cytokine-targeted siRNA and DNA vaccine to antigen-presenting cells. *Molecular Therapy*, *16*(12), 2011–2021. doi:10.1038/mt.2008.206

Singh, A., Suri, S., & Roy, K. (2009). In-situ crosslinking hydrogels for combinatorial delivery of chemokines and siRNA-DNA carrying microparticles to dendritic cells. *Biomaterials*, *30*(28), 5187–5200. doi:10.1016/j.biomaterials.2009.06.001

Solsona, I. A., Smith, R. B., Livingstone, C., & Davis, J. (2006). Metabolic mimics: thiol responsive drug release. *Journal of colloid and interface science*, *302*(2), 698–701. doi:10.1016/j.jcis.2006.06.042

Son, Y.-J., & McConville, J. T. (2008). Advancements in dry powder delivery to the lung. *Drug Development and Industrial Pharmacy*, *34*(9), 948–959. doi:10.1080/03639040802235902

Spicer, P. P., & Mikos, A. G. (2010). Fibrin glue as a drug delivery system. *Journal of Controlled Release*, *148*(1), 49–55. doi:10.1016/j.jconrel.2010.06.025

Steinbüchel, A., & Matsumura, S. (2003). *Biopolymers: Miscellaneous biopolymers and biodegradation of synthetic polymers*.

Sumer, B., & Gao, J. (2008). Theranostic nanomedicine for cancer. *Nanomedicine (London, England)*, *3*(2), 137–140. doi:10.2217/17435889.3.2.137

Sung, J. C., Pulliam, B. L., & Edwards, D. A. (2007). Nanoparticles for drug delivery to the lungs. *Trends in Biotechnology*, *25*(12), 563–570. doi:10.1016/j.tibtech.2007.09.005

Suri, S., & Schmidt, C. E. (2009). Photopatterned collagen-hyaluronic acid interpenetrating polymer network hydrogels. *Acta biomaterialia*, *5*(7), 2385–2397. doi:10.1016/j.actbio.2009.05.004

Suri, S., & Schmidt, C. E. (2010). Cell-laden hydrogel constructs of hyaluronic acid, collagen, and laminin for neural tissue engineering. *Tissue engineering Part A*, *16*(5), 1703–1716. doi:10.1089/ten.tea.2009.0381

Suzuki, Y., Tanihara, M., Nishimura, Y., Suzuki, K., Kakimaru, Y., & Shimizu, Y. (1998). A new drug delivery system with controlled release of antibiotic only in the presence of infection. *Journal of Biomedical Materials Research*, *42*(1), 112–116.

Ta, H., Dass, C., & Dunstan, D. (2008). Injectable chitosan hydrogels for localised cancer therapy. *Journal of Controlled Release*.

Tabata, Y. (2003). Tissue regeneration based on growth factor release. *Tissue engineering*, *9 Suppl 1*, S5–15. doi:10.1089/10763270360696941

Tae, G., Scatena, M., Stayton, P. S., & Hoffman, A. S. (2006). PEG-cross-linked heparin is an affinity hydrogel for sustained release of vascular endothelial growth factor. *Journal of Biomaterials Science, Polymer Edition*, *17*(1-2), 187–197.

Taqvi, S., Dixit, L., & Roy, K. (2006). Biomaterial-based notch signaling for the differentiation of hematopoietic stem cells into T cells. *Journal of Biomedical Materials Research Part A*, *79*(3), 689–697. doi:10.1002/jbm.a.30916

Tauro, J. R., & Gemeinhart, R. A. (2005a). Extracellular protease activation of chemotherapeutics from hydrogel matrices: a new paradigm for local chemotherapy. *Molecular Pharmaceutics*, *2*(5), 435–438. doi:10.1021/mp050028n

Tauro, J. R., & Gemeinhart, R. A. (2005b). Matrix metalloprotease triggered delivery of cancer chemotherapeutics from hydrogel matrixes. *Bioconjugate Chemistry*, *16*(5), 1133–1139. doi:10.1021/bc0501303

Tauro, J. R., Lee, B.-S., Lateef, S. S., & Gemeinhart, R. A. (2008). Matrix metalloprotease selective peptide substrates cleavage within hydrogel matrices for cancer chemotherapy activation. *Peptides*, *29*(11), 1965–1973. doi:10.1016/j.peptides.2008.06.021

Thissen, H., Chang, K.-Y., Tebb, T. A., Tsai, W.-B., Glattauer, V., Ramshaw, J. A. M., & Werkmeister, J. A. (2006). Synthetic biodegradable microparticles for articular cartilage tissue engineering. *Journal of Biomedical Materials Research Part A*, *77*(3), 590–598. doi:10.1002/jbm.a.30612

Thompson, A. D., Betz, M. W., Yoon, D. M., & Fisher, J. P. (2009). Osteogenic differentiation of bone marrow stromal cells induced by coculture with chondrocytes encapsulated in three-dimensional matrices. *Tissue engineering Part A*, *15*(5), 1181–1190. doi:10.1089/ten.tea.2007.0275

Thornton, P. D., & Heise, A. (2010). Highly specific dual enzyme-mediated payload release from peptide-coated silica particles. *Journal of the American Chemical Society*, *132*(6), 2024–2028. doi:10.1021/ja9094439

Thyagarajapuram, N., Olsen, D., & Middaugh, C. R. (2007). The structure, stability, and complex behavior of recombinant human gelatins. *Journal of Pharmaceutical Sciences*, *96*(12), 3363–3378. doi:10.1002/jps.21022

Tokatlian, T., Shrum, C. T., Kadoya, W. M., & Segura, T. (2010). Protease degradable tethers for controlled and cell-mediated release of nanoparticles in 2- and 3-dimensions. *Biomaterials*, *31*(31), 8072–8080. doi:10.1016/j.biomaterials.2010.07.030

Tong, L., Wei, Q., Wei, A., & Cheng, J.-X. (2009). Gold nanorods as contrast agents for biological imaging: optical properties, surface conjugation and photothermal effects. *Photochemistry and Photobiology*, *85*(1), 21–32. doi:10.1111/j.1751-1097.2008.00507.x

A Truskey, G., Yuan PhD, F., Yuan, F., & F Katz, D. (2004). *Transport phenomena in biological systems*.

Tsapis, N., Bennett, D., Jackson, B., Weitz, D. A., & Edwards, D. A. (2002). Trojan particles: large porous carriers of nanoparticles for drug delivery. *Proceedings of the National Academy of Sciences of the United States of America*, *99*(19), 12001–12005. doi:10.1073/pnas.182233999

Tønnesen, H. H., & Karlsen, J. (2002). Alginate in drug delivery systems. *Drug Development and Industrial Pharmacy*, *28*(6), 621–630. doi:10.1081/DDC-120003853

Uebersax, L., Merkle, H. P., & Meinel, L. (2009). Biopolymer-based growth factor delivery for tissue repair: from natural concepts to engineered systems. *Tissue engineering Part B, Reviews*, *15*(3), 263–289. doi:10.1089/ten.TEB.2008.0668

Urech, L., Bittermann, A. G., Hubbell, J. A., & Hall, H. (2005). Mechanical properties, proteolytic degradability and biological modifications affect angiogenic process extension into native and modified fibrin matrices in vitro. *Biomaterials*, *26*(12), 1369–1379. doi:10.1016/j.biomaterials.2004.04.045

van Blitterswijk, C.A., & Thomsen, P. (2008). Tissue engineering.

van de Weert, M., Hennink, W. E., & Jiskoot, W. (2000). Protein instability in poly(lactic-co-glycolic acid) microparticles. *Pharmaceutical Research*, *17*(10), 1159–1167.

van de Wetering, P., Metters, A. T., Schoenmakers, R. G., & Hubbell, J. A. (2005). Poly(ethylene glycol) hydrogels formed by conjugate addition with controllable swelling, degradation, and release of pharmaceutically active proteins. *Journal of Controlled Release*, *102*(3), 619–627. doi:10.1016/j.jconrel.2004.10.029

Vartak, D. G., & Gemeinhart, R. A. (2007). Matrix metalloproteases: underutilized targets for drug delivery. *Journal of drug targeting*, *15*(1), 1–20. doi:10.1080/10611860600968967

Vauthier, C., Schmidt, C., & Couvreur, P. (1999). Measurement of the density of polymeric nanoparticulate drug carriers by isopycnic centrifugation. *Journal of nanoparticle research : an interdisciplinary forum for nanoscale science and technology*.

Velasco, D., Elvira, C., & San Román, J. (2008). New stimuli-responsive polymers derived from morpholine and pyrrolidine. *Journal of materials science Materials in medicine*, *19*(4), 1453–1458. doi:10.1007/s10856-007-3315-z

Verestiuc, L., Nastasescu, O., Barbu, E., Sarvaiya, I., Green, K. L., & Tsibouklis, J. (2006). Functionalized chitosan/NIPAM (HEMA) hybrid polymer networks as inserts for ocular drug delivery: Synthesis,in vitro assessment, andin vivo evaluation. *Journal of Biomedical Materials Research Part A*, *77A*(4), 726–735. doi:10.1002/(ISSN)1552-4965

Veronese, F. M., & Pasut, G. (2005). PEGylation, successful approach to drug delivery. *Drug Discovery Today*, *10*(21), 1451–1458. doi:10.1016/S1359-6446(05)03575-0

Wacker, B. K., Alford, S. K., Scott, E. A., Thakur, Das, M., Longmore, G. D., & Elbert, D. L. (2008). Endothelial cell migration on RGD-peptide-containing PEG hydrogels in the presence of sphingosine 1-phosphate. *Biophysical Journal*, *94*(1), 273–285. doi:10.1529/biophysj.107.109074

Wanakule, P., & Roy, K. (2012). Disease-responsive drug delivery: the next generation of smart delivery devices. *Current drug metabolism*, *13*(1), 42–49.

Wanakule, P., Liu, G. W., Fleury, A. T., & Roy, K. (2012). Nano-inside-micro: Disease-responsive microgels with encapsulated nanoparticles for intracellular drug delivery to the deep lung. *Journal of Controlled Release*, *162*(2), 429–437. doi:10.1016/j.jconrel.2012.07.026

Wang, C.-K., Ho, M.-L., Wang, G.-J., Chang, J.-K., Chen, C.-H., Fu, Y.-C., & Fu, H.-H. (2009). Controlled-release of rhBMP-2 carriers in the regeneration of osteonecrotic bone. *Biomaterials*, *30*(25), 4178–4186. doi:10.1016/j.biomaterials.2009.04.029

Wang, J. (2008). In vivo glucose monitoring: towards "Sense and Act" feedback-loop individualized medical systems. *Talanta*, *75*(3), 636–641. doi:10.1016/j.talanta.2007.10.023

Wang, W. (1999). Instability, stabilization, and formulation of liquid protein pharmaceuticals. *International Journal of Pharmaceutics*, *185*(2), 129–188.

Wee, S., & Gombotz, W. (1998). Protein release from alginate matrices. *Advanced Drug Delivery Reviews*, *31*(3), 267–285.

Wijaya, A., Schaffer, S. B., Pallares, I. G., & Hamad-Schifferli, K. (2009). Selective release of multiple DNA oligonucleotides from gold nanorods. *ACS nano*, *3*(1), 80–86. doi:10.1021/nn800702n

Wong, C., Stylianopoulos, T., Cui, J., Martin, J., Chauhan, V. P., Jiang, W., Popović, Z., et al. (2011). Multistage nanoparticle delivery system for deep penetration into tumor tissue. *Proceedings of the National Academy of Sciences of the United States of America*, *108*(6), 2426–2431. doi:10.1073/pnas.1018382108

Wood, M. D., MacEwan, M. R., French, A. R., Moore, A. M., Hunter, D. A., Mackinnon, S. E., Moran, D. W., et al. (2010). Fibrin matrices with affinity-based delivery systems and neurotrophic factors promote functional nerve regeneration. *Biotechnology and bioengineering*, *106*(6), 970–979. doi:10.1002/bit.22766

Wood, M. D., Moore, A. M., Hunter, D. A., Tuffaha, S., Borschel, G. H., Mackinnon, S. E., & Sakiyama-Elbert, S. E. (2009). Affinity-based release of glial-derived neurotrophic factor from fibrin matrices enhances sciatic nerve regeneration. *Acta biomaterialia*, *5*(4), 959–968. doi:10.1016/j.actbio.2008.11.008

Woodruff, M. A., Rath, S. N., Susanto, E., Haupt, L. M., Hutmacher, D. W., Nurcombe, V., & Cool, S. M. (2007). Sustained release and osteogenic potential of heparan sulfate-doped fibrin glue scaffolds within a rat cranial model. *Journal of molecular histology*, *38*(5), 425–433. doi:10.1007/s10735-007-9137-y

Wu, Y., MacKay, J. A., McDaniel, J. R., Chilkoti, A., & Clark, R. L. (2009). Fabrication of elastin-like polypeptide nanoparticles for drug delivery by electrospraying. *Biomacromolecules*, *10*(1), 19–24. doi:10.1021/bm801033f

Wygrecka, M., Markart, P., Ruppert, C., Petri, K., Preissner, K. T., Seeger, W., & Guenther, A. (2007). Cellular origin of pro-coagulant and (anti)-fibrinolytic factors in bleomycin-injured lungs. *The European respiratory journal : official journal of the European Society for Clinical Respiratory Physiology*, *29*(6), 1105–1114. doi:10.1183/09031936.00097306

Xiong, M., Forrest, M., Karls, A., & Kwon, G. (2007). Biotin-Triggered Release of Poly (ethylene glycol)– Avidin from Biotinylated Polyethylenimine …. *Bioconjugate Chemistry*.

Xu, X., Yee, W.-C., Hwang, P. Y. K., Yu, H., Wan, A. C. A., Gao, S., Boon, K.-L., et al. (2003). Peripheral nerve regeneration with sustained release of poly(phosphoester) microencapsulated nerve growth factor within nerve guide conduits. *Biomaterials*, *24*(13), 2405–2412.

Yaguchi, T., Fukuda, Y., Ishizaki, M., & Yamanaka, N. (1998). Immunohistochemical and gelatin zymography studies for matrix metalloproteinases in bleomycin-induced pulmonary fibrosis. *Pathology international*, *48*(12), 954–963.

Yamamoto, M., Takahashi, Y., & Tabata, Y. (2006). Enhanced bone regeneration at a segmental bone defect by controlled release of bone morphogenetic protein-2 from a biodegradable hydrogel. *Tissue engineering*, *12*(5), 1305–1311. doi:10.1089/ten.2006.12.1305

Yang, B.-B., Lum, P. K., Hayashi, M. M., & Roskos, L. K. (2004). Polyethylene glycol modification of filgrastim results in decreased renal clearance of the protein in rats. *Journal of Pharmaceutical Sciences*, *93*(5), 1367–1373. doi:10.1002/jps.20024

Yap, T. A., Carden, C. P., & Kaye, S. B. (2009). Beyond chemotherapy: targeted therapies in ovarian cancer. *Nature Reviews Cancer*, *9*(3), 167–181. doi:10.1038/nrc2583

You, J.-O., & Auguste, D. T. (2008). Feedback-regulated paclitaxel delivery based on poly(N,N-dimethylaminoethyl methacrylate-co-2-hydroxyethyl methacrylate) nanoparticles. *Biomaterials*, *29*(12), 1950–1957. doi:10.1016/j.biomaterials.2007.12.041

Young, S., Wong, M., Tabata, Y., & Mikos, A. G. (2005). Gelatin as a delivery vehicle for the controlled release of bioactive molecules. *Journal of Controlled Release*, *109*(1-3), 256–274. doi:10.1016/j.jconrel.2005.09.023

Zhang, G., Drinnan, C. T., Geuss, L. R., & Suggs, L. J. (2010). Vascular differentiation of bone marrow stem cells is directed by a tunable three-dimensional matrix. *Acta biomaterialia*, *6*(9), 3395–3403. doi:10.1016/j.actbio.2010.03.019

Zhang, L., Furst, E. M., & Kiick, K. L. (2006). Manipulation of hydrogel assembly and growth factor delivery via the use of peptide-polysaccharide interactions. *Journal of Controlled Release*, *114*(2), 130–142. doi:10.1016/j.jconrel.2006.06.005

Zisch, A. H., Lutolf, M. P., & Hubbell, J. A. (2003a). Biopolymeric delivery matrices for angiogenic growth factors. *Cardiovascular pathology : the official journal of the Society for Cardiovascular Pathology*, *12*(6), 295–310.

Zisch, A. H., Lutolf, M. P., Ehrbar, M., Raeber, G. P., Rizzi, S. C., Davies, N., Schmökel, H., et al. (2003b). Cell-demanded release of VEGF from synthetic, biointeractive cell ingrowth matrices for vascularized tissue growth. *The FASEB Journal: Official Publication of the Federation of American Societies for Experimental Biology*, *17*(15), 2260–2262. doi:10.1096/fj.02-1041fje

Vita

Prinda Wanakule was born in Austin, Texas in May of 1985 to Nisai and Paulla Wanakule. She attended Palm Harbor University High School, where she was enrolled in the Center for Wellness and Medical Professions program, and worked part time as a Nurse Helper/Nursing Assistant in the Emergency Room of Mease Countryside Hospital. In August 2003, Prinda began attending the University of Florida in Gainesville, FL on a full scholarship from the Florida Bright Futures Scholarship Program, and additional scholarships from the Environmental Protection Agency, National Science Foundation Particle Engineering Research Center, Engineering Dean's Scholarship, and the University Scholars Program. While at the University of Florida, Prinda conducted nearly four years of undergraduate research in the Department of Environmental Engineering Sciences (Dr. Chang-Yu Wu) and the Department of Mechanical & Aerospace Engineering (Dr. Malisa Sarntinoranont), and ultimately received a Bachelor of Science degree in Agricultural and Biological Engineering with a minor in Biomechanics. She was also heavily involved in the College of Engineering student organizations, serving as President of the Society of Women Engineers and Vice President of Programs for the Benton Engineering Council. In recognition of her academics, research, and service, she was the recipient of the Class of 2007 Gator Engineering 4-Year Scholar award.

Following graduation in May 2007, Prinda began pursuing her Ph.D. in Biomedical Engineering at the University of Texas at Austin as a National Science Foundation Graduate Research Fellow, with additional support from the University in the form of THRUST, Bruton, Heuer and Women in Engineering Program Fellowships, as

well as the Society of Women Engineers Jill S. Tietjen Scholarship. Working in Dr. Krishnendu Roy's Laboratory for Cellular and Macromolecular Engineering, Prinda's graduate studies focused on enzyme-responsive biomaterials, hydrogels, and disease-responsive drug delivery systems. Towards the end of her graduate career, Prinda held five peer reviewed journal publications, one book chapter in press, a patent application, and over 25 conference proceedings related to her research, as well as her work in engineering education-related topics. In 2011, Prinda was recognized by the Society of Women Engineers as the *Outstanding Graduate Collegiate Member* for her leadership and dedication in promoting engineering education and research. That same year, she was also recognized as one of the leading young women scientists in the nation, and invited to meet First Lady Michelle Obama at the White House in Washington, D.C.

Prinda is currently continuing research in disease-responsive drug delivery and biomaterials, while continuing to engage in the improvement and promotion of education in science, technology, and engineering.

Permanent email: prinda.wanakule@gmail.com or prinda@utexas.edu

This dissertation was typed by Prinda Wanakule.